The Measurement of Particle Velocity and Suspension Density in Pneumatic Coal Injection Systems

by

Stephen Robert Woodhead

Thesis submitted in partial fulfilment of the
requirements for the award of the degree of
Doctor of Philosophy
under the conditions of the award of
higher degrees of
The University of Greenwich

The University of Greenwich

in collaboration with

Blue Circle Cement PLC

August 1992

The Measurement of Particle Velocity and Suspension Density in Pneumatic Coal Injection Systems

Stephen R. Woodhead

Abstract

This thesis describes a programme of work which has been undertaken with the objective of obtaining data relating to the performance of on-line mass flow rate meters as applied to pulverised coal injection systems. Such injection systems are utilised widely in power generation, cement and steel manufacture.

A technology review was carried out, incorporating an extensive literature survey. This review precipitated the conclusion that a number of techniques have been proposed, which may be applicable to the measurement under investigation. However, very little experimental verification of sensing systems based on these techniques had been undertaken.

A test facility, suitable for such verification was therefore developed and an extensive programme of tests were carried out, of a sensing system based on an electrostatic technique. The development of a mathematical model of the sensor operation has also been undertaken, in an attempt to explain some of the more unusual aspects of the experimental results.

The overall conclusion is that some aspects of the measurement can be achieved without major difficulties, whilst problems have yet to be resolved in respect of other aspects of the measurement system. The principle of the measurement system is such that the independent measurement of average particle velocity and suspension density are required in order to measure mass flow rate. The measurement of average particle velocity was shown to be achievable by either of two techniques, whilst the measurement of suspension density proved more problematic.

Recommendations for further work, aimed at addressing these remaining aspects are detailed.

Acknowledgements

This project could not have been completed, or even initiated, without the help and support of a number a people and organisations.

Firstly, I would like to thank Professor Alan Reed, the Director of The Wolfson Centre For Bulk Solids Handling Technology, The University of Greenwich (formally Thames Polytechnic) for his involvement. It was he who in conjunction with Mr Roger Barnes persuaded me to initiate the programme of work described in this volume. He also undertook the task of second supervisor for the project, provided stimulating conversations throughout the programme and proof read the final document.

The involvement of Mr Roger Barnes, the Director of Studies of the programme is also gratefully acknowledged, having provided stimulating conversations and proof read the final document, in addition to having had a significant role in persuading me to initiate the programme.

Dr Mike Bradley, the Manager of The Wolfson Centre has also contributed in the form of some significant stimulating conversations and his input is also gratefully acknowledged.

The support of both The Wolfson Centre and School of Engineering technician staff, in particular: Messrs. Len Parrish, Mike Holman, John O'Connor and Jim Wood is gratefully acknowledged, as is the support of a number of members of both Wolfson Centre and School of Engineering staff, particularly Dr Matthew Reynolds and Mr Andrew Pittman.

Drs John Coulthard and Ben Byrne, and Messrs Ron Hampton and Yong Yan of Teesside Polytechnic have also provided advice and the loan of equipment.

I would also like to thank my family and friends who have had to "put up with me"

throughout the programme, which I am sure at times has not been easy!

Financial support and the loan of equipment from the Science and Engineering Research Council, the Department of Energy, Blue Circle Cement PLC, Babcock Energy PLC, Tealgate Limited, Kevex (U.K.) Limited, Teesside Polytechnic and The Wolfson Foundation is also gratefully acknowledged.

Finally, I would like to thank Mr Trevor Wilson of Hitchin School (now Boyes Lyon School, Hitchin) for persuading me to follow the path which ultimately lead me to undertake this work.

Author's Note

All of the work in this thesis is the sole and original work of the author, except where stated otherwise by acknowledgement or reference.

Contents

Chapter 1 Introduction

1.0 Introduction

The technological evolution which has been taking place over a period of decades has allowed industry to operate with continuously increasing efficiency. Much of this efficiency increase has resulted from increased automation of what had traditionally been labour intensive and/or skilled manual operations.

Two of the corner-stones of this evolution have been the increased use of automatic control systems, and the increased use of conveying systems to transport a wide range of goods from liquids to cars.

It is in these areas that the programme of work reported in this thesis is focused. For many years pulverised coal has been conveyed pneumatically from mills to boilers, kilns and furnaces in the electrical power generation, cement manufacturing and steel manufacturing processes. All of these industries are under continuous pressure to improve production efficiency and product quality, whilst at the same time reduce atmospheric emissions and energy consumption for environmental reasons.

The plant utilised in these industries is heavily dependent on electronic automatic control systems for its operation, and the control techniques are coming under increasing scrutiny for the reasons outlined above. All such control systems are entirely dependent on data supplied by sensors at various points in the process, the reliability and accuracy of which are of vital importance to the efficient operation of the plant.

The flow rate of pulverised coal supplied to the burners in such plants is usually controlled by loss-in-weight feeders or belt weighers on the coal feed into the mills. A combination of oxygen, carbon dioxide and carbon monoxide sensors in the exhaust stacks are then used to provide a feedback signal to the control system, which is used to adjust the coal flow rate in an attempt to operate the plant under optimum conditions

whilst having regard to satisfactory levels of emissions in the exhaust stack.

This technique although widely used suffers from two major drawbacks:

1. The time lag between any change in coal flow rate taking place at the input to the mill and being detected by the stack sensors is significant, sometimes being of the order of 100 seconds. This makes the application of conventional closed loop control techniques inappropriate. As a consequence, manual intervention is commonly utilised. The time taken for the coal feed system to reach optimum conditions can then be protracted, and continuous manual monitoring is then required.

2. Most multi-burner installations have a number of burners fed from a single mill, with a large conveying pipeline from the mill bifurcating up to three times before the pulverised coal reaches the burners. Clearly it is desirable that the split ratio of the pulverised coal at each bifurcation is equal in order that each burner operates with the same stoichiometric ratio, which, for obvious reasons, should be close to the optimum. However, experience has shown that it is difficult to engineer an approach capable of providing a stable split ratio for extended periods.

From the foregoing it is clear that an on-line system for measuring the flow rate of pulverised coal from the mill to the boiler, kiln or furnace would afford a number of advantages.

Such a sensing system would allow the feed of pulverised coal to each burner to be monitored. This data could then be utilised in an automatic control system to ensure that all of the burners in a multi-burner installation were balanced, and thus ensure that the plant was operating at its most efficient condition. The monitoring of the flow rate of pulverised coal to single burner installations, such as cement kilns, would allow closed loop automatic control of the stoichiometric combustion ratio to ensure efficient use of fuel and minimise undesirable atmospheric emissions.

The development of such a sensing system has been addressed by many engineers over the years and many technical papers have been published with respect to principles which may be applied to such a measurement problem. However, despite the significant number of publications relating to the subject matter, very little experimental verification has been reported. Thus, the performance of sensors based on such principles, under various operating conditions, particularly those found in relevant industries, remains largely unknown.

It was precisely this fact which the programme of work in this thesis set out to address.

1.1 Programme Objectives

The major objective of the programme of work reported in this thesis was to obtain information which would allow the performance of an on-line mass flow rate measurement system, applied to pulverised coal in pneumatic injection systems, to be determined under conditions which are relevant to the power generation, cement manufacturing and steel manufacturing industries.

In order to achieve this overall objective, it was recognised that a number of component objectives would have to be achieved:

1. A literature survey would need to be undertaken.

2. Detailed experimental verification of the performance of one or more sensing systems would need to be undertaken, under relevant test conditions.

3. In order to achieve 2 above, a suitable test facility would need to be made available to the programme.

4. It was also considered desirable to improve the understanding of the operating principle of such sensing systems, since it was clear from an initial survey of the technology that there was a lack of understanding in this area, which was impeding the evaluation of sensor performance from a more fundamental

standpoint .

1.2 Programme Preview

This section will briefly describe the work which was undertaken in an attempt to satisfy the programme objectives. The work outlined in this section is then documented in much greater detail in the following chapters and appendices.

In order to assess the existing state of the relevant technology, a technology review was undertaken in the early stages of the programme. This is detailed in Chapter 2. The results of a literature survey were supplemented by a small amount of information which was gained by the author in the form of first hand experience in the use of some sensing systems. The major conclusion of this review was that while a number of techniques had been proposed and instruments constructed, there was, however, a lack of experimental test data to validate the approaches. This was largely attributed to the lack of availability of suitable test facilities to the academic community, the latter being the source of the majority of publications.

As a direct consequence of this fact, the decision was made to design and construct a dedicated industrial scale test facility in which the most promising sensing system could be subjected to close scrutiny. The design and construction of this facility is detailed in Chapter 3.

A programme of experimental test work was then undertaken in order to assess the performance of a sensing system based on an electrostatic principle, this having been isolated as being the most promising of the approaches available. These tests were carried out under conditions which were as representative as possible of those found in industrial systems. This work is detailed in Chapters 4 and 6. A detailed analysis of the experimental test data was then carried out, and the results presented and discussed. This work is detailed in Chapters 5 and 6.

Some of the experimental test data yielded results which were not as initially expected, and in an attempt both to explain these results and to gain a better understanding of the

operating principle of the sensing head, a model of the sensor operation was developed. The model was then used to examine the effect of a number of variables on the performance of the sensor. The development of the model is detailed in Chapter 7 along with some discussion with respect to the implications of the modelling work on the experimental results.

Finally, the conclusions of the programme, along with recommendations for further work are presented in Chapter 8.

Chapter 2

A Review of Technology Applicable to Mass Flow Rate Measurement in Pulverised Fuel Injection Systems

2.0 Introduction to the Review

A literature survey was undertaken as the initial element of the programme of work reported in this thesis. The purpose of this survey was to identify technologies which had been, or could, in the future, be applied to the measurement of the mass flow rate of pulverised fuel (PF) in pneumatic injection systems of the type introduced in Chapter 1. A number of techniques were identified. Some were reported to have undergone trials in PF injection or other pneumatic conveying systems, whilst others had not but could perhaps be used in the application under consideration.

This information was then supplemented with some direct experience gained by the author. This additional information was obtained by obtaining appropriate equipment on loan from suppliers and carrying out either bench scale tests or on-line trials.

2.1 Summary of Proposed Measurement Techniques

The literature survey showed that a number of techniques had been proposed. The principles of these techniques will be introduced and an analysis of each author's work will then be given. Where appropriate, the experiences, at this stage, of the author of this work will also be given.

It is apparent that many of the proposed techniques derived their value of mass flow rate from the measurement of two separate variables. These variables are the density of the flowing suspension (ρ_s) and the average velocity of the particles in the suspension (V_{pa}). These two values were then combined, usually using an equation of the form below:

$$Mass\ Flow\ Rate = V_{pa} . \varrho_s . Constant$$

There are, however a small number of papers which report instruments based on principles which derive the mass flow rate by a more direct method. These instruments are usually of an intrusive type, based on differential pressure meters commonly used for the measurement of flow rate of single phase flows.

2.1.1 Techniques Proposed for the Measurement of Suspension Density (ρ_s)

The literature survey yielded three principles by which the measurement of the suspension density might be achieved. These were as follows :

1. Sensing the charge induced on an electrode inside the pipeline by the flowing particles contacting the electrode. This is generally termed an electrostatic technique or a triboelectric technique by different authors respectively, but will be termed an electrostatic technique here for the purposes of clarity. A typical sensor head is shown in Figure 2.1.

2. Sensing the change in the relative permittivity of the pipeline cross section by making the pipeline cross section into the dielectric of a capacitor and measuring the change in the value of the capacitor. This will be termed a capacitive technique. A typical sensing head is similar to that shown in Figure 2.I, although the signal processing will obviously be different to that used in 1. above.

3. Sensing the change in the attenuation of a beam of radiation passing through the pipeline cross section. This will be termed a radiation attenuation technique. The principle of this type of sensor is shown in Figure 2.2. The types of radiation proposed for such an approach are β-particles, X-rays and visible light.

2.1.2 Techniques Proposed for the Measurement of Average Particle Velocity (V_s)

Four principles were identified by which the measurement of average particle velocity might be achieved. Two are potentially applicable to real industrial installations, and

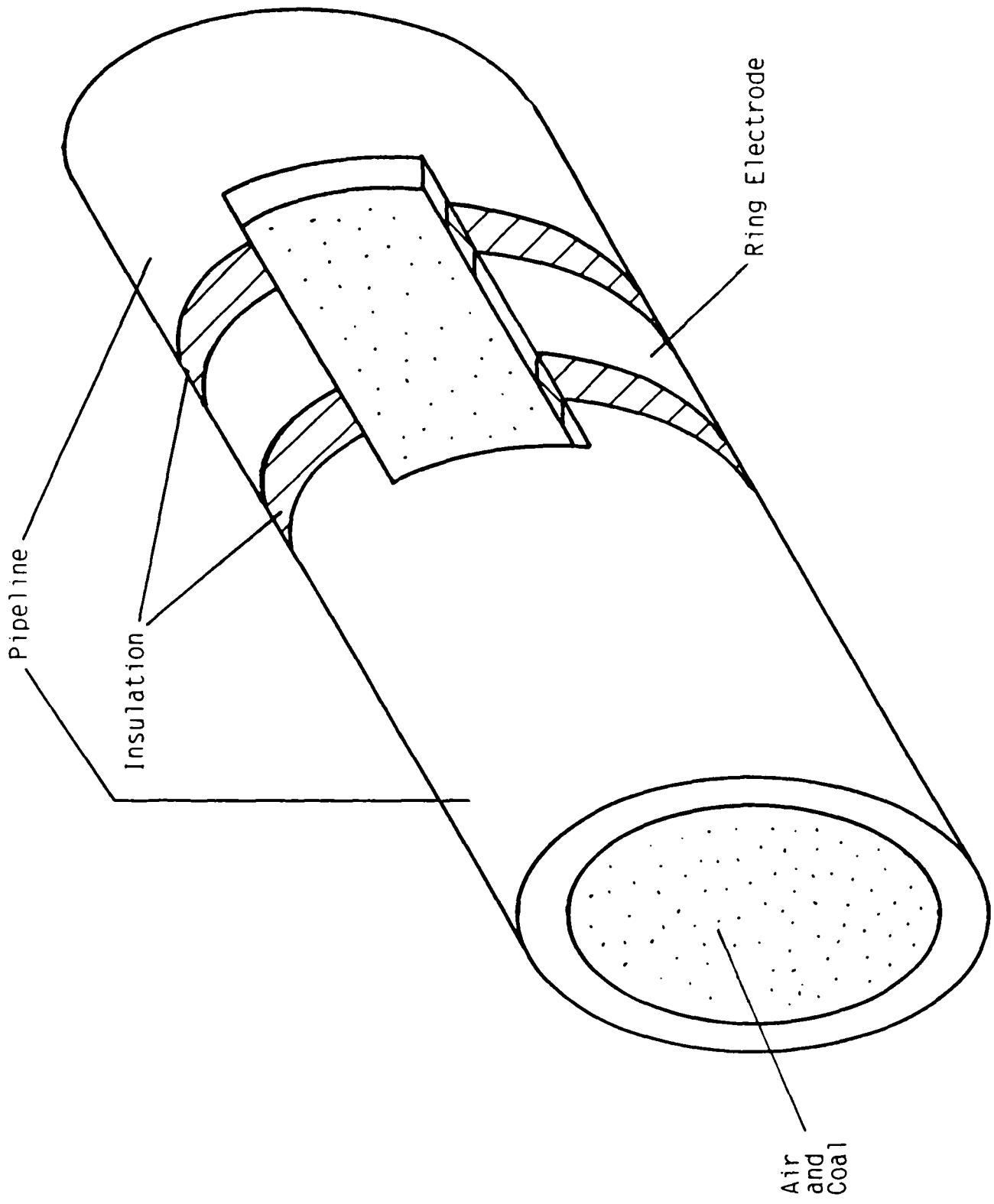

Figure 2.1 Typical Electrostatic Sensing Head

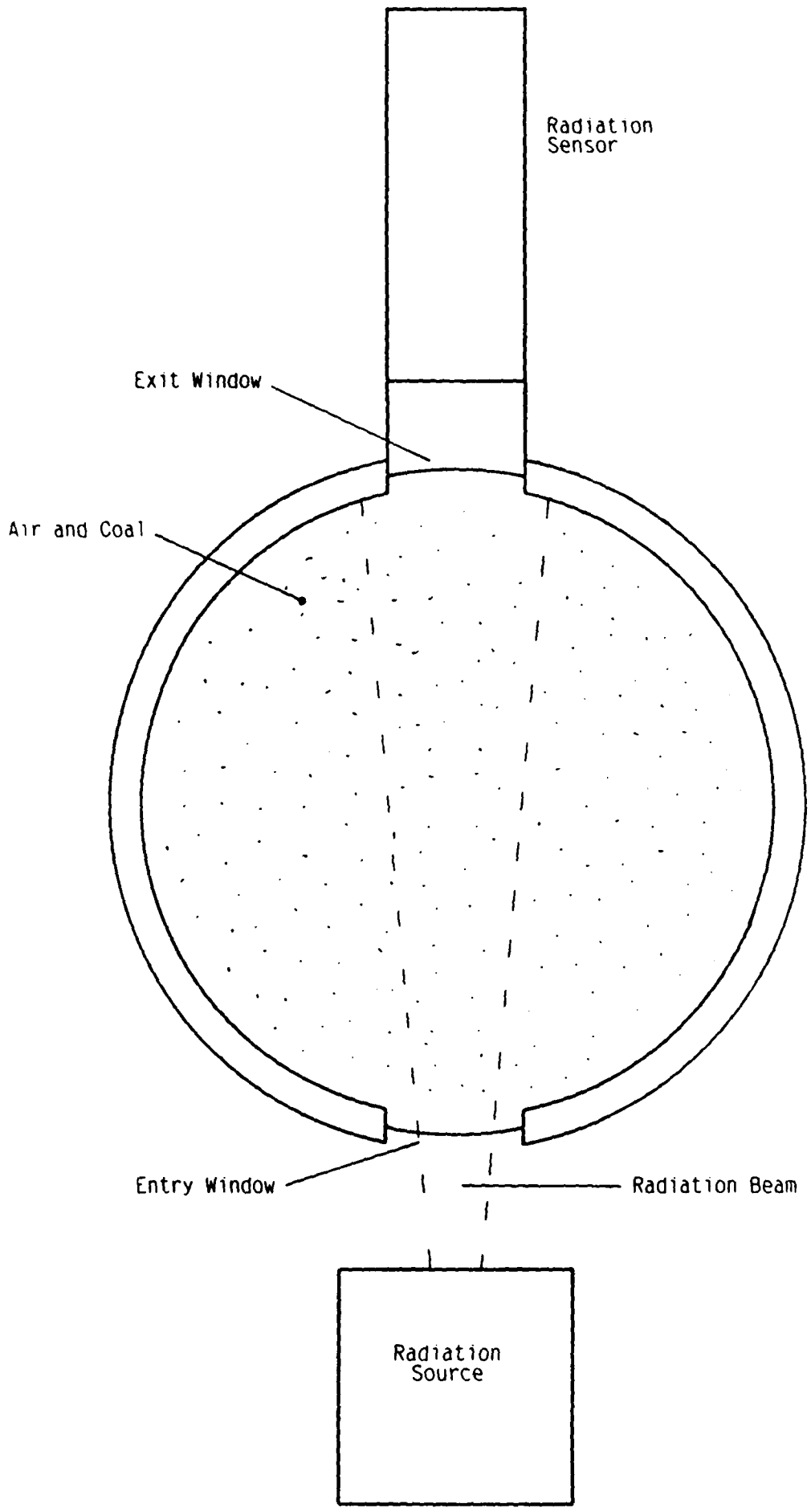

Figure 2.2 Principle of the Flow Modulated Radiation Technique

these will be outlined first, whilst the other two are only suitable for research work in the laboratory and will be dealt with second.

1. Utilisation of electronic hardware or computer software to calculate the cross correlation function of the signals from two suspension density sensors spaced axially along the pipeline. The transit time between the two sensors and hence the velocity may then be determined from the cross correlation function. This will be termed a cross correlation technique, the principle of which is shown in Figure 2.3.

2. Determination of the conveying air velocity using a knowledge of the air volumetric flow rate and the cross sectional area of the pipeline. This value is then used in conjunction with the estimation of the particle slip in the air stream to estimate the average particle velocity. This will be termed a slip velocity technique.

3. Utilisation of laser doppler velocimetry, the principles of which are described in detail in Chapter 4, to measure the average particle velocity.

4. Utilisation of tracer particles, such as radioactive isotopes, to measure the transit time between points spaced axially along the pipeline, from which the velocity may be determined. This will be termed the transit time technique.

2.1.3 Techniques Proposed Which Derive Mass Flow Rate Directly

All of the instruments in this category are based on adaptations of differential pressure techniques commonly used in the field of single phase fluid flow measurement. Both orifice meters and venturi meters are proposed.

2.1.4 Classification of the Work of Others

For the purposes of clarity it was decided to attempt to classify the work of various authors into various categories. Since many of the techniques discussed require two

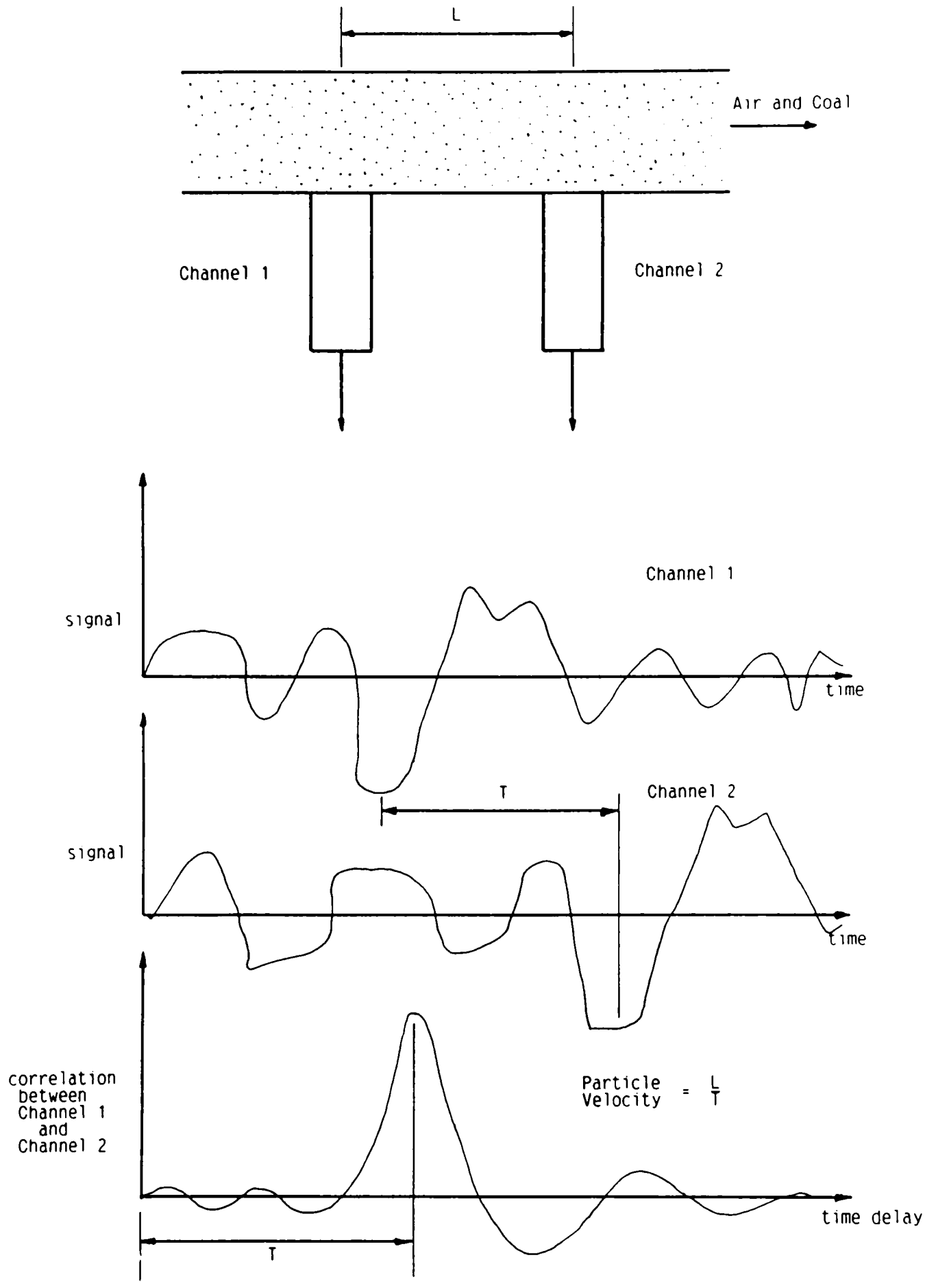

Figure 2.3 Average Particle Velocity Measurement Using the Cross Correlation Technique

separate measurements and different authors use different combinations it was not possible to do this definitively. As a consequence these classifications are intended only as a guide.

2.2 Techniques Based on Adaptations of Single Phase Flow Rate Meters

The work of two authors is dealt with here. Both of the references cited detail techniques which were originally proposed in the 1950's but were not taken up at that time. The techniques were investigated again in the early 1970's. However as far as may be determined these techniques have not been adopted in industry and no published work has been found dated after 1971.

2.2.1 McVeigh and Craig

A single paper by McVeigh and Craig[A1] was identified by the survey as being relevant to the work of this thesis. This publication is particularly useful since the first part of the paper undertakes a review of the work of a number other authors dating back to the 1940's. It is reported that experiments have been carried out with both orifice meters and venturi meters in order to evaluate their applicability to the mass flow rate measurement of P.F. in pneumatic conveying systems.

McVeigh and Craig report that the majority of these trials were unsuccessful for various reasons:

1. Some of the meters were unable to differentiate between a change in air flow rate and a change in solids flow rate.

2. Many of the meters exhibited unacceptable sensitivity to upstream pipeline fittings such as bends which are difficult to avoid when retrofitting such technology to existing PF injection systems.

3. The calibration of the meters drifted with time due to wear of the internal parts of the meter caused by the abrasive nature of the PF.

4. Blockages in the duct work were found to occur in the region of the meter, apparently due to the increased pressure drop imposed by the meters installation.

McVeigh and Craig then report the results of experimental tests carried out to evaluate the performance of an annular type venturi meter applied to PF mass flow rate measurement. The trials were carried out in a pilot scale test rig, the exact scale of which is not given. Although some experimental results are given, showing a sensitivity to product mass flow rate, no tests were carried out to evaluate the effect of wear and pipeline fittings on the meter. Thus a full assessment of the applicability of the meter may not be made from the reported results.

2.2.2 Farbar

Fabar[A2] reports the results of tests carried out on a venturi type meter in a 17mm bore conveyor. Tests results are reported for a range of conditions and it is clear that the meter has the ability to give a reading proportional to product mass flow rate. However, none of points 2 to 4 in Section 2.2.1 are addressed.

It is apparent that whilst it is possible that these early techniques derived from single phase flow measurement techniques could be developed in such a way that they are largely immune to points 1 and 2 in Section 2.2.1. It seems unlikely that the problems outlined in points 3 and 4 can ever be fully overcome. It seems to the author of this thesis that this may account for the fact that, despite this technology having been identified some 40 or 50 years ago, it has not found use in industry.

It is for these reasons that the decision was taken not to pursue this technology further as part of the work reported in this thesis.

2.3 Techniques Based on Electrostatic Sensors

The work of a number of authors is dealt with here, some proposing and/or reporting the use of single sensors in isolation for the measurement of suspension density and

some proposing and/or reporting the use of sensors spaced axially along the pipeline in conjunction with a cross correlator, for the measurement of average particle velocity.

2.3.1 Dechene and Averdieck

Five papers were sourced by Dechene and Averdieck. These will be dealt with in chronological order.

The first paper[B1], published in 1985, reports the use of a single electrostatic sensor to detect an increase in dust level in a duct, such as may be caused by the failure of a bag filter. A diagram of the reported installation is shown in Figure 2.4. The dust concentrations reported were of the order of 3.0×10^{-5} grains/m^3, which corresponds to approximately 2.0×10^{-9} kg/m^3. Typical air velocities past the probe were reported as 18m/s. Dust particle sizes were reported as around 10μm.

The sensor was intended to give a signal only when a threshold of dust concentration was exceeded. No information on the possible linearity of a sensor of this type was given. Although the air velocity and dust particle sizes reported were similar to those commonly found in PF injection systems, the suspension density was around nine orders of magnitude lower.

The second paper[B2], published in 1986, reports the use of several sensors of the type described in the paper of the previous year, but gives no technical details of these installations. This paper also proposes the use of a linear version of the sensor, giving an analogue output to give continuous dust level monitoring. Again no technical details of the installation are given.

The third paper by Dechene and Averdieck[B3], published in May 1987, again proposes the use of an analogue type sensor with an output proportional to flow rate. A graph relating sensor output and flow rate is given, but the units of the flow rate axis are not given, and no details of the installation, such as conveyed material, air velocity or

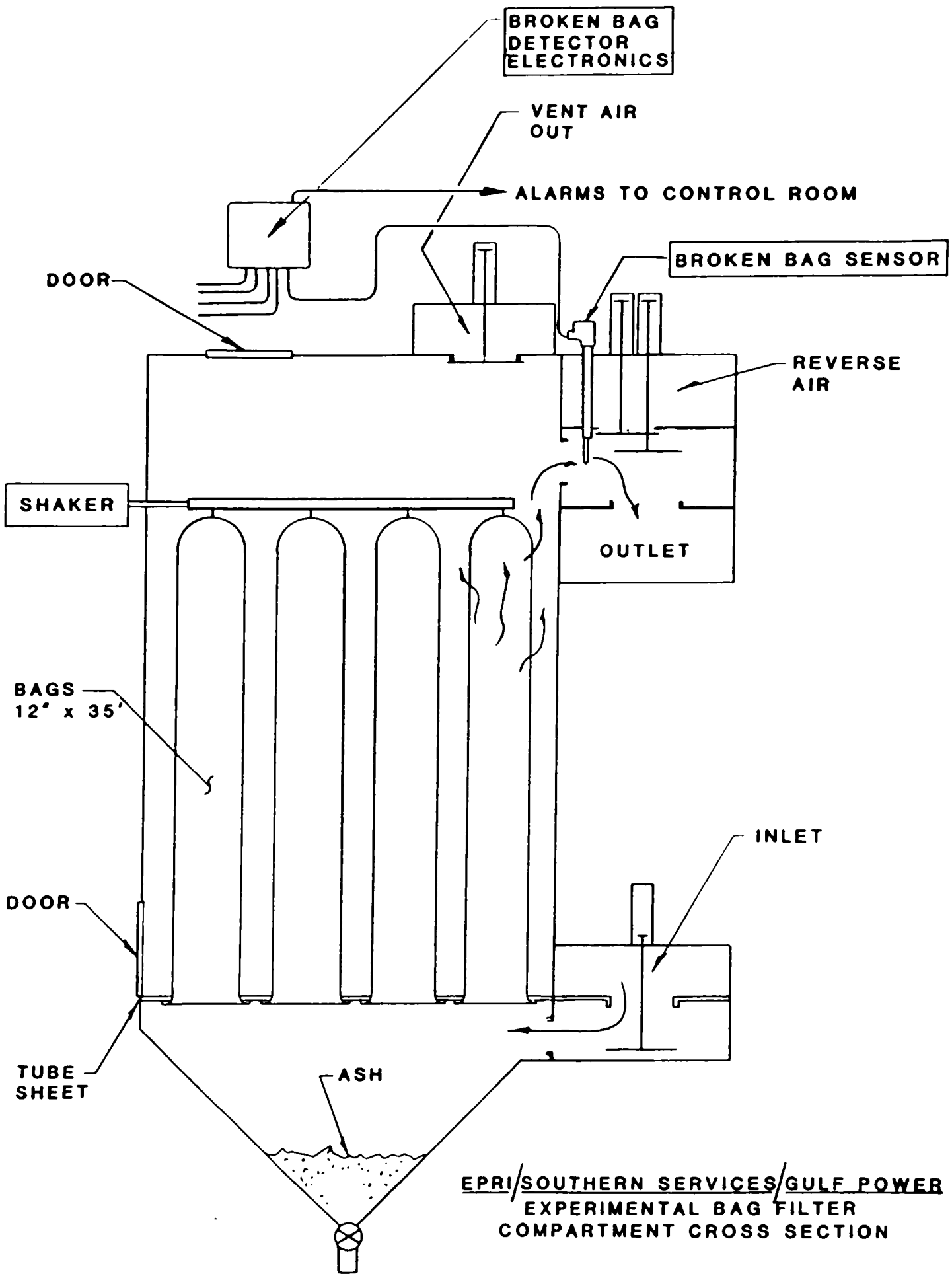

Figure 2.4 Installation of Dust Sensor Reported by Dechene[B1]

suspension density are given. This paper also proposes the use of two axially spaced sensors connected to a cross correlator in order to measure the average particle velocity. It is also proposed that the output from the analogue flow sensor is sensitive to both velocity and suspension density and that by combining both the analogue flow sensor and a cross correlation system, mass flow rate can be calculated. The paper indicates that such a meter has been constructed, but does not report the results of any test work.

The fourth paper[B4], published in June 1987, does not propose any new principles or report the results of any tests which have not already been documented in previous papers.

The fifth paper[B5], published in 1988, gives further details of the design of a mass flow rate meter using both an analogue suspension density meter and cross correlation. However, no test results were reported.

In summary, Dechene and Averdieck have proposed the use of electrostatic type sensors in conjunction with cross correlation techniques to measure the mass flow rate of materials in a pneumatic conveyor. No test results are reported.

2.3.2 Gajewski and Szaynok

Two relevant papers were published by Gajewski and Szaynok. The first, published in 1981[B6], reports laboratory tests carried out to measure the charging tendency of PVC powder under various conditions. The reported tests were carried out with an "inductive ring probe", few details of which are given.

However, the reported results are of interest, since they give information on the effect of a number of variables on the charging tendency of PVC powder with a particle size below 60μm. The effects of moisture content, flow velocity and mass of powder are reported. Graphs illustrating the reported results are shown in Figure 2.5. The results

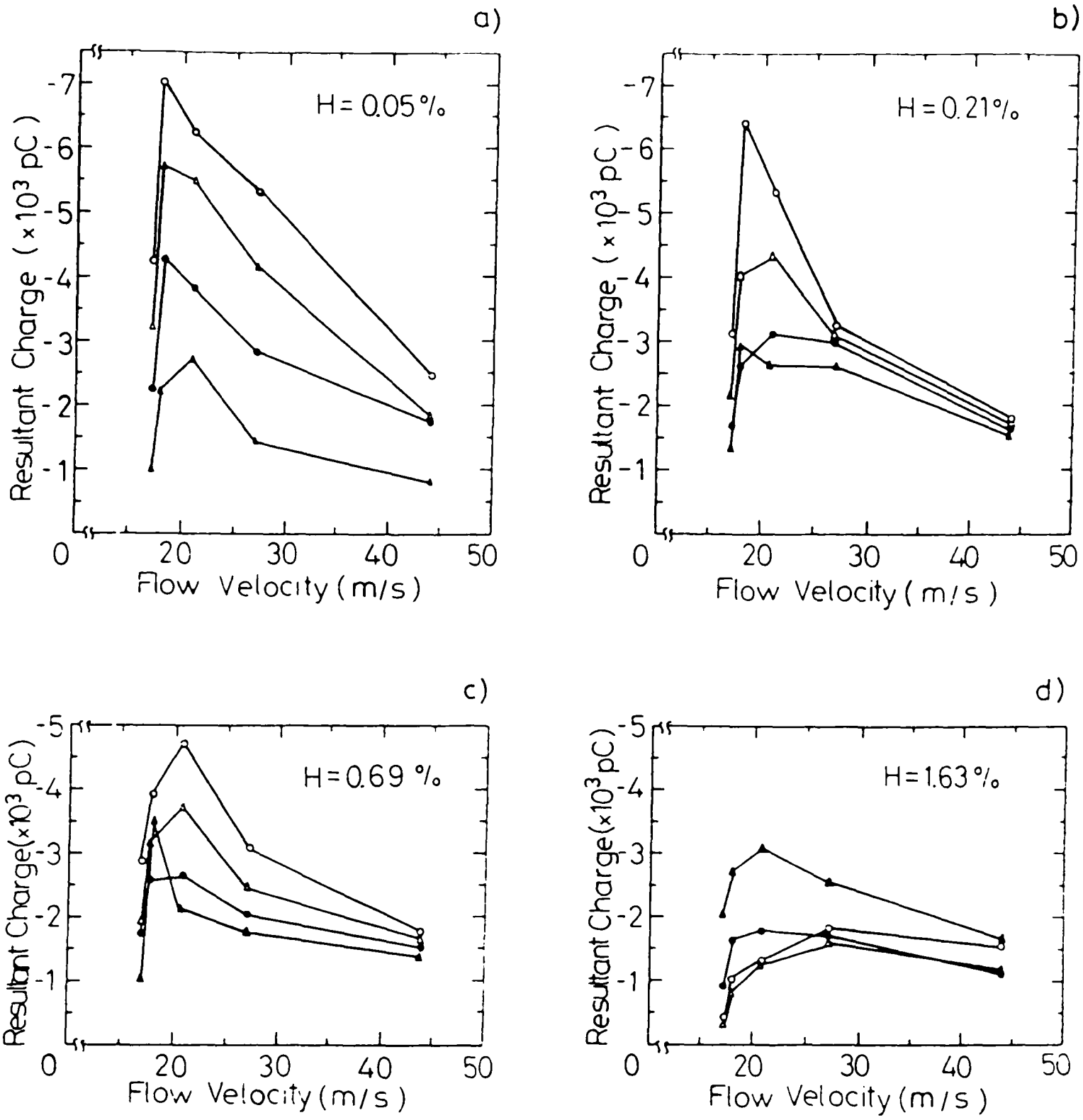

The resultant charge of the PVC dust flux as a function of flow velocity: (o)m = 0.212g; (△)m = 0.159g; (●)m = 0.106 g; (▲)m = 0.053g, and of the equilibrium moisture contents: a) 0.05%, b) 0.21%, c) 0.69%, d) 1.63%.

Figure 2.5 Graphs Showing Results Reported by Gajewski and Szaynok [B6]

indicate that with increasing moisture content, the charging tendency of the powder decreases. With increasing flow velocity, the charging tendency has a maximum value around 20m/s, dropping off rapidly below 20m/s and dropping off more slowly for increasing flow velocity. Generally the larger the mass of material used for the test, the larger the charging tendency of the powder.

The second paper by Gajewski[B7] is essentially a continuation of the first, reporting results obtained using the same apparatus as in the first paper, but testing a range of powdered materials of different composition and particle size.

Tests were carried out using polymethylmethacrylate (PMMA), saccharose and nichrome powders. For each material, tests were carried out with powders of three different particle sizes, $<60\mu$m, 60-120μm and 120-200μm. For the PMMA, the charging tendency of the powder increases with increasing particle size. For both the saccharose and the nichrome, the charging tendency of the powder decreased with increasing particle size. The PMMA had the greatest charging tendency, followed by the saccharose and then nichrome.

Although no mass flow rate measurement technique is reported, the work of Gajewski and Szaynok is of interest, since it reports the charging tendencies of various powders. This tendency is a property upon which the operation of the electrostatic type sensors clearly depends and so is of indirect interest to the programme of work reported in this thesis.

2.3.3 Singh

One paper by Singh was found to be relevant to the work of this thesis.

This paper[B8], was published in 1983 and reports the results of tests carried out to investigate the charge tendency of high density polyethylene (HDPE) powder during pneumatic conveying. Silo current measurements were made of the current flowing between an isolated silo and ground during the filling of the silo from a pneumatic

conveyor. Currents in the region of 2.0μA were recorded with an HDPE mass flow rate of approximately 4kg/s through a 100mm diameter pipeline. This corresponds to a charge on the HDPE of approximately 0.6 μC/kg. The charge to mass ratio was found to decrease with increasing mass flow rate. The results also indicate that the charging tendency is dependent on relative humidity (RH), decreasing with increasing RH (as noted by Gajewski and Szaynok) with a distinct change in the charging of the powder occurring at an RH of 35%. Thus, in order to minimise the possibility of electrostatic discharges and their associated explosion hazards in pneumatic conveying systems the paper recommends operation at high material flow rates and RH's above 35%.

Although this paper does not propose any techniques which may be applicable to mass flow rate measurement, the results, like those of Gajewski and Szaynok, are of relevance in terms of understanding something of the charging characteristics of the powder.

2.3.4 Shackleton

The work of Shackleton is reported in a Master of Philosophy thesis dated 1982[B9].

This thesis reports the design and development of an electrostatic type sensor very similar to that reported by Dechene and Averdieck. Although Shackleton's work pre-dates that of Dechene and Averdieck, it is not cited by these authors.

Shackleton reports the design of a single electrostatic type sensor, as well as the use of cross correlation techniques in conjunction with axially spaced sensors to evaluate average particle velocity. However, unlike Dechene and Averdieck, some test results are given using 4mm poly-vinyl chloride (PVC) chips and 280μm steel shot. The reported results are limited and indicate that the single electrostatic sensor gives an output which is not proportional to flow rate even at constant air velocity. Cross correlation functions and spectral analyses are given for the sensor outputs, but no comparisons are made with actual particle velocities. Thus, it is difficult to gauge the

potential accuracy of the cross correlation technique from the results.

2.3.5 Masuda et al

A single paper by Masuda et al[B10], published in 1977, was identified as relevant to the work reported in this thesis. This paper reports results of tests carried out to measure the current flowing between an isolated section of pipeline and earth, as induced by the flow of particles when the pipeline sections were incorporated in a pneumatic conveying system. Trends are reported for the effects of using bare metal and insulated lined pipes, as well as the position of pipeline bends and product feeders. The measurement technique reported is a less well developed version of that reported by Shackleton and Dechene and Averdieck and predates the work of both. The work of Masuda et al is cited by Dechene and Averdieck, but not by Shackleton.

This work is of indirect interest in the same way as that of Gajewski and Szaynok and Singh.

2.3.6 King

The literature survey identified one paper by King[B11], published in 1973.

King reports the results of tests carried out using a single electrostatic sensor in a pneumatic conveying pipeline. The tests used PVC powder (particle size around 1mm) and wheat flour. They were carried out over a limited range of conveying conditions in a 50mm nominal bore pipeline. The reported results are illustrated in Figure 2.6. The output of the sensor increases with material mass flow rate up to a certain value, with the output then levelling off. This levelling off occurred at a suspension density of approximately 3.5 kg/m^3 using a conveying velocity of approximately 20 m/s with flour. The corresponding value for PVC powder was 6.4 kg/m^3.

This paper also reports the sensitivity of this single sensor to conveying velocity and moisture. The conveying velocities were measured by a cross correlation method of which unfortunately few details are given. However, the test results demonstrate the

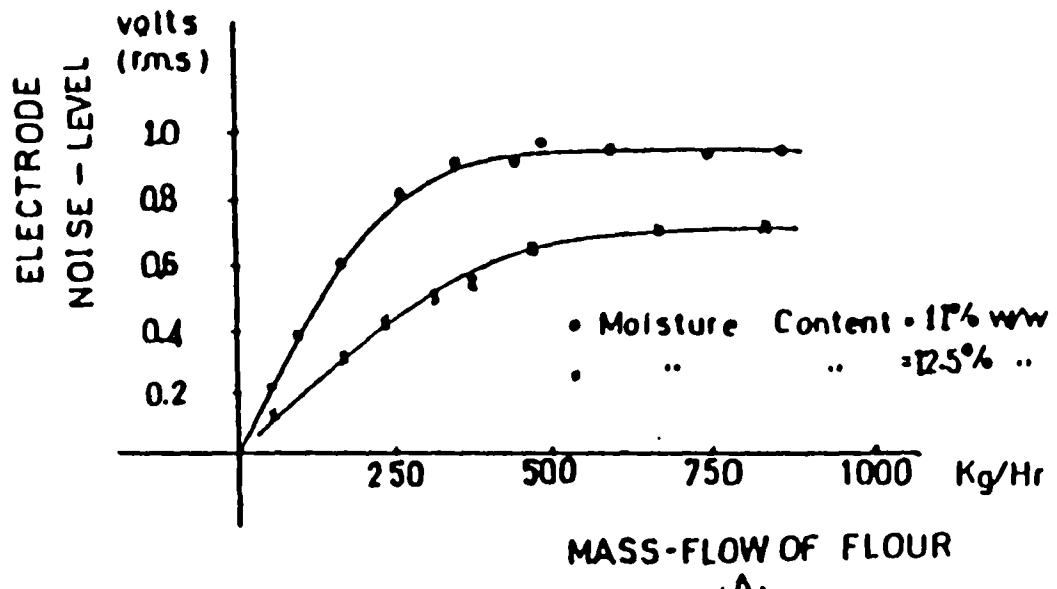

Variation of noise level ($\hat{V}$) with mass flow rate of flour, at constant Humidity values.

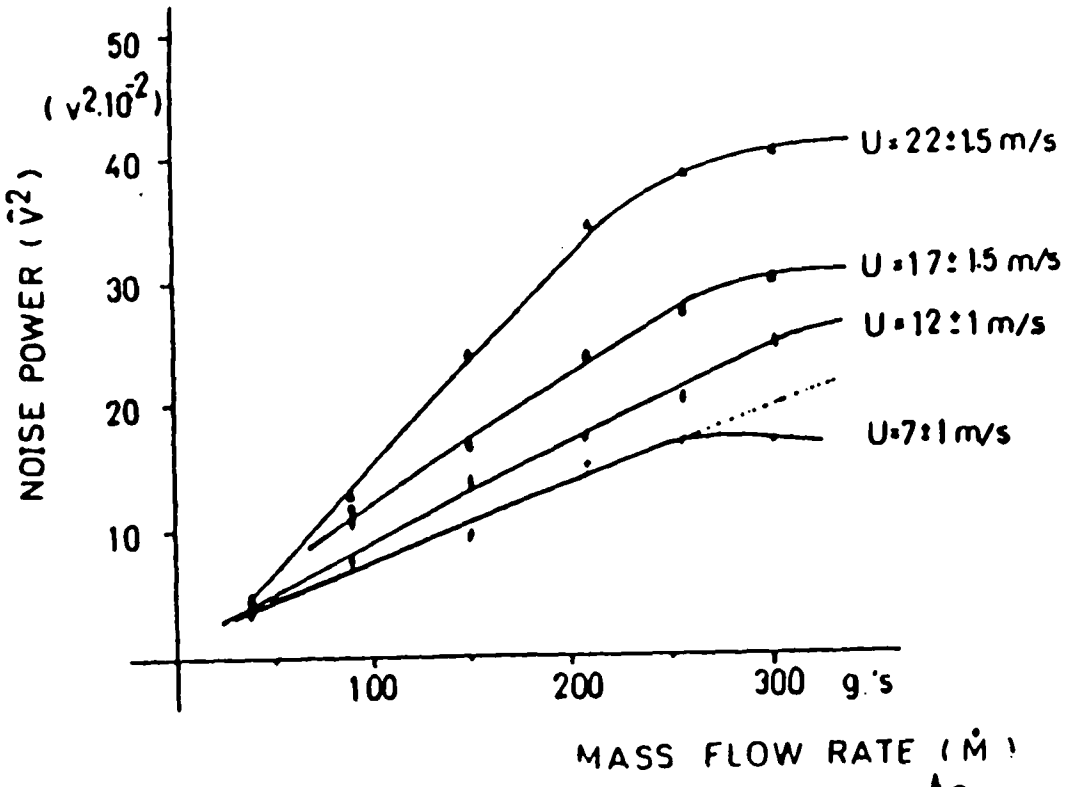

Linear plots of measured noise power ($\hat{V}^2$) against PVC mass flow ($\dot{M}$) at specified values of mean transport velocity (U).

Figure 2.6 Graphs Showing Results Reported by King[B11]

sensitivity of the sensor to conveying velocity, with the sensor output increasing with conveying velocity.

This paper is clearly of great interest, since it is, thus far, the only report of any significant test work carried out with this type of sensor. However, the range of test conditions was limited and little information was given on the velocity measurement technique used. Also of interest is the fact that this publication pre-dates those of Dechene and Averdieck and Shackleton by some 8-10 years, and in the most part gives more comprehensive information. King's work is cited by Shackleton (as would be expected since they carried out their work at the same university), but is not cited by Dechene and Averdieck.

2.3.7 Kittaka et al

A single paper by Kittaka et al[B12] was identified by the literature survey. They report the results of measurements carried out using an electrometer connected to a powder sampling device. The tests were carried out using several polymer powders by circulating them at low velocities (1.4-2.8m/s) in a closed loop pneumatic conveyor. The times needed for the polymer powders to reach the saturation charge were then determined. The value of the saturation charge was also recorded. The reported results show that both the charging time and the saturation charge value increase with increasing velocity. The charging time increases with decreasing suspension density, and the saturation charge value is independent of suspension density. These results are broadly in agreement with those reported by Singh.

This work, like that of Gajewski and Szaynok , Singh and Masuda et al, is of indirect interest.

2.3.8 Klinzing et al

The literature survey identified three papers by Klinzing et al proposing or reporting the use of electrostatic techniques. These being published between 1982 and 1987. These will be examined in chronological order.

Klinzing et al published a single paper in 1982[B13]. In common with the work of Singh, Gajewski and Szaynok, Masuda et al and Kittaka et al, none of these papers propose or report any new techniques which could be applied to mass flow rate measurement. However they do provide information on the charging tendency of powders under conditions of pneumatic transport and are therefore of indirect interest.

Reference B13 reports the results of tests undertaken to evaluate the effect of particle size, suspension density and relative humidity (RH) on the charging tendency of glass beads with particle sizes in the region of 100μm. The reported trends are that the charging tendency of the powder increases with decreasing RH, decreasing particle size and increasing suspension density. With the exception of the last point, these findings are in broad agreement with the reported findings of the other authors discussed.

The second paper of Klinzing et al[B14] reports the results of tests carried out using the cross correlation of two axially spaced electrostatic sensors to evaluate particle velocity. This work was carried out in the vertical section of a pneumatic conveyor using 150μm glass beads and air velocities in the region of 20m/s. The results are presented as graphs of particle slip velocity against voidage fraction, and make the assumption that the particle velocity as evaluated by the cross correlator is the actual average particle velocity, from which in conjunction with the air velocity, the slip velocities were calculated.

No direct measurements of the average particle velocity are made, and so no information is given with respect to the accuracy of the cross correlation velocity measurement technique.

The third paper by Klinzing et al[B15], published in 1987, reports the results of tests carried out using the cross correlation principle applied to two axially spaced electrostatic type sensors. The tests were carried out in a horizontal section of a pneumatic conveyor using air velocities in the range of 10 to 20m/s. The conveyed material was crushed glass with a mean particle size in the region of 270μm.

The reported results again compare the particle velocity measured using the cross correlation technique with the actual air velocity. The slip velocity so calculated increases with increasing air velocity over the range of conditions tested.

The last two references by Klinzing et al[B14,B15] contain the only reports from which any evaluation of the cross correlation technique applied to electrostatic sensors might be made. Although no actual particle velocity measurements are reported for comparison, the velocities evaluated by the cross correlation technique are generally slightly below the air velocities indicating that this technique at least has some potential.

The last paper[B15] is also important because it proposes that the electrostatic sensors used do not need to be in contact with the flowing suspension. That is the signal picked up by the probes is induced by the electrostatic field associated with the charged particles rather than being induced by actual charge transfer by contact. The work of all the other authors cited propose that the charge is induced by charge transfer on contact with the flowing particles.

2.3.9 Woodhead et al

The author of this thesis carried out some initial tests using a single electrostatic suspension density sensor and a cross correlation technique using two electrostatic sensors to evaluate velocity. The results of these tests are reported in a paper[B16], published by the author and others in 1990.

These results are shown in Figures 2.7 and 2.8. The results show that the velocity given by the cross correlation technique is generally somewhat below the air velocity, as we might expect. The output of the suspension density sensor increases with increasing suspension density, however it is difficult to assess the linearity of the sensor from the small number of test data points obtained.

2.4 Techniques Based on Laser Doppler Velocimetry

The work of several authors is examined in this section, most of which report the

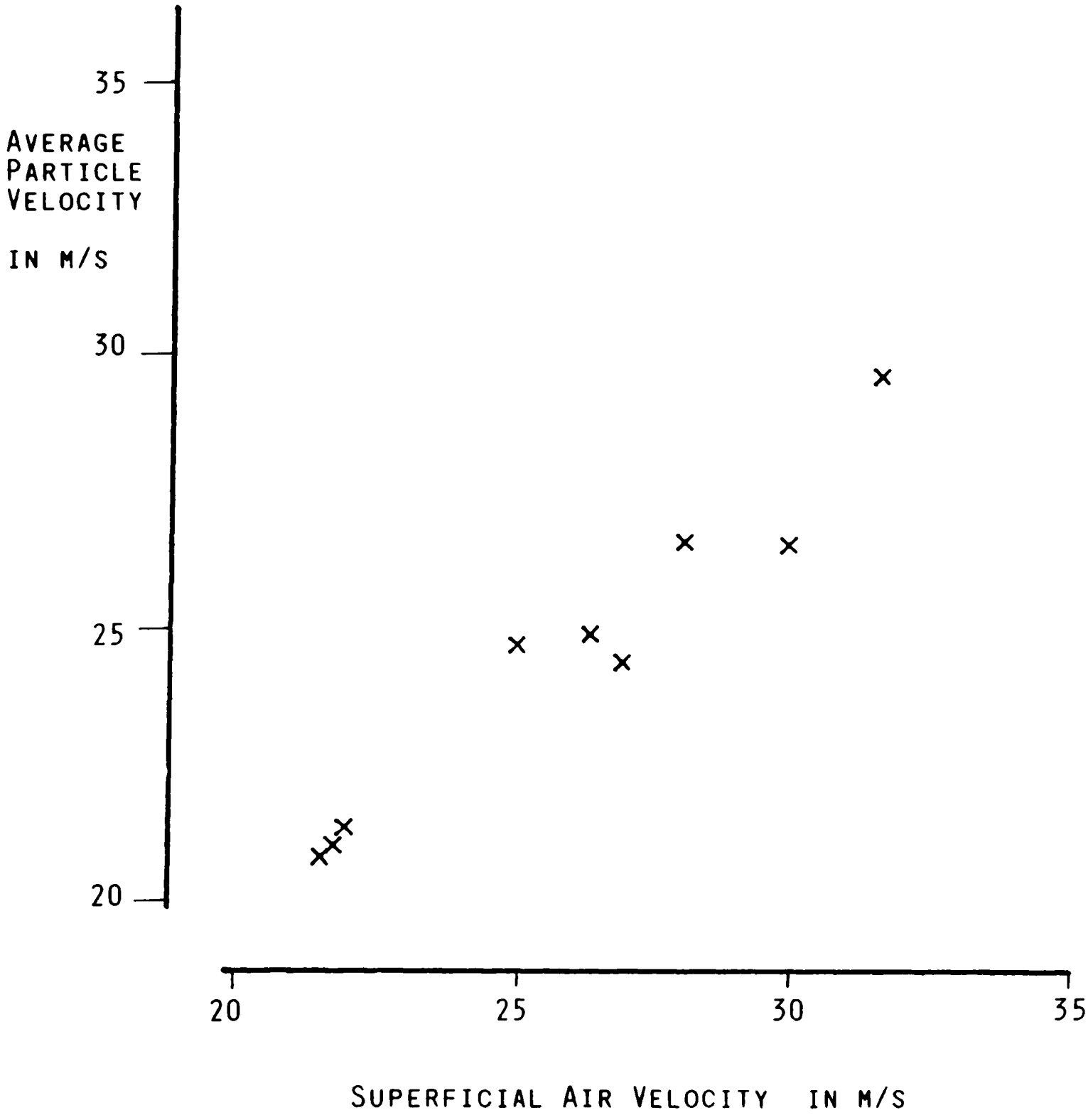

Figure 2.7 Graph Showing Results Reported by Woodhead et al [B16]

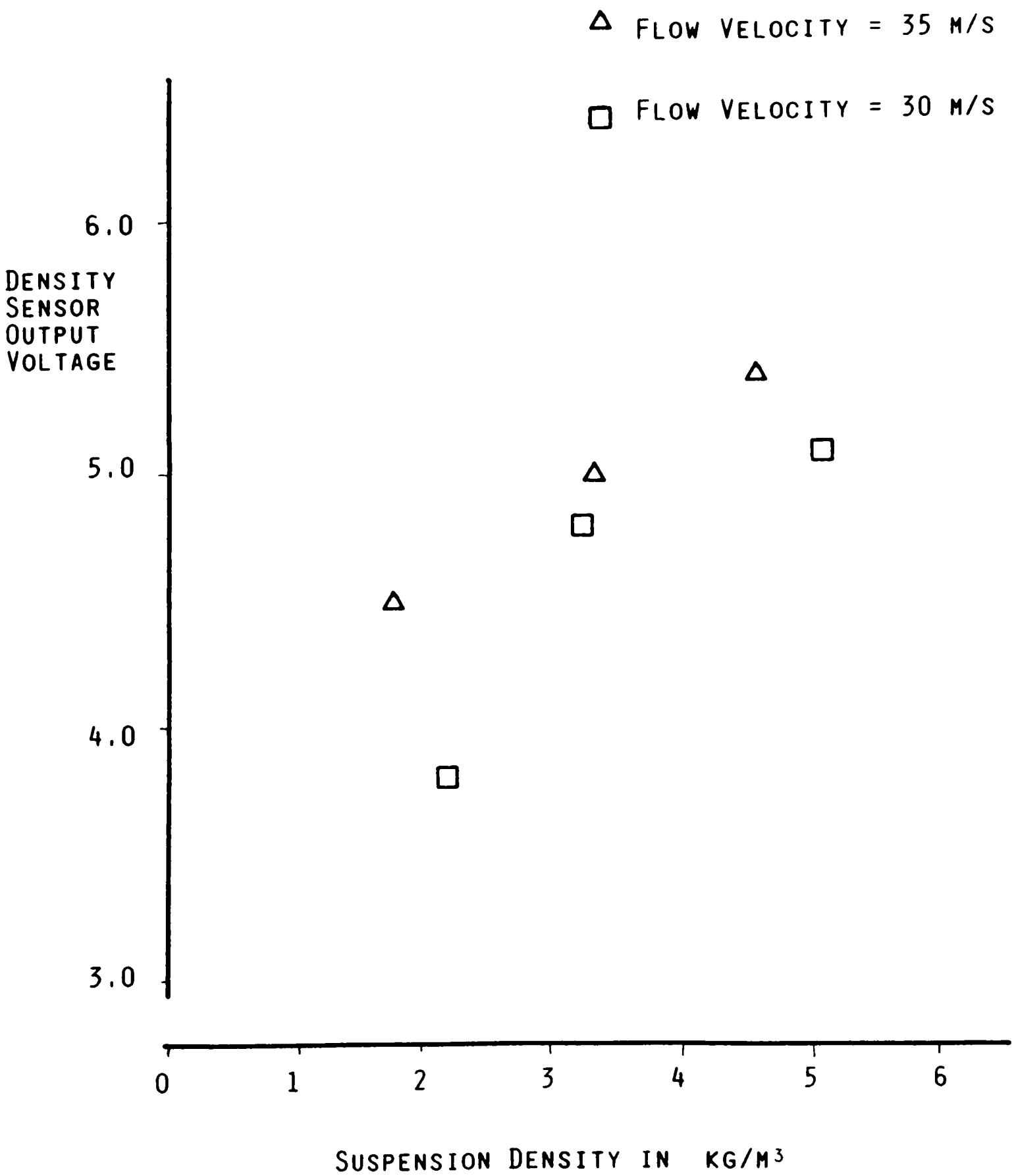

Figure 2.8 Graph Showing Results Reported by Woodhead et al [B16]

results of tests carried out to evaluate the air and/or particle velocities inside the pipelines of pneumatic conveying systems. In all of the references cited, laser doppler velocimetry instrumentation was used.

2.3.1 Tsuji and Morikawa

The literature survey identified a single paper by Tsuji and Morikawa[C1], published in 1982. This paper details tests carried out to measure the velocity of both the air and particles in a pneumatic conveying system simultaneously using laser doppler velocimetry.

Tests were carried out using plastic pellets of 3.4mm and 200μm mean particle size. The most comprehensive results are given for the 200μm particles, showing that the particle velocity is generally slightly below the air velocity for all conditions tested.

Figures for average velocities are not given and so it is not possible to make any accurate estimation of the particle slip velocities.

2.4.2 Riethmuller and Ginoux

The literature survey identified a single paper by Riethmuller and Ginoux. This[C2] reports tests carried out to measure the velocity of solid particles in a pneumatic conveyor. Although the paper states that the test facility is capable of operating over a very wide range of conveying velocities from 2 to 100m/s, and with suspension densities up to 6kg/m^3, only a small number of experimentally obtained data points are presented. The results quoted indicate that the difference between the air and particle velocities is approximately 12m/s for a gas velocity of around 20m/s. These tests were carried out with glass beads of mean particle size 500μm at suspension densities in the region of 1.0kg/m^3.

2.4.3 Birchenough and Mason

Two references by Birchenough and Mason were identified by the literature survey. These were published between 1975 and 1977.

The first paper by Birchenough and Mason[C3], reports the results of experimental tests carried out to measure the average particle velocity of alumina powder in a pneumatic conveying duct. The powder had a mean particle size of approximately 21μm, and was conveyed over a range of conveying air velocities between 16.8 and 56m/s. The tests were also carried out over a range of suspension densities between 0.226 and 2.26kg/m^3. A pipeline of 49mm bore was used.

Values of particle slip between 1 and 20% of actual air velocity were reported, with the slip increasing with both increasing air velocity and increasing suspension density.

A comparison was also made between two different methods for obtaining the average particle velocity:

1. Particle velocity profiles were obtained by traversing the laser doppler velocimetry system across the pipeline cross section using a small sample volume. The average particle velocity was then obtained from this data by integration (the exact method is not given).

2. A large sample volume was used to interrogate the whole pipeline cross section simultaneously and the average doppler frequency taken.

Results obtained by both methods were found to be within 2.8% overall.

The second paper by Birchenough and Mason[C4] reports the results of tests carried out to measure the velocities of particles close to the pipeline wall when being conveyed vertically upwards in a pneumatic conveying system.

The results are of no direct relevance to the programme of work reported in this thesis, since only velocities close to the pipeline wall were measured. However, the results are of indirect interest, since they give some insight into the minimum air velocity required

to convey the particles.

2.5 Other Techniques Based on Cross Correlation

A number of authors have published work which proposes and/or reports the use of cross correlation techniques to measure the velocity of flows. The work of authors which have utilised electrostatic type sensors has already been discussed in Section 2.2. The work of authors using other types of sensors in conjunction with cross correlation techniques will be discussed in this section.

2.5.1 Coulthard and Keech

This paper[D1] reports the development of a multichannel cross correlator for the purposes of flow measurement. The cross correlator is designed to operate with up to six input channels (sensors spaced axially along the pipeline), which is reported to improve the transient response of a velocity meter based around this correlator. The correlator was designed to operate with ultrasonic transducers in pipelines carrying liquid and gas mixtures.

No test results are reported, and so no assessment of the performance of the system may be made.

2.5.2 Beck and Green et al

Seven references by Beck and Green et al were identified by the literature survey, they will be discussed in chronological order.

The first paper[D2] is divided into two parts, and as a consequence, these will be dealt with separately.

The first part proposes a method by which the signals from two capacitive transducers may be cross correlated to yield the average particle velocity in a pneumatic conveyor. The results of some limited tests are also reported, using flour of mean particle size 50μm. The reported average particle velocities were between 0.90 and 0.97 of the air

velocity. Unfortunately insufficient information is given to allow the suspension densities under which these tests were carried out to be calculated.

The second part of the paper proposes a method by which a single capacitive transducer may be used to evaluate the density of the suspension flowing inside a pneumatic conveyor. Again, the results of very limited tests are reported, but they do indicate a sensor response which is close to linear for three conveyed materials namely, flour, wheat and beans. Unfortunately, once again insufficient information is given to enable the exact test conditions to be calculated.

The second paper[D3] contains much of the same information as the first, but goes on to propose a technique by which conductivity sensors may be used in slurry pipelines in much the same way as it is proposed that capacitive sensors are used in pneumatic conveyors. Once again limited test results are reported.

The third paper[D4] proposes the use of a microprocessor based cross correlator in place of the analogue hardware or mainframe digital techniques previously reported. This new proposal is reported to result in a very considerable reduction in the capital cost of the equipment. No test results are reported.

The fourth paper[D5], by Green et al proposes the use of sensors based on the capacitive type sensors in conjunction with cross correlation signal processing, as described in previous papers. The application is in 370mm diameter pulverised coal injection line. Details of the design and construction of such a system are reported. The results of very limited tests are reported, using 4mm polyethylene chips. It is somewhat unclear as to weather these tests were carried out in the 370mm duct, or in some other system. No tests are reported with pulverised coal. This is somewhat disappointing, since the description of the proposed system was comprehensive, and yet the results of tests using pulverised coal are not quoted.

The fifth paper[D6] proposes the application of cross correlation flow measurement

techniques to a number of flow measurement problems. No new techniques which may be applied to pulverised fuel injection systems or pneumatic injection systems in general are reported.

The sixth and final paper[D7] identified by the literature survey published by Beck et al proposes the incorporation of a cross correlation based particle velocity measurement instrument in a closed loop control system to control the particle velocity in a pneumatic conveying system.

Tests were carried out in a 75mm bore pneumatic conveyor, at particle velocities of around 10m/s and suspension densities of around 5kg/m^3. The limited data reported indicates that the performance of the control system is encouraging.

Beck also published a book[G5] with Plaskowski in 1987, however, this contains little information which had not already been published in the papers discussed above.

2.5.3 Mesch and Kipphan

This paper[D8] proposes the use of both capacitive and optical sensors in conjunction with a cross correlation signal processor to determine average particle velocity in a pneumatic conveyor.

Test results are reported in the form of cross correlation functions for various flow conditions using both sensors. Although these are of indirect interest, the tests were carried out at suspension densities which were far below those under investigation in the programme of work reported in this thesis. Detailed analysis of the reported results was not therefore undertaken.

2.5.4 Boeck

Two papers by Boeck were identified by the literature survey. These will be dealt with in chronological order.

Boeck's first paper[D9] proposes the application of capacitive type transducers in conjunction with cross correlation signal processing to evaluate particle velocity. The measurement of suspension density is also proposed using a single capacitive transducer. No experimental test results are reported. These proposals are very similar to those of Beck and Green et al, whose work is not cited by Boeck in this paper despite the fact that their work predates his by some 15 years.

Boeck's second paper[D10] initially describes the principles of the cross correlation signal processing technique. It then goes on to describe the design and construction of a microprocessor based cross correlator. A number of sensors are then proposed for use with the cross correlator for flow measurement. These are based on optical, capacitive, ultrasonic and microwave techniques.

Of the above list, it is proposed that optical and capacitive type sensors are applicable to measurement of both velocity (using cross correlation) and suspension density in pneumatic conveying systems. The results of limited tests in a 250mm diameter pipeline are reported for both types of sensor.

At low suspension densities, below approximately 0.5kg/m^3 the system incorporating the optical type sensors gave an output of mass flow rate which follows the rotational speed of the feeder, and therefore the approximate solids mass flow rate, well. However frequent calibration was needed because of the variable nature of the optical properties of the particles upon which the measurement technique depends. Problems were also encountered with wear and 'fogging' of the optical windows in the pipeline walls. No results are given for suspension densities above 0.5kg/m^3. This makes the applicability of the technique questionable, since the majority of PF injection systems in industry tend to operate at suspension densities between 1.0 and 5.0kg/m^3.

Experimental test results are also reported for the measurement system incorporating capacitive type sensors. These tests were carried out at suspension densities above 1.0kg/m^3. Again, the output of the measurement system follows the actual mass flow

rate measured by a loss in weight feeder, it is however difficult to assess the accuracy of the system.

Much of the work reported by Boeck in both of his papers is very similar to that of Beck and Green et al and that of Mesch and Kipphan, all of whom published their work some 15 years prior to Boeck. Boeck cites both of these other groups in his second paper, and so must have been aware of this work.

2.5.5 Midttveit and de Silva

A single paper by Midttveit and de Silva[D11] was identified as being relevant to the work reported in this thesis.

Midttveit and de Silva report the results of a series of tests carried out to evaluate the performance of a mass flow rate meter of the type described by Boeck. The results of tests are reported for a number of different sensor positions within a pilot scale test facility pipeline, both vertical and horizontal.

Throughout the reported results there is a significant discrepancy in the value of the average particle velocity, this commonly being of the order of 30% of the air velocity. Middttveit and de Silva comment that these values are difficult to believe, and concede that the sensor readings are unreliable. A possible source of the error being cited as stratification of the flow.

This paper is clearly of interest, since it reports the results of actual tests carried out in a pilot scale test rig. However, the usefulness of the results is brought into serious question by the particle velocity measurements.

2.5.6 Work Carried Out by the Author

Having reviewed the work of other authors as discussed above, it was considered that the use of capacitive type suspension density sensors in combination with cross correlation signal processing techniques had some potential as a means of measuring

the mass flow rate of PF in a pneumatic injection system.

It was therefore decided to undertake an initial evaluation of such a sensing system. The system, very similar in design to that of Beck and Green et al was installed in a pneumatic conveying test plant, and a number of tests carried out using PF having a mean particle size of approximately 80μm. The tests were carried out using conveying air velocities in the region of 25m/s and suspension densities between 1.0 and 10.0kg/m^3. A 53mm bore pipeline was used.

The output voltage from the suspension density sensor was not at all stable under stable flow conditions in the pipeline. The correlation between the sensor output voltage and the actual suspension density was very poor, and for much of the range of test conditions the output voltage was off of the top of the sensor scale for all reasonable values of sensor gain and zero offset.

The cross correlation velocity meter was not able to provide a sensible velocity reading. The readings obtained bore no resemblance to the estimated actual particle velocity, with errors of 100% and more being shown. The velocity reading was also very unstable and on some occasions went off the top of the scale for no apparent reason.

Following this somewhat disappointing performance, a fault within the measurement system was suspected. The manufacturers of the system were contacted and offered some advice with respect to fault finding and sub system testing. No faults were found. The performance of the sensing system did not improve during a further programme of tests, and so given this adverse experience, further testing with this system was abandoned.

2.6 Techniques Based on Ionising Radiation

The work of a number of authors is examined in this section. All of the work discussed proposes or reports the use of the attenuation of ionising radiation to measure

the density of the flowing suspension in a pneumatic conveying system. The basic principle of this technique is explained in Section 2.1.1. A transit time technique utilising radioactive tracer particles is also discussed.

2.6.1 Howard

A single paper by Howard was identified by the literature survey.

This paper[E1] reports the results of tests carried out using an ionising radiation attenuation technique to evaluate the concentration of pulverised coal in a 660mm diameter PF injection pipeline. Strontium-90 β-particle sources were used.

The detector and source arrangement is shown in Figure 2.9, three sources and a single scintillation counter being used. Nylon windows were utilised in the pipeline wall to allow the passage of the β-particles.

The sensor is reported as having been tested on a power station installation. However no comparisons are given of the sensor reading against actual suspension density. It is not therefore possible to make any assessment of the potential accuracy of such a technique.

Howard also reports the results of tests carried out using a microwave technique to evaluate both particle velocity and suspension density. It is emphasised that this technique was in the early stages of development, and that certain problems with wear of the sensors incorporated into the walls of pipeline bends had been experienced. Although limited test results are reported, because of the practical problems reported by Howard, a detailed analysis of these was not considered necessary.

2.6.2 Parkinson and Hiorns

A single paper by Parkinson and Hiorns was identified as being relevant to the work reported in this thesis.

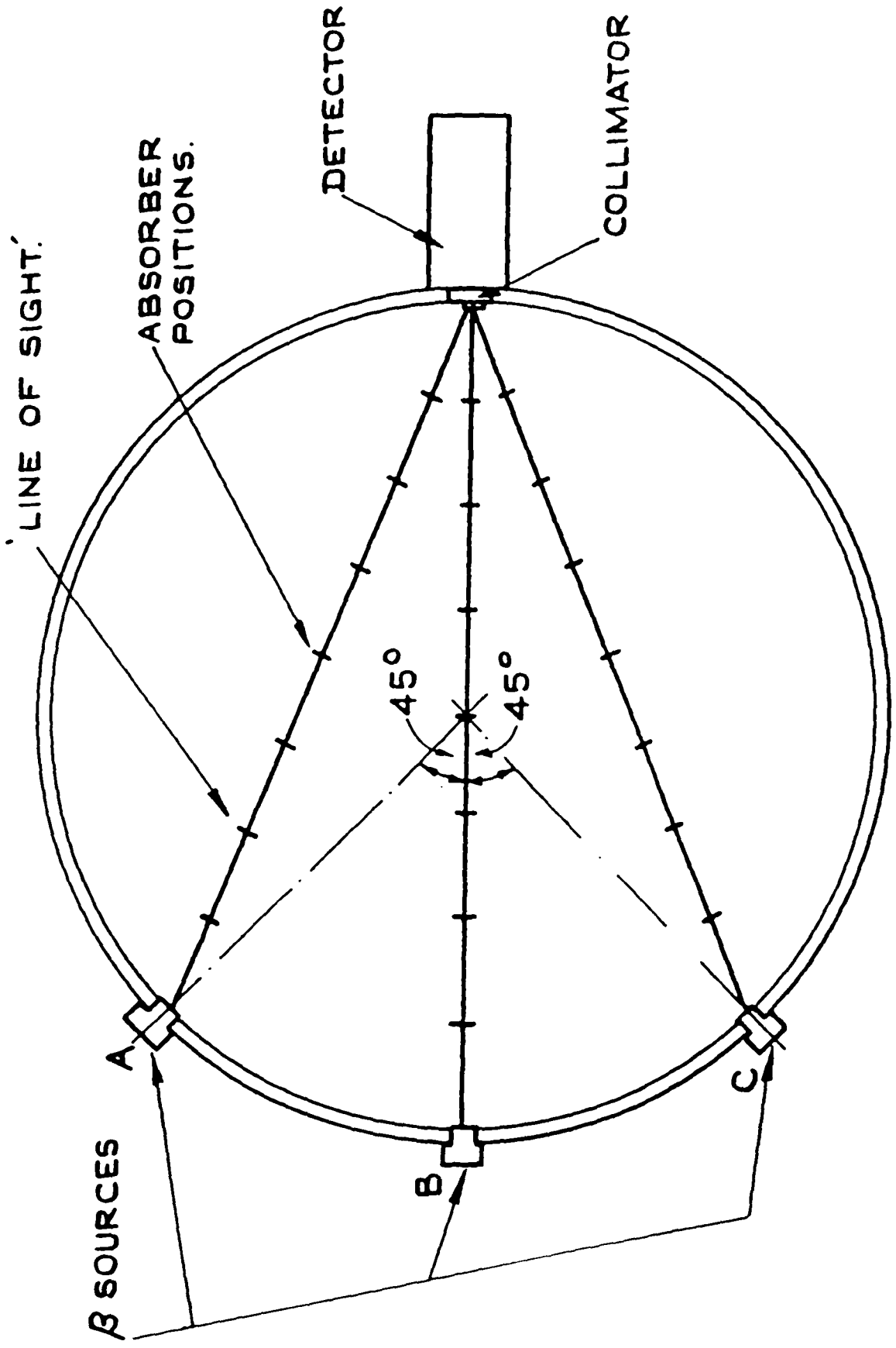

Figure 2.9 Source and Detector Arrangement as Reported by Howard[E1]

Parkinson and Hiorns[E2] describes the design and construction of an ionising radiation attenuation type suspension density sensor. An ultrasonic transit time velocity measurement sensor is also detailed.

The design of the β-particle meter is very similar to that of Howard, with the exception that only a single strontium-90 source was used. The very limited test results indicate that the meter gave readings which were in close agreement with those obtained by another method (few details of which were given). The work of Parkinson and Hiorns is cited by Howard. No experimental results are reported for the velocity meter.

2.6.3 Hours and Chen

A single paper by Hours and Chen[E3] was identified by the literature survey.

This paper may usefully be divided into two sections. The first deals with the measurement of average particle velocity by means of a tracer particle method. The second part deals with the measurement of suspension by a ionising radiation attenuation method. The parts will be dealt with in order.

Hours and Chen describe a technique by which a small quantity of radioactive tracer particles are introduced into a pneumatic conveying pipeline. Indium 113 or gold 198 γ-ray emitting isotopes were used with half lives of 100 minutes and 2.7 days respectively. Activities of 0.2-0.3mcuries were used.

The reported results give the particle velocities as between 0.5 and 0.8 that of the air for a range of air velocities between 15 and 20m/s, and suspension densities around 5.0kg/m^3. The main drawback of the technique was that the apparatus had to be left to "cool" for up to 7 half lives before it could be worked on after a test - clearly this causes problems with the Gold isotope. It also seems to the author of this thesis that significant hazards exist should a leak occur in the conveying system, and therefore its use is limited to obtaining information in test facilities in laboratory environments.

The second part of this paper describes the construction of a radiation attenuation suspension density meter, once again based on β-particles. No experimental results are reported. The layout of the sensor is very similar to that of Parkinson and Hiorns whose work is not cited by Hours and Chen despite the fact that it predates the latter by some seven years. The work of Hours and Chen is not cited by Howard.

2.6.4 Work Carried Out By the Author

Having reviewed the work of other authors as discussed above, it was considered that the application of a suspension density sensor based upon the ionising radiation attenuation principle to PF injection systems was worthy of further investigation. No sensor of this type was available commercially, and so a feasibility study into the design, construction and testing of such a sensor was undertaken.

Two important points arose from this study:

1. There was found to be a certain amount of opposition to the use of radioactive isotopes in industry as a whole, largely as a result of anxiety expressed by the workforce regarding the safety of such equipment.

2. During some consultations with other workers in this field[G7], the suggestion was made that the use of an X-ray source may be more appropriate than the use of β-particle emitting isotopes.There were two reasons for this:

   Firstly, by employing an X-ray source with variable target voltage and current, the photon energy and intensity of the X-rays could be varied over a wide range and thus optimised. This should result in a more accurate instrument.

   Secondly, the use of an X-ray source would allow the ionising radiation source to be safely disabled, simply be shutting down the power supply. This would go some way towards allaying the concerns of employees servicing the

equipment, and thus lessen the opposition encountered in industry.

It was therefore decided to pursue the design, construction and evaluation of a suspension density sensor based upon the attenuation of X-rays.

A number of bench tests were carried out by the author to evaluate the feasibility and potential accuracy of such an instrument. These are detailed below.

The layout of the bench scale test apparatus is shown in Figure 2.10. A section of 18mm thick oak, along with a 0.7mm thick sheet of aluminium were used to simulate the combined window material. This corresponds to a total mass per unit area of 14.5kg/m^2, which in turn corresponds to 1.9mm of mild steel, thus allowing 0.95mm of mild steel per window. It was considered that this was enough to allow windows to be constructed from a suitable material.

A sheet of aluminium having a mass per unit area of 0.05kg/m^2 was used to simulate the solids phase in the pipeline. This corresponds to a suspension density of 0.85, which is at the low end of the conditions normally experienced in PF injection systems, thereby providing a worst case suspension density on which to base the tests. Four tests were carried out, and the results are shown in Table 2.1 below.

Test No.	Target Voltage (kv)	Target Current (μA)	Counter Output Without Solids (MHz)	Counter Output With Solids (MHz)	Diff. in Freq. (kHz)	Useable Accuracy (Khz)	Useable Accuracy ($\pm$%)
1	20	40	2.8866	2.8104	76.2	3.39	4.5
2	20	100	5.7584	5.6304	128.0	4.80	3.8
3	25	10	3.7872	3.7194	67.8	3.89	5.7
4	25	30	7.1889	7.0952	93.7	5.36	5.7

Table 2.1. Initial evaluation of X-ray Sensor - Results Summary

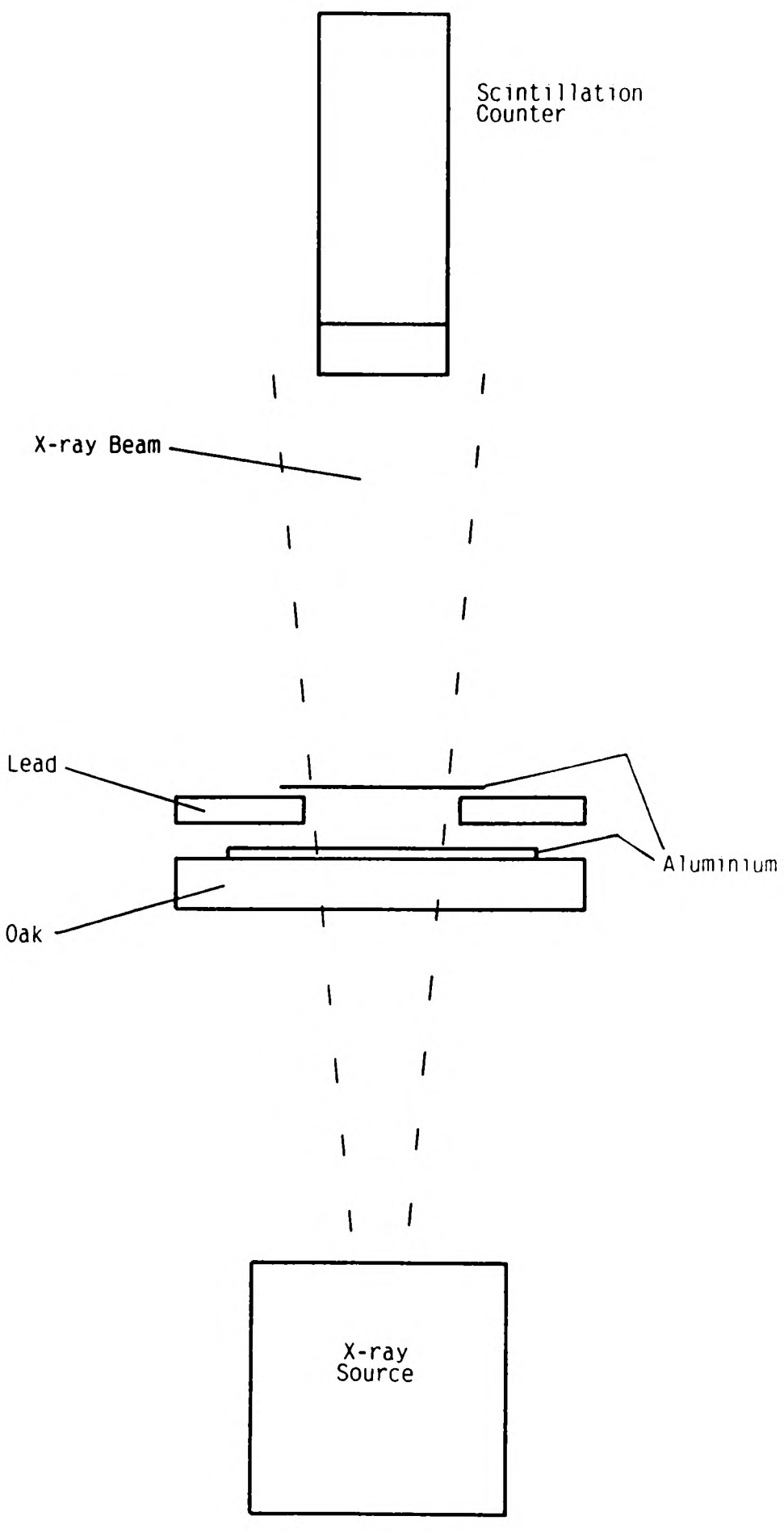

Figure 2.10 Layout of Bench Scale Test Equipment

The output frequency of the scintillation counter was recorded for a number of X-ray source settings, with, and without the simulated solids phase present. For each setting of the X-ray source, the two frequencies were then subtracted to give the difference in frequency. On the basis that, for the high count rates used, the standard deviation of the scintillation counter frequency counts could be taken as the square root of the actual count[1], the accuracy of the frequency counts was calculated. The percentage accuracy of the sensor was then calculated.

Table 2.1 shows that the achievable accuracies were generally in the range ± 3 to $\pm 6\%$. It was considered at that time that with some additional refinement, the achievable accuracy of an on line instrument could well be of the order of ± 1 to $\pm 2\%$. Thus, the application of such a sensor to the measurement problem under investigation seemed technically feasible.

The financial feasibility of the design of an on line sensor based upon this principle was next considered. It was estimated that the cost of the design, construction and initial on line testing of such a sensor would probably be in the region of £150k Sterling (1989 prices). Clearly this is a significant sum, which was not readily available at that time, and so the programme of designing such a sensor was deferred until a time when such funds become available.

2.7 Conclusions of the Review

The work of a large number of authors was reviewed. This resulted in the identification of a number of potential techniques which might be applied to mass flow rate measurement in coal injection systems. Other techniques were eliminated at this stage, since they were not considered to be worthy of further examination.

The techniques which were considered to be worthy of further investigation at this stage were as follows:

---

[1] This is an approximate evaluation which seems to be accepted. It was considered to be adequate for the purpose, since the study under discussion was only intended as an initial feasibility study.

1. The electrostatic technique for suspension density measurement and velocity measurement in conjunction with a cross correlator. Four particular authors have proposed the use of this type of instrumentation for this or similar applications, namely Dechene and Averdieck, King, Klinzing et al and Shackleton. The author of this work has also carried out limited trials of such a system, the results of which indicated that it was worthy of further study.

2. The laser doppler velocimetry technique for average particle velocity measurement. It was considered that this technique, although because of it's complex and delicate nature confined to closely controlled environments such as research laboratories, could be a valuable tool, in that it provided a technique by which the average particle velocity could be definitively measured to a good degree of accuracy. Thus, if incorporated into a test plant, the average particle velocities so derived could be used as calibration standards against which other meters could be assessed.

3. The evaluation of the average particle velocity by measurement of the conveying air velocity and estimation of the average particle slip. This technique had not been proposed by other authors, but was considered to be worthy of further investigation in this study.

The techniques which were rejected at this stage are as follows:

1. Intrusive techniques derived from single phase fluid flow rate measurement techniques. The shortcomings of instruments based on these principles are essentially that they suffer from wear due to the abrasive nature of the PF and their intrusive nature. Duct blockages were also a problem. These problems have consequently resulted in this thesis being focused on instruments of a non-intrusive nature. It is also apparent that no work has been published in this area for some 20 years and therefore seems to the author of this work that the community generally seems to have reached a similar conclusion.

2. The capacitive technique for suspension density measurement and velocity measurement in conjunction with cross correlation signal processing. Although a number of authors have proposed the use of this technique for the application under investigation and similar applications, there is a singular lack of test data for such a technique in this application. The experiences of the author of this work, although possibly due to less than perfect equipment, were also not encouraging. It was therefore decided not to investigate this technique any further at this stage.

3. The optical technique proposed by Boeck and Mesch and Kipphan. This technique was not considered feasible since it was considered that a system applied to PF injection systems would be highly sensitive to abrasion and 'fogging' of the optical windows. The only test data for this technique was limited to suspension densities below 0.5kg/m^3, due to the fact that the light was not able to penetrate suspensions of greater density. This, in the light of the fact that most PF injection systems operate at suspension densities between 1.0 and 5.0kg/m^3, also contributed to the decision not to pursue further investigation of this technique.

4. The ionising radiation attenuation technique. The cost of designing, constructing and testing a sensor based on this principle resulted in a decision being made not to pursue instruments based on this method further.

The review of the work of other authors also indicated that there was a considerable lack of reliable test data. In particular there was very little test data for systems applied to PF injection systems, despite the fact that this is an important application for such technology.

Of the small amount of test data published, the quality of the data was generally very poor. Where the results of tests of suspension density sensors were reported, they

were often calibrated against the speed of the solids feeder, or not at all, giving poor quality test results. Where the results of tests of velocity sensors were reported, these were not compared with actual average particle velocities obtained by any other method. Thus, it was not usually possible to make any accurate assessment of the performance of such sensing systems.

It was considered that this lack of good quality test data could be due to two factors:

1. Lack of availability of suitable test plants. The cost of designing and constructing even a small pilot scale test plant is probably large in comparison with the cost of developing a sensing system. Thus, the availability of such plants to the academic community, which is the source of most of the publications reviewed, is probably, at best, very limited. In reality, in many cases the availability of such a facility will be reliant on the cooperation of a sympathetic industrial organisation, who may make a plant available for a limited period for such trials.

2. Inadequate test plant instrumentation. As already discussed, in many cases the test plant will not be fully under the control of the researcher, and so it will probably not be sufficiently well instrumented to allow the exact conditions inside the pipeline to be determined. Most industrial pneumatic conveying plants, for economic reasons, have very little instrumentation. Indeed, this is usually confined to the bare minimum required for normal operation, and are thus somewhat inadequate for research work.

As a direct result of the foregoing, a decision was made to design and construct a fully instrumented pilot scale test plant for the purposes of evaluating such sensors. It was considered that this was essential in order to obtain a reliable set of test data upon which the applicability and accuracy of a flow meter could be judged. This process is described in Chapter 3.

The measurement techniques which were considered to be worthy of further investigation, as outlined above would then undergo comprehensive evaluation in the test facility. The tests undertaken and the results obtained are then described in Chapters 4 to 7.

Chapter 3 The Design and Development of the Test Facility

3.0 Introduction to the Test Facility

In order to evaluate the measurement techniques under investigation, it was necessacary to develop a suitable facility in which such work could be carried out. A system was needed which could convey PF pneumatically under a range of conditions similar to those commonly found in PF injection systems.

It was also most important for the test facility to be fully instrumented, in order that the flow rates of both the air and coal could be determined with a sufficient degree of accuracy. It was considered that this had been a major problem in the development of such instrumentation. A number of meters have been proposed, as detailed in Chapter 2. However, very few results have been published of tests carried out in instrumented test facilities, where an accurate calibration can be carried out against known operating conditions.

The test facility was developed and built specifically for this programme of work. With the exception of the design of the main air control sub-system, which is similar to a system originally designed by Bradley[G1], the entire test facility was designed and developed by the author. The test facility forms an integrated system made up from a number of sub-systems. In order to describe the design and development of the complete facility, it will be broken down into the various sub-systems, each of which will be described separately. The following sub-system classifications will be used:

- PF Storage Hopper and Filter
- PF Feeder
- Air Control
- Test Pipeline
- Data Logger
- Control System
- Computer

A brief overview of the entire facility will be given initially, in order that the reader may appreciate the position of each sub-system with respect to the whole. The design and development of each sub-system will then be presented in detail.

3.1 Overview of Entire Facility

Figure 3.1 shows a block diagram of the various sub-systems, and indicates how they are interconnected. Figure 3.2 shows a photograph of the PF storage and feeder assembly. PF is stored in a hopper, which is located above the PF feeding sub-system, this hopper is mounted on load cells, which are, in turn, connected to the data logging sub-system, thereby allowing the mass flow rate of PF to be determined.

Compressed air is provided by the main laboratory air supply, which is served by three reciprocating compressors. The air mass flow rate is controlled and metered by the air control sub-system, which is interfaced to both the data logging and control sub-systems, allowing the flow rate of air to be controlled and monitored by the operator.

The PF feeder operates in a batch fashion, taking a batch from the PF storage hopper and feeding it into the conveying pipeline. The PF is then conveyed around the pipeline, and returns to the storage hopper. The storage hopper incorporates a filter to disengage the PF from the air, before the air passes to atmosphere outside the building.

The sensor undergoing evaluation is installed in the pipeline and connected to the data logging sub-system. Pressure and temperature sensors are incorporated in the test pipeline adjacent to the sensor, these are also connected to the data logging sub-system.

3.2 PF Storage and Filter Sub-System

3.2.1 Requirements of the PF Storage and Filter Sub-System

This sub-system serves two purposes, that of a storage vessel for the PF and also that of a disengaging device, separating the coal and air after conveying.

The requirements of the sub-system were as follows;

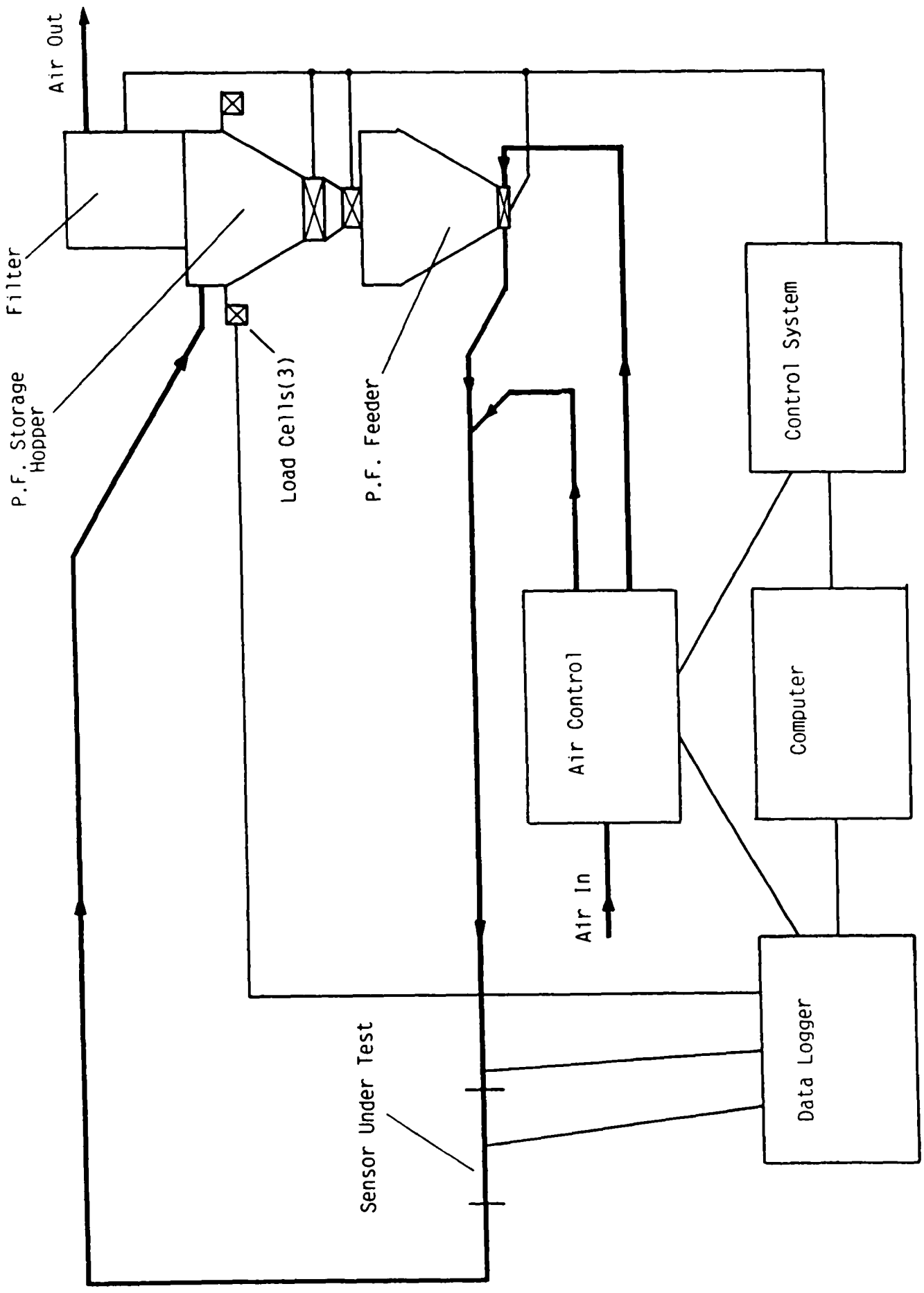

Figure 3.1 Block Diagram of Test Facility

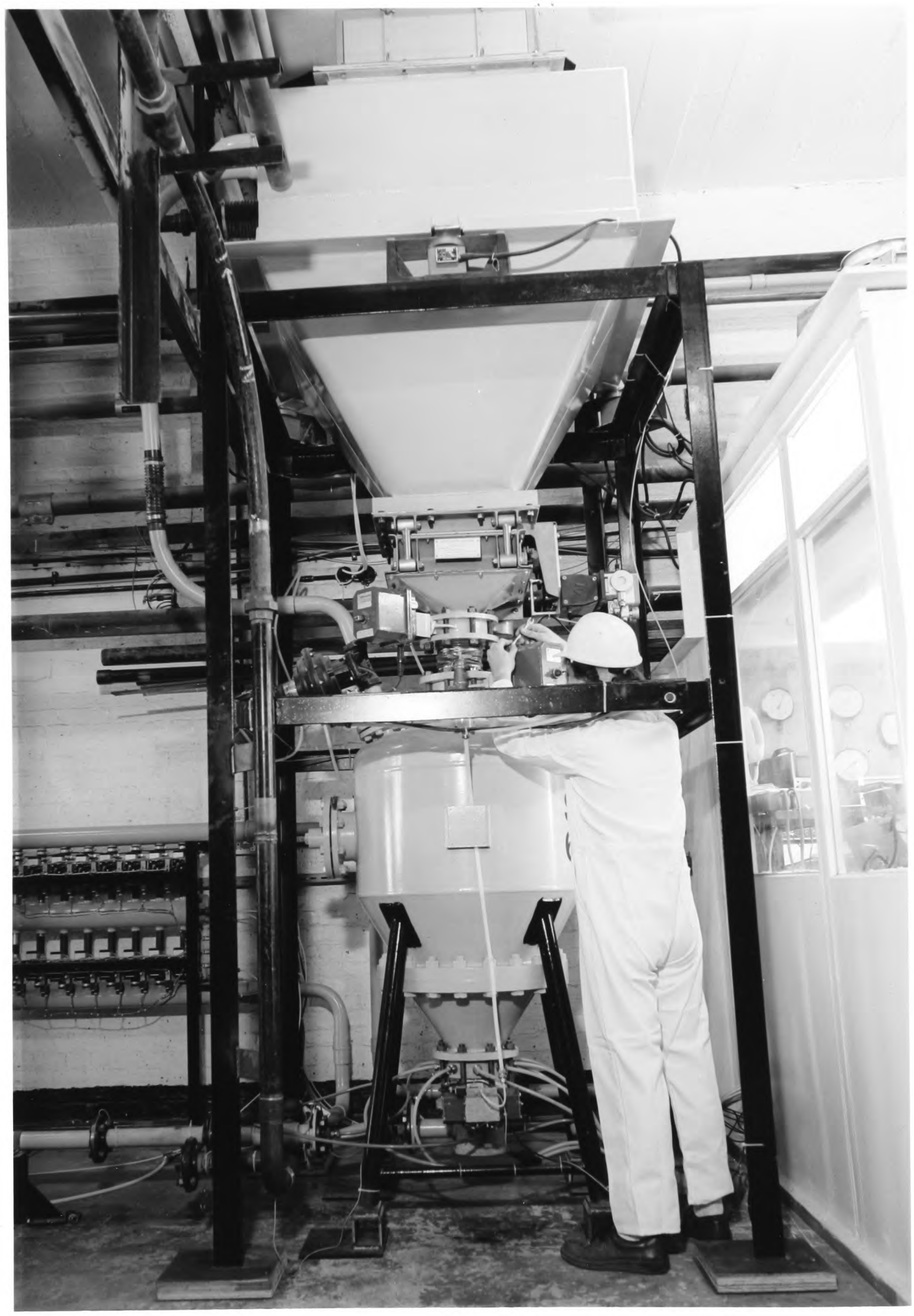

Figure 3.2 Photograph of the PF Storage and and Feeder Assembily

1. To store approximately $0.4m^3$ of PF, having a mass of some 200kg.

2. The completed assembly needed to be mounted above the PF feeder on load cells and within the height available in the laboratory.

3. A filter suitable for filtering $0.15m^3/s$ of the returning coal-air suspension was required above the storage hopper.

4. The hopper discharge needed to incorporate a flow control valve, to control the flow of PF into the feeder.

3.2.2 Specification of the Filter

The required flow rate of the coal-air suspension has already been stated, and a filter suitable for disengaging this amount of suspension was required. The guidelines available[G2], are largely based on experience and give a required maximum air velocity through a woven fabric filter of 0.016m/s, which for the required flow rate gave a required cross section of filter material of $9.38m^2$. A filter of $9.26m^2$ was readily available commercially and so this was chosen.

3.2.3 Design of the PF Storage Hopper

The major problem which needed to be overcome in the design of the main storage hopper was that of the height constraint placed by the building roof. The storage hopper needed to be mounted above the PF feeder, the height of which was fixed. A suitable filter as discussed above, which was also of fixed geometry, was to be installed on top of the hopper. This left the storage hopper height as the only variable.
Following some consultations[G3], it was apparent that a hopper of the geometry dictated would not allow the PF to flow from it reliably under gravity alone. It was therefore decided to incorporate a 'Hogan' type vibratory discharger on the hopper bottom, to aid the flow of the PF into the feeder below.

A hopper of the dictated geometry complete with a suitable discharger were therefore chosen.

3.2.4 Discharge Control Valve Assembly

A suitable discharge control valve was required on the outlet of the hopper, in order to control the flow of PF into the feeder. Two matters needed to be addressed here, firstly, the valve assembly needed to be airtight, since the feeder could be pressurised to 0.5 barg, secondly it was important that none of the weight of the hopper could be coupled to the feeder, since this would prevent the load cells from sensing the correct weight, and thus indicating the correct mass of PF in the hopper.

It was therefore decided to use two valves separated by a flexible tube, thus preventing any weight coupling. Butterfly type valves were used, since these have been shown to be reliable when subject to similar duties in a laboratory environment.

3.2.5 Load Cells and Installation

The hopper, filter, vibratory discharger and discharge valve assembly were installed on a supporting framework on three load cells. The load cells were of a suitable rating to withstand the combined weight of the hopper, filter, vibratory feeder, discharge valve assembly and the maximum weight of PF.

3.3 PF Feeder

3.3.1 Requirements of the Feeder

This sub-system has the purpose of feeding the PF into the conveying pipeline. The requirements of the feeder are as follows:

1. To feed the PF against a pressure of up to 0.5 barg.

2. To provide feed rates in the range 0.001kg/s to 2kg/s.

3. To provide the smoothest possible feed, that is with the minimum of pulsations or variations in the specified feed rate.

Because of the exacting requirements in terms of both feed rate, turndown ratio, and smoothness of feed, it was not considered feasible to use a commercially available

feeder of any of the conventional designs. A combination of two widely used techniques was therefore chosen, and a feeder developed to incorporate these.

3.3.2 Principle and Characteristics of Blow Tank Type Feeder

A typical bottom discharge blow tank feeder is shown in Figure 3.3. With the air supply turned off, the discharge valve closed and the vent line valve open, the tank is charged from above with a batch of material by opening the charging valve. The charging valve is then closed, the vent line valve closed and the tank pressurised using the tank air control valve. The tank discharge valve and the supplementary air control valve are then opened simultaneously and conveying begins. When the batch is exhausted, the air supply is shut off, the discharge valve closed and the vent line opened. The cycle is then repeated.

The upper limit on the pressure to which the blow tank will feed is limited only by the rating of the tank and air supply system. Thus a very wide range of conditions are achievable. The lower limit of feed rate from a blow tank is usually determined by the required stability of the discharge. Blow tanks will operate at low feed rates, but the flow becomes unstable and tends to adopt a pulsating mode of flow.

3.3.3 Principle and Characteristics of Venturi Type Feeder

A typical venturi feeder is shown in Figure 3.4. The pressure in the throat region of the venturi will be below that up or down stream. This reduction in pressure may be utilised to reduce locally the pressure in the pipeline and therefore allow solid material to be introduced.

The upper limit on the pressure to which the venturi will feed is limited by the pressure reduction which may be achieved in the throat section. This may be modelled hydrodynamically by a number of approaches. In practice, the maximum pressure reduction for a practical venturi feeder operating with air is found to be around 0.25 bar. Thus it is not possible to feed to systems operating above this pressure. The lower limit of feed rate from a venturi feeder is sufficiently low as to make it inapplicable in conventional pneumatic conveying systems where the maximum

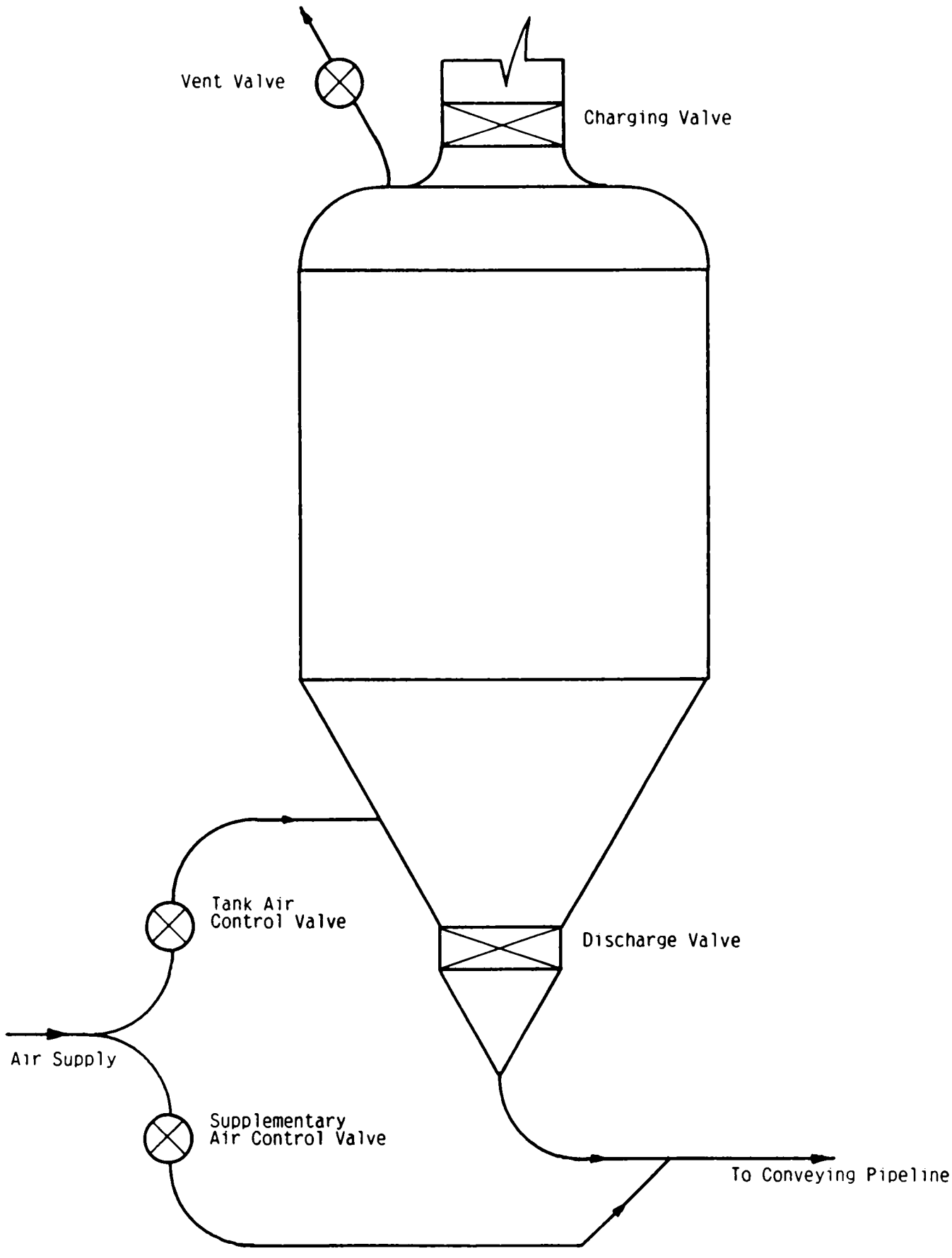

Figure 3.3 Typical Bottom Discharge Blow Tank

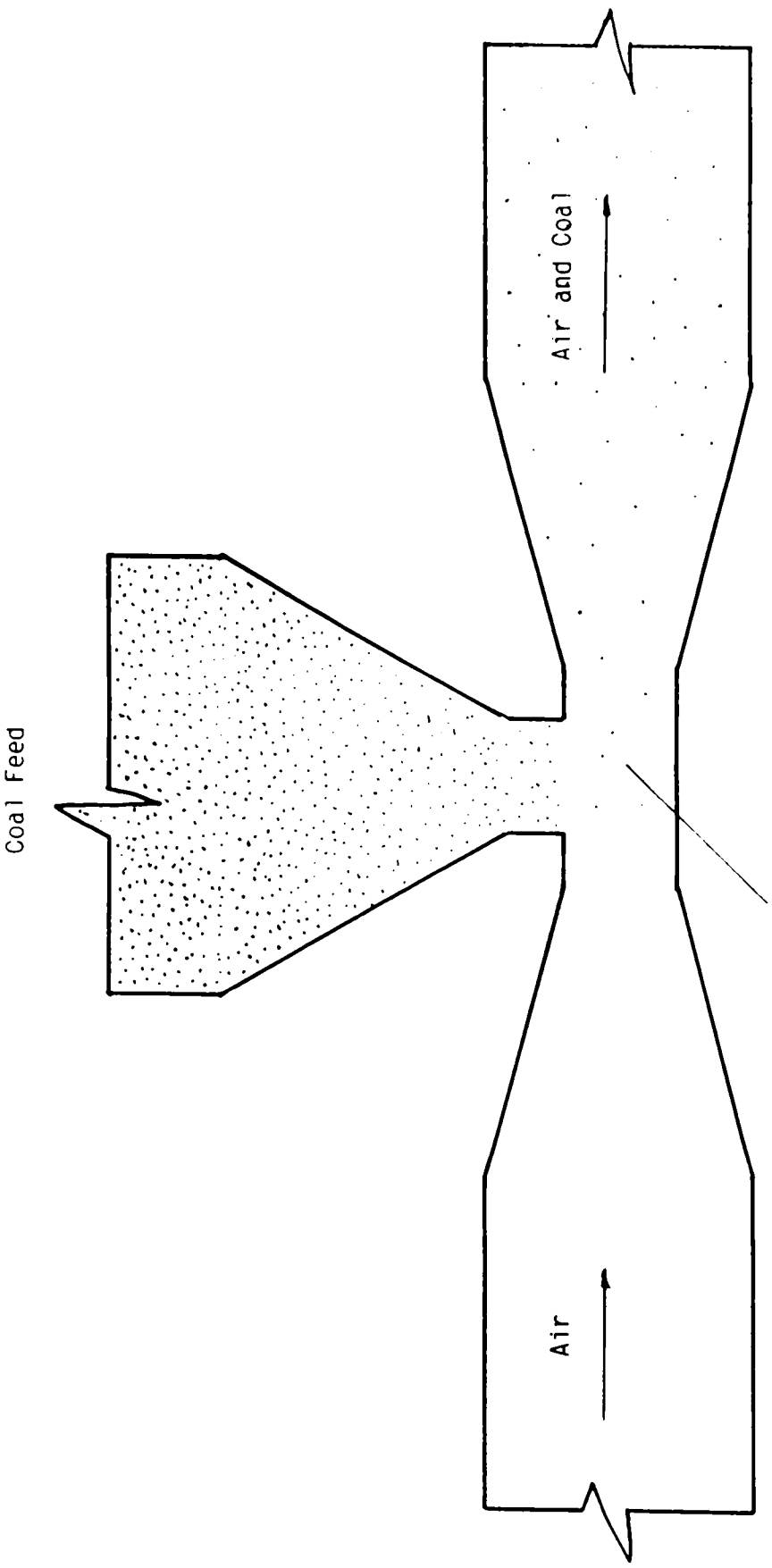

Figure 3.4 Typical Venturi Feeder

throughput for a given plant size is the primary requirement. The stability of the flow from the venturi feeder is very good under most operating conditions.

3.3.4 Principle of Operation of the Test Facility Feeder

A schematic diagram of the test facility feeder is shown in Figure 3.5. It is a combination of a conventional bottom discharge blow tank and a venturi feeder. The philosophy behind this is that the blow tank will allow the feeder to operate at higher pressures than the venturi alone, but at the same time, the stable feeding characteristic of the venturi will be preserved.

At low feed rates, and therefore low suspension densities, the feeder operates purely as a venturi, with some additional air being added after the venturi in order to provide better control over air velocity and suspension density. The venturi and supplementary air flow rates are therefore controlled by the air control sub-system with the blow tank air valve remaining closed and the vent line left open. In this mode of operation, the choking valve in the supplementary air feed line is fully open.

When the test pipeline pressure is required to exceed 0.2 barg., due to higher pipeline pressure drops caused either by high air velocity or high suspension density, a different mode of operation is used. Firstly, the choke valve position is adjusted to give a pressure of approximately 2.0 barg. upstream of the valve. The vent valve is closed, the blow tank air valve opened, and the pressure regulator, which now has 2.0 barg. at the inlet, is set to a low output pressure in the range 0.05-0.3 barg. Air then flows into the blow tank and pressurises it to the specified pressure. The choke valve is required because the pressure regulator has a burden of at least 1.0 bar, which means that the upstream pressure of the regulator must always be at least 1.0 bar above the outlet pressure to maintain regulation.

The venturi then has a lower pressure across it for any given pipeline pressure and is able to operate at pipeline pressures up to 0.5 barg. thereby allowing a wider range of conditions to be achieved than with the standard venturi configuration alone.

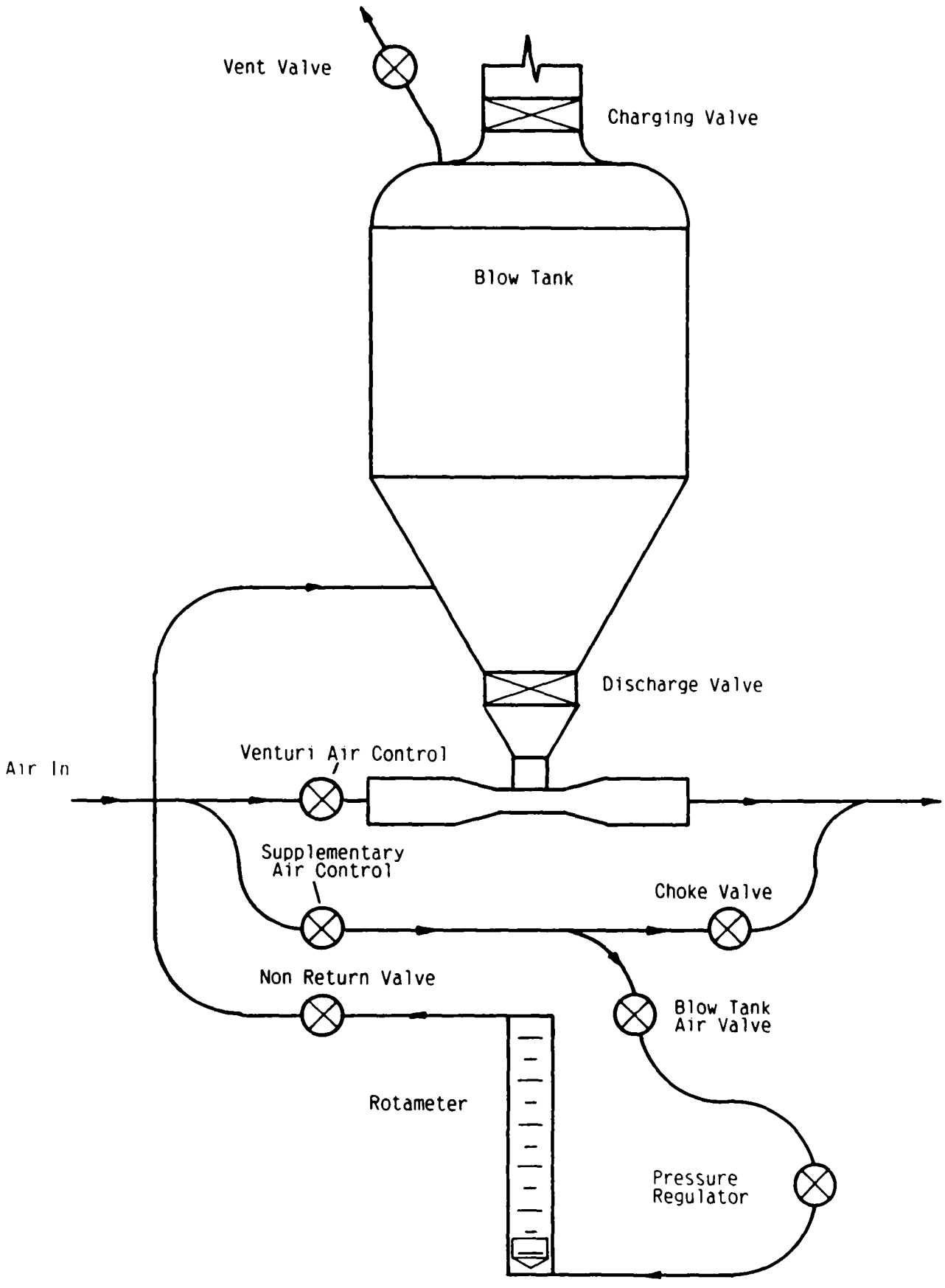

Figure 3.5 Test Facility P.F. Feeder

This type of feeder was installed in the test facility.

3.4 Air Control[1]

3.4.1 Requirements of the Air Control Sub-System

This sub-system has the purpose of controlling and metering the total amount of air supplied to the test pipeline.

The requirements for the air control sub-system are as follows:

1. To meter up to $0.15m^3/s$ of air feeding both the venturi and supplementary feeder input points.

3. To be able to do this by remote control from the control room.

4. To be able to meter the air to an accuracy of $\pm 2\%$ or better.

5. To be able to supply the air at pressures up to 2.5 barg.

3.4.2 Principle of Operation of the Air Control Sub-System

These requirements were achieved using two banks of choked flow nozzles the air feeds to which were individually controlled by pneumatically actuated ball valves. Figure 3.6 shows a photograph of the completed system and Figure 3.7 shows a schematic diagram of a single nozzle and valve assembly. Eight nozzles were used in each bank, arranged in a x2 series, so that nozzle number 2 was of twice the rated flow rate of number 1, number 3 was twice that of number 2 and so on. Thus, a design turndown ratio of 255 to 1 is achievable.

The main laboratory air supply is rated at $0.39m^3/s$ free air at 6 barg. Thus, the volumetric flow rate available is over twice that required. The pressure is reduced to

[1]As previously stated, this sub-system is a direct copy of that developed by Bradley[G1]. A brief description will be included in this text for the purposes of completeness , but the reader is directed to Bradley's work for the definitive description.

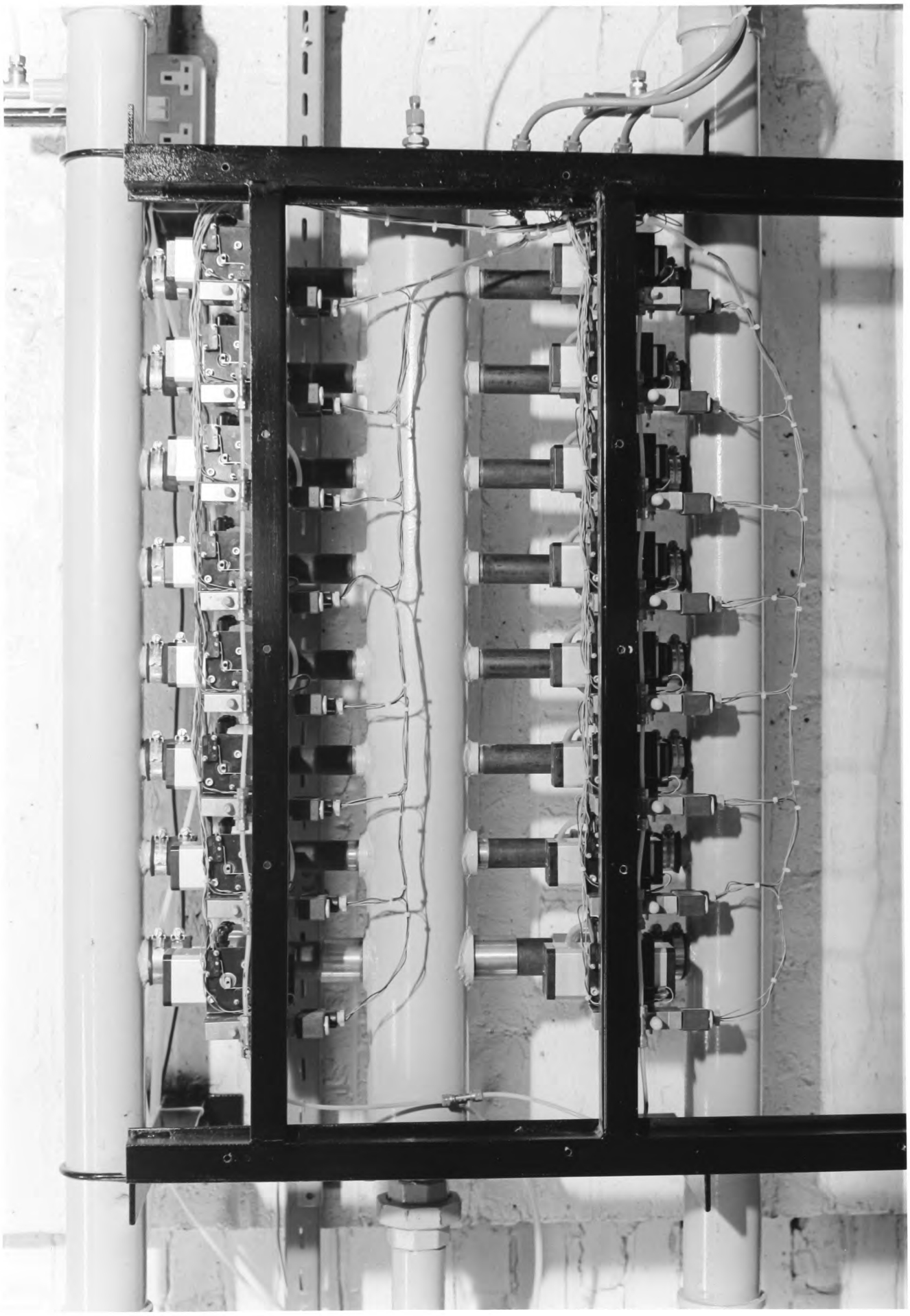

Figure 3.6 Photograph of the Air Control Sub System

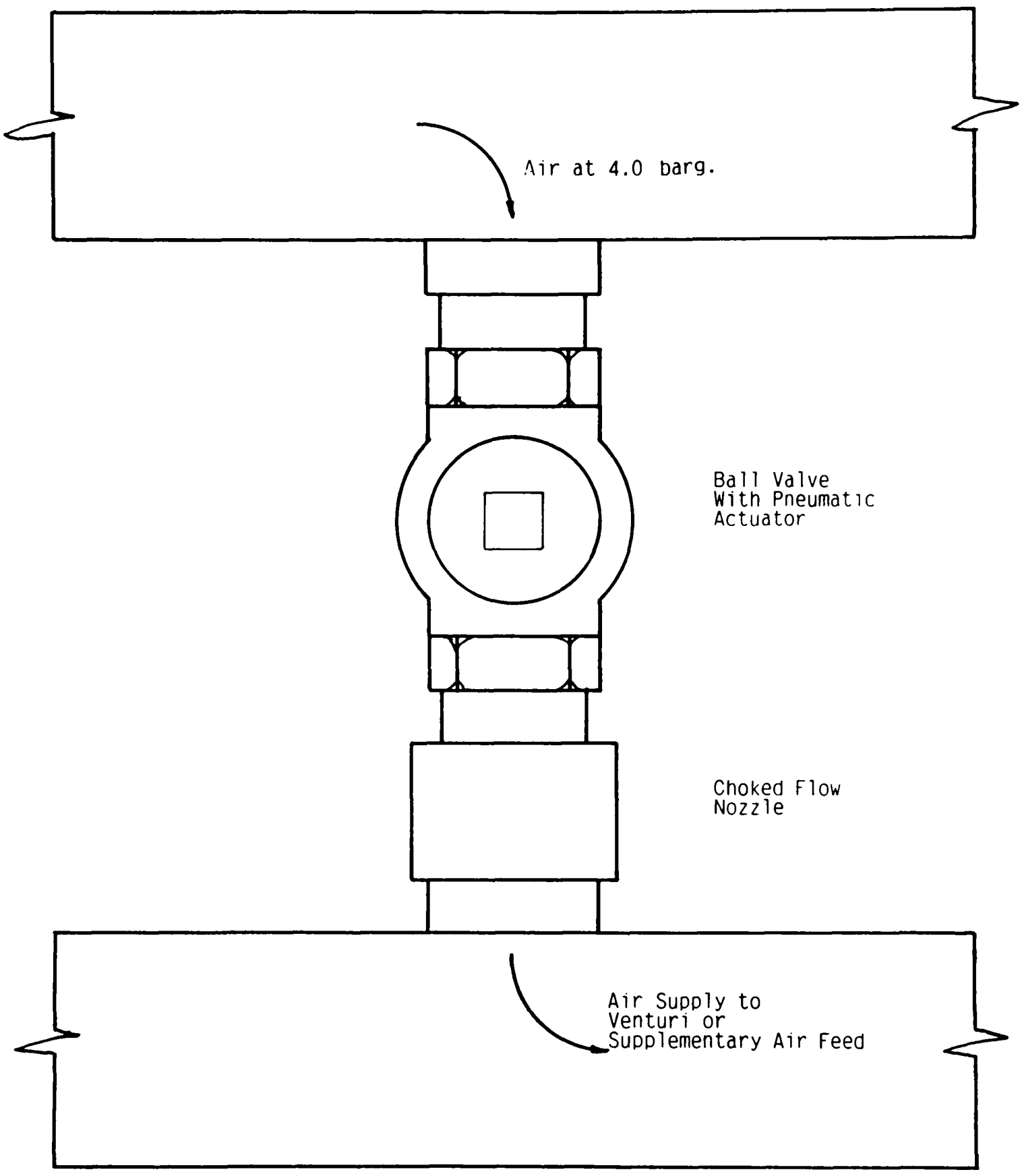

Figure 3.7 Single Nozzle and Valve Assembily

4.0 barg using a suitable pressure regulator situated before the inlet to the nozzle bank. Therefore, with an absolute pressure ratio of 70% across the nozzles, the output pressure could be raised to 2.5 barg without any possibility of the nozzles becoming unchoked.

The pneumatic actuators on each of the ball valves were, in turn, controlled by electrically actuated spool type solenoid valves, which were connected to the control sub-system.

3.4.3 Calibration of the Nozzles

In order to obtain the required flow rate accuracies, it was necessacary to calibrate each nozzle against a standard flow meter. An orifice meter conforming to BS 1042[G4] was chosen for this purpose. Each nozzle was calibrated for a range of downstream pressures, in order to verify the pressure at which the nozzles unchoke and the actual air flow rate. The flow rate for each nozzle for a supply air pressure of 4.0 barg. and supply air temperature of 20°C is given in Table 2.1. The real time data processing software then carries out compensation for any variations from these values.

Nozzle Number	Venturi Nozzle Flow Rate in m^3/s	Supplementary Nozzle Flow Rate in m^3/s
1	0.00155	0.00131
2	0.00260	0.00260
3	0.00503	0.00494
4	0.01060	0.01010
5	0.02030	0.02030
6	0.04010	0.04000
7	0.08000	0.08000
8	0.14900	0.14820

Table 2.1 Mass Flow Rates For Each Nozzle at 4.0 barg. and 20°C.

3.5 Test Pipeline

3.5.1 Requirements of the Test Pipeline

The test pipeline takes the flowing suspension from the feeder and conveys it via the sensor under test to the storage hopper and filter.

The requirements of the test pipeline are as follows:

1. To feed the flowing suspension to the sensor under test with sufficient straight length before the sensor to ensure that the flow has reached a stable condition. This allows the sensor to be evaluated with minimal flow disturbances upstream.

2. During specified tests to feed the flowing suspension to the sensor under test via one or more bends at specified distances from the sensor. This allows the sensitivity of the sensor to flow disturbances upstream to be evaluated.

3.5.2 Layout of the Test Pipeline

Two basic pipeline layouts were adopted, in order to satisfy 1 and 2 above. The configuration of the straight pipeline is shown in Figure 3.8. The configurations of the pipelines used to evaluate the effect of bends upstream of the sensor in a real PF injection system are detailed in Section 6.3.4.

3.6 Data Logging

3.6.1 Requirements of the Data Logging Sub-System

It was decided to use a computer based data logging sub-system, since this would allow data to be collected and processed in real time much more rapidly than if the task were carried out manually.

The requirements of the Data Logging Sub-System were as follows:

1. To be able to log up to 16 channels of various analogue sensor outputs.

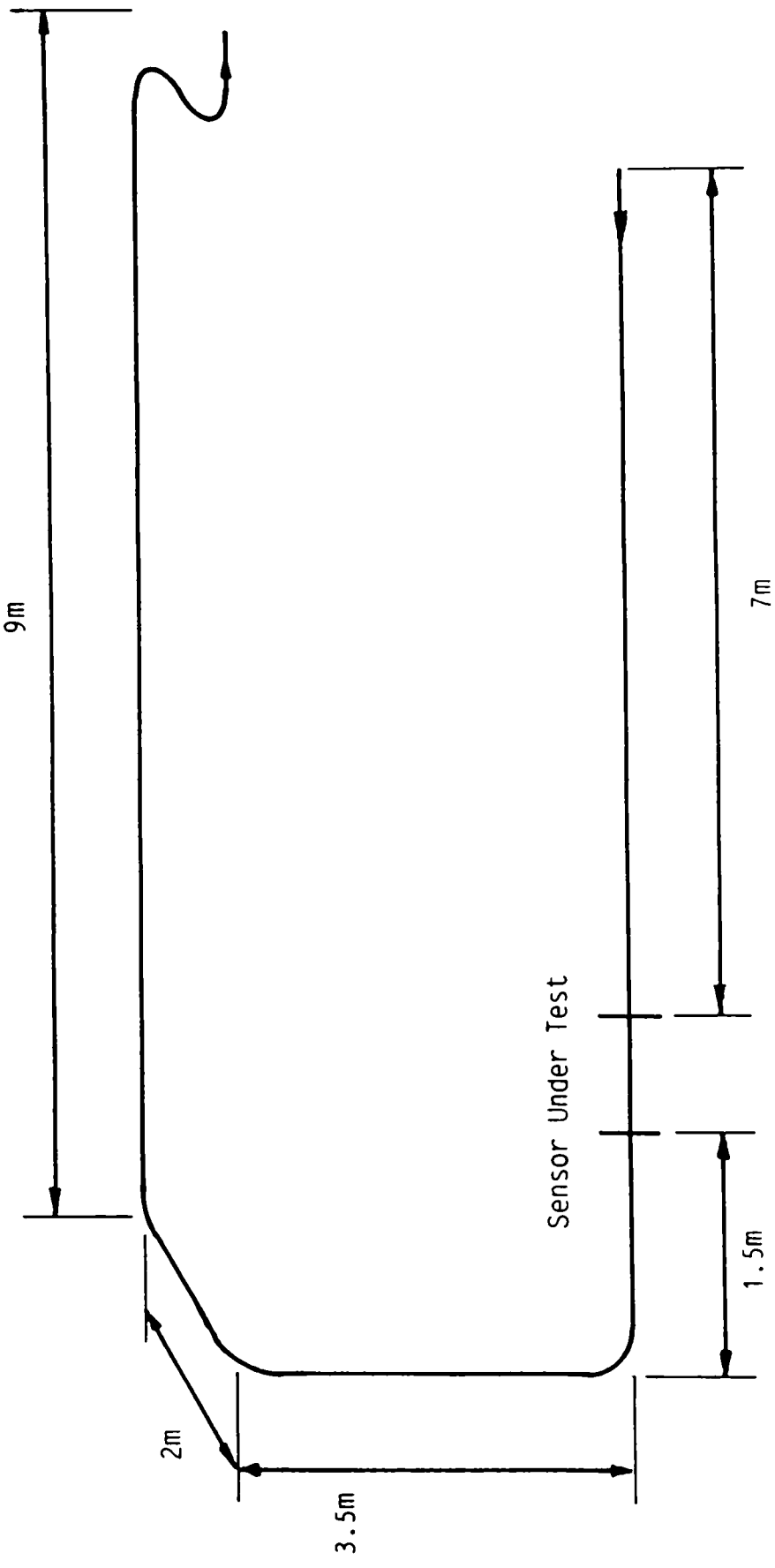

Figure 3.8 Configuation of Pipeline With Straight Section Upstream Of Sensor

2. To be able to store this data on the computer.

3. To be able to process enough of the data in real time to provide the operator with sufficient data to monitor the performance of the test being carried out.

4. An accuracy of $\pm 0.25\%$ for each channel and up date rate of 1Hz including real time processing.

5. To be able to operate in an electrically noisy environment with sensors located up to 1km from the control room[2].

3.6.2 Outline of the Data Logging Sub-System

The data logging sub-system is a complex electronic system, which will be dealt with in sections. Initially an overview of the whole system will be given in order that the reader may see the position of each section within the whole.

Figure 3.9 gives a schematic diagram of the complete sub-system. The front end units are located close to the sensors and provide stabilised power supplies to them. The signal from each sensor is then amplified and converted to a frequency for transmission along a 50 ohm cable to the opto-isolators. The opto-isolators electrically isolate the front end units from the rest of the system. The various signal frequencies are then multiplexed into the counters, where the frequency is converted to a binary number. The binary numbers are then read by the computer via the interface.

The sensors used were:

1. Storage hopper load cells. These were used to monitor the mass of the storage hopper, and thus the flow rate of the returning PF.

---

[2]This distance was specified on the basis that should a suitable sensor be developed, the sensor and data logging equipment would be installed in a large cement manufacturing facility where such distances are usual. The maximum length of cable run in the laboratory is around 20m.

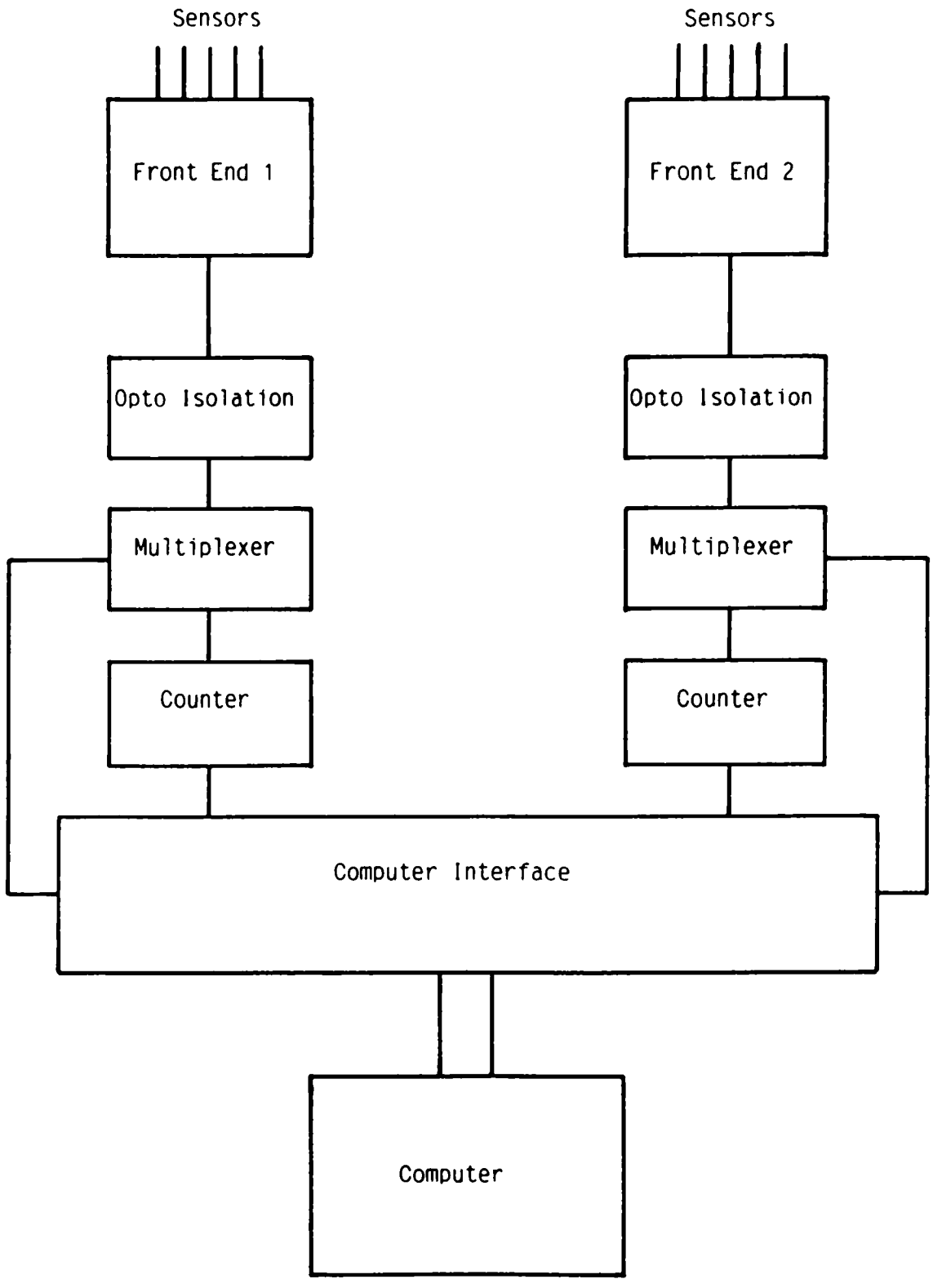

Figure 3.9 Block Diagram of Data Logging Sub System

2. Air pressure in the air control sub-system supply manifold. This measurement was used to carry out real time compensation of the air flow rates, for any variation in the nozzle upstream pressure.

3. Air temperature in the air control sub-system supply manifold. This measurement was used for the same purpose as 2.

4. Air pressure on the output of the air control sub-system feeding the venturi. This measurement was used in combination with 2. to ensure that the pressure ratio across the choke flow nozzles did not fall below 70%.

5. As 4. but for the supplementary air feed.

6. Air Pressure in the test pipeline close to the sensor under test. This measurement was used in combination with 7. and a knowledge of the nozzle valve positions to calculate the volumetric flow rate of the air at this point in the pipeline. The superficial air velocity, V_{as} is then calculated since the cross sectional area of the pipeline is known.

7. Air temperature in the test pipeline close to the sensor under test. Used as in 6.

8. Air relative humidity in the exhaust air from the main disengaging filter. This measurement is logged by the computer. Its use is explained in detail in section 6.6.

9. Air temperature in the exhaust air from the filter. Used as in 8.

10. Suspension density reading supplied by the sensor under test. This measurement was recorded by the computer for later analysis.

The particle velocity given by the system under test was not logged by the computer,

since it was not available from the sensing system in the necessary form. It was therefore logged manually.

3.6.3 Data Logging Front End

A block diagram of one channel of a front end unit is shown in Figure 3.10. The function of which is as follows.

A stabilised D.C. power supply is available to power the sensor. The incoming signal from the sensor, either floating differential or single ended, is amplified using high precision low noise amplifiers and fed into a precision voltage to frequency (V to F) converter. The output of the V to F converter is then fed to the 50 ohm line driving circuits and thence to the transmission line.

3.6.4 Opto-Isolation, Counters and Multiplexers

At the control room end of the 50 ohm line, each signal passes through an opto-isolator, this serves two purposes. It prevents the formation of large ground loops which can lead to high levels of noise being induced on the signal lines. It also prevents any unexpected high voltages on the incoming lines, such as those which may be caused by power cables accidentally coming into contact with the transmission lines, from causing any major damage to the multiplexers, counters and computer interface.

Each signal then passes to the multiplexer, which under computer control selects one of the incoming signals and connects it through to the counter input.

Again under computer control, the counter then runs a 20ms count on the incoming frequency and passes the resulting binary number to the computer. By sampling the incoming frequency over 20ms, any noise which has a period equal to an integer multiple of 20ms, such as 50Hz mains noise will be filtered out.

3.6.5 Real Time Data Processing

A flow diagram of the real time data processing software algorithm is given in Figure 3.11. This was written in Motorola 68000 machine code and C, listings of the source

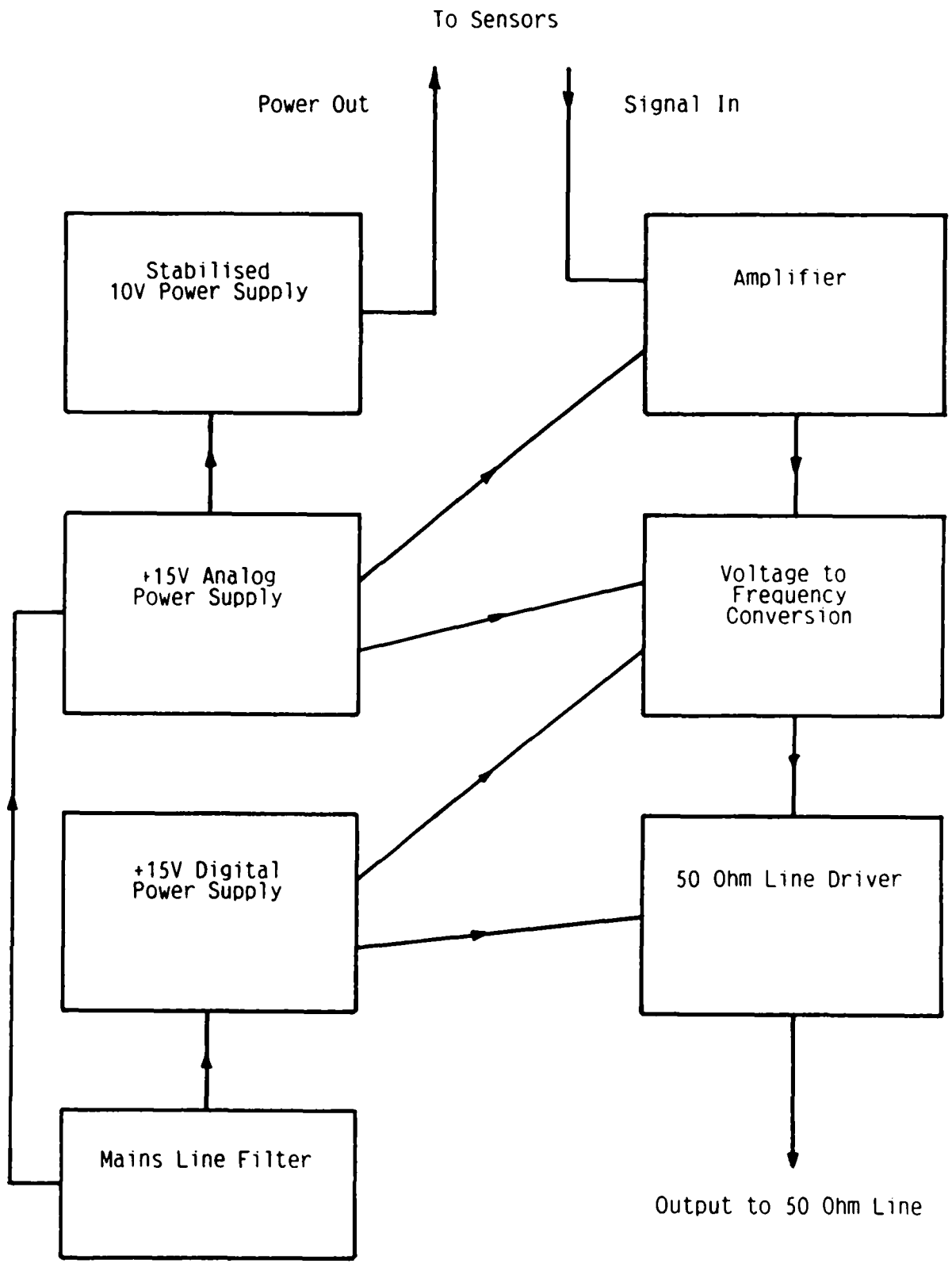

Figure 3.10 Block Diagram of One Channel of Front End Unit

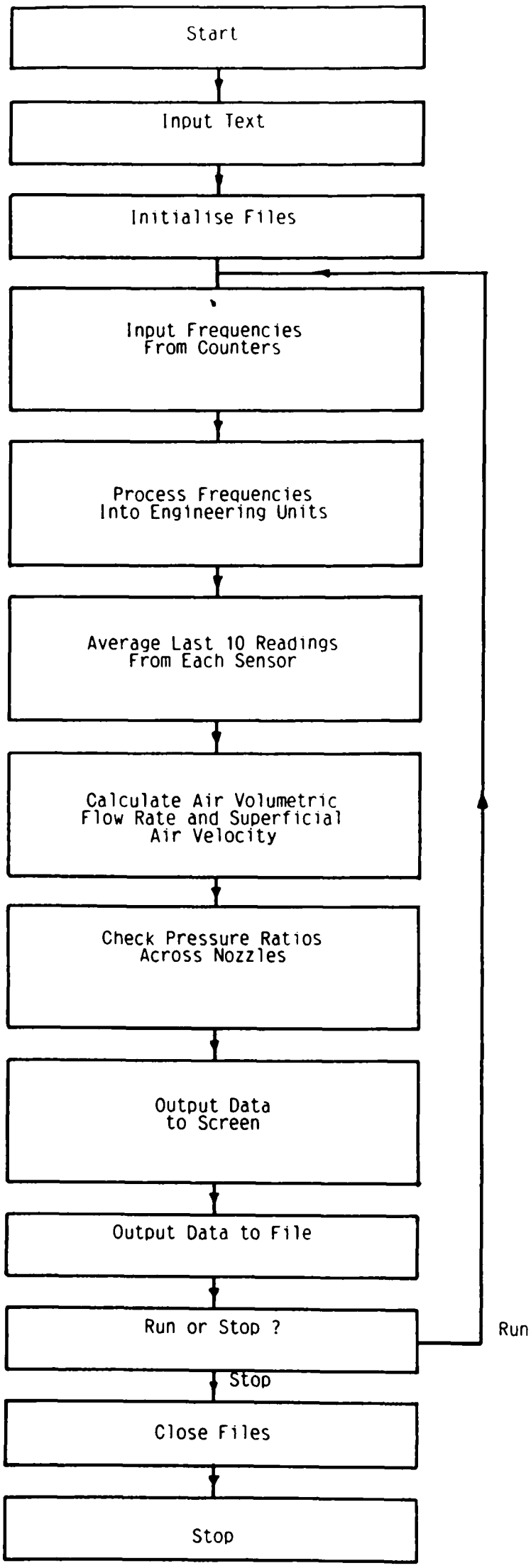

Figure 3.11 Flow Diagram of Real Time Data Processing Software

code are given in Appendix 5.

When the programme is initiated, data is first requested from the keyboard regarding the run number, output file name etc. The files containing the calibration constants and the output file are then opened. A loop is then entered, which continues until further input from the keyboard is received.

Each time the loop is executed, the following tasks are carried out. The counters are run with each of their sensor inputs connected in turn. The resulting binary numbers being stored in the computer memory. Each binary number is then converted to appropriate engineering units using constants stored in the calibration file. The average of each sensor reading for the last ten inputs in then calculated. The volumetric flow rate of the air in the test pipeline adjacent to the sensor under test is calculated. The value for V_{as} is then calculated. A check is then carried out to ensure that the pressure ratio across the choke flow nozzles in the air control sub-system is satisfactory. The calculated data is then both output to the screen and logged to file. If no input has been received from the keyboard, the loop is executed again.

If any input is received from the keyboard, the files are closed and the programme terminated.

3.7 The Control Sub-System

3.7.1 Requirements of the Control Sub-System

The purpose of the control system is to allow the test facility to be fully controlled from a remote control room, thus saving the time on manual effort.

The requirements of the control system are as follows:

1. To provide a control panel inside the control room from which the test facility could be fully controlled.

2. To connect all of the necessary actuators and motors to the control panel.

3. To provide feedback signals so that the operator may see when a motor or actuator has failed to reach the specified position.

3.7.2 Control Panel and Driver Circuits

A photograph of the control panel is shown in Figure 3.12. The control panel was designed so that each of the actuators could be driven either by a switch on the panel or by the computer via the interface. Thus, the control panel switches control 5v logic levels. In order to drive the various actuators, it was necessacary to convert these low voltages to 24v control signals. Some of these 24v control signals operate solenoid actuators directly, while others operate relays to switch 240v single phase or 415v three phase to run various motors.

A 24v driver circuit card was therefore designed and built for this purpose. This card incorporates the control panel switches and forms an integral part of the panel.

3.7.3 Feedback and Error Checking Circuits

A schematic diagram of a single control and feedback channel is shown in Figure 3.13. Each of the actuators was equipped with position sensors so that position signals could be sent back to the control panel. Each of the feedback signals is displayed on the control panel. The feedback signals and the outgoing control signals are then compared electronically using an error detection card designed for the purpose. Should any error be detected, the error checking card lights a control panel indicator so that the operator may see that a specified actuator operation has not been achieved. The error indicator signals are also available to the computer via the interface.

3.7.4 Safety Interlocks

It was decided to install a number of safety interlocks in the control system circuitry, in order that certain combinations of actuator positions which were potentially dangerous could not occur.

The function of these are as follows:

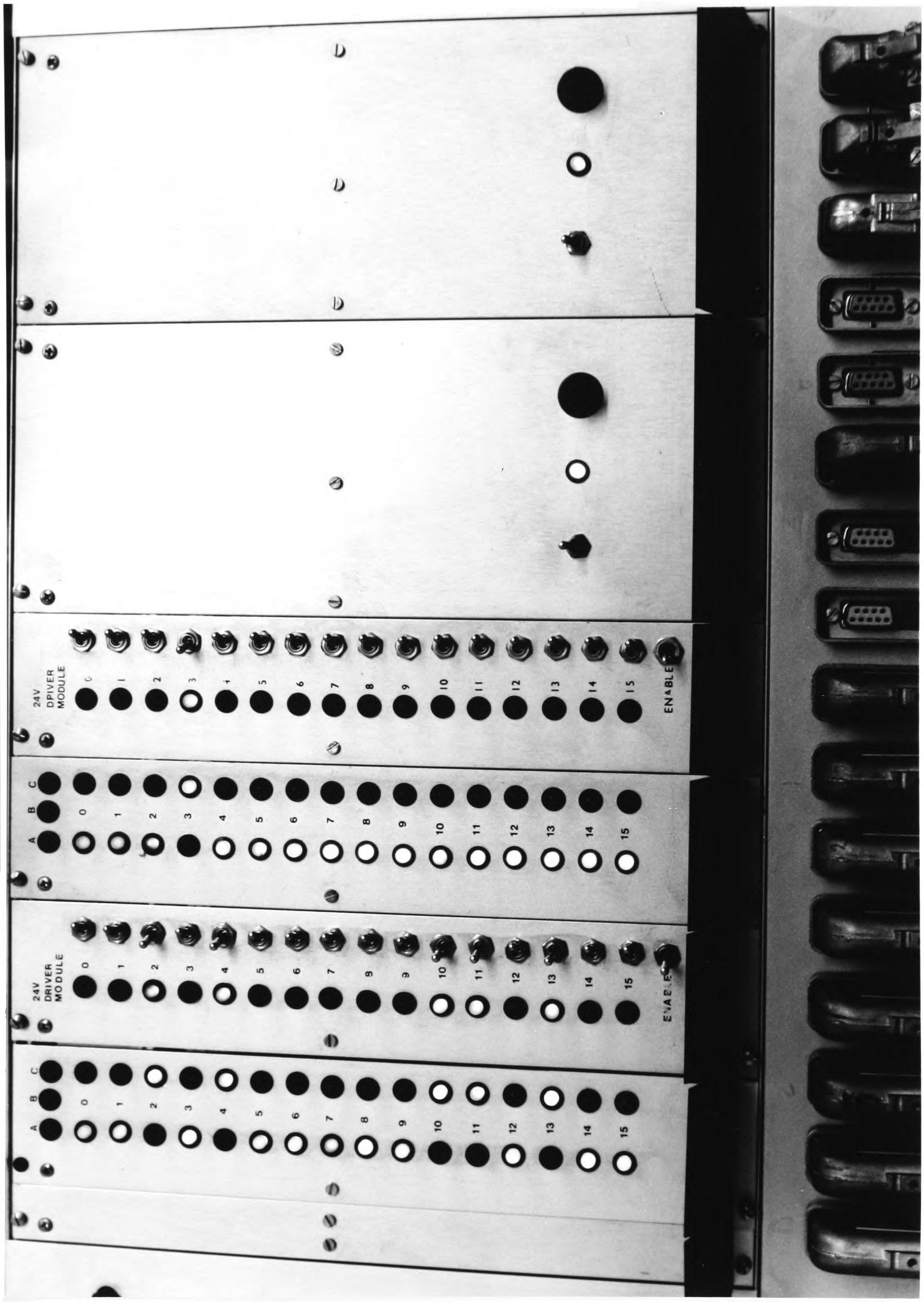

Figure 3.12 Photograph of the Test Facility Control Pannel

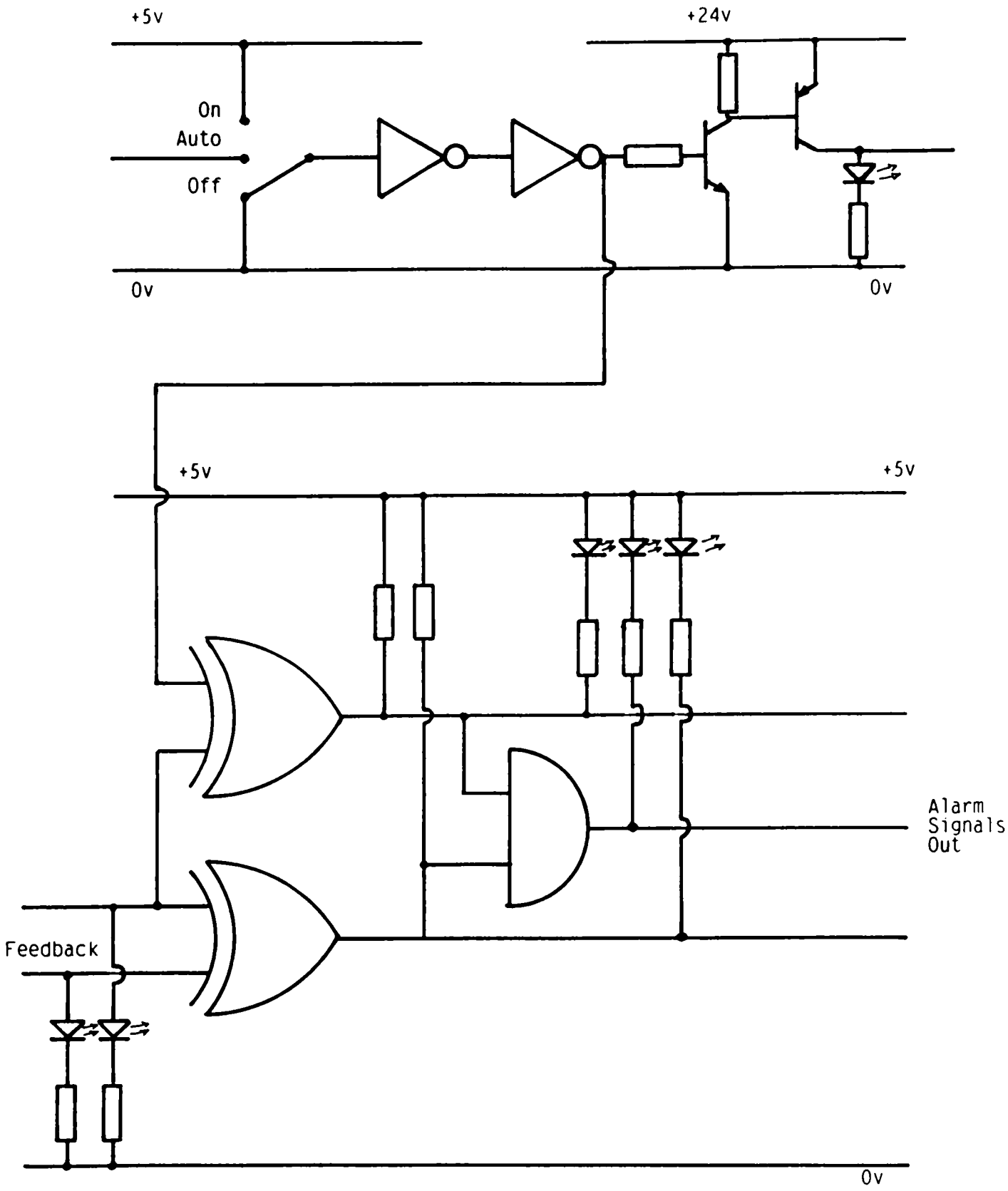

Figure 3.14 Circuit Diagram of Single Channel of Control System

1. If the safe working pressure of the blow tank is exceeded, the air supply is shut off and the vent valve is opened.

2. The storage hopper discharge valve assembly cannot be opened unless the vent line valve is fully open.

The function of the first is self explanatory. The function of the second is to prevent the hopper discharge valves from being opened when the blow tank is pressurised, thus preventing a large volume of air being discharged into the storage hopper which may damage the filter.

3.8 Computer and Interface

A Motorola 68000 based Atari 1040STFM personal computer was chosen for the system computer. This choice was made for two reasons:

1. The author was familiar with the 68000 microprocessor, and its programming.

2. At the time of specification (early 1988) this was the most economic computer available of comparable processor power.

Of consideration also was the fact that software for the Atari was much more economically priced than that of other similar machines.

The computer interface system was developed to plug into one of the ports of the Atari and provide a number of 16 and 8 bit parallel ports. These ports are then utilised by connecting them to the data acquisition sub-system and the control sub-system.

3.9 Commissioning of the Test Facility

The test facility was installed as detailed in Sections 3.1 to 3.8. Initial tests showed some minor problems, mainly with software. These were easily overcome in a relatively short time.

One item which required major modification was the main disengaging filter. After a short period of testing at the high end of the range of air velocities, the differential pressure across the filter became too great for the filter housing to withstand. The resulting failure caused contamination of the laboratory with PF.

This was highly unsatisfactory, since it required the temporary evacuation of the laboratory, and consequent disruption to work.

It was therefore decided to install an additional filter on top of the storage hopper, in order to give a larger filter area and reduce the differential pressure across it. Another filter of the same specification as the original was installed next to it, and the original repaired. This provided twice the original filter cloth area and proved to be entirely satisfactory throughout the test programme.

Chapter 4
The Laser Doppler Velocimetry Test Work

4.0 Introduction to the Laser Doppler Velocimetry Test Work

Laser doppler velocimetry instrumentation is a totally non-intrusive technique by which the velocity of flowing particles may be evaluated, potentially to a very high degree of accuracy. Although undoubtably the technique is a valuable research tool, because of the complex and delicate nature of the equipment, it's use is largely confined to research environments.

As discussed in Chapter 2, the on line evaluation of the mass flow rate of pulverised coal (PF) in an injection system by most techniques currently proposed requires the measurement of both the average velocity of the particles (V_{pa}), and the density of the flowing suspension (ρ_s). In order to be able to evaluate any proposed sensing system, it was important to be able to compare both measurements with known values.

The evaluation of the suspension density is accomplished using a knowledge of the PF and air mass flow rates as outlined in Section 3.6. The evaluation of V_{pa} is not as straight forward, since although the superficial air velocity (V_{as}) is known, it seems unlikely that the particles travel at exactly the same velocity. In fact it is widely accepted that they do not[B1,B3,B6,B9,B10].

A technique was therefore needed to enable V_{pa} to be measured directly. For laboratory based research, laser doppler velocimetry is very well suited to this application and was therefore chosen to measure this variable.

4.1 Objectives of the Laser Doppler Velocimetry Test Work

There were two objectives of the laser doppler velocimetry test work. These were:

1. To evaluate the slip of the particles in the air stream and to attempt to find a relationship between the slip and other more easily measurable quantities.

2. To compare the actual particle velocity with the particle velocity evaluated by the electrostatic sensing system.

Information from 1 above will determine whether a simple model can be developed which will predict the average particle velocity from a knowledge of the values of more easily measurable quantities. This model could be utilised in a measurement system to evaluate the average particle velocity from the more easily measurable quantities, such as air velocity and suspension density.

The work carried out under 2 will provide a calibration of the electrostatic sensing system, for velocity measurement, so that it's performance is known over a range of operating conditions. Clearly, should the performance of this system be satisfactory, then it may be utilised directly in PF injection systems.

4.2 Principle of Operation of the Laser Doppler Velocimetry Instrumentation

In this section the principle of operation of the laser doppler velocimetry instrumentation is described.

When two beams of monochromatic coherent electromagnetic radiation cross at an angle as shown in Figure 4.1, interference fringes will be formed, as shown. The spacing of these fringes is a function of the beam intersection angle and the wavelength of the radiation.

If a particle then passes through the region of beam intersection in the direction indicated by the arrow A in Figure 4.1, it will reflect pulses of light. The frequency of these pulses is termed the doppler frequency and is a function of the velocity of the particle in the direction A in the plane of the paper and the fringe spacing only.

Thus if the light pulses are detected and the doppler frequency measured, the geometry of the beam intersection known and the wavelength of the radiation known, the velocity of the particle may be determined.

A schematic drawing of the general arrangement of a simple laser doppler velocimeter

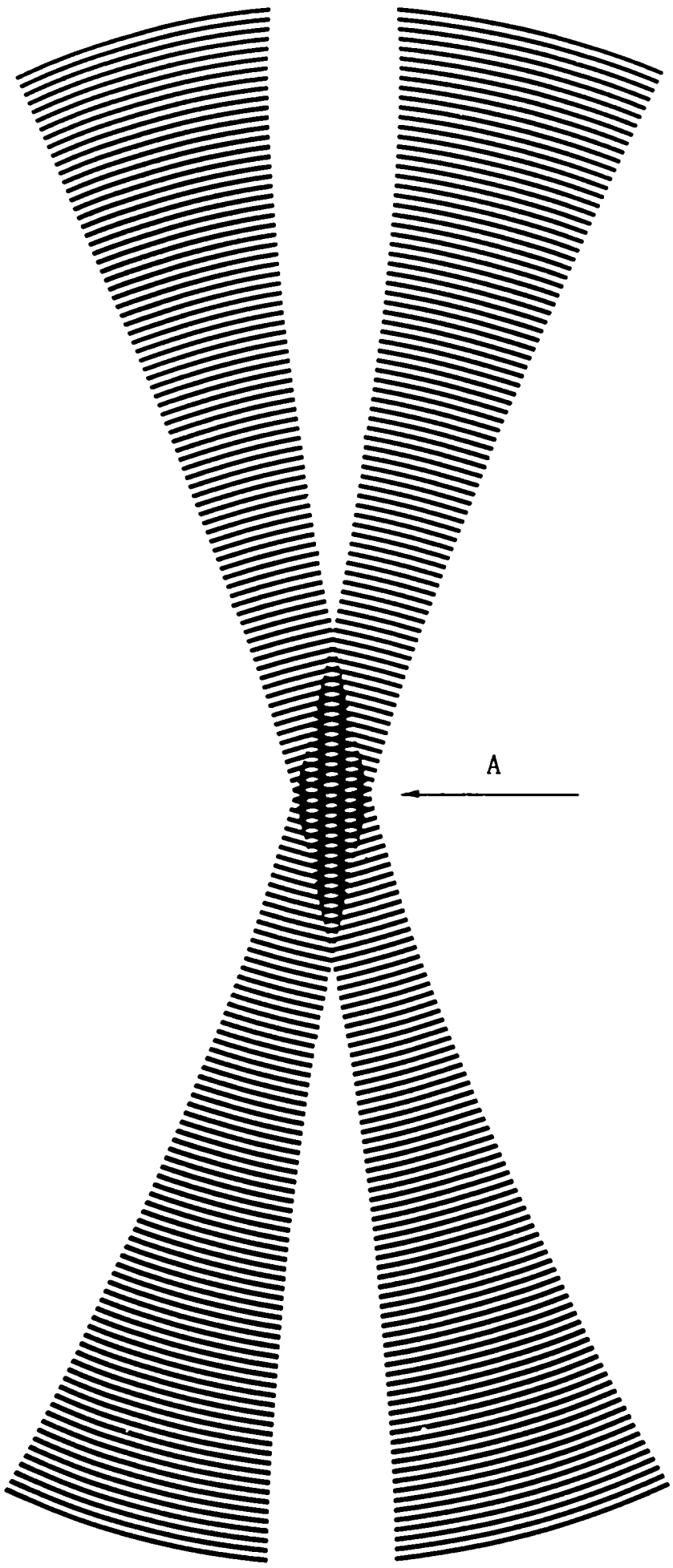

Figure 4.1 Illustration of Interference Fringes

is shown in Figure 4.2.

In practice a laser forms a convenient source of monochromatic coherent light, having a suitably narrow beam. The beam may be split to form two beams, which can then be deflected by mirrors and/or lenses to intersect at the required angle as shown in Figure 4.2.

4.2.1 Determination of the Relationship Between the Wavelength of the Laser Light, the Beam Intersection Angle, the Doppler Frequency and the Velocity of the Particle

A drawing showing the individual wave fronts within the region of intersection of the beams is shown in Figure 4.3. The wavelength of the laser light is denoted by λ, the spacing of the fringes by δ and the angle of beam intersection by 2θ.

Figure 4.4 shows one of the diamond shapes bounded by the wave fronts shown in Figure 4.3. From this figure it is possible to determine the relationship between λ, δ and 2θ.

From the smaller inner triangle of Figure 4.4, it may be seen that:

$$Cos\ \theta = \frac{\lambda}{a}$$

From either of the larger inner triangles it may be seen that:

$$Tan\ \theta = \frac{a}{2\delta}$$

From simple trigonometric relationships:

$$Sin\ \theta = Tan\ \theta\ .\ Cos\ \theta$$

$$\therefore \quad Sin\ \theta = \frac{a}{2\delta} \cdot \frac{\lambda}{a} = \frac{\lambda}{2\delta}$$

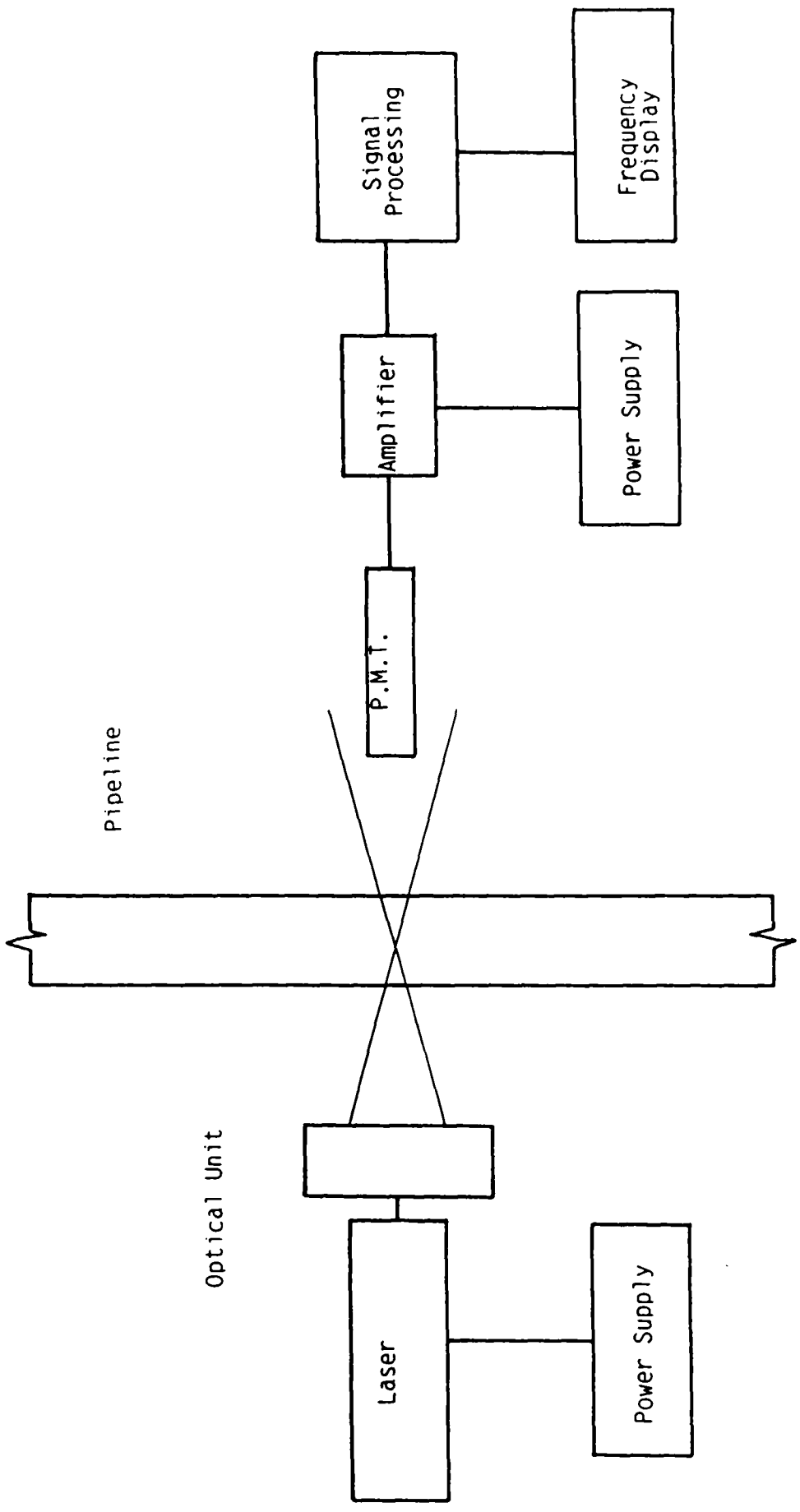

Figure 4.2 Block Diagram of Laser Doppler Velocimeter

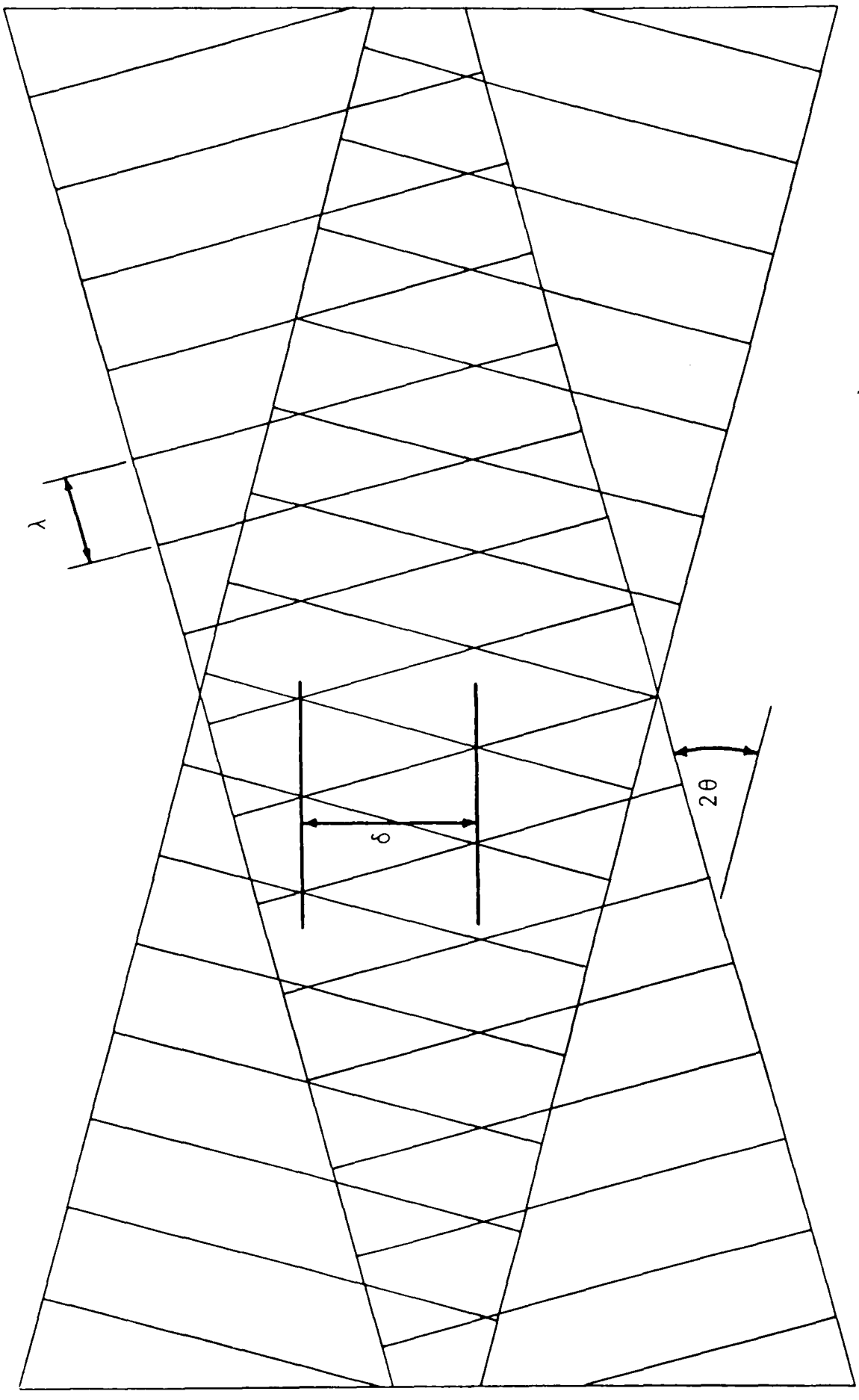

Figure 4.3 Showing the Relationship Between λ, δ and 2θ

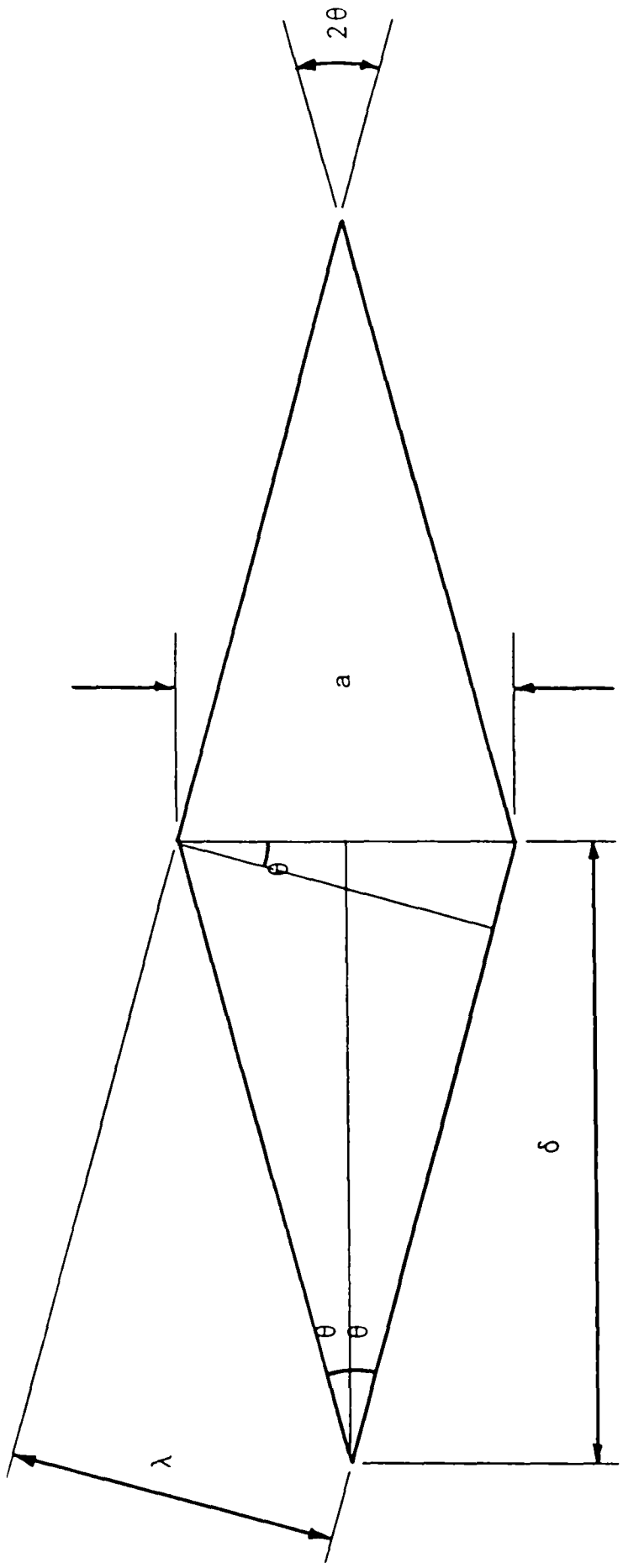

Figure 4.4 Showing Relationship Between λ, δ and 2θ in More Detail

$$\therefore \quad \delta = \frac{\lambda}{2 \sin \theta}$$

Thus, for any values of λ and 2θ, δ may be calculated from this simple relationship. From δ, V_p can be determined from the following relationship:

$$V_p = f_d . \delta$$

Where f_d = Doppler Frequency

V_p = Velocity of the Particle

Low power Helium-Neon lasers up to 25mW are commonly used for simple laser doppler velocimetry work, although Argon-Ion lasers having higher powers are often used when the flow conditions are less favourable, or when simultaneous velocity measurements are being made in different directions.

4.2.2 Space Volume Illuminated by Fringe Pattern

At the point of intersection of the light beams, a volume of space will be illuminated by a fringe pattern. The laser beam has a Gaussian intensity distribution and the illuminated volume takes the form of an ellipsoid, as shown in Figure 4.5. The diameter of the laser beam may be defined as the distance between the points at which the laser beam intensity is greater than $1/e^2$ of its maximum value. The dimension ΔX is equal to the diameter of the laser beam waist at the cross over point. This is given by[C3]:

$$\Delta X = 2b_0 = \frac{4 f_L \lambda}{\pi 2b}$$

where f_L = focal length of lens

$2b$ = initial diameter of laser beam

$2b_o$ = beam diameter at cross over point

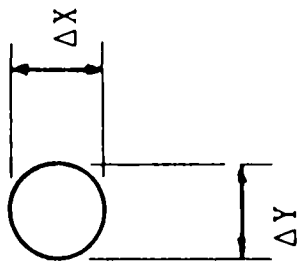

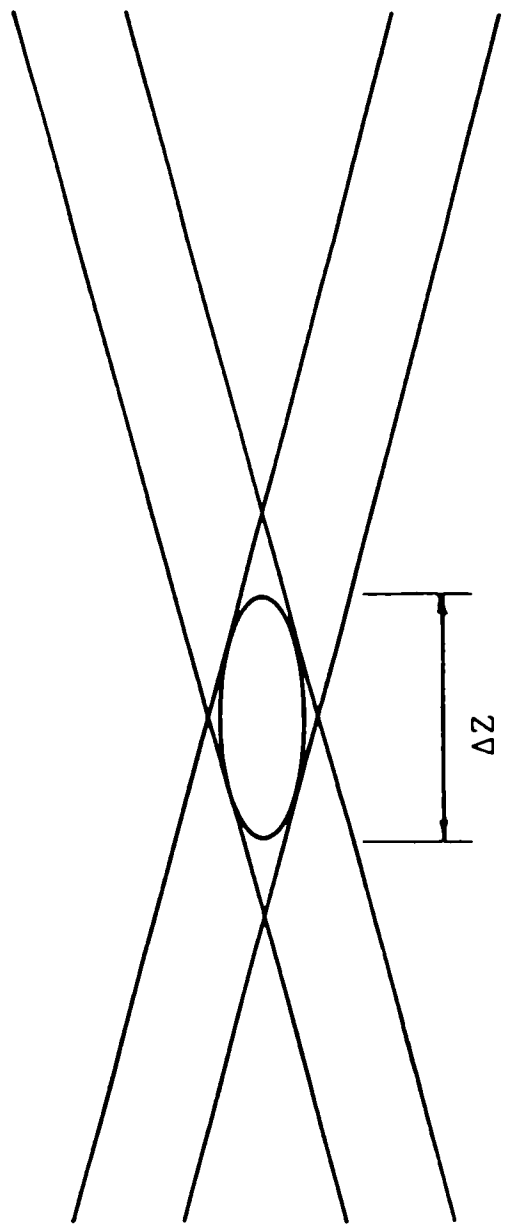

Figure 4.5 Illuminated Volume Dimensions

The dimensions ΔY and ΔZ are given by[C3]:

$$\Delta Y = \frac{2b_0}{Cos\theta}$$

$$\Delta Z = \frac{2b_0}{Sin\theta}$$

For the equipment used, the dimensions were 0.12, 0.12 and 5.5mm respectively.

4.2.3 Doppler Frequency Sensors

The light sensors used to sense the doppler frequency light pulses are usually one of two basic types.

The avalanche photo-diode has relatively low sensitivity and is used in simple systems where flow conditions are favourable and the doppler signal high. The photomultiplier sensor has higher sensitivity, and so is used in systems where flow conditions are not the most favourable, and where the doppler signal is lower. In practice, this applies to most systems.

The sensor usually incorporates a system of lenses and apertures as shown in Figure 4.6. These allow an image of part of the illuminated volume to be formed on a target, which incorporates a pinhole at the centre. By the selection of lens arrangement and pinhole size, the portion of the illuminated volume sensed by the sensor may be set.

4.2.4 Signal Processing Techniques

In practice, it is very common for the doppler signal at the output of the photomultiplier or photo-diode to have a relatively low signal to noise ratio. In order to be able to measure the doppler frequency accurately, it is therefore usual to process the raw signal before attempting to measure the doppler frequency.

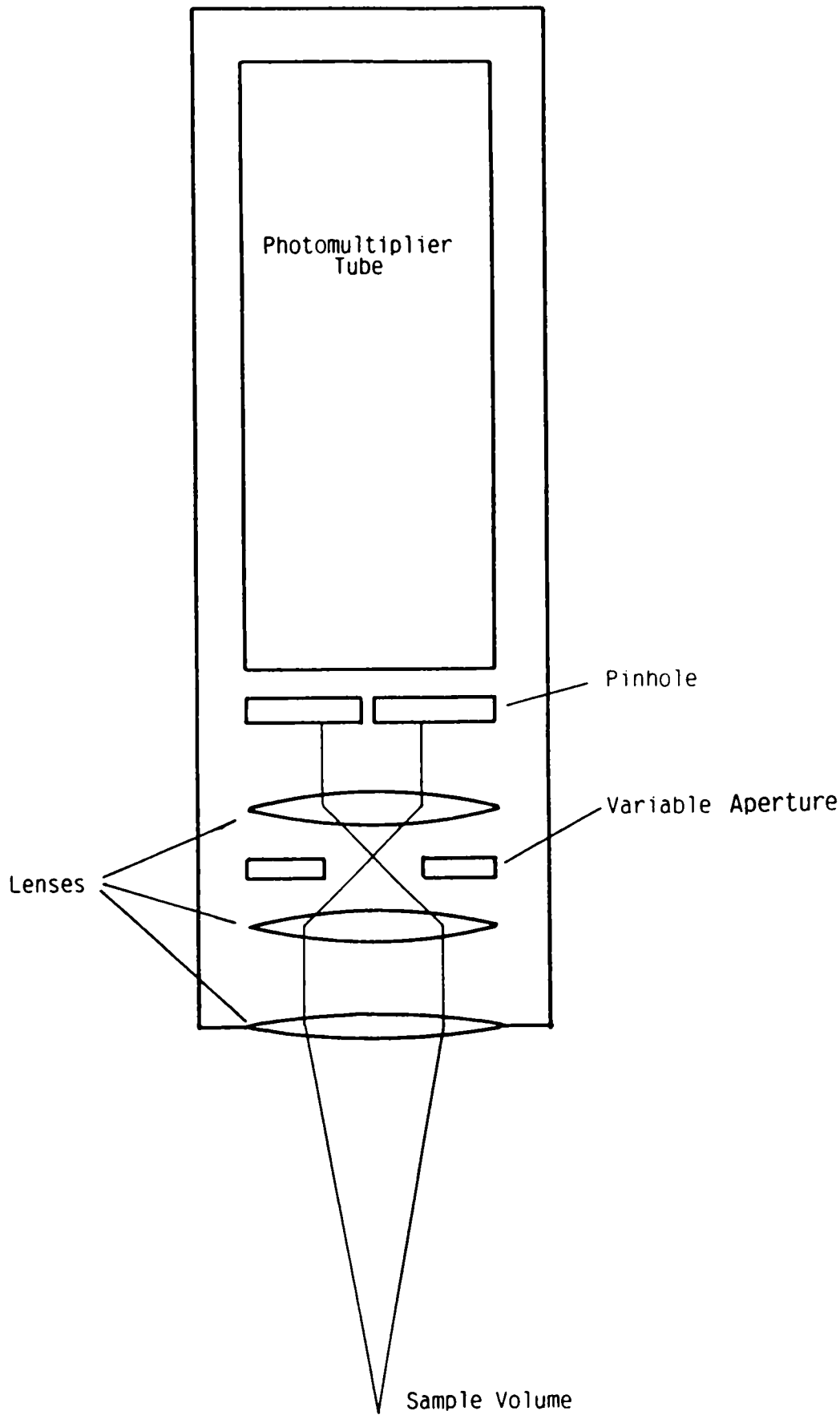

Figure 4.6 Typical Light Sensor, Lens and Aperture Arrangement

This processing usually takes one of two forms. In some systems the signal undergoes spectral analysis, using Fourier transformation or a sweeping filter, the doppler frequency may then be readily identified from the spectrum. In other systems the signal is fed to a tracking filter, which is designed to track the doppler frequency. Thus, the output of the tracking filter will be the doppler frequency alone, which may be fed to a frequency counter for measurement.

The spectral analysis technique is often more useful for signals which have a low signal to noise ratio.

The tracking filter technique is better suited to situations where the doppler signal has a high signal to noise ratio, where because of it's ability to count the doppler frequency directly, it provides superior accuracy.

4.3 The Laser Doppler Velocimetry Equipment Used for the Test Work

The description of the laser doppler velocimetry equipment will be divided into a number of sections as follows:

1. A description of the laser and the optical arrangement used to split and cross the beams.
2. Details of the procedure used to calibrate the laser optical arrangement.
3. A description of the photomultiplier tubes and the optical arrangement used to focus the image of the sample volume.
4. Details of the mounting arrangement employed for the laser doppler instrumentation.
5. A description of the signal processing techniques which it was proposed to use.

4.3.1 The Laser and Optical Arrangement

A photograph of the laser and optical unit is shown in Figure 4.7, a corresponding diagram showing the principle of the arrangement is shown in Figure 4.8. A Helium-Neon laser having an output power of 6mW and manufactured by Spectra Physics Limited was used. A Disa 55L optical unit was also used since this was also readily available.

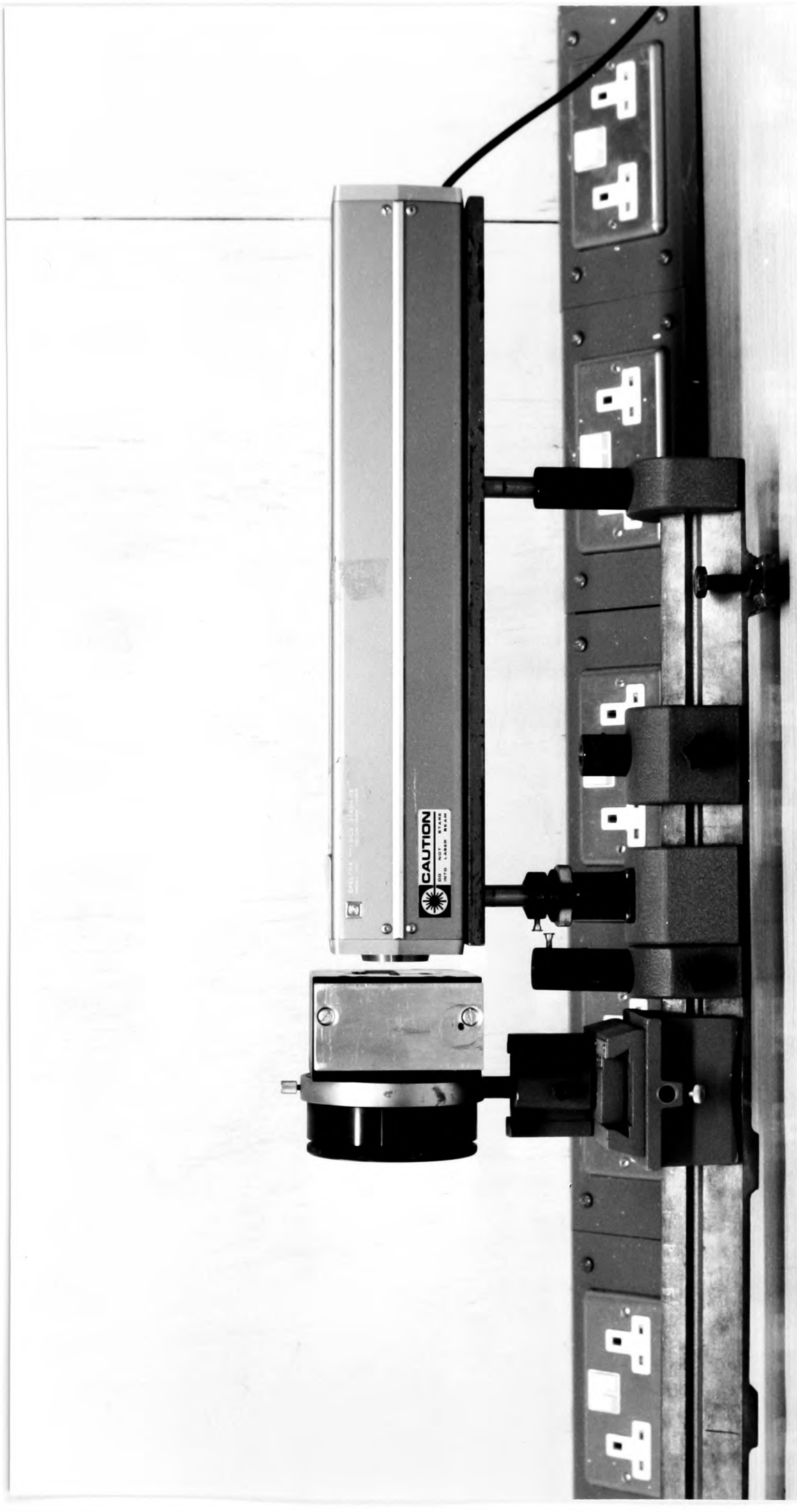

Figure 4.7 Photograph of the Laser and Optical Unit

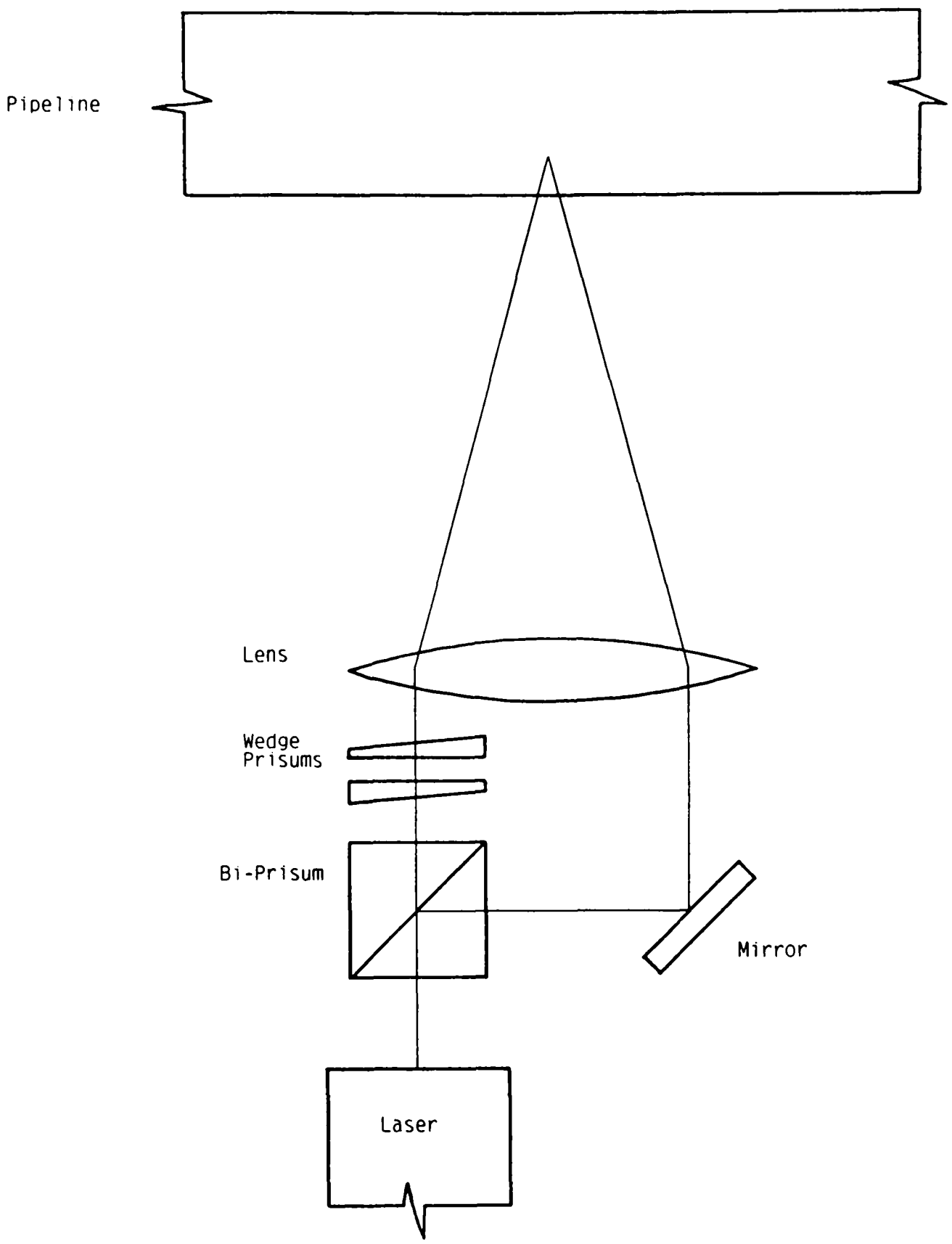

Figure 4.8 Principle of Operation of the Beam Splitting Optical Unit

In the optical unit the light beam first enters a biprism, where it is split into two beams of equal intensity. One beam passes straight through the biprism, whilst the other is deflected through 90°. The first beam passes through two wedge shaped prisms which may be rotated, thus allowing minor adjustments of beam position. The second beam is deflected through 90°, again by a mirror. The position of the mirror is adjustable in order to allow the beam spacing to be set.

Both beams then pass through a lens, which focuses them, causing them to cross at the required point.

It will be seen from Section 4.2.1 that in order to be able to evaluate the particle velocity, three other variables must be known, namely, the wavelength of the laser light, the doppler frequency and the geometry of the intersecting laser beams. The wavelength of light emitted by a Helium-Neon laser is well defined, and has a value of 632.8nm. The doppler frequency may be evaluated with sufficient accuracy utilising one of the techniques outlined in section 4.2.3. The determination of the angle of intersection of the beams is the third variable and is obtained by calibration, the procedure for which is described in the following section.

4.3.2 Calibration of the Optical Arrangement

A drawing of the equipment used for the calibration of the optical arrangement is shown in Figure 4.9. The laser and optical arrangement is mounted on an optical bench, which is secured by three adjustable legs to a rigid bed. A X-Y traversing mechanism is also secured to the bed. A quadrant photo-diode is mounted on the traversing mechanism.

The legs of the laser and optical arrangement are first adjusted so that the crossing beams are in the same plane as the movement of the X-Y traversing mechanism. The height of the quadrant diode is then adjusted so that the diode is at the same height as the centre of the laser beams.

The X-Y mechanism is then adjusted until the quadrant diode is exactly aligned with the centre of one of the laser beams. The position of the X-Y traversing mechanism

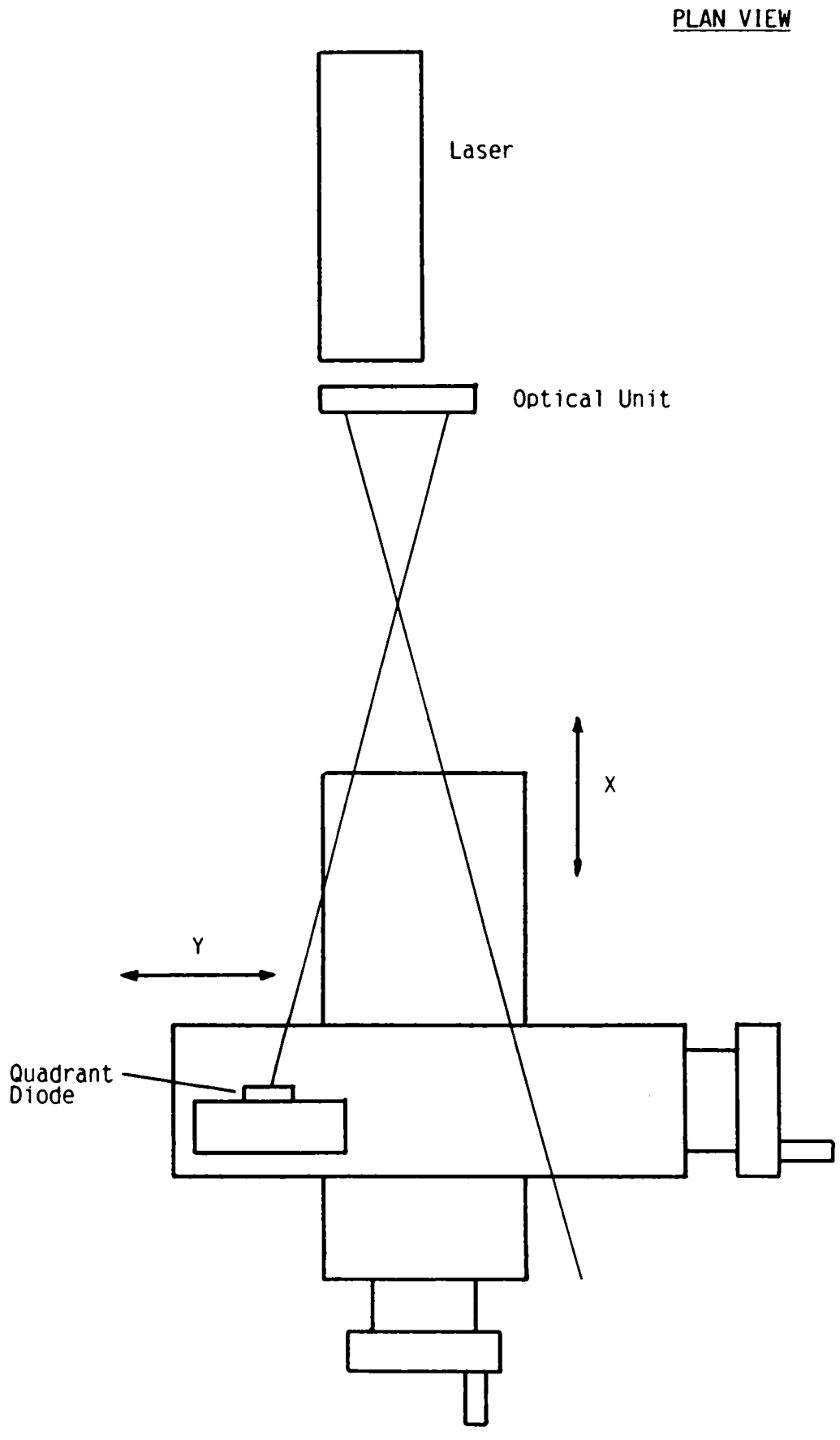

Figure 4.9 Equipment Used to Calibrate the Laser Doppler Velocimeter Optical Unit

is then noted. The Y slide is then adjusted until the second beam is at the centre of the diode, and the position of the X-Y traversing mechanism noted. This gives an accurate measurement of the distance between the beams for a given value of X.

The X slide is then traversed by a fixed distance, and the process repeated. The measurements thus obtained are shown in Figure 4.10. The angle of intersection of the beams is then obtained using simple trigonometric relationships.

4.3.3 Photomultiplier Tubes and Associated Optical Arrangement

Two DISA type 55L10 photomultiplier assemblies were utilised. The photomultiplier assemblies were positioned as shown in Figure 4.11. The first was positioned in forward scatter mode, i.e on the opposite side of the pipeline to the laser. The second was positioned on in backscatter mode, on the same side of the pipeline as the laser.

Two photomultiplier tubes were utilised since it was considered that the relative quality of the signal from each may vary with flow conditions, and the position of the measurement volume inside the pipeline. Figure 4.12 shows the arrangement of the tubes and their associated optical assembly. The diameter of the area interrogated by the photomultiplier assembly may be calculated from the relationship below, using simple lens theory[G8].

$$d_{ia} = d_{ph} \cdot \frac{300}{115}$$

where d_{ia} = diameter of the interrogated area

d_{ph} = diameter of the pin hole

4.3.4 Mounting of the Laser Doppler Velocimetry Instrumentation

The laser doppler velocimetry instrumentation was mounted on a rigid steel section, which, in turn was mounted on a slide, thereby allowing the complete assembly to traverse across the diameter of the pipeline. A drawing of this arrangement is shown in Figure 4.13.

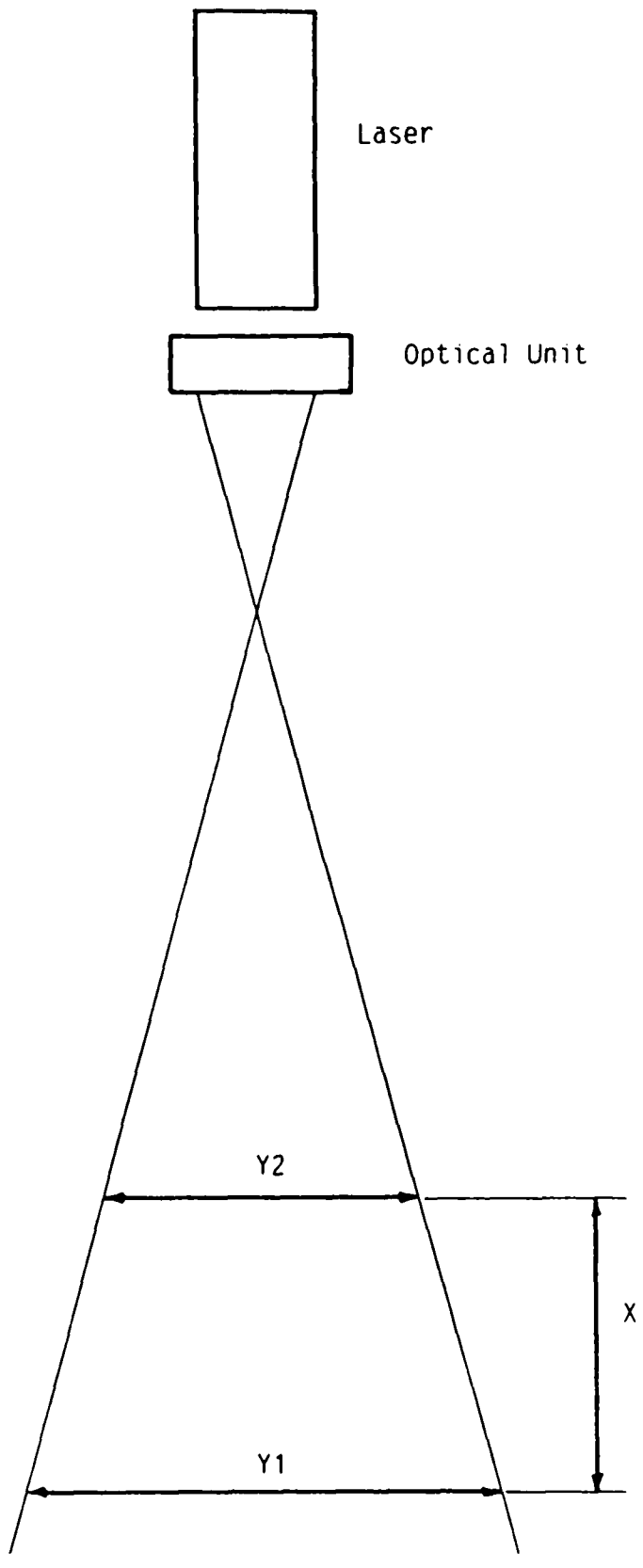

Figure 4.10 Measurements Obtained During Calibration

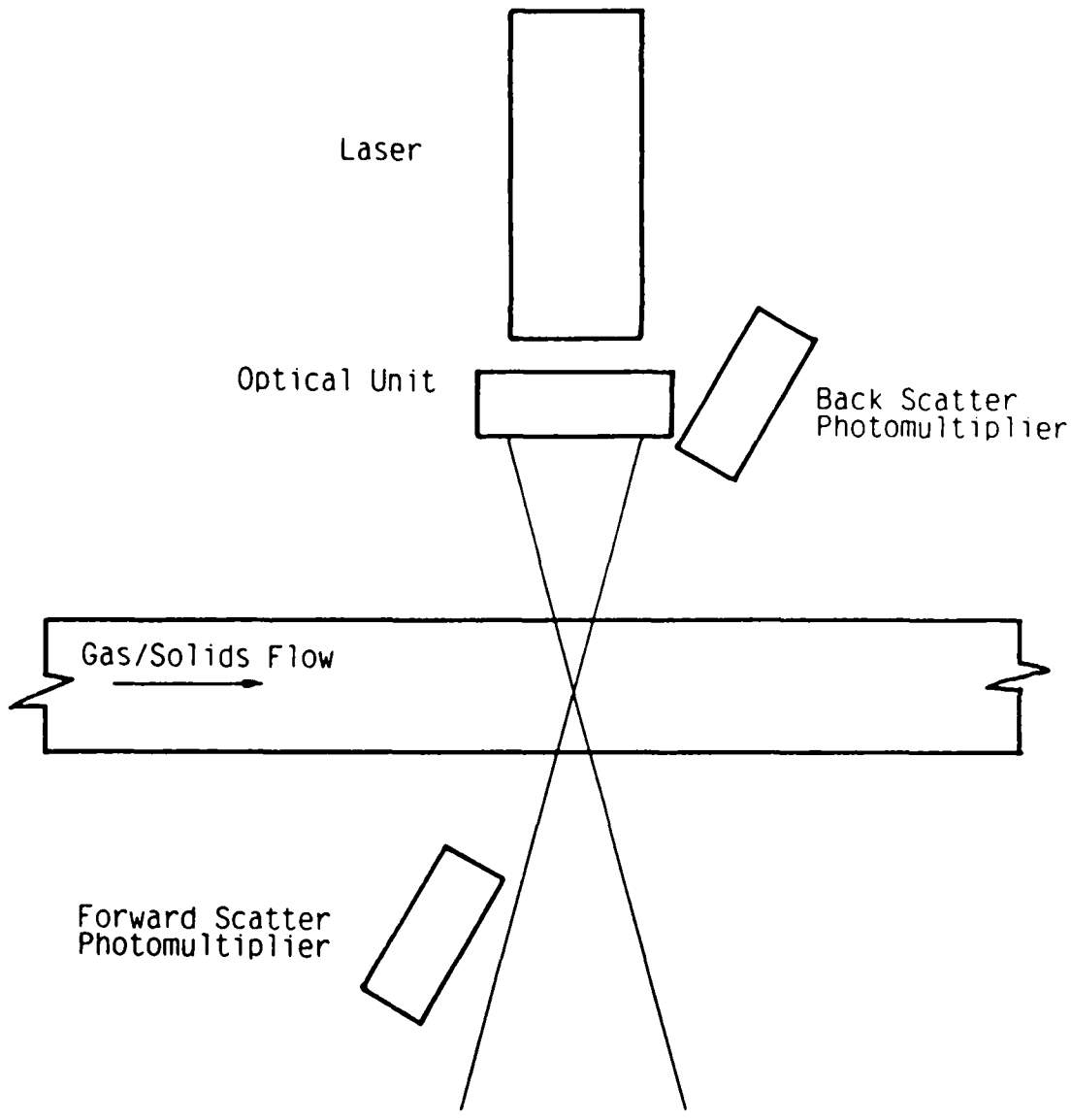

Figure 4.11 Position of the Photomultiplier Tubes

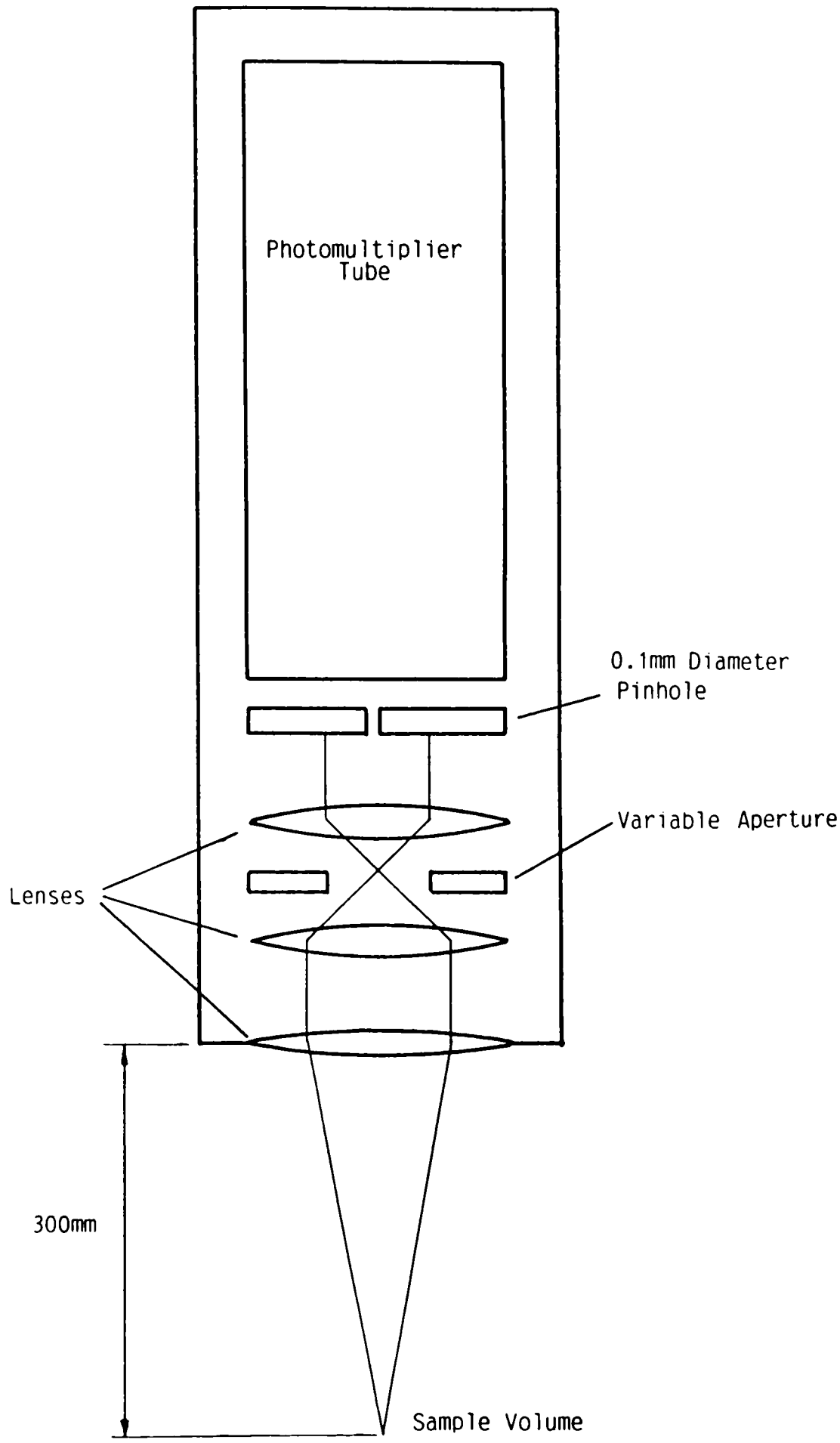

Figure 4.12 Arrangement of the Photomultiplier Tube and Optics in the Disa 55L10

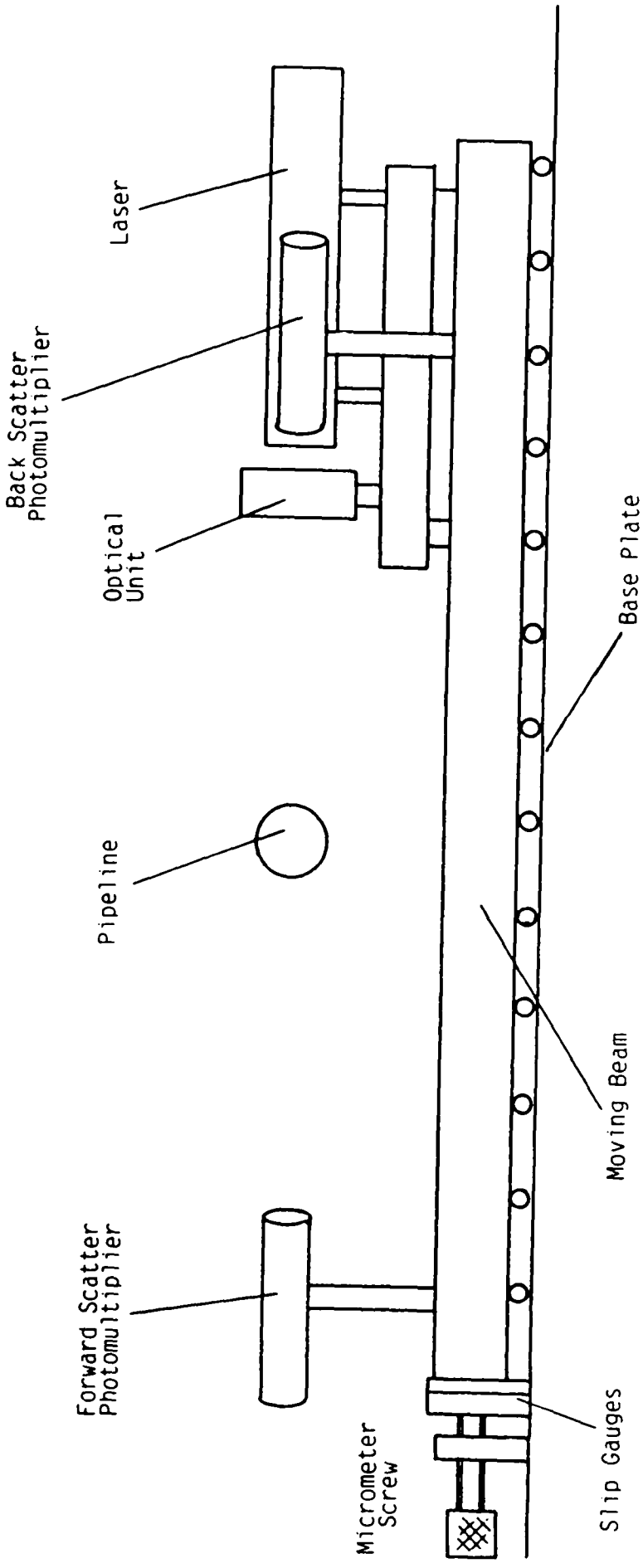

Figure 4.13 Laser Doppler Velocimeter Mounting Details

The position of the laser doppler system in the horizontal plane, relative to the pipeline was adjusted using a micrometer screw and slip gauges. Thus, once the centre of the interference fringe pattern had been initially positioned, the actual position could be determined at any time by reference to the micrometer scale, and the slip gauges used.

4.3.5 Signal Processing Techniques

A laser doppler velocimeter signal processor of Cambridge Consultants type CC02 was initially used, having the capability to process the doppler signal using either the tracking filter or spectral analysis techniques described in Section 4.2.3.

4.4 Commissioning of the Laser Doppler Velocimetry Instrumentation

The complex and delicate nature of the laser doppler velocimetry instrumentation dictated that a certain amount of commissioning work was required before reliable measurements could be obtained. This commissioning work was focused on two areas:

1. Optimisation of the signal processing techniques used.
2. Determination of the flow conditions in the test pipeline over which reliable signals could be obtained.

The initial commissioning tests were not encouraging. No reliable frequency reading could be obtained regardless of the signal processing technique used. On closer examination of the signal directly from the photomultipliers on an oscilloscope, two problems were noted. Firstly, the signal to noise level relative to the wide band noise was very low and secondly, there were strong noise levels at approximately 100kHz and 13MHz. The expected 1.2MHz signal was barely discernable from the wide band noise, the 100kHz noise was 20dB above the signal, and the 13MHz noise was approximately 3dB above the signal. Consequently, the signal processor was not able to distinguish the 1.2MHz signal from the 100kHz and 13MHz noise, despite having a band pass filter on its input.

At this stage, two measures were adopted. Firstly, the PF being conveyed by the test plant was replaced with wheat flour. The particle size distribution and density being

comparable with PF, but the flour was white rather than black. This caused a moderate increase in the magnitude of the signal to noise ratio at the output of the photomultiplier with respect to the wide band noise. However, the 100kHz and 13MHz noise signals were still present at similar magnitudes.

The second measure to be adopted at this stage was that of modifying the signal processing equipment.

4.4.1 Modification of the Signal Processing Equipment

It was clear that the bandpass filter on the input of the signal processor was not adequate. On examination of the exact specification, it was found to have a pass band from 70kHz to 1.7MHz with only 20dB/Decade roll off at both ends. It was therefore decided to design and build a better filter. The range of velocities used in the test work were expected to yield frequencies in the range 800kHz to 1.7 MHz, and so it was decided to design a filter with this pass band. It was then necessary to determine the required roll off in order to fully specify the filter.

There was some trade off here since the design and construction of filters having a steep roll off is complex, yet considerable attenuation of the 100kHz noise was necessary in order to obtain a reliable doppler frequency reading. It was decided to carry out a calculation to determine the attenuation of the 100kHz signal with a lower corner frequency of 800kHz and a roll off of 40dB/decade (a second order filter).

This was done graphically and is shown in Figure 4.14. At 100kHz, the noise will have been attenuated by approximately 37dB, or by a factor of 70. Thus, the signal at 1.2MHz will have approximately 7 times the magnitude of the 100kHz noise, which originally had a magnitude of ten times that of the 1.2MHz signal. Clearly, the 13MHz noise will be well below the level of the signal.

It was therefore decided to design and build a second order band pass filter having a pass band from 800kHz to 1.7MHz. This filter was tested with a signal generator and oscilloscope over the full working frequency range, with performance being close to the design expectations in most respects.

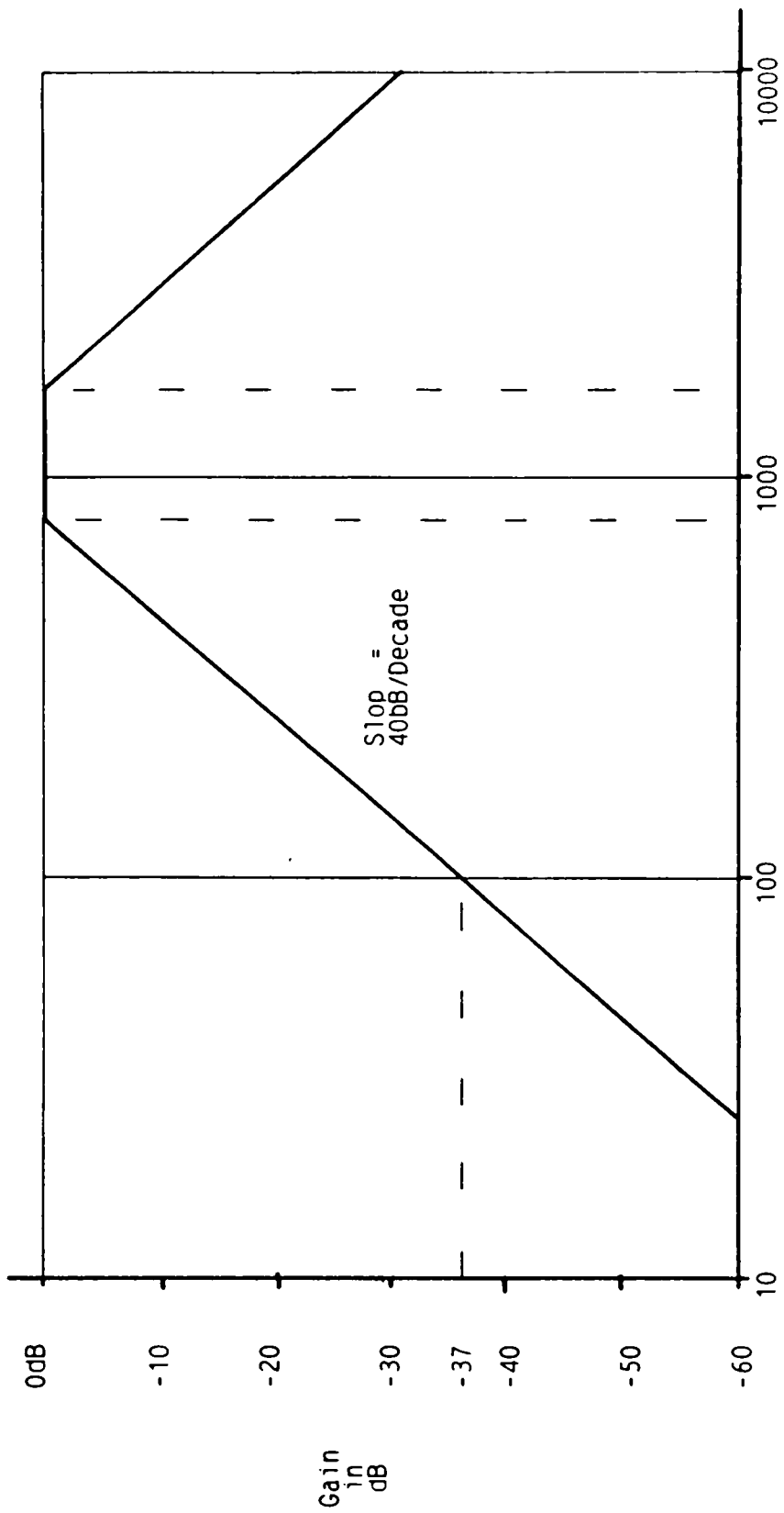

Figure 4.14 Graph of Frequency Response of Proposed Filter

On testing the laser doppler equipment with the new filter installed before the signal processor, it was found that the processor operated satisfactorily in spectrum analyzer mode, but no reading could be obtained using the tracking filter mode. The filtered signal was also displayed on the oscilloscope, from which a good estimation of the doppler signal frequency could be obtained. Thus, it was decided to take doppler signal readings from both the spectrum analyzer and the oscilloscope. The readings would then be analyzed accordingly.

4.4.2 Determination of the Flow Conditions Under Which the Laser Doppler Velocimetry Instrumentation will Operate

A number of tests were carried out at various flow conditions. No major limitations were encountered in terms of the value of the conveying air velocity, 25m/s was the lowest value tested, since it was considered that some settlement of the flour in the pipeline might occur below this velocity and 43m/s was the highest value used because of the limitations imposed by the design of the test facility. Most commercial PF firing systems operate in the range from 25 to 35m/s, and so the operating range of the test facility was considered adequate.

At suspension densities below 0.005 kg/m^3 the laser doppler velocimetry instrumentation became unreliable, the level of the signal being very low due to the small number of particles present in the flow. At suspension densities above 0.5kg/m^3 the quality of the signal once again deteriorated since the laser light was not able to penetrate the flow.

4.5 The Laser Doppler Velocimetry Test Programme

Having established the operational limits of the instrumentation, it was possible to prepare a proposed programme of tests in the light of the programme objectives. It was decided to carry out a range of tests to compare the particle velocity determined by the electrostatic sensors and the cross correlator with the particle velocity determined by the laser doppler velocimetry instrumentation. The suspension density indicated by the electrostatic sensor was also compared with the actual suspension density derived by the data logger as outlined in section 3.6. It was considered that the results of such tests would satisfy the objectives of the test programme as layed

down in Section 4.1.

The decision then had to be made as to how many test runs to carry out. There was a requirement for some compromise to be considered here since is was desirable to have a comprehensive data set, but at the same time the commissioning tests had shown that the procedure involved in operating the laser doppler velocimetry instrumentation was very time consuming, and so a large number of test runs would be costly in terms of time.

It was therefore decided to carry out tests at nominal superficial air velocities of 25,33,27 and 43m/s. For each air velocity the aim was to carry out tests at three different suspension densities within the operating limits of the instrumentation. Because of the unpredictable nature of the PF feeder it was not possible to accurately specify the suspension densities in advance, and so the actual values of suspension density tested do not follow any predetermined pattern.

The control system was first set to provide the required air flow rates. The feed of PF or flour was then started by setting the feed rate (approximately) and the opening of the butterfly valve on the bottom of the blow tank. A period of time was then required for the feeder to settle down to a steady feed rate before any measurements were taken. This time varied considerably from run to run, but was generally between 5 and 30 minutes. Generally, a longer settling time was required at low product flow rates. A range of readings were taken by the data logger as described in Section 3.6, with the velocity indicated by the cross correlator being recorded by hand throughout the test run.

For one position of the measurement volume inside the pipeline the doppler frequencies indicated by the laser doppler velocimetry instrumentation were recorded for both the forward and backscatter photomultipliers. These frequency readings were taken from both the spectrum analyzer and the oscilloscope display.

The laser doppler system was then traversed a fixed distance across the pipeline cross section and the new doppler frequencies recorded. This process was repeated until the

whole cross section of the pipeline had been interrogated.

Chapter 5 The Laser Doppler Velocimetry Data Analysis

5.0 Introduction to the Laser Doppler Velocimetry Data Analysis

This chapter will detail the data analysis techniques utilised to process the data obtained during the laser doppler velocimetry test work, which was described in the previous chapter. This work will be divided into a number of sections:

1. A technique to allow an initial validation of the test data to be undertaken. This is detailed in Section 5.1.

2. A method to evaluate the average particle velocity from the discrete particle velocity data points obtained experimentally. This is described in Section 5.2.

3. Slip velocity values and other data are then presented in a graphical form. The resulting data is then discussed.

5.1 Comparison of Actual Particle Velocity Distributions With Air Only Velocity Distributions Obtained From Modelling

During the commissioning of the laser doppler velocimetry instrumentation the relatively complex nature of the equipment meant that a need was identified to be able to carry out a relatively simple analysis of the raw doppler frequency data in order to check that there was not an error in the reading due to operator error or equipment malfunction. It was of some importance that this analysis could be carried out relatively quickly in order that any faults or errors could be identified at an early stage before more data was generated having the same shortcoming.

A simple technique was therefore developed to allow the raw discrete velocity data points to be plotted on the same graph as a curve giving the air velocity predicted using a well established model for the air only condition[G6].

5.1.1 Derivation of Discrete Particle Velocity Data Points

For each position of the interrogated volume across the pipeline diameter, four readings of doppler frequency were recorded. Frequency readings were taken from both the forward and backscatter photomultipliers, the value of each being displayed on both the oscilloscope and the spectrum analyzer.

For much of the range of test conditions and interrogated volume position, these readings were in close agreement, often within 1%. Under such circumstances all four readings were averaged. However, under some flow conditions and with the interrogated volume in certain positions on the pipeline diameter (notably close to the pipeline walls), some of the readings became less reliable, and in some cases, no reading could be obtained from one photomultiplier. Under these conditions, the less reliable readings were omitted from the averaging process. Thus, an average doppler frequency for each discrete position of the interrogated volume across the pipeline diameter was obtained.

Using the calibration technique described in Section 4.3.2, the relationship between the doppler frequency and the particle velocity was obtained. Each average doppler frequency was multiplied by this value to obtain the corresponding discrete particle velocity data point.

5.1.2 Derivation of Air Only Velocity Distributions Based a Model

The Reynolds number of the flow in the pipeline for a superficial air velocity of 25m/s was calculated as $Re = 8.2 \times 10^4$. Prandtl[G6] reports that a one seventh power law model is adequate to predict the velocity distribution in a pipeline when the Reynolds number is in the region of 10^5. This model is illustrated in Figure 5.1 along with other power law models for reference.

For the purposes of the data under discussion, it was considered that it might be more useful to normalise the velocity values to the average air velocity, based on the air volumetric flow rate and the pipeline bore, rather than the peak value, since the value of the average was reliably known, and ultimately it was the average velocities that were to be compared. The discrete particle velocity data points were also normalised

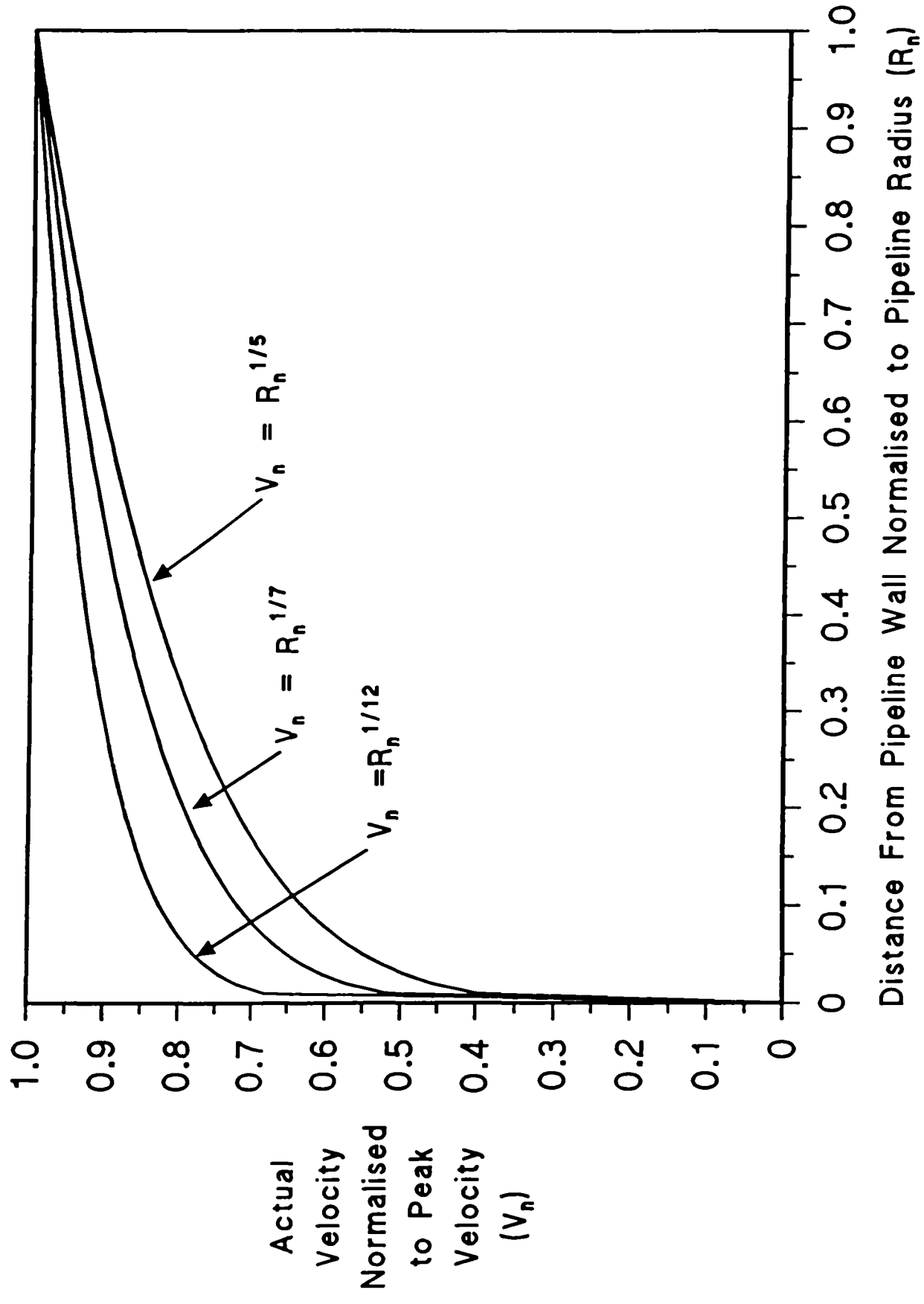

Figure 5.1 Illustration of Power Law Models

to the average air velocity and the points plotted on the same graph as the air only air velocity curve. Thus, for each test run, a graph was obtained similar to that shown in Figure 5.2.

5.1.3 Analysis of Comparison Data

Immediately after each test run had been completed, the data analysis process described above was carried out and a graph plotted. A visual inspection then allowed a simple assessment of the validity of the recorded and computed results.

5.2 Derivation of Average Particle Velocity Data

In order to obtain a value for the average particle velocity it was necessary to carry out an integration of the discrete velocity data points obtained at various points across the pipeline cross section. Two techniques were considered:

1. A numerical technique. Each discrete velocity value could be multiplied by the area of the annular part of the cross section appropriate for that data point. The volumes thus obtained for each discrete velocity data point could then be summed to give the average particle velocity.

2. An analytical technique. A best fit line through the discrete data points could be determined. The equation describing this line could then be integrated analytically using a volume of revolution technique.

The numerical technique suffers from the inaccuracies inherent in this technique when applied to a limited number of discrete data points. On the other hand, the analytical technique relies on being able to determine a best fit line which can be adequately described with a relatively simple equation which will lend itself to the volume of revolution integration technique. Some experimentation was needed at this stage before a choice of technique could be made.

Initially a power law model was considered as the basis for a best fit straight line. The details of this technique are given in Section 5.2.1 below. This was found to provide a fit of good accuracy for all of the test results. This also had the added advantage of

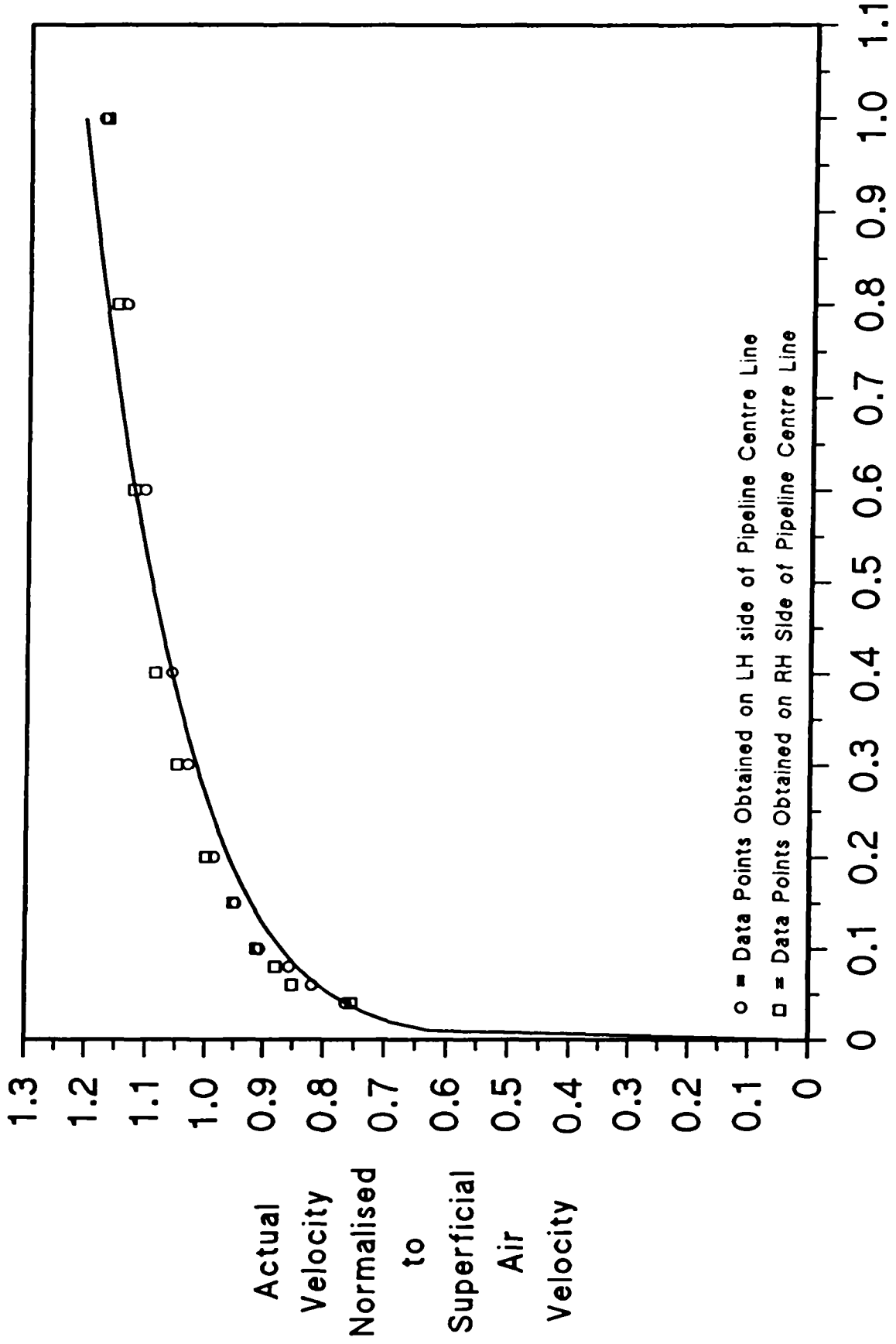

Figure 5.2 Graph Showing the Descrete Part
Plotted on the Same Graph as the Modelle

indicating a power law model for the data from each test run, thus providing some simple variables by which the measurements taken at various test conditions might be compared.

The decision was thus made to adopt the analytical integration technique.

5.2.1 Curve Fitting of Actual Particle Velocity Data Points

As noted in the previous section a power law model of the form below was initially considered.

$$Y = A.X^n$$

Where X is the distance of the particle velocity measurement point from the pipeline wall normalised to the pipeline radius.

Y is the value of the measured particle velocity normalised to the superficial air velocity.

n and A are constants.

It was considered that the most straight forward method by which the value of A and n might be determined would be by taking logarithms of the equation to obtain the straight line equation as shown below.

$$Log(Y) = Log(AX^n)$$

Therefore

$$Log(Y) = Log(A) + n.Log(X)$$

The standard least squares best fit technique[G9] could then be used to fit the straight line equation to the logarithms of the data points. The power law model coefficients A and n are then obtained by taking antilogarithms of the best fit linear equation. The value of A and n for each set of test data are tabulated in Appendix 3.

5.2.2 Validity of Power Law Model Close To Pipeline Wall

It was considered that there was some question as to whether equations of the best fit curves derived in the way outlined above accurately modelled the particle velocities close to the pipeline wall. The closest discrete data point to the pipeline wall was 1mm away from it, and although this point was generally very close to the best fit line, it was considered that there was some uncertainty as to the validity of the equation closer to the pipeline wall. The area of the annulus between the pipeline wall and 1mm into the pipeline was calculated as 7.8% of the pipeline cross sectional area, thus any significant error in the velocity value taken for this annulus could be significant in the overall calculation of the average particle velocity.

It is clear that at the pipeline wall, for the power law models to hold, the particle velocity must be zero. However, a particle cannot exist with it's centre line at the pipeline wall because all particles have a finite size, the average particle size of the coal and flour used for the test work being approximately 70μm. So there must be a region close to the pipeline wall where the models of the experimental data are not applicable.

It was considered that the most important question was how close to the pipeline wall are the models valid? If the percentage of the pipeline cross section in which they are not valid is very small, then it was considered that the resulting error could be ignored.

Clearly there will be a discrepancy in the 50 or so microns close to the pipeline wall because particles having diameters up to 100μm cannot have their centre lines within this region, and so the model cannot be valid. We also know that the models seem to hold 1mm from the wall because the data points agree with the models at that point.

It was considered that there would be considerable disturbance to the flow in the 50 to 100μm closest to the pipeline wall because of particles coming into contact with the pipeline wall or because of particles undergoing high accelerations caused by the very steep air velocity gradient in this region. However, it was considered that the models derived from the test data would represent good approximations to the true particle velocities more than 100μm from the pipeline wall. If this was the case, the area of

the pipeline cross section for which the models do not hold will be only 0.8% of the total.

Thus, it was concluded that the error introduced into the calculations by taking the models derived from the test data to be valid across the whole pipeline cross section will be less than 0.8%. Since the accuracy of the calibration of the laser doppler velocimetry instrument was 1% this was considered satisfactory.

5.2.3 Derivation of Average Particle Velocity Data

Having determined the equation of the best fit power law model, it was then necessary to integrate this equation across the pipeline cross section in order to evaluate the average particle velocity. A small problem was encountered here, since the volume of revolution about the pipeline centre line was required, whereas the values of normalised pipeline radius used to find the best fit model (x) were relative to the pipeline wall. Thus, a simple substitution of x = (1-x) was required.

The standard volume of revolution formula for revolution about the y axis[G9] is:

$$V = 2.\pi \int_{x_1}^{x_2} x.y dx$$

Therefore in our case

$$V = 2.\pi.G \int_{0}^{1} x.(1-x)^{n}.dx$$

Where G = Ratio of peak particle velocity to average particle velocity

n = power of the power law model

This was evaluated by the standard integration by parts technique[G9], giving

$$V = 2.\pi.\frac{G}{(n+1).(n+2)}$$

G and n were then substituted for each data set, and the expression evaluated. The results are tabulated in Appendix 3.

5.3 Particle Slip Velocity Data

Having evaluated the average particle velocity as determined by the laser doppler velocimetry technique, by comparing these values with those of the air velocity it was possible to calculate the average particle slip for the range of conditions tested. The percentage difference between the superficial air velocity (V_{as}) and the average particle velocity obtained by the laser doppler velocimetry method (V_{pldv}) was therefore calculated. This will be termed the slip velocity and will be expressed as a percentage of V_{as}. The percentage difference between the average particle velocity obtained by cross correlation (V_{pcc}) and V_{pldv}, giving an indication of the accuracy of the cross correlation technique, was also calculated. These values are also tabulated in Appendix 3.

Graphs were then plotted of the percentage differences against suspension density (ρ_s). The first graph is shown in Figures 5.3 and will be discussed in the next section. Presentation and discussion of the second graph will be deferred until Chapter 6, where the other data relating to the performance of the electrostatic sensing system will be presented and discussed.

5.3.1 Discussion on Particle Slip Velocity Data

With reference to Figure 5.3, the first point of note is that with the exception of two data points, over the range of conditions tested V_{pldv} is within $\pm 2\%$ of V_{as}. In light of the fact that the combined error of the sensors used to evaluate V_{as} was of the order of $\pm 1\%$, and the calibration accuracy of the laser doppler instrument was of a similar value, it was considered that these results show that over the range of conditions tested, no particle slip was discernable.

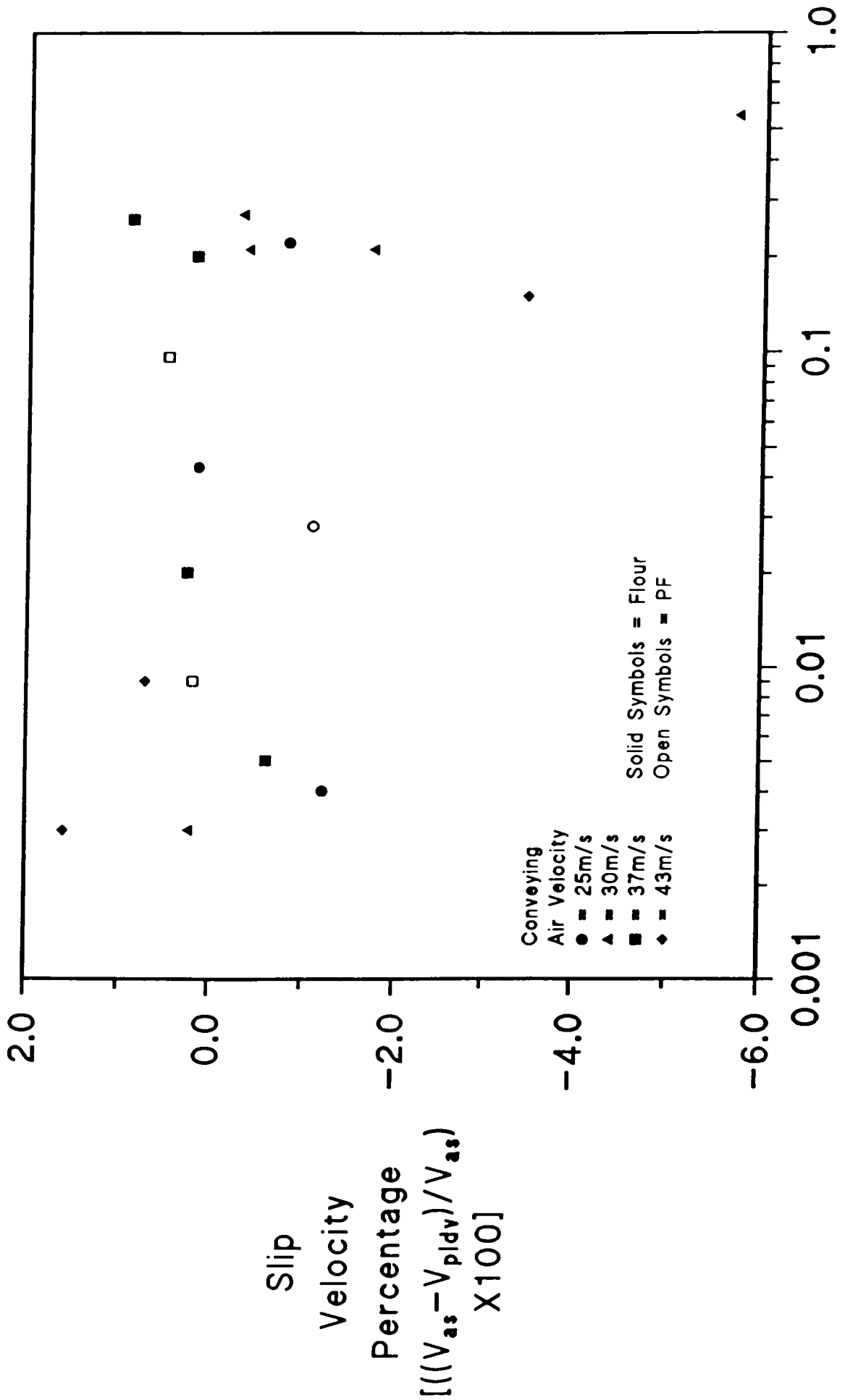

Figure 5.3 Graph of Particle Slip Velocity as Determined by the LDV Against Suspension Density for a Range of Conveying Air Velocities

This was a very interesting result, because the work of other authors as discussed in Chapter 2 give values between 5 and 50% for different conveyed materials and conditions. One might expect the values obtained to be towards the low end of this range, since the work was carried out with fine particles (mean particle size approximately 70μm - see Appendix 2) and at low suspension densities. However, the value of zero is still lower than might have been expected.

It is also worthy of note that the data from the three test runs carried out with PF is consistent with the data from those carried out using wheat flour as discussed in Section 4.4. No distinction will therefore be made between these materials during the remainder of the discussion.

With respect to the two data points which fall outside the tolerance of $\pm 2\%$, it was considered that some analysis was required here in attempt to decide whether they are due to experimental error or any real effect. Both points suggest V_{pldv} above V_{as}, which initially seems impossible. It poses the question as to whether there are any circumstances by which the particles travel faster than the air? A possibility which was considered was that the superficial air velocity(V_{as}) determined from measurements was lower than the actual average air velocity.

The superficial air velocity in the pipeline test section was calculated by the data logging sub system of the test rig, which calculates the mass flow rate of air into the pipeline, calculates the equivalent volumetric flow rate at the pressure and temperature in the pipeline test section, and then calculates the air velocity from a knowledge of the pipeline internal diameter. No account is taken of the volume occupied inside the pipeline by the particles. Clearly, the volume occupied by the particles will increase with suspension density, and both data points occur at the high end of the suspension density range tested.

A calculation was therefore carried out to determine the percentage of the pipeline volume occupied by the particles at various suspension densities. At a suspension density of 1.0kg/m^3, which represents the worst case for the test results under

consideration, the volume occupied by the particles is 0.1%. Clearly this is insignificant in comparison to the discrepancies of 3 or 4% under consideration and the volume occupied by the particles was therefore discounted.

It was therefore decided to scrutinise the reliability of the data points in question. The reliability of the measurements made by the laser doppler velocimetry instrumentation at the high end of the range of suspension densities tested was considered to be less than that at lower suspension densities. This is due to the fact that less of the laser light was able to penetrate the pipeline because of attenuation by the particles present. This in turn caused a reduction in the signal to noise ratio of the doppler signal, making it more difficult for the operator to read the value of the doppler frequency from the oscilloscope or spectrum analyzer, introducing a possible source of error.

Both the data points in question occur at the top end of the range of suspension density and so the data points outside the $\pm 2\%$ tolerance considered to be attributable to this reduction in reliability of the instrumentation.

5.4 Power Law Model Data

In addition to providing a best fit line of the discrete data points, the power law model constants obtained in Section 5.2.1 allow some comparison of the characteristics of the particle velocity profiles obtained over the range of conditions tested. The significant constant with respect to the velocity profile shape is n, the power in the power law model. The value of n was therefore plotted against ρ_s yielding the graph shown in Figure 5.4.

5.4.1 Discussion of Power Law Model Data

Although significant scatter of the points is present, a consistent trend of increasing n with increasing ρ_s is observed for fixed V_{as}.

As noted in Section 5.1.2, Prandtl[G6] reports that a one seventh power law model is applicable to air only flows in circular pipelines having a Reynolds number(Re) in the region of 10^5. Prandtl also suggests that this value increases with increasing Re. (for an air only flow) up to a one tenth power law for flows having Re up to 10^6.

It may be seen from Figure 5.4 that the power of the power law model for low values of ρ_s is between 6.5 and 8.5. As ρ_s increases, the value of n increases to between 8.0 and 10.5.

It must be noted here that Prandtl's work was based on single phase flows, and concerns the modelling of the air only velocity profiles. The test work from which Figure 5.4 is derived measured particle velocities in a two phase flow. However, the average particle and air only velocities obtained during the test work are in good agreement, and so it seems reasonable to assume that the velocity distributions will be similar for both gas and solids phases over the range of conditions tested.

If this is accepted, then it seems that by introducing solid particles into an air only flow, the flow behaves in some respects in the same way as a single phase flow having a higher Re.

This increasing Re with increasing ρ_s may also be considered from the point of view of taking Re as an indication of the relative predominance of momentum and frictional forces acting within a flowing fluid. For relatively high values of Re, momentum forces may be considered to predominate, whilst at low values of Re, frictional forces associated with the viscosity of the fluid predominate.

Thus, by introducing small particles having a high density, and which flow at the same velocity as the fluid, the momentum forces acting within the fluid will be enhanced relative to the frictional forces, which may in fact be reduced by the presence of the solid particles interfering with the molecular structure of the fluid.

5.5 Boundary Layer Width Data

Having established that there was considerable variation in the characteristics of the measured particle velocity profiles, it was considered that it would be of interest to calculate a value for the width of the so called turbulent boundary layer of the flow inside the pipeline. This could then be plotted for various values of ρ_s and V_{ss} in an attempt to isolate any underlying relationships.

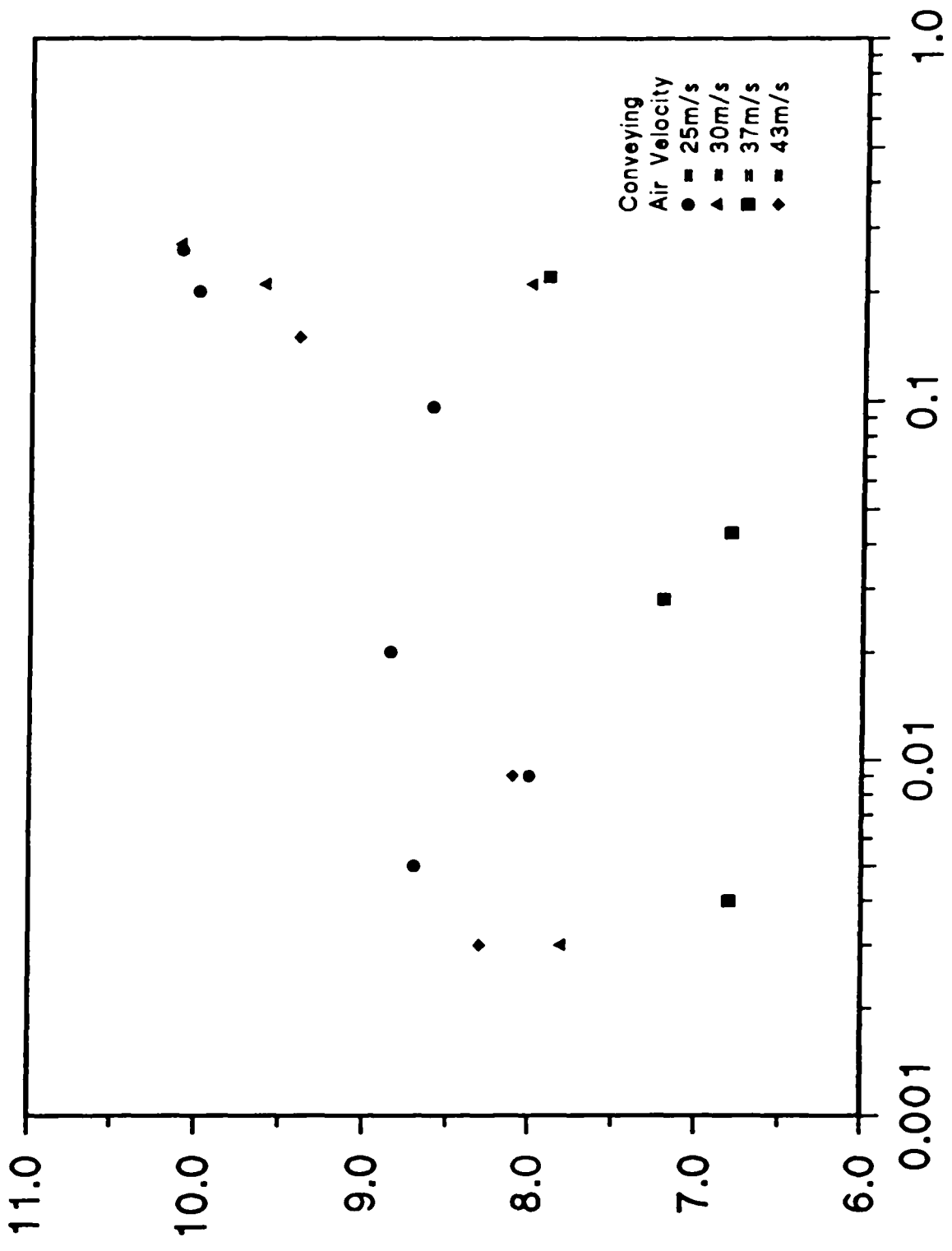

Figure 5.4 Graph of the Power Law Model Power Against Suspension Density for a Range of Conveying Air Velocities

5.5.1 Derivation and Presentation of Boundary Layer Width Data

Having made this decision, the first question was how to define the width of the boundary layer. No definitive definition of the boundary layer was available, other than the fact that it was a region of rapidly increasing velocity gradient and turbulence close to the pipeline wall. Since no definition was available, it was decided to take the distance between the pipeline wall and the point at which the velocity profile fell to 70% of it's peak value, as an arbitrary value for the width of the boundary layer. The values of the boundary layer width (d_{BL}) so defined, are tabulated in Appendix 3 for each test condition.

A graph of d_{BL} against ρ_s for a range of values of V_{as} was plotted and is shown in Figure 5.5.

5.5.2 Discussion of Boundary Layer Width Data

As would be expected following the discussion of Section 5.4, for a fixed value of V_{as}, d_{BL} generally decreases with increasing ρ_s.

With the reduction in d_{BL} at higher values of ρ_s, there will be a consequent flattening of the velocity profile, as would be expected for higher values of n, the power law model power(see Figure 5.1). Thus, the proportion of the pipeline cross section over which the flow velocity is close to the peak velocity is increased at high values of ρ_s. Since a higher velocity is present over a larger proportion of the cross section, all other variables being unchanged, we might expect some reduction in the energy required to force the fluid along the pipeline.

An implication of this is that by introducing fine solid particles into a gas flow it may be possible to reduce the pipeline pressure drop and thus the energy required to pump or compress the gas.

Unfortunately, it was not possible to quantify this reduction in pressure loss in the test rig. This was due to the fact that the pipeline pressure drop measured by the data logging sub system of the rig was sensitive to a range of other variables, such as air velocity and filter pressure drop, both of which will vary with varying suspension

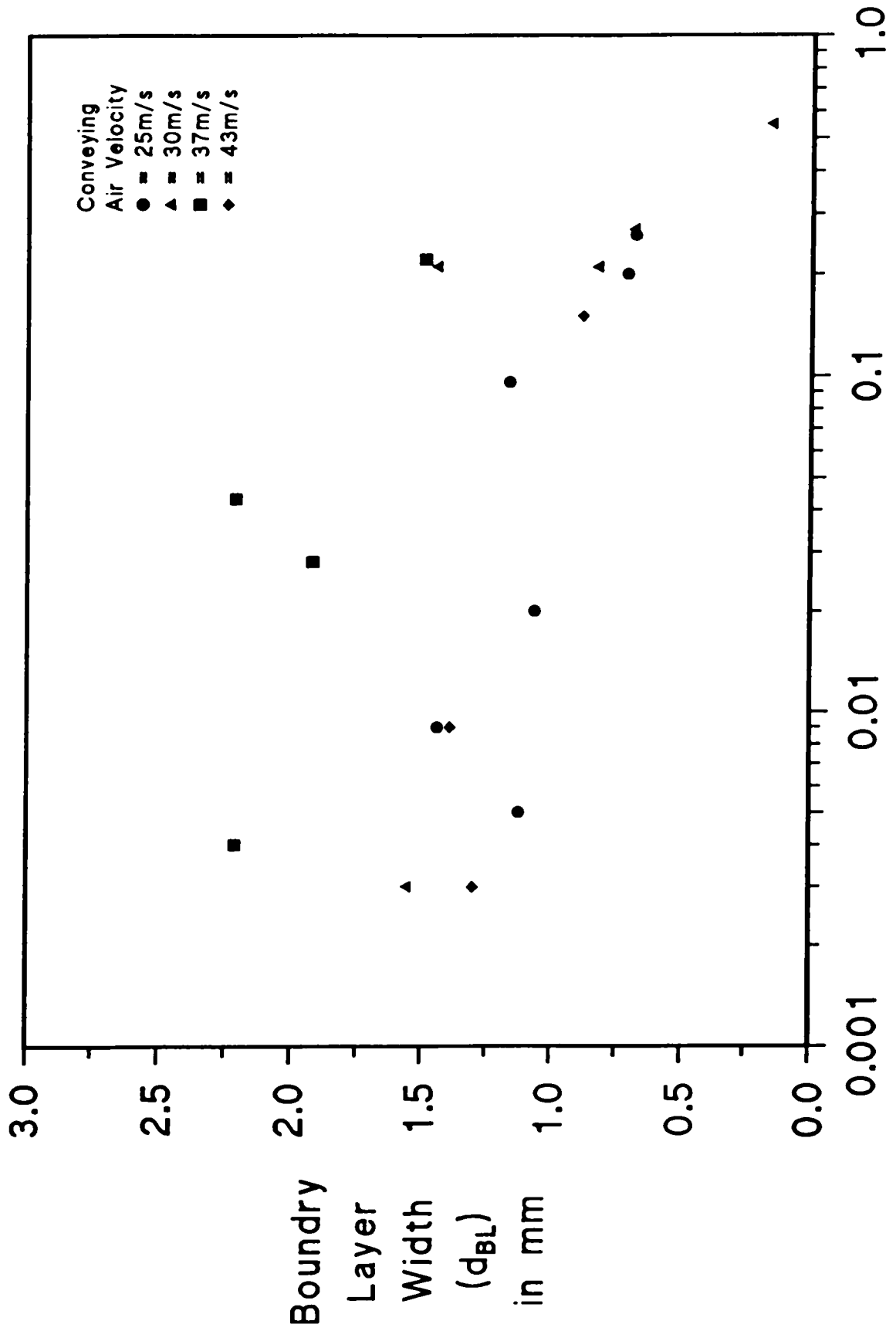

Figure 5.5 Graph of Nominal Boundry Layer Width Against Suspension Density for a Range of Conveying Air Velocities

density in the test rig.

However, the effect, commonly referred to as 'drag reduction', has been documented by a number of other authors, notably Soo[C1] and Kolansky et al[C2]. If this pressure loss reduction can be realised in real systems, such as long distance gas pipelines, it is conceivable that significant energy savings could result.

Chapter 6 The Electrostatic Sensor Test Work

6.0 Introduction to the Electrostatic Sensor Test Work

As outlined in Section 2.6, following the literature survey and some limited trials carried out by the author, it was decided that a PF mass flow rate measurement system based on the electrostatic principle was worthy of further investigation.

This chapter details the programme of work undertaken, using the experimental test rig described in Chapter 3, to assess the applicability and accuracy of such a system. As detailed in Section 2.1, the measurement of mass flow rate by this technique requires the evaluation of both suspension density and average particle velocity. A programme of work to assess the ability of the electrostatic sensing system to measure these variables was therefore undertaken and will be described.

The results of the test work will then be presented, and discussed. A more detailed discussion with respect to some aspects of the experimental results will be deferred until Chapter 7, where these results will then be discussed in the light of a mathematical model describing the operation of such sensors.

6.1 Objectives of the Test Work on Electrostatic Sensors

The major objective of this aspect of the programme was to assess the applicability and accuracy of the electrostatic sensing system when applied to average particle velocity and suspension density measurement in pulverised fuel (PF) injection systems.

It was considered that the best way to achieve this task was to define a number of component objectives, such that when all had been achieved, the major objective would also have ben achieved.

The component objectives were as follows:

1. Assess the accuracy with which the single electrostatic sensor was able to

measure suspension density.

2. Assess the accuracy with which the sensors, in combination with the cross correlator could measure the average particle velocity.

3. Assess the sensitivity of the electrostatic sensing system to major operational variables such as: particle size distribution of PF; conveying air relative humidity and upstream pipeline geometry.

6.2 Principle of Operation of the Electrostatic Sensing System

The principle of operation of the electrostatic sensing system is shown in Figure 6.1. Two steel ring type probes are incorporated into the wall of the test pipeline, each being separated from the steel pipeline by nylon insulating rings. A guard ring is also incorporated between the two probes, this being connected to the main pipeline sections which are in turn connected to earth.

Each of the two axially spaced sensor rings are connected to the input of their own charge amplifier. The output of each charge amplifier is then connected via a buffer to the input channels of the cross correlator. The cross correlator evaluates the transit time between the two signals and thus the velocity of the particles inducing the signals as detailed in Section 2.1.2. The velocity thus obtained is then displayed on the front panel of the correlator.

The output from one charge amplifier is is also taken to the input of an RMS to DC converter, the output of which gives the DC value of the charge induced on the electrode, and thus an indication of the suspension density.

Further discussion of the mechanism of charge transfer onto the ring probes will be deferred until Chapter 7.

6.3 The Electrostatic Sensing System Test Programme

The test programme was divided into a number of sections, in order to satisfy the

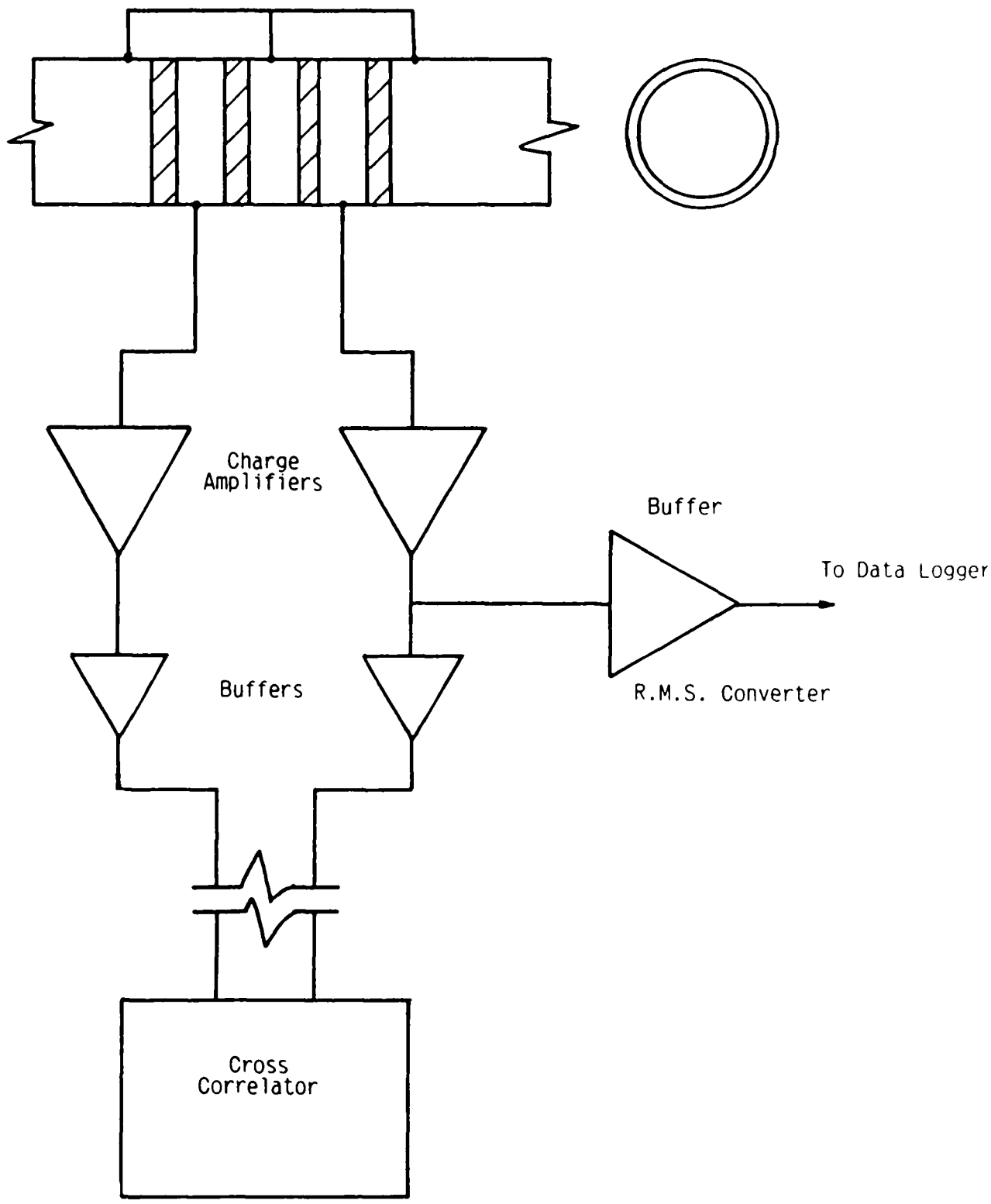

Figure 6.1 Block Diagram Showing Principle of Operation of Electrostatic Sensing System

objectives set out in Section 6.1.

6.3.1 Suspension Density and Average Particle Velocity Tests

The electrostatic sensing system had already undergone tests to evaluate it's performance with respect to the measurement of average particle velocity over a limited range of test conditions. The limitations were imposed by the operational limit of the laser doppler velocimetry instrument. This test programme has been described in Section 4.5, the results of which will be presented and discussed in Section 6.4.

A more complete evaluation of both the suspension density and the average particle velocity measurement techniques required the evaluation of their accuracy over a wider range of suspension densities than the laser doppler velocimetry instrument would operate. The upper limit of suspension density at which the laser doppler velocimetry instrumentation would operate was approximately 0.5kg/m^3. However, commercial PF injection systems operate in the range 0.5 to 5.0kg/m^3. Thus in order to be able to evaluate the sensing system fully, under conditions representative of those utilised in real systems, a wide range of tests would need to be carried out outside the operational range of the laser doppler velocimetry instrumentation. Although the data logging sub system was able to calculate the actual suspension density(ρ_s) inside the pipeline over the full required test range for comparison, the actual particle velocity could not be directly measured over the range of test conditions which would be representative of those found in real systems.

However, it may be seen from Section 5.3 that over the range of conditions that the laser doppler velocimetry instrument was able to operate, the average particle velocity was very close to the superficial air velocity. It was therefore decided to carry out an evaluation of the velocity measurement capability of the electrostatic measurement system by comparing the average particle velocity determined by the cross correlator (V_{pcc}) with the superficial air velocity (V_{as}).

The range of conveying air velocities employed in commercial systems is usually in the range 25 to 35m/s and so it was considered that the range of test conditions should also

include this range.

Tests were therefore carried out over a range of test conditions representative of those found in real PF injection systems. The results are presented and discussed in Section 6.4.

6.3.2 Particle Size Tests

The work of a number of authors, as discussed in Section 2.2, reports that the size of solid particles can have a significant effect on the charge per unit mass held by a powder. Thus, it was considered that the particle size of the conveyed PF may have a significant effect on the performance of the electrostatic suspension density sensor.

It was considered that the particle size would not have any effect on the velocity measurement system, since this relied on calculating the time delay between two signals and was not significantly sensitive to the absolute value of those signals.

Tests of the suspension density sensor were therefore carried out using PF having three different particle sizes distributions, details of which are given in Appendix 2. For each grade of PF, the output voltage of the suspension density sensor was recorded for a range of values of ρ_s. The value of V_{as} was maintained at approximately 27m/s throughout this section of the test work. The results of these tests are presented and discussed in Section 6.5.

6.3.3 Relative Humidity Tests

The work of a number of authors, as discussed in Section 2.2, also reports that the relative humidity (RH) of the conveying air in a pneumatic conveying system can have a significant effect on the particle charging mechanism. It was therefore decided to carry out a number of tests to evaluate the effect of this reported sensitivity on the performance of the suspension density sensor. It was not considered necessary to carry out any tests on the velocity measurement system for the same reasons as outlined in Section 6.3.2.

Section 6.3.2.

The range over which the RH of the conveying air could be varied was somewhat limited by the capability of the air supply to the test rig, the latter not having originally been designed with this purpose in mind. Once again, for each value of RH, the value of the suspension density output voltage was recorded for a range of values of ρ_s, while the value of V_{ss} was maintained at approximately 27m/s. The results of the limited tests undertaken are presented and discussed in Section 6.6.

6.3.4 Pipeline Geometry Tests

It was considered that the performance of the sensing system could be adversely affected by the positioning of the sensor in close proximity to upstream flow disturbances such as pipeline bends. It seems to be widely accepted that this is indeed a problem with many single phase flow measurement methods[G11].

It was therefore decided that in order to be able to fully assess the applicability of the sensing system, some assessment of this effect was necessary. A number of tests were therefore carried out for three different configurations of pipeline. For each configuration, and distance between the sensor and bend(s), the electrostatic density sensor output voltage was recorded for a range of values of ρ_s, again with the value of V_{ss} being maintained at approximately 27m/s. The cross correlation coefficients calculated by the cross correlator were also recorded. The pipeline configurations used were:

1. The pipeline was configured as shown in Figure 6.2a, with a single bend in the horizontal plane positioned at various distances upstream of the sensor.

2. The pipeline was configured as shown in Figure 6.2b, with two bends, one directly after the other in different planes positioned at various distances upstream of the sensor.

3. The pipeline was configured as shown in Figure 6.2c, with a single bend in the vertical plane positioned at various distances upstream of the sensor.

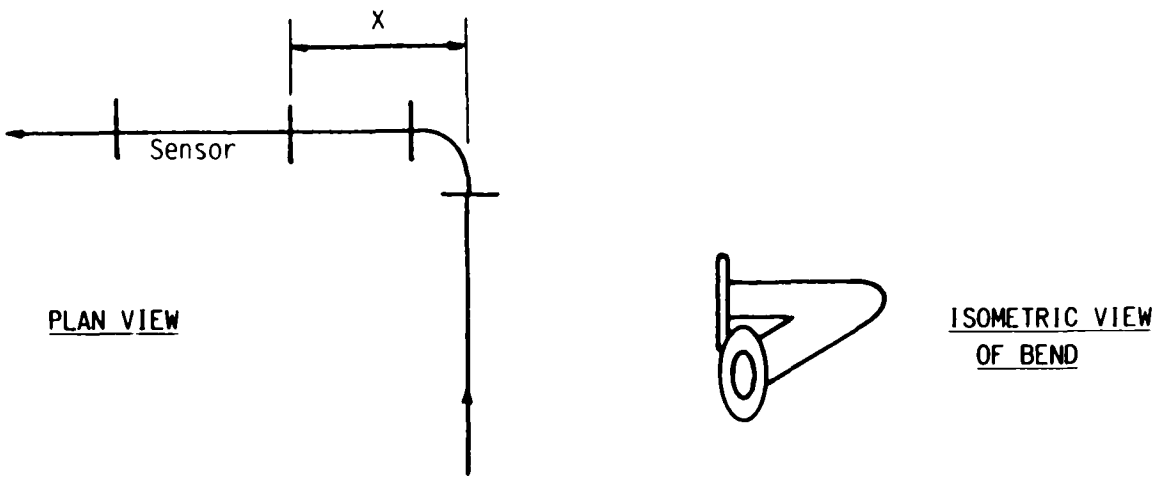

a) Single Bend in Horizontal Plane

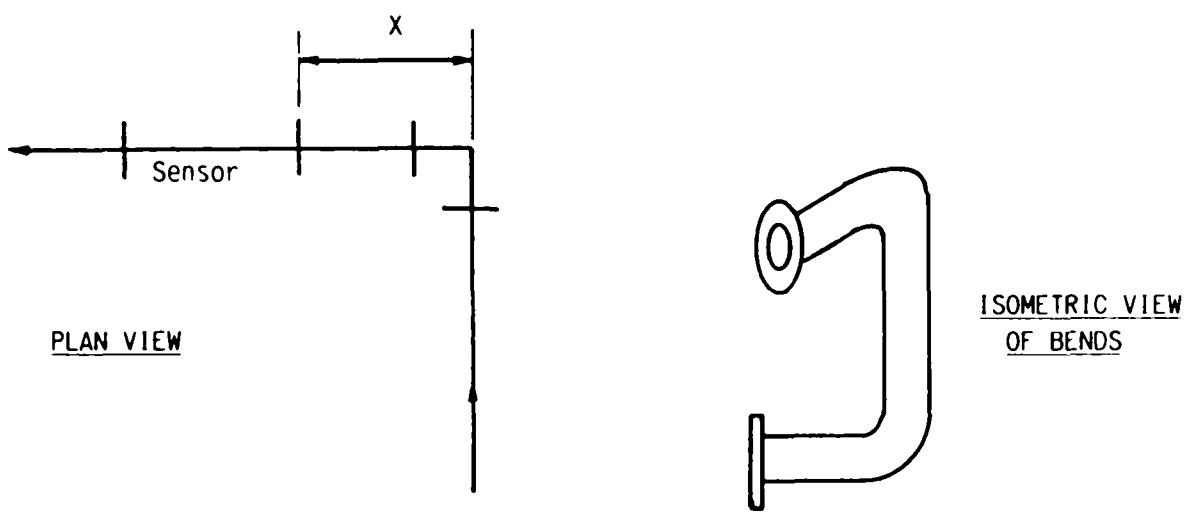

b) Double Bend

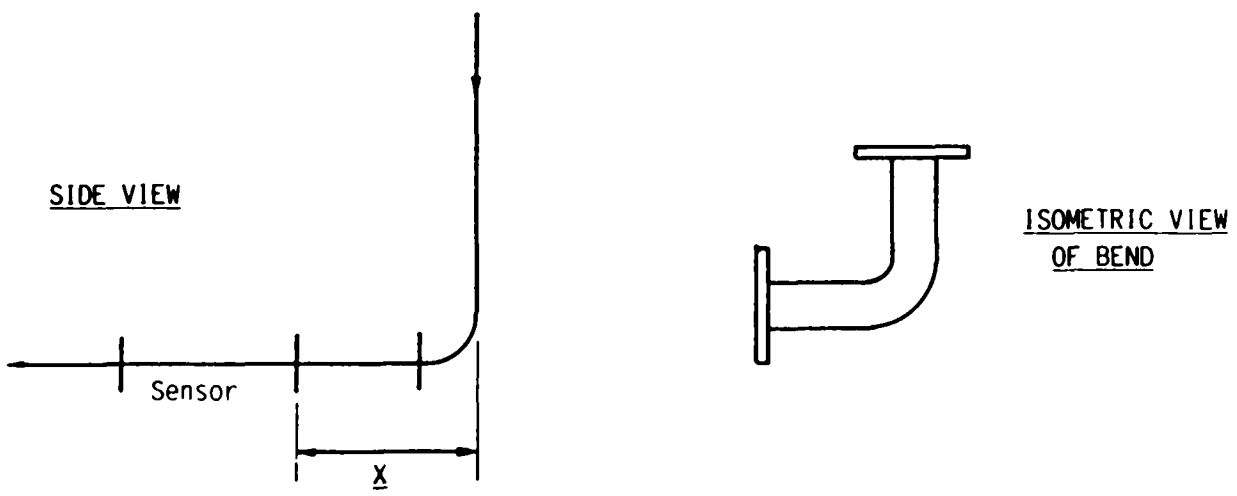

c) Single Bend in Vertical Plane

Figure 6.2 Pipeline Configurations Used

For each configuration, a straight pipeline section of at least 4.5m was used upstream of the bend(s), since it was considered that this would minimise the effect of any flow disturbances further upstream.

The results of these tests are presented and discussed in Section 6.7.

6.4 Suspension Density and Average Particle Velocity Test Results

The results of three sets of tests will be presented and discussed in this section:

1. Comparisons between V_{pcc} and the average particle velocity determined by the laser doppler velocimeter (V_{pldv}) over the limited range of conditions imposed by the operational limits of the laser doppler velocimeter.

2. Comparisons between V_{pcc} and V_{ss} over a wide range of conditions considered to be fully representative of those found in industrial PF injection systems.

3. Comparisons between the electrostatic suspension density sensor reading and the actual suspension density calculated by the data logging sub system (ρ_s) over the same range of conditions as 2. above.

6.4.1 Comparisons Between V_{pcc} and V_{pldv}

The percentage difference between V_{pcc} and V_{pldv} were calculated and are tabulated in Appendix 3. A graph of the percentage difference against ρ_s is shown in Figure 6.3.

Clearly, it may be seen from Figure 6.3 that V_{pcc} is consistently below V_{pldv}, generally by approximately 10%. Discussion of possible explanations for this result will be deferred until Chapter 7. However, over the range of conditions tested, the error is generally consistent to within $\pm 3\%$. As discussed in Section 5.3.1, the accuracy of the data derived from the laser doppler velocimetry test work is only reliable to $\pm 1\%$ and the quoted best accuracy of the correlator is of a similar value. Thus, much of the $\pm 3\%$ scatter of the points in Figure 6.2 may be accounted for in these tolerances.

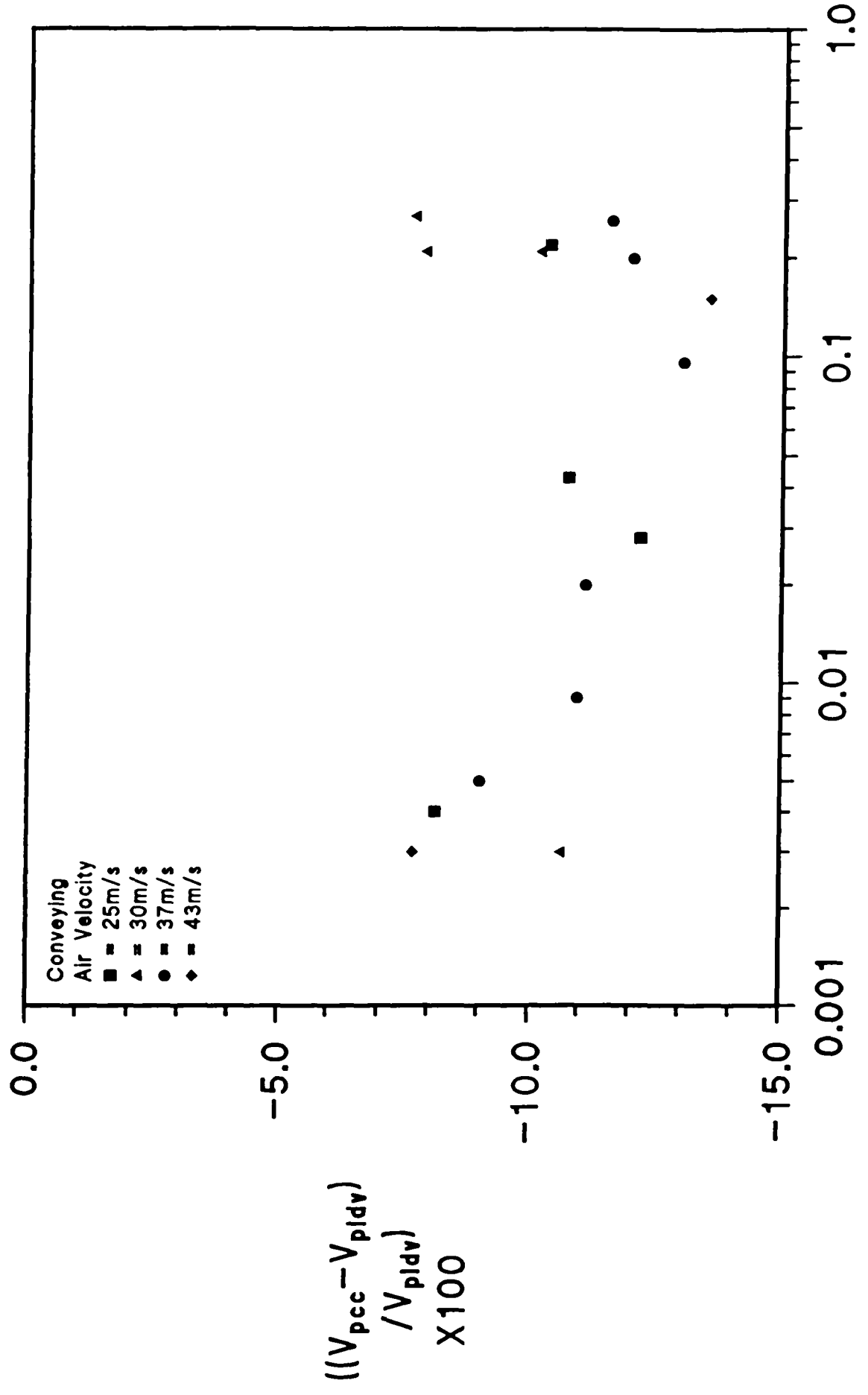

Figure 6.3 Graph of Difference Between V_{pcc} and V_{pldv} Against Suspension Density for a Range of Conveying Air Velocities

Because the -10% error is consistent over the range of conditions tested, it was concluded that this may be removed by calibration, and so the potential accuracy of the technique is in the region of $\pm 3\%$ over the range of suspension densities examined.

6.4.2 Comparison Between V_s and V_{pcc}

The percentage differences between these values were calculated, and these are tabulated in Appendix 3. A graph of the percentage difference against ρ_s was plotted and is shown in Figure 6.4.

There are two points which are worthy of discussion at this point with respect to this data:

1. For values of ρ_s between 0.1 and 0.5kg/m^3, there is significant scatter on the graph. This is consistent with the data presented in Figure 6.3, where the scatter is also significant over a similar range of ρ_s. In addition there is an mean offset in the region of -8%, which is slightly above the value of -10% for the data presented in Figure 6.3. However, generally it seems that the two data sets are consistent, as one would expect.

2. For values of ρ_s between 0.6 and 7.0kg/m^3, there is less general scatter, but some dependency on ρ_s, with the average difference ranging from -7% at a ρ_s of 0.6kg/m^3 to around 0% for a ρ_s value of 6.0kg/m^3. Although this adds some complexity to the data processing, it seems that it should be possible to compensate for this dependency during the derivation of mass flow rate from V_p and ρ_s values. If such a compensation could be carried out, it seems from Figure 6.4 that the accuracy of the cross correlation technique over the range of conditions normally found in PF injection systems could be of the order of $\pm 2\%$.

6.4.3 Comparison Between Density Sensor Output Voltage and ρ_s

The electrostatic suspension density sensor output voltage was plotted against ρ_s for a

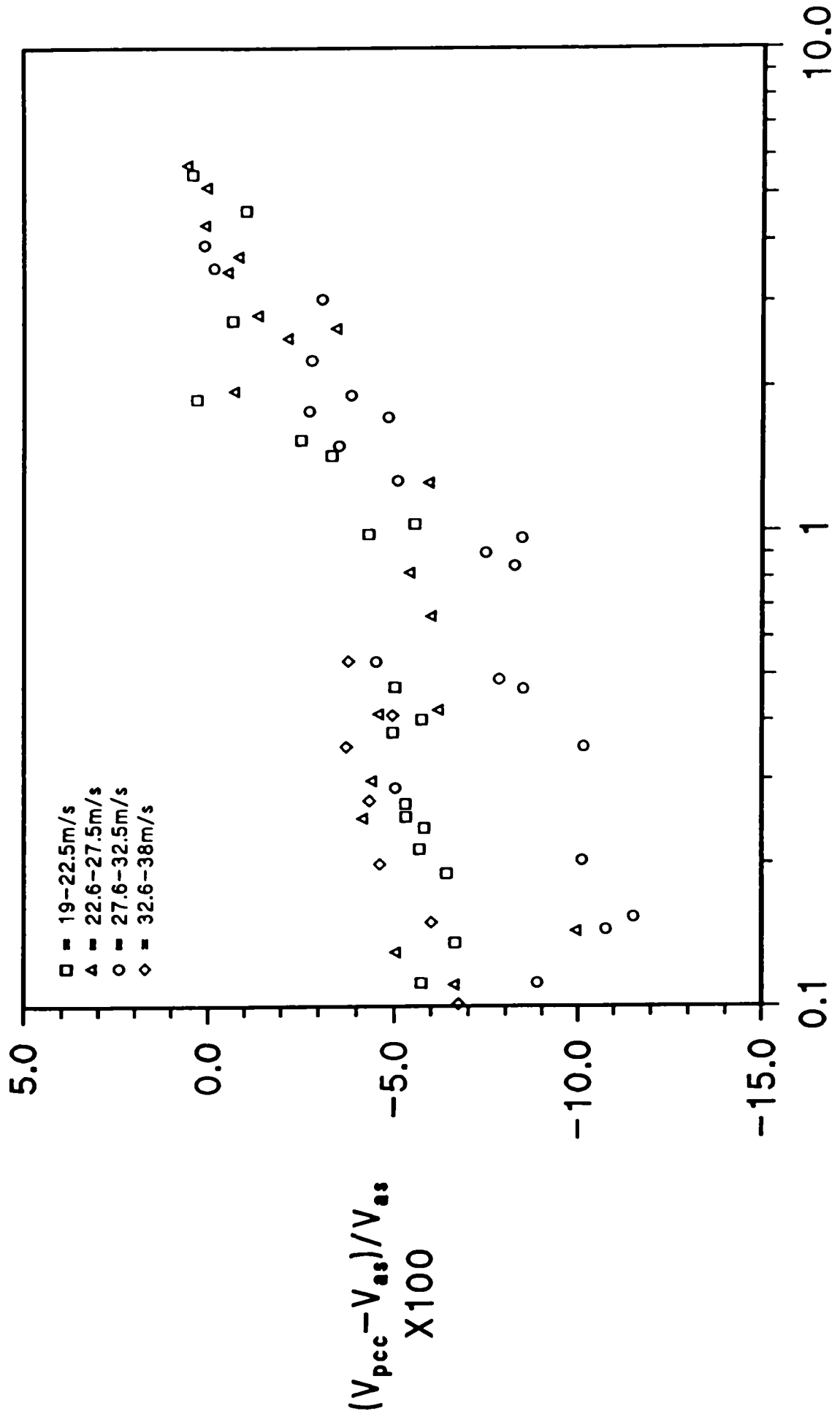

Figure 6.4 Graph of Difference Between V_{pcc} and V_{as} for a Range of Conveying Air Velocities

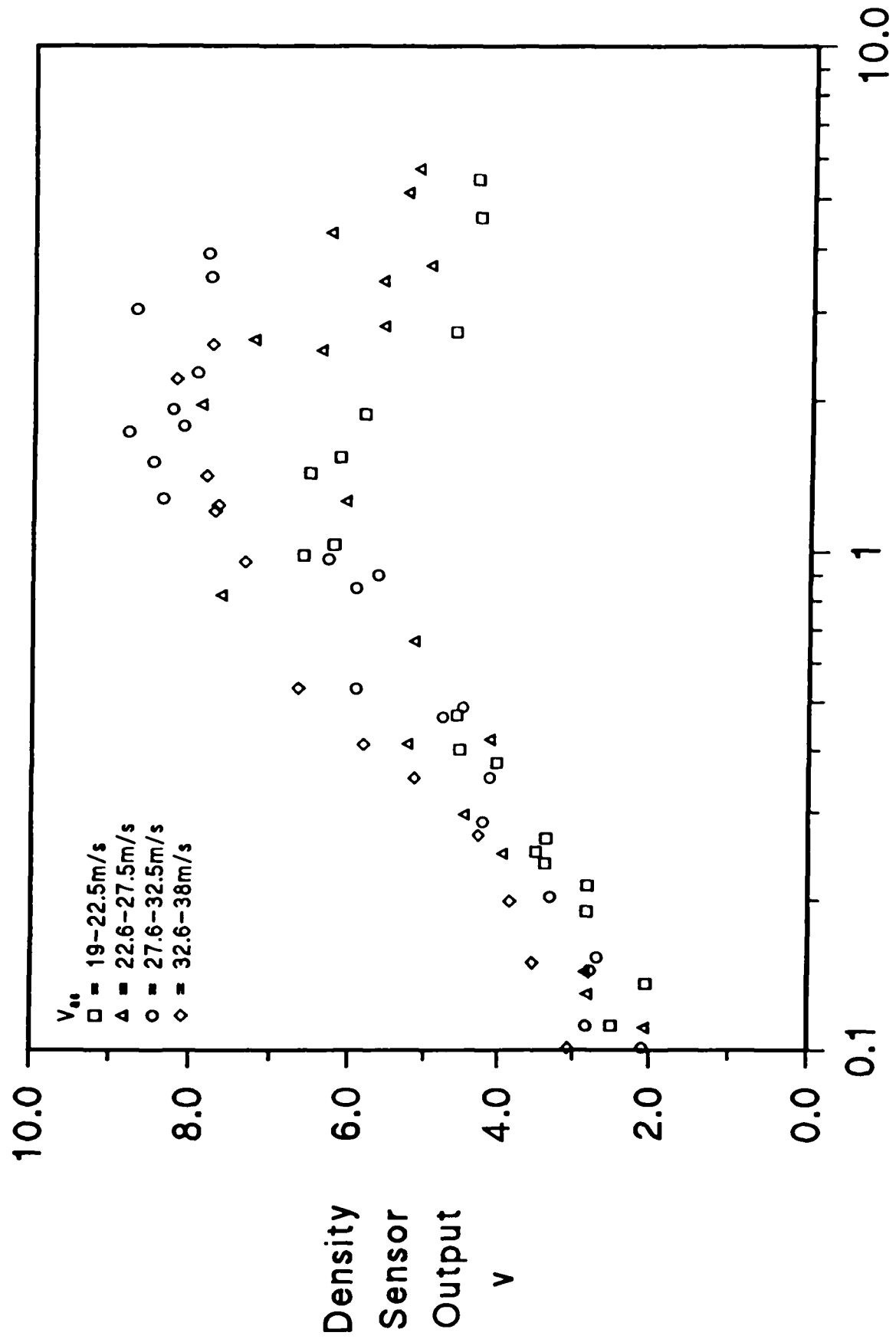

Figure 6.5 Graph of Electrostatic Density Sensor Output Against Suspension Density for a Range of Conveying Air Velocities

range of conveying air velocities. This graph is shown in Figure 6.5. There are two points worthy of discussion at this point:

1. For the range of ρ_s values between 0.1 and 0.5, there is a small amount of scatter on the data points. There is also a discernable sensitivity to conveying air velocity. If the output voltage dependency on conveying air velocity is disregarded on the basis that it is possible to remove it in the PF mass flow rate calculation, then the scatter of the points from visual inspection is in the region of $\pm$0.3v, which represents $\pm$3% of the full scale sensor output. Thus, it seems that for ρ_s values between 0.1 and 0.5kg/m^3 the performance of the sensor is adequate. However, unfortunately most PF injection systems operate at values of ρ_s above 0.5kg/m^3.

2. For values of ρ_s between 0.5 and 7kg/m^3, the performance of the sensor is very different. The scatter, even for a fixed value of air velocity increases markedly. The sensitivity to air velocity increases and above a ρ_s value of approximately 2.0kg/m^3, the sensor has negative sensitivity, with the output voltage decreasing with increasing with ρ_s. This leads to the conclusion that this sensor is not, at least in it's present form, able to reliably measure suspension density over the range of condition normally found in PF injection systems.

6.5 Particle Size Test Results

A graph was plotted of sensor output voltage against ρ_s for each grade of coal, and is shown in Figure 6.6. It was considered that the data points for the different grades of coal were sufficiently close together that it may be assumed that the sensor has negligible sensitivity to the particle size of the coal.

This result was somewhat unexpected following the test results reported by other authors, as detailed in Chapter 2.

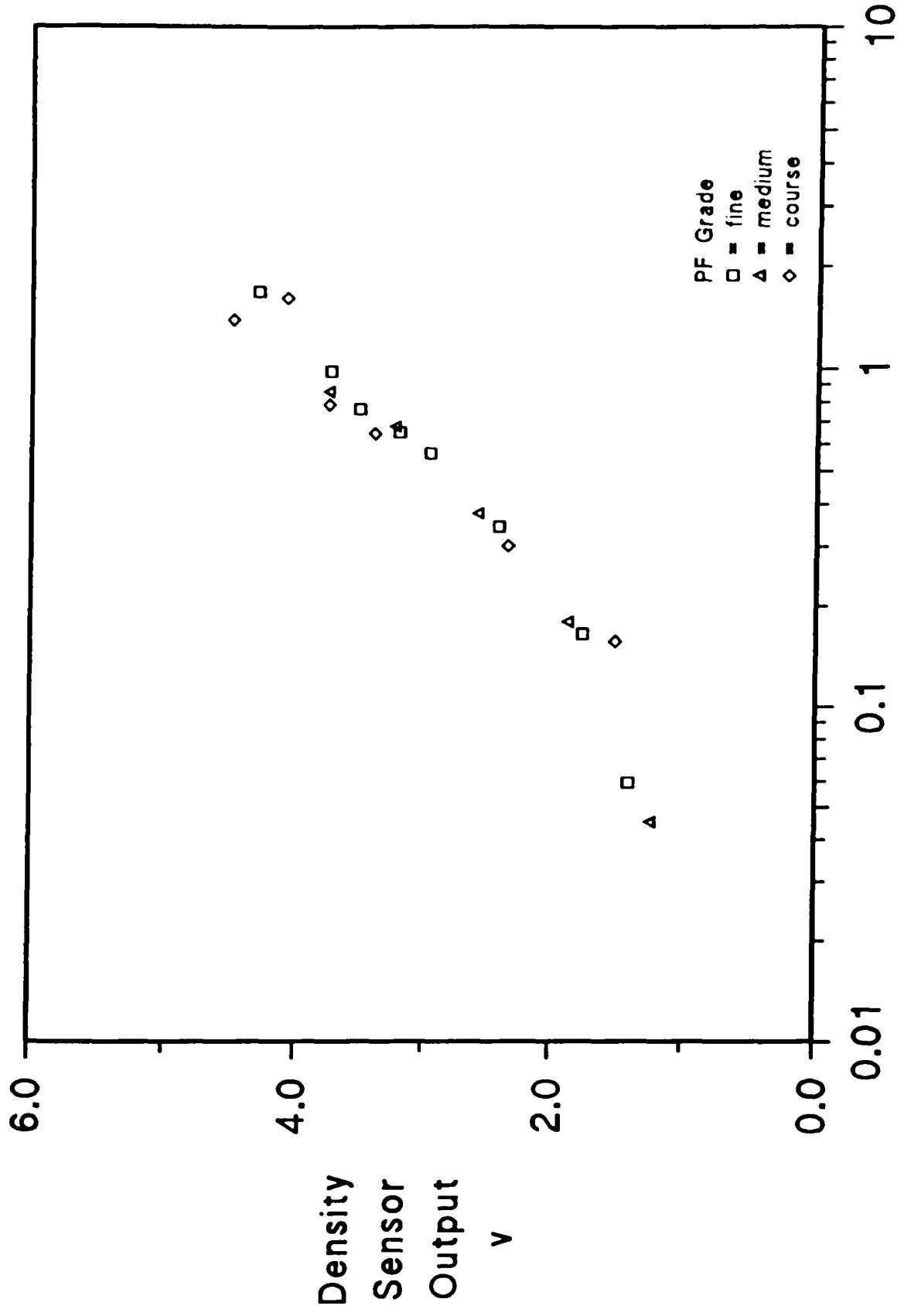

Figure 6.6 Graph of Electrostatic Density Sensor Output Against Suspension Density for a Range of Grades of Coal

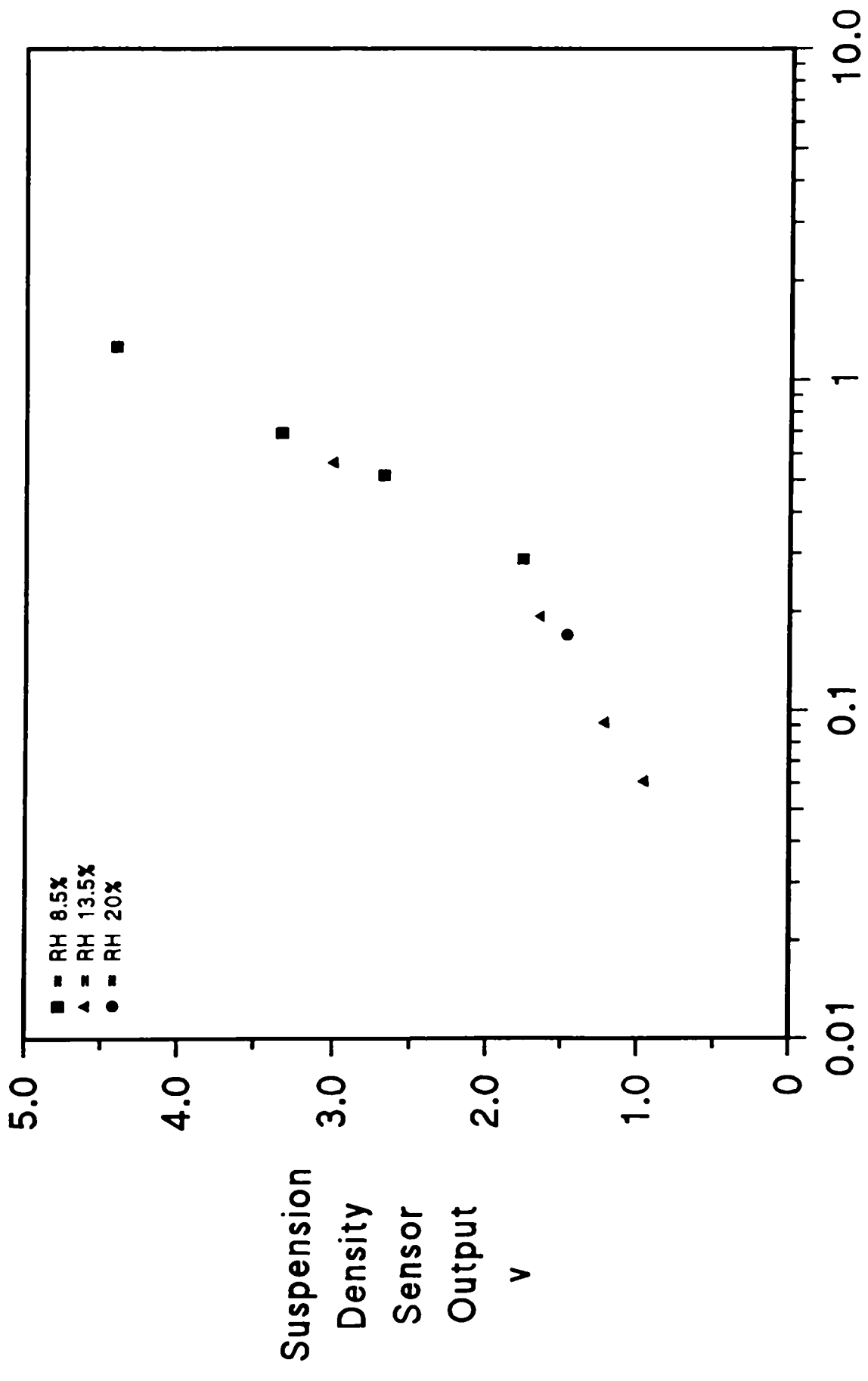

Figure 6.7 Graph of Electrostatic Density Sensor Output Against Suspension Density for a Range of Values of Air Relative Humidity

6.6 Relative Humidity Test Results

A graph was plotted of sensor output voltage against ρ_s for each value of RH, and is shown in Figure 6.7. As discussed in Section 6.3.3, the number of test points is somewhat limited, but it was considered that the data points show that if the suspension density sensor is sensitive to RH, this sensitivity is small. Clearly, the exact effect of RH cannot be determined without more comprehensive test data.

6.7 Pipeline Geometry Test Results

For each of the pipeline configurations used as detailed in Section 6.3.4, a graph was plotted of density sensor output voltage against ρ_s for constant V_{ss} and various values of distance between the bend(s) and the sensor:

- Figure 6.8 shows the graph of the results obtained with a single bend in the horizontal plane.

- Figure 6.9 shows the graph of the results obtained with two bends in different planes, one immediately after the other, in perpendicular vertical planes.

- Figure 6.10 shows the graph of the results obtained with a single bend in the vertical plane.

It may be seen from these graphs that for all of the configurations tested, a flow disturbance in close proximity to the sensor in the upstream pipework has a very significant effect on the performance of the sensor. In both cases where a single bend was tested, when the bend is 0.4m from the sensor, the sensor exhibits negative sensitivity. In all cases, the effects caused by the flow disturbances decrease as the disturbance is moved further away from the sensor, as would be expected.

With respect to the effect of the flow disturbances on the velocity measurement technique, values of V_{cc} and the cross correlation coefficient (C_{cc}) are tabulated in Appendix 4. The values of V_{cc} are not significantly different from those measured with

no flow disturbance present. However, the value of C_{cc} was found to vary significantly when a flow disturbance was present. For all of the tests prior to the pipeline configuration work, C_{cc} was found to be in the range 0.35 to 0.40. In all three cases tested, when a bend or bend combination was situated 0.4m from the sensor, the value of C_{cc} was in the range 0.20 to 0.22. This value was found to increase as the distance between the flow disturbance and the sensor was increased, as would be expected.

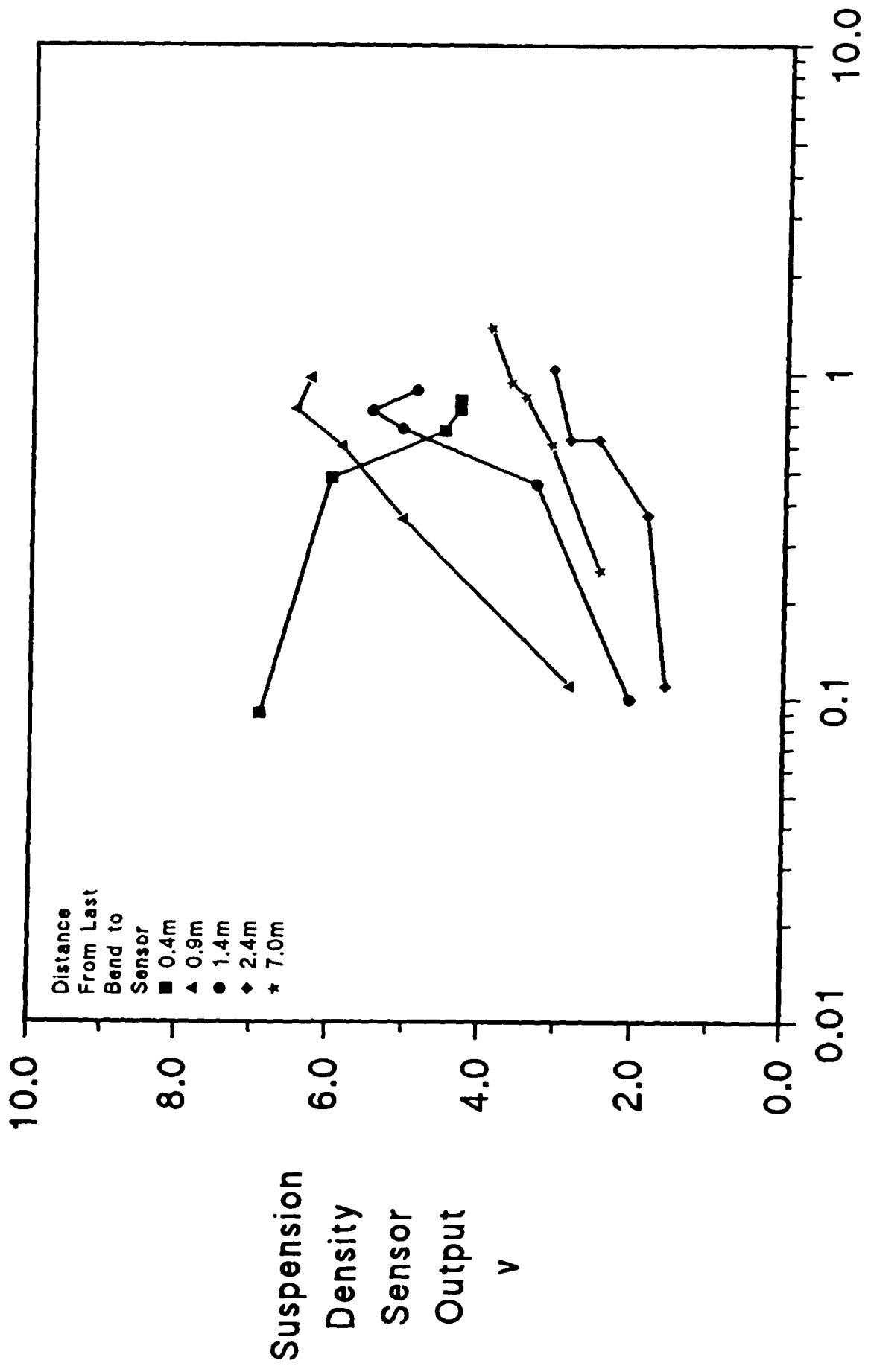

Figure 6.8 Graph of Electrostatic Density Sensor Output Against Suspension Density for a Range of Distances Between Sensor and Upstream Horizontal Bend

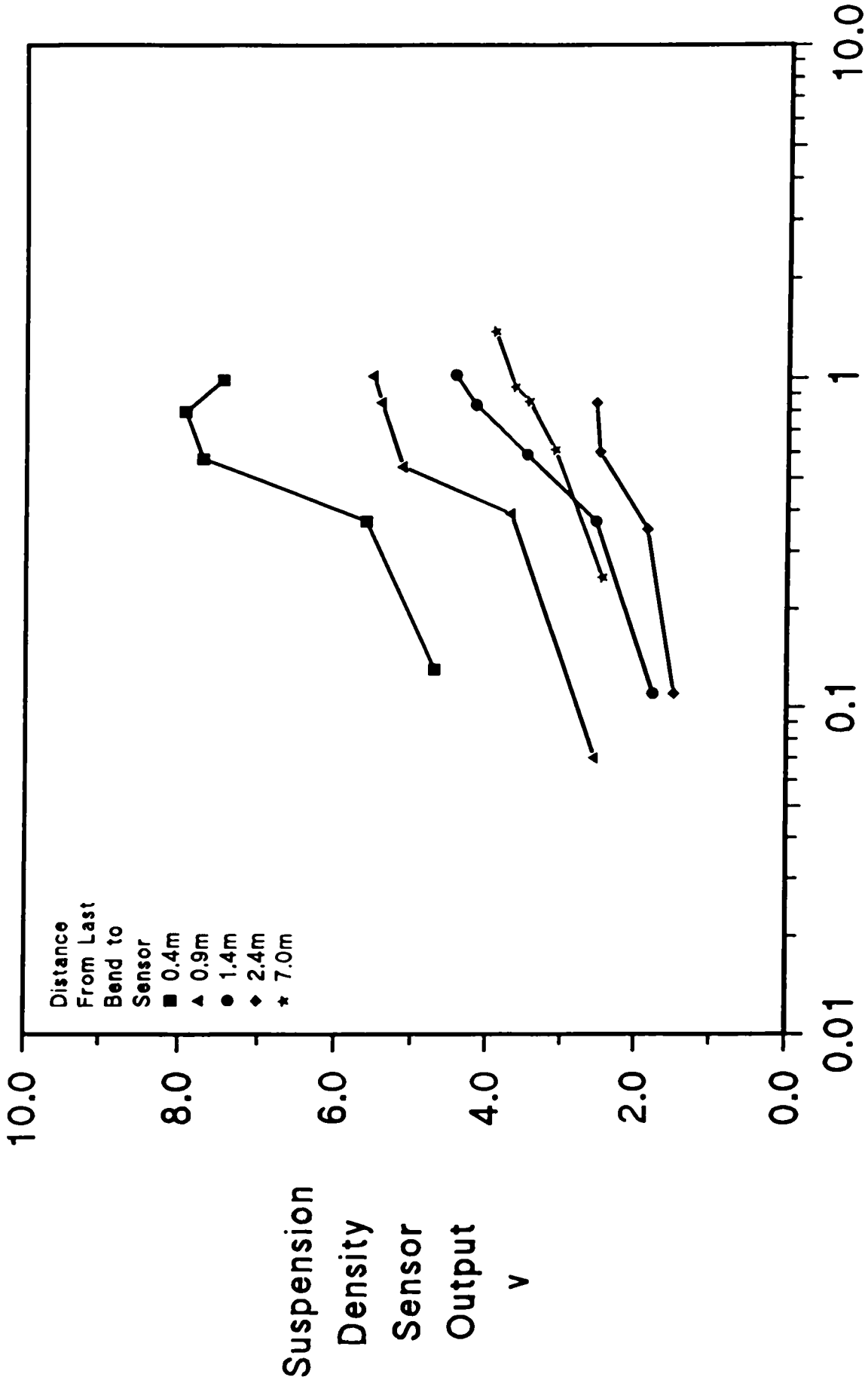

Figure 6.9 Graph of Electrostatic Density Sensor Output Against Suspension Density for a Range of Distances Between Sensor and Double Bend Upstream

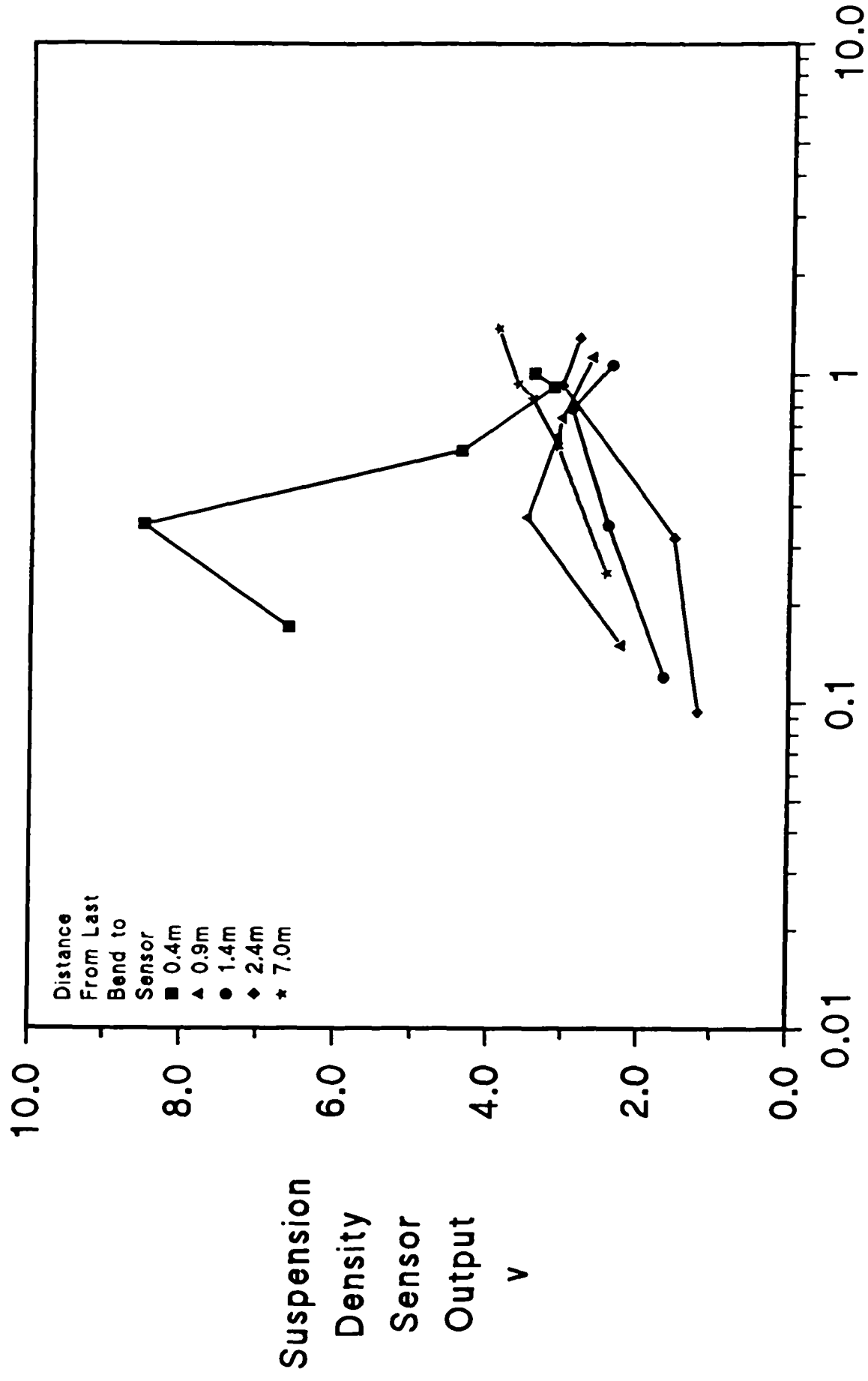

Figure 6.10 Graph of Electrostatic Density Sensor Output Against Suspension Density ffor a Range of Distances Between Sensor and Single Vertical Upstream Bend

Chapter 7 Modelling of the Electrostatic Sensor Operation

7.0 Introduction to the Modelling Work

Chapter 6 has reported on a comprehensive programme of tests that have been undertaken to evaluate the performance of electrostatic type sensors when applied to mass flow rate measurement of PF in pneumatic injection systems. The results of the test work have also been presented and discussed in that Chapter.

Some of the results obtained were not as might have been initially expected and this, combined with the fact that there are some discrepancies in the work of other authors, as well as in the experience of the author of this work, contributed to the decision to develop a model of the mechanism responsible for the operation of the sensor.

Initially it was considered that there was a significant question as to whether the flowing particles needed to come into contact with the sensing rings in order to induce a charge on them. The work of a number of authors discussed in Section 2.2 reports that the charge measured on the sensing rings is induced by charge transfer during contact between the solid particles in the flowing suspension and the sensing ring, as shown in Figure 7.1a. The term "triboelectric" being commonly used to describe the effect.

However, as noted in Section 2.2, Klinzing et al[B13,B15] report that contact is not necessary, and that the charge is induced by the charged particles passing close to the sensing ring without contact taking place, as shown in Figure 7.1b. This work is in agreement with work recently carried out by other workers in the field[G12], and with observations by the author of this thesis.

A further consideration leading to doubt about the triboelectric effect is relevant to the use of the electrostatic sensors for velocity measurement by cross correlation. This consideration relates to the point that if charge transfer takes place between a charged particle and an electrode and a charge is deposited on the electrode, how can the

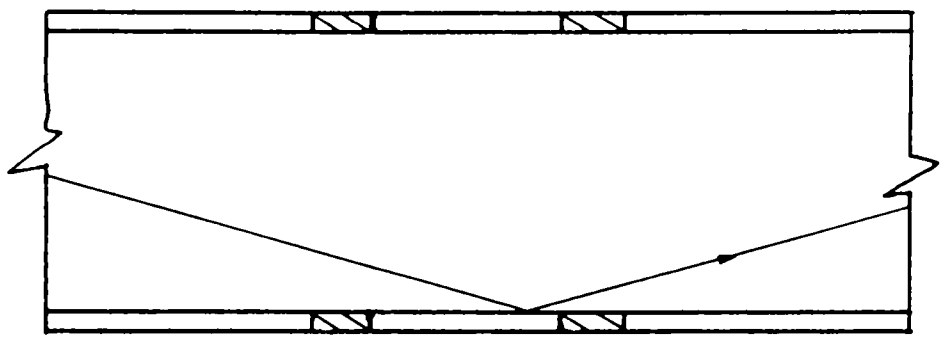

a) Charge Transfer by Contact

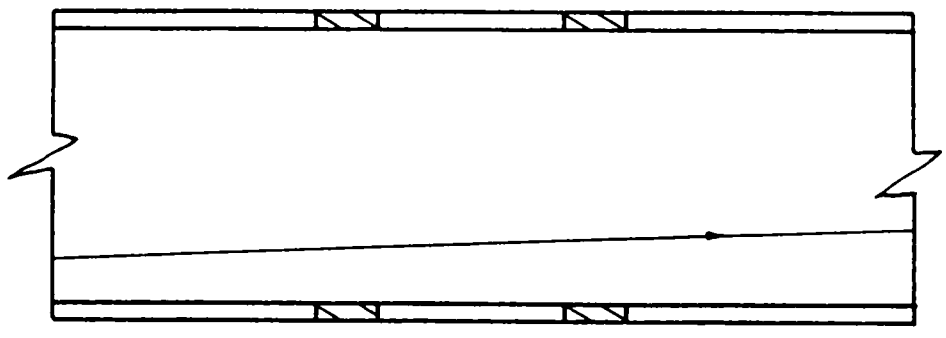

b) Charge Induction by Disturbance of Electrostatic Field

Figure 7.1 Illustration of the Two Mechanisums of Electrostatic Sensor Operation

particle then also deposit a similar charge on another electrode a short distance downstream? It is not unreasonable to assume that the charge on the particle will have been significantly changed during the contact with the first electrode. This brings into question whether the cross correlation technique will work at all if the only mechanism of charge inducement is charge transfer on contact. Indeed, it seems then that any signal induced on the electrode by charge transfer will be seen as noise by the cross correlator, since there will be no correlation between the charge transfers at axially spaced electrodes. Thus, it is suggested that signal induced by charge transfer will, in fact, reduce the cross correlation coefficient (C_{cc}), and so the accuracy of the velocity measurement. If this is accepted then this makes the signal induced by charge transfer undesirable. This will be discussed in more detail in Section 7.4.3.

It was considered, therefore, that it was necessary to establish some fundamental understanding of the mechanism by which a charge could be induced on the probe without any contact between the charged particles and the probe taking place.

It became clear that some localised disturbance to the electrostatic field in the region of the probe, caused by the passage of the charge particles was probably responsible for the charge inducement on the probe when particles did not come into contact with the probe. It seemed then, that two mechanisms were at work: that of charge transfer by contact; and that of charge inducement by disturbance to the electrostatic field in the region of the probe.

Following some consultations[G13], it was decided to attempt to develop a model, which would allow the investigation of the effect of a charged particle on the electrostatic field in close proximity to the sensor, and thereby facilitate some investigation into the mechanism of the charge inducement.

7.1 Development of the Basic Mathematical Model

In order to develop the mathematical model, it was necessary to find a fundamental physical model which could be used as a basis upon which to build a more complex model. Weber[E4] describes a technique which he terms the method of images, the

principle of which is illustrated in Figure 7.2.

An equipotential plane will exist between two equal and opposite charges as shown in Figure 7.2a. This fact may be used to model the effect of a single charge above an equipotential plane on the induced charge density on that plane. An image charge, having equal and opposite magnitude to the real charge is placed such that it forms a mirror image of the real charge about the equipotential plane as shown in Figure 7.2b. The equipotential plane is analogous to the pipeline wall, the latter being at earth potential. The electrode forming part of the pipeline wall may be considered as a section of the equipotential plane since it will be maintained at earth potential by the charge amplifier. The charge density at any point P on the equipotential plane (or the electrode) will then be given by[G4]:

$$\sigma = \frac{Q}{2\pi} \cdot \frac{h}{r^3}$$

where σ = charge density in C/m^2

Q = charge in C

h = height of Q above z=0 in m

r = distance from Q to P in m

so,

$$r = \sqrt{x^2+y^2+z^2}$$

where x = the component of r in the plane of the paper in Figure 7.2b

y = the component of r in the horizontal plane perpendicular to the paper in Figure 7.2b

z = the vertical component of r in Figure 7.2b

Thus, the value of the charge induced onto an electrode may be evaluated by integrating the above function with respect to x and y. Thus Q_{total} on the electrode

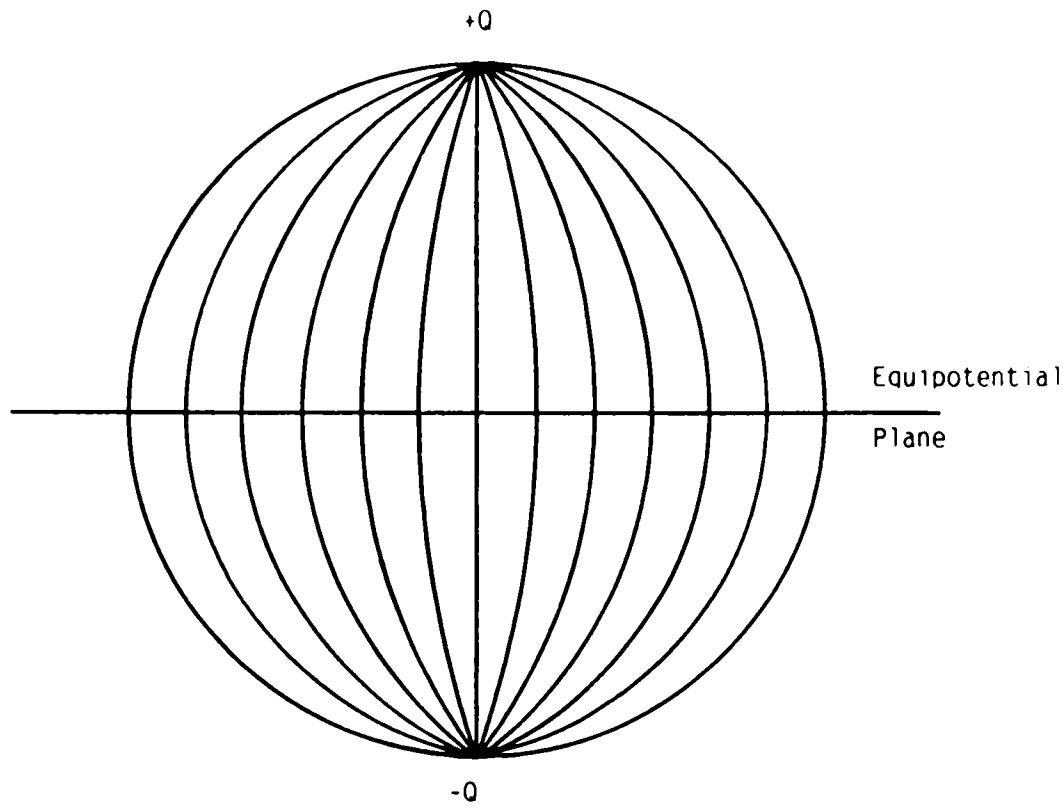

a) Equipotential Plane Between Two Equal and Opposite Charges

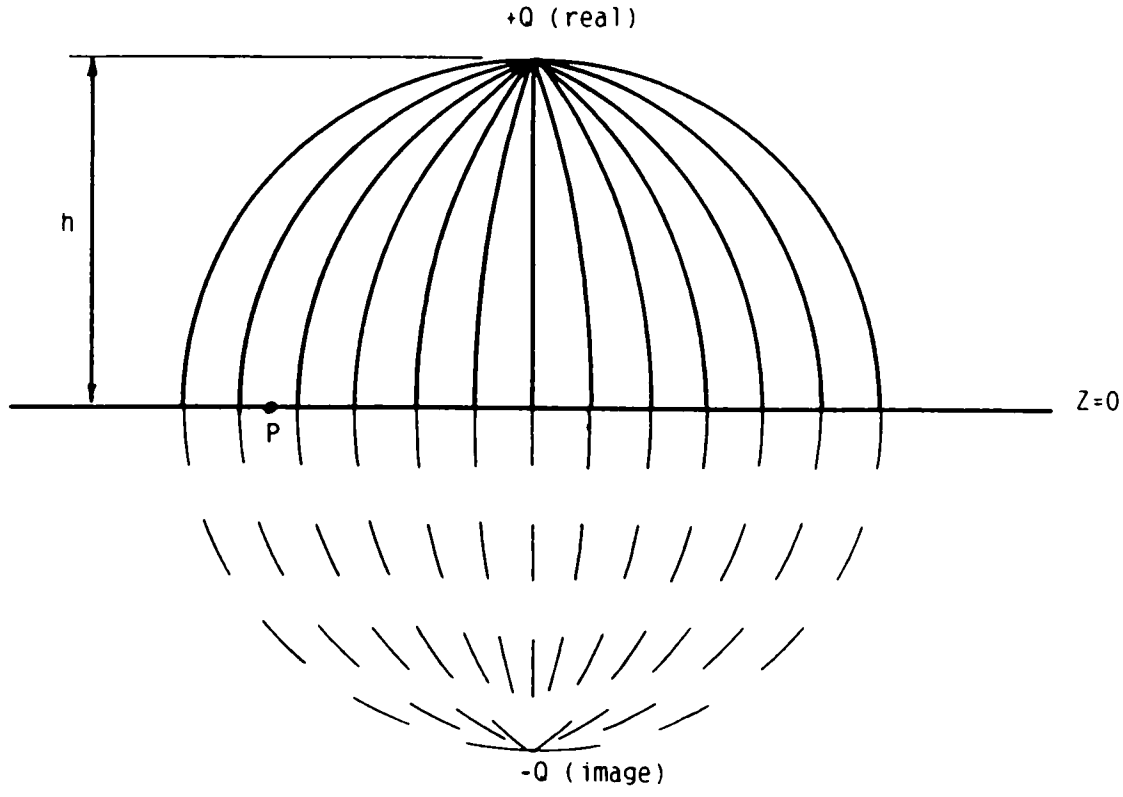

b) Image Charge, -Q, on opposite side of equipotential plane to real charge, +Q.

Figure 7.2 Principle of the Method of Images

bounded by x_1,x_2,y_1 and y_2 will be given by:

$$Q_{total} = -\frac{Qh}{2\pi}\int_{x_1}^{x_2}\int_{y_1}^{y_2}(x^2+y^2+h^2)^{-\frac{3}{2}}dydx$$

Evaluating this integral with respect to y, we obtain:

$$Q_{total} = -\frac{Qh}{2\pi}\int_{x_1}^{x_2}-\frac{1}{x^2+h^2}\left(\frac{y_1}{\sqrt{y_1^2+x^2+h^2}}-\frac{y_2}{\sqrt{y_2^2+x^2+h^2}}\right)dx$$

The analytical evaluation of this integral with respect to x was not easily achieved, and so computer software was developed to carry out the integration numerically. The software is listed in Appendix 5.

This software was then further developed to allow the charge induced on a strip of the equipotential plane, analogous to the sensing ring in the pipeline wall, to be evaluated for a series of different positions of the charge in the horizontal plane. The software was also written to allow the charge height and modelled electrode width to be varied. A plot of induced charge against horizontal distance between the charge and electrode centre line is shown in Figure 7.3.

This graph is based on a charge value of 1 unit, and clearly shows that even when the charge is 25mm away from the equipotential plane, an induced charge of approximately 0.05 units will exist when the particle is directly over the centre line of the electrode.

7.1.1 Limitations of the Model

The model described above is based on a single charge passing over a flat equipotential plane, which is clearly not the same as a particle passing through a cylindrical section of pipeline having a ring type probe incorporated in the pipeline wall. However, the model which has been developed demonstrates that charge inducement can take place

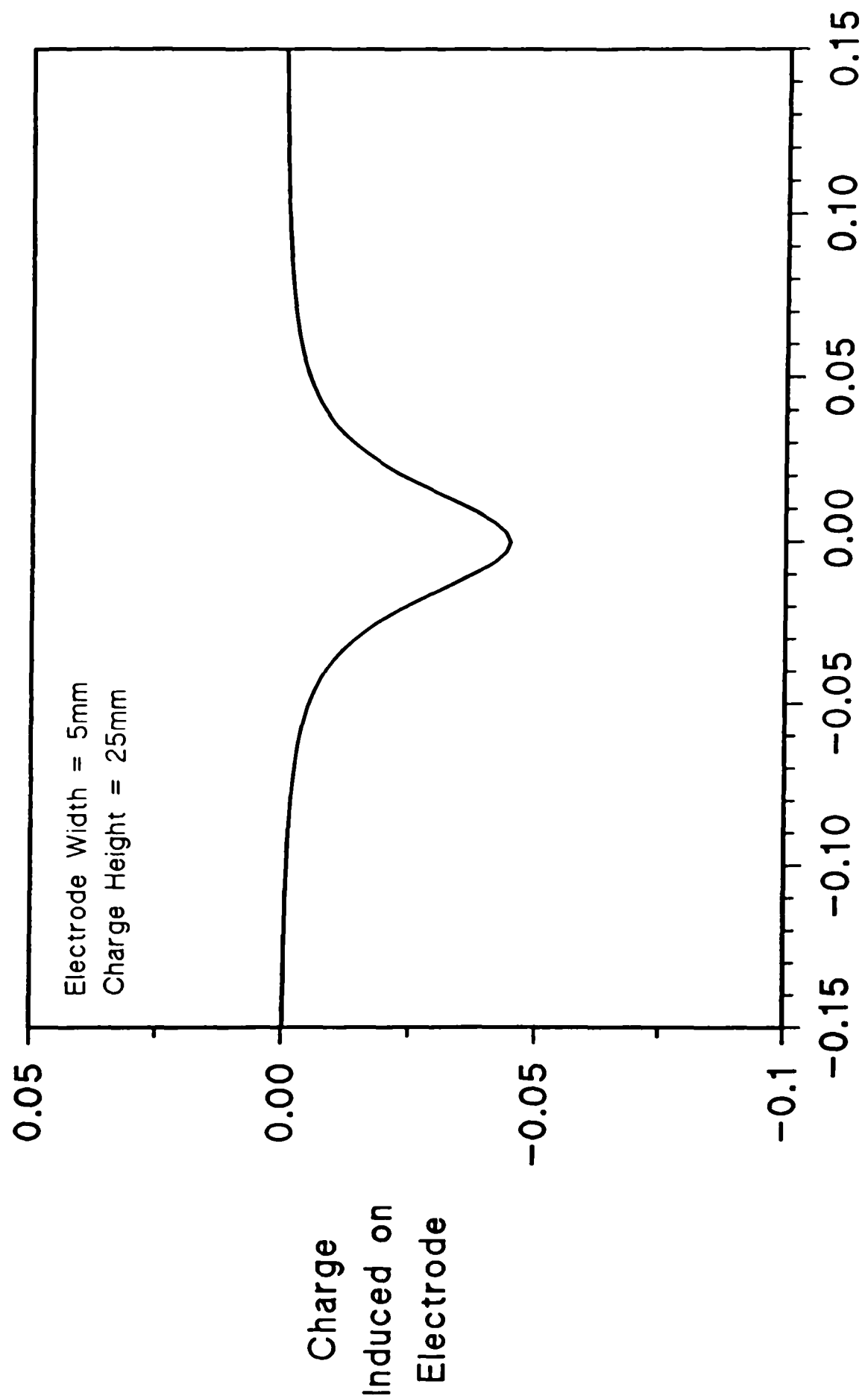

Figure 7.3 Graph of Induced Charge Against Horizontal Distance

without contact between the charged particle and the electrode.

Clearly, the fact that the modelled electrostatic field configuration is different from that of the real sensor places limitations on the validity of any data derived from this model. As a consequence,the possibility of developing a more complex model having a geometry much closer to the real sensor was considered. However, no physical model on which to build a mathematical model of a cylindrical electrode was available. The possibility of developing a finite element model based on a more fundamental physical model was also considered. However, the cost of purchasing suitable computer hardware and software was considered to be beyond the scope of the project and consequently this idea was abandoned.

It was therefore decided to carry out some investigations using the model developed on the previous pages. Whilst recognising that the quantitative validity of the results would be suspect, it was considered that some qualitative data would be generated which would provide a better understanding of the effect of some variables such as electrode width and charge height on the performance of the sensor.

7.2 Investigative Work Carried Out Using the Mathematical Model

The investigative work was focused in two areas. The first area of work was that of examining the effect of electrode width on the charge induced on the electrode, with the second being that of exploring the effect of the height of the inducing charge above the equipotential plane (or electrode).

7.2.1 The Effect of Electrode Width

For a given value of electrode width, the charge induced on the electrode was calculated for a range of values of horizontal distance between the charge and the electrode centre line. This process was then repeated for a range of values of electrode width.

The modelled results are presented in graph form in Figure 7.4. The graph clearly shows that the induced charge increases with increasing electrode width.

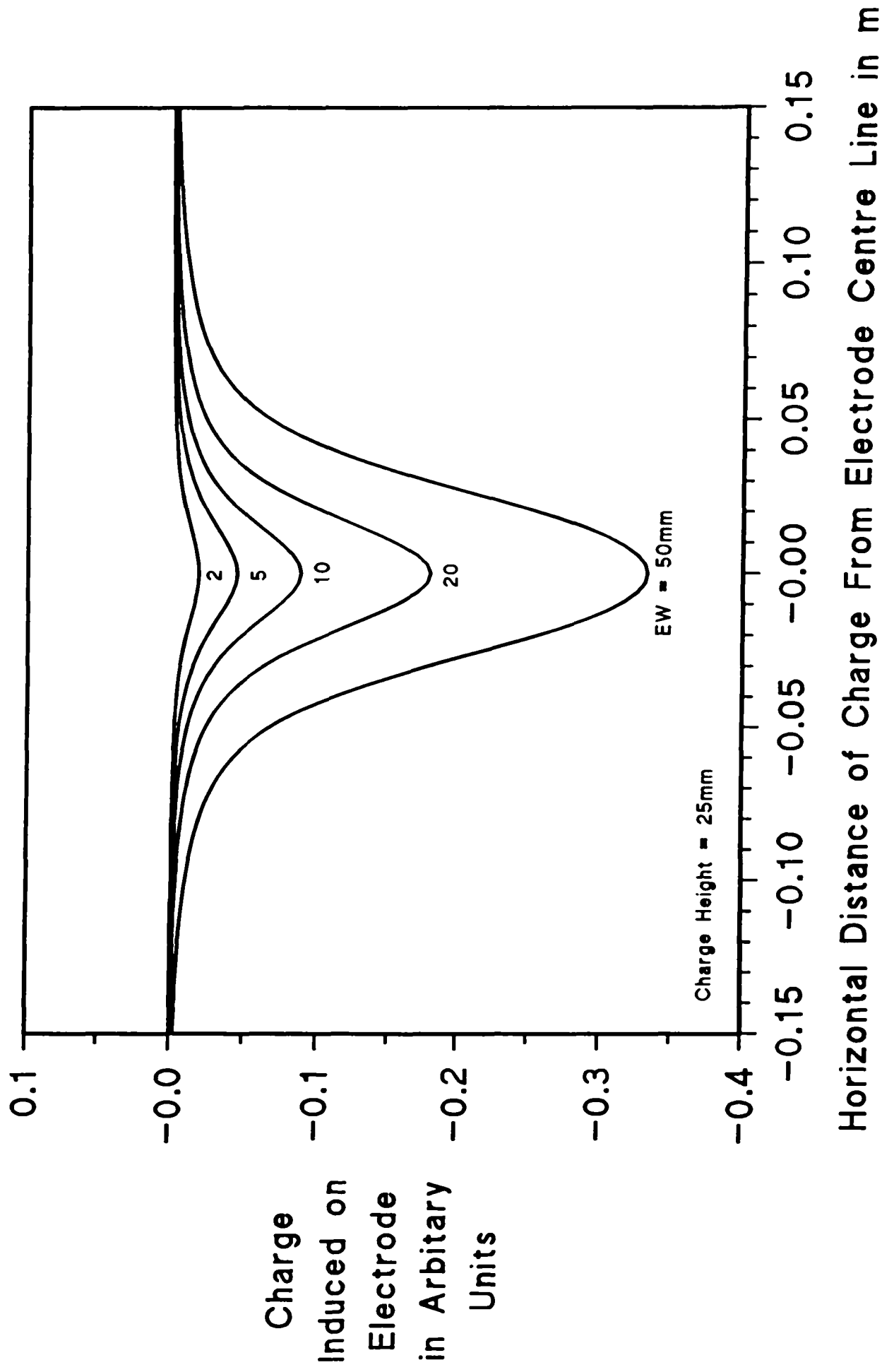

Figure 7.4 Graph of Charge Induced on Electrode for a Range of Values of Electrode Width

7.2.2 The Effect of Charge Height

Along similar lines to that of the previous section, for a given value of charge height, the charge induced on the electrode was calculated for a range of values of horizontal distance between the charge and the electrode centre line. This process was then repeated for a range of values of charge height.

The modelled results are presented graphically in Figure 7.5. The graph clearly shows that the peak induced charge increases with decreasing height of the charge above the electrode.

7.3 Principle and Limitations of Cross Correlation Signal Processing

The cross correlation function of two time varying signals x(t) and y(t) may be expressed as the average of the product of x(t) and y(t-τ) over a given observation time T. Where τ = a time delay between the two signals. This may be expressed mathematically as follows:

$$R_{xy}(\tau) = \lim_{T\to\infty} \frac{1}{T} \int_0^T x(t).y(t-\tau)\,dt$$

where $R_{xy}(\tau)$ = Cross correlation function of x and y.

A typical symmetrical cross correlation function is shown in Figure 7.6a. The value of τ at which the peak of the cross correlation function occurs (τ^*) is the value determined for the time delay between x(t) and y(t). In the application of flow measurement, this will be taken as the transit time from one axially spaced sensor to another.

A problem with the interpretation of the cross correlation function occurs when the function is not symmetric about the peak value as shown in Figure 7.6b. Under such circumstances, which occur commonly in the field of flow measurement due to the flow having a distribution of velocities, the value τ_{peak} does not represent an accurate value

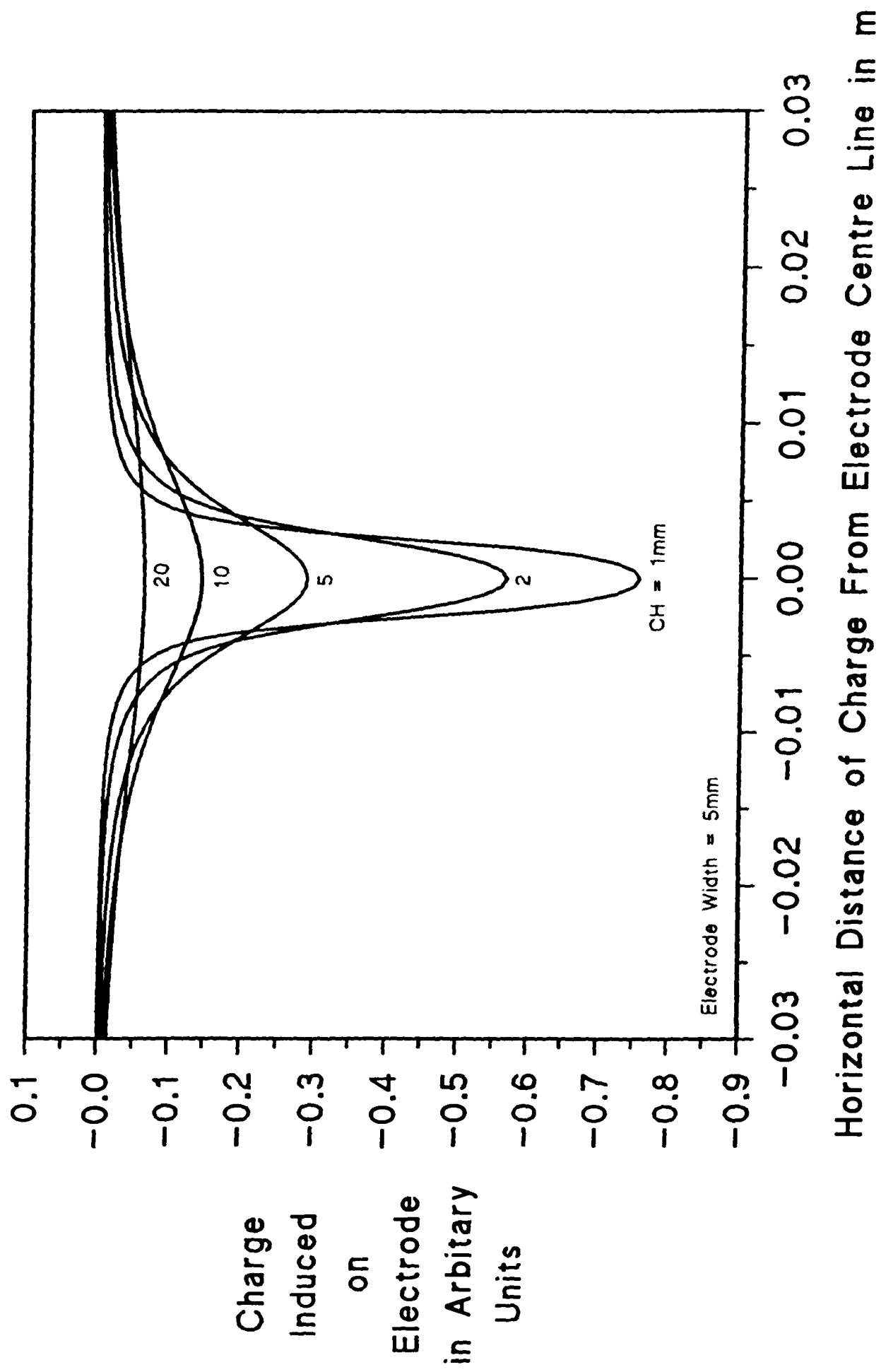

Figure 7.5 Graph of Charge Induced on Electrode for a Range of Values of Charge Height

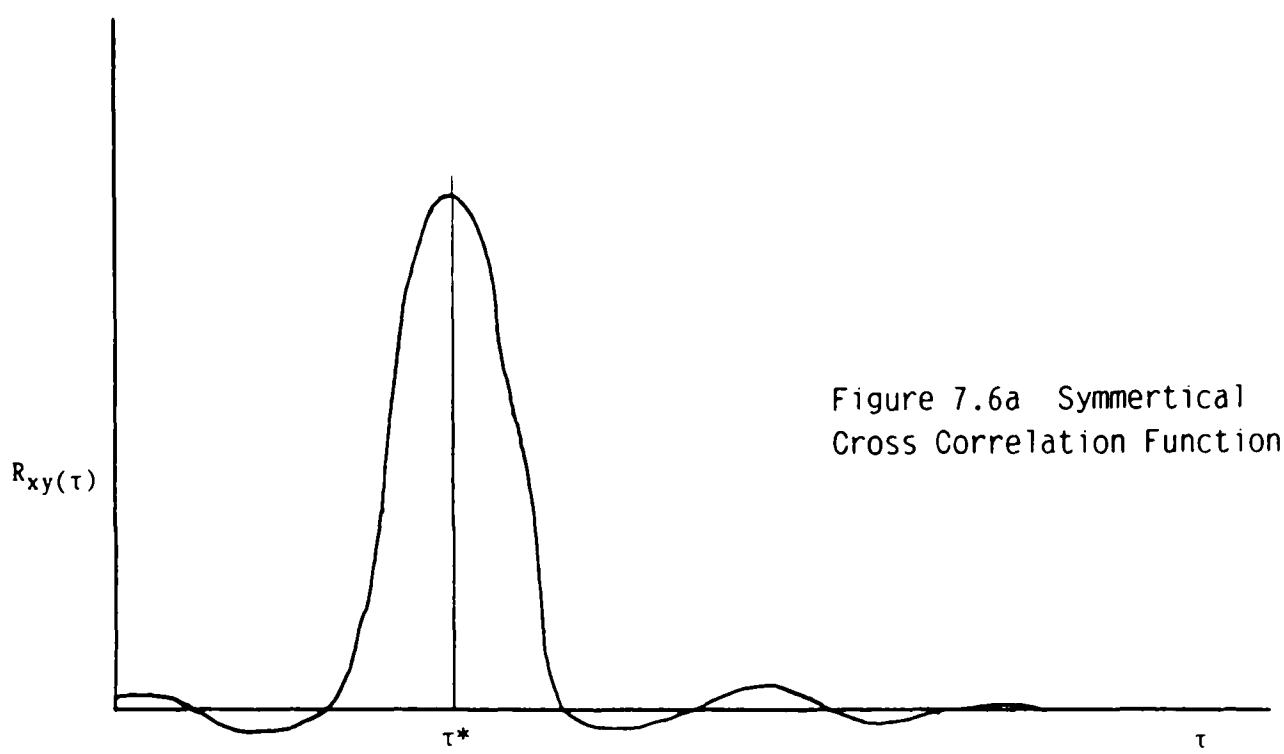

Figure 7.6a Symmertical Cross Correlation Function

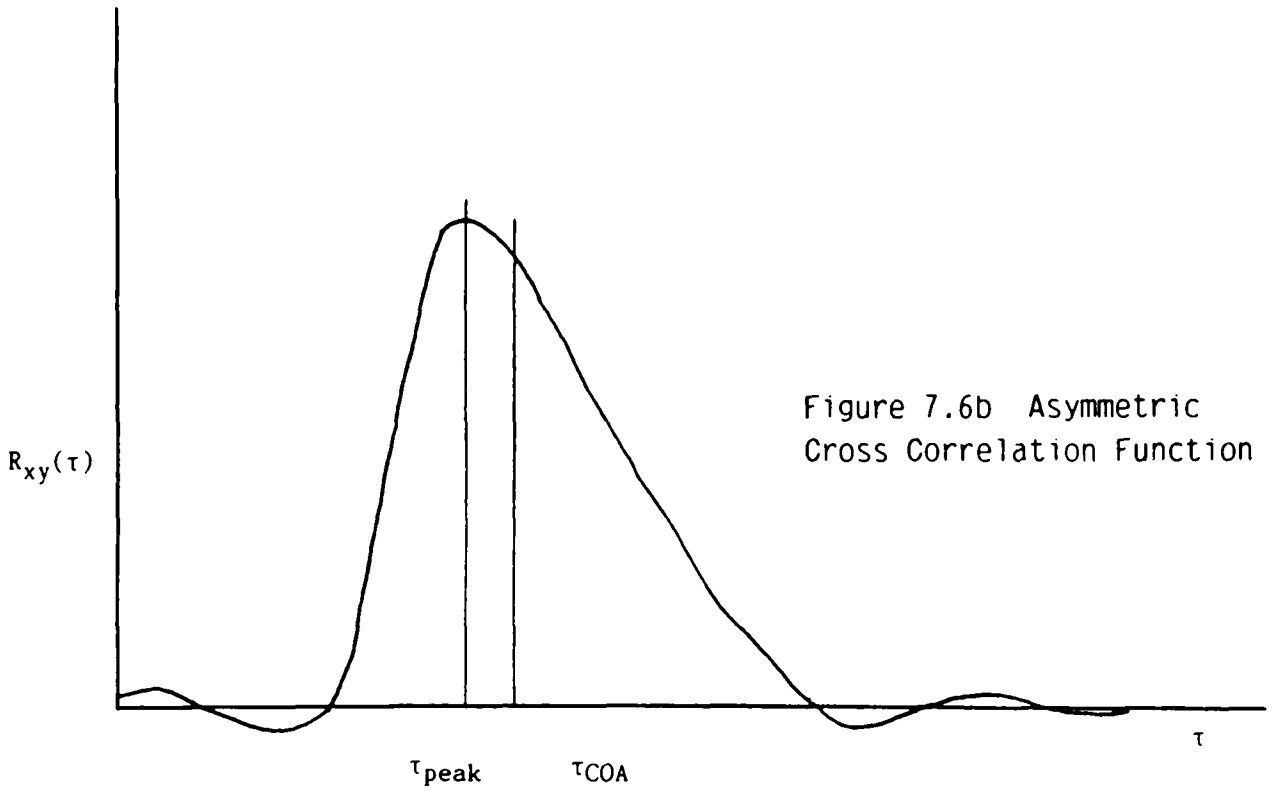

Figure 7.6b Asymmetric Cross Correlation Function

of the average transit time. An alternative approach which is therefore sometimes used involves calculating the centre of area of the cross correlation function, which will take into account any asymmetry in the function. The value τ_{COA} shown in Figure 7.6b illustrates this technique.

The cross correlator used for the test work reported in this thesis used the centre of area technique to evaluate the average time delay of the flow. The average particle velocity was then calculated using the sensor spacing programmed into the cross correlator.

7.4 Discussion of Test Results in the Light of Modelling Results

At this stage, it was decided to re-examine the experimental test results presented in Chapter 6 in the light of the qualitative results presented in the previous section. Three sections of the experimental results were re-examined, on the basis that there were aspects of these results which could not be easily accounted for. It was considered that the re-examination of these results in the light of the foregoing modelled data might allow some of the unusual aspects of the results to be explained.

7.4.1 Discussion on Data Relating to Particle Velocity

The experimental results relevant to conditions usually encountered in commercial PF injection systems are presented in Figure 6.4. As discussed in Section 6.4, V_{pcc} is below V_{as} (and therefore V_{ps} from Figure 5.3) for much of the range of ρ_s tested. The error also decreases with increasing ρ_s.

It has been noted in Section 7.2.2 that the peak charge induced onto the electrode by a charged particle passing close to the electrode increases rapidly as the height of the charge above the equipotential plane decreases. Thus, it may be considered that a charged particle passing very close to the pipeline wall (having a small charge height in the model) will induce a much larger peak charge on the electrode than a charge passing at a greater distance form the pipeline wall.

Thus, it may also be concluded that the electrostatic sensor has greater sensitivity to

particles close to the pipeline wall than to particles closer to the centre of the pipe. Since the velocity profiles obtained during the laser doppler velocimetry test work clearly show that the particle velocities close to the pipeline wall are lower than the average particle velocity, it is was concluded that the fact that the electrostatic cross correlation velocity meter indicates a lower value is an indication that it is more sensitive to particles close to the pipeline wall, where the particle velocities themselves are lower.

The laser doppler velocimetry test work also showed that the power of the power law model which models the particle velocity distribution increases with increasing ρ_s. Thus, as the velocity profile becomes flatter, the faster moving particles become closer to the pipeline walls. It is suggested that this may account for the reduction in the difference in the reading of the electrostatic cross correlation velocity meter with increasing suspension density.

It may also be seen from Figure 7.5 that the rate of change of induced charge with charge height decreases with increasing charge height. Thus, it would appear that if charged particles could be prevented from getting to within, say, 5mm of the electrode, the effect of the characteristics outlined in the previous two paragraphs could be reduce. If this is accepted, then it is suggested that this could be achieved by recessing the electrode rings into the wall of the pipeline and providing, say, 5mm of insulating material between the electrode and the pipeline bore.

This would also have the added effect of preventing any contact between the charged particles and the electrode thereby reducing the possible mechanisms of charge inducement from two to one. The possible benefits of this will be discussed in more detail in Section 7.4.3.

7.4.2 Discussion on Data Relating to Suspension Density

The results of the test work undertaken on the electrostatic suspension density sensor are shown in Figure 6.5, and as noted in Section 6.4, the sensor in its present form is not able to give reliable readings of ρ_s over the range of operating conditions usually

found in commercial PF injection systems.

At the present time, the principle characteristic of the electrostatic suspension density sensor which makes its performance unsatisfactory is that the output saturates at a given value of suspension density. If the cause of this saturation could be identified, then it may be possible to carry out some modifications to either the electrode or the processing electronics to reduce or even alleviate this effect. Should this be possible, then a satisfactory technique for measuring the suspension density would result. Since a technique to evaluate the average particle velocity has already been proven, it follows that a complete mass flow rate system will also result.

It was anticipated that the development of the model of the sensor operation would provide some explanation for the undesirable features of the experimental test results. However, none of the data derived from the model was considered to contribute to an explanation of this aspect of the experimental results.

One possible explanation for the saturation phenomenon is the possibility that the R.M.S. converter may not have a linear transfer characteristic over the whole output voltage range. Details of the type of circuit used to carry out this conversion were not available from the meter manufacturers for reasons of commercial confidentiality, and so further investigation of this possibility was not possible.

7.4.3 Discussion on Data Relating to Pipeline Geometry

The results of the experimental test work relating to pipeline geometry are shown in Figures 6.8 to 6.10. As noted in Section 6.7, the performance of the electrostatic density sensor and the cross correlation velocity meter decayed significantly when a flow disturbance was situated immediately upstream of the sensor head unit.

It was considered that much of the deterioration in performance could be accounted for by the possible increase in charge induced on the electrodes by contact between the charged coal particles and the electrodes. This increase in contact could be caused by the centrifugal force exerted on the charged particles as they round the pipeline bend

forcing the particles to slide along the pipeline wall rather than being carried in the centre of the pipeline by the air, as would normally be the case.

The increase in prevalence of the contact or 'triboelectric' mechanism could have two effects on the measurement system. Firstly, the increase in charge transfer could lead to an increase in the output of the suspension density sensor. This could be compounded by the presence of a large number of charged coal particles close to, but not in contact with the electrode, since as noted in Section 7.2.2, the sensor is much more sensitive to charged particles close to the electrode. This is in agreement with the experimental results shown in Figures 6.8 to 6.10, which show a significant increase in sensor output when a pipeline bend is positioned upstream of the sensing head.

The second effect could be to reduce the value of the cross correlation coefficient (C_{cc}). This could be caused by the increase in proportion of the sensor signals derived from charge transfer, rather than charge inducement. As discussed in Section 7.0, the correlation between the signals from the two sensors will be good when the signals are caused by charge inducement because the charged particles induce a charge on the electrodes without charging their own charge. Thus the same charge will be induced on each of the axially spaced electrodes. However, the correlation between the signals derived from charge transfer will be poor, since in order to provide a signal, the charged particle must deposit some or all of it's charge and will not therefore have the same effect on the second sensor.

If the foregoing is accepted, then the modification to the sensing head as discussed in Section 7.4.1, to insulate the electrode from the pipeline bore and thus remove any possible charge transfer by contact, would reduce to some extent the dependency of the sensor performance on pipeline geometry, as well as alleviating the problems discussed in Section 7.4.1.

7.5 Concluding Remarks

In conclusion, it is noted that the foregoing relatively simple modelling exercise has

provided an number of points of interest.

- The demonstrated sensitivity of the sensor to particles close to the pipeline wall has provided a possible explanation for the unusual aspects of both the particle velocity measurement performance and the performance of the density sensor with respect to upstream pipeline fittings.

- Some plausible explanations have been developed for the non linear performance of the suspension density sensor.

- A modification to the sensing head has been proposed, which may improve some important aspects of the performance of the sensing system.

It is therefore concluded that despite the inherent limitations of the model which has been developed, a significant amount of useful information has resulted.

Chapter 8 Conclusions

The programme of work undertaken in an effort to satisfy the programme objectives has been detailed in the preceding six chapters. This work will now be discussed in the light of the programme objectives as set out in Section 1.1.

In accordance with the first component objective, a review of the technology has been undertaken, incorporating a literature survey, as well as information gathered as a result of some more direct experience gained by the author. The major conclusions of this review were that although a number of measurement techniques had been proposed, there was a significant lack of test data to verify any of the techniques proposed, particularly when applied to the mass flow rate measurement of pulverised coal in pneumatic injection systems.

This lack of test data was largely attributed to lack of industrial scale instrumented pneumatic conveying test facilities within the academic community. It was considered that the availability of such a facility was an important prerequisite for the successful completion of the project.

The decision was therefore taken to design and construct an instrumented test facility in order that trials with sensors based on the promising techniques could be undertaken under the full control of the author, rather than in a plant belonging to a third party, with the inevitable associated constraints.

The design and construction of the test rig was completed in the early stages of the programme, and thus the third component objective was achieved.

The test facility so developed was then utilised to undertake a range of experimental tests in order to evaluate the performance of various aspects of the most promising measurement system, in order to satisfy the second component objective of the programme as discussed in Section 1.1. This work is described in Chapters 4 and 6.

The results of the experimental tests are presented and analyzed in Chapters 5 and 6. Some of the experimental test results were not as would have been initially expected, and so a model was developed in an attempt to explain some of the less expected features of the experimental results. This work also satisfies the fourth component objective. Chapter 7 details the development of the model to describe the sensing mechanism.

Thus all four of the component objectives layed out in Section 1.1 were satisfied. The resulting data satisfies the overall objective of the work programme which was to obtain information which would allow the performance of a mass flow rate measurement system to be determined. The conclusions drawn from the work are as follows:

1. The electrostatic sensing system in conjunction with the cross correlator has the capability, in it's present form to measure the mean particle velocity to an accuracy in the region of $\pm 2\%$. This result is as might have been expected, but more importantly the performance of the sensing system has now been proven through extensive experimental testing over a range of conditions found in industry.

2. The average particle velocity can also be evaluated under the conditions tested by the evaluation of the superficial air velocity, the two being equal to within $\pm 2\%$ for the range of conditions tested. This result, whilst very encouraging, was rather unexpected, since a the work of a number of authors discussed in Chapter 2 propose values of particle slip between 3 and 20% for similar conditions. This result is very important since it allows the average particle velocity to be evaluated with ease in many plants where the air flow rate is known or can be inferred. However, in many plants this is not possible and so the electrostatic cross correlation technique will be useful under such conditions.

3. The performance of the electrostatic suspension density sensor in it's present form is unsatisfactory. This was somewhat disappointing, since the measurement of particle velocity has been accomplished to a good degree of accuracy. However, this result reinforces the fact that experimental testing and verification is extremely important.

   Some possible causes of this problem are proposed in Section 7.4.2. Possible modifications to the sensor in order to overcome this problem have also been proposed and are discussed in that section.

4. The sensitivity of the electrostatic sensing system to the relative humidity of the conveying air and particle size of the conveyed product has been determined as very small. This result is of significance because the particle size of the PF used in injection systems does vary over a period of time as the performance of the mills varies between service intervals. The insensitivity to relative humidity is also important since this may change in an industrial system with a change in ambient environmental conditions.

   These results were somewhat unexpected, since the work of a number of authors discussed in Chapter 2 have reported significant sensitivities to these variables, albeit over a much wider range of these variables.

5. The sensitivity of the electrostatic sensing system to upstream flow disturbances has been determined as highly significant. This is another important result, since with the requirement to retrofit this technology to existing plant, the positioning of sensors with respect to flow disturbances in many cases may be very limited.

   Possible modifications to reduce this sensitivity have been discussed in Section 7.4.

A mathematical model to describe the principle of operation of the electrostatic sensor

has been developed, demonstrating that the charge induced on the sensor by the charged coal particles does not require contact between the sensing ring and the particle. This result is very significant because the work of a number of authors discussed in Chapter 2 have reported that charge transfer by contact is the only mechanism responsible for the signal generation.

Furthermore, it has been proposed in Section 7.4.1 that the charge induced on the electrostatic sensor by contact can, in fact, be detrimental to the performance of the sensor, and that it is the charge induced by the disturbance of the electrostatic field which is of vital importance to the successful operation of the sensor. In an attempt to reduce the sensitivity of the sensing system to charge induced by contact, possible modifications to the sensing head have been considered and are discussed in Section 7.3.1.

With respect to the accuracies stated in 1. and 2. above, it should be noted that these figures are based on an estimated accuracy of $\pm 1\%$ for the laser doppler velocimetry instrumentation, which is perhaps rather optimistic, and so should be regarded with a caution.

In addition to achieving the original programme objectives, a number of other ideas have been proposed in the light of the experimental test data obtained.

The analysis of the data from the laser doppler velocimetry test work has, in addition to providing a calibration of the electrostatic velocity meter, provided data of interest to the understanding of two phase gas/solids flow at low suspension densities. This has been discussed in Sections 5.4 and 5.5.

As a direct result of some of the laser doppler velocimetry test data, it has also been proposed that some reduction in the head losses in pipelines may be possible by seeding the gas stream with a small quantity of solid particles. This provides some confirmation of similar phenomenon proposed by Soo[F1] and Kolansky et al[F2]. This work is discussed in Section 5.5.

8.1 Recommendations for Further Work

It will be apparent from the foregoing that significant progress has been made towards identifying a mass flow rate measurement system for PF in pneumatic injection systems. However, there are a number of areas in which it is recommended that further work could usefully be carried out, with a view to arriving at a complete, self contained unit for meeting this goal:

1. Possible modifications to the electrostatic sensing system have been proposed in Chapter 7, and it is recommended that a sensing head conforming to the suggested modified design be manufactured and subjected to a programme of on-line evaluation in a suitably instrumented test facility.

2. The work proposed in 1. above could also benefit from the development of better mathematical model in order to better investigate the effect of sensor geometry on its operation. Due to the lack of a suitable fundamental model upon which to base a mathematical model , it is recommended that finite element methods be considered. A number of computer software packages are available, and it is recommended that the capabilities of these packages be assessed, with a view to utilising such technology for this task.

3. Should it be possible to alleviate the shortcomings of the present sensing system, it is recommended that the developed sensing technique should undergo trials in a larger scale test rig, in order to evaluate the effect of scale on the system performance. Clearly this will require the use of a larger scale instrumented test facility than that described in Chapter 3, the development of which could perhaps be undertaken jointly by the major industries which would benefit from the development of such technology. Should these trials be successful, then it is recommended that full scale plant trials be undertaken, once again in collaboration with the major potential beneficiaries.

Appendix 1 References

This appendix contains a list of the references cited in the thesis text by superscript alphanumerics.

References

A1 McVeigh, M.A.; Craig, R.W. Metering of Solids/Gas Mixtures Using An Annular Venturi Meter, Proceedings of the First International Conference on the Pneumatic Transport of Solids in Pipes, Cambridge, England 1971.

A2 Farbar, L. The Venturi as a Meter for Gas-Solids Mixtures, Transactions of The American Society of Mechanical Engineers, 1953.

B1 Dechene, R.L.; Averdieck, W.J. Triboelectricity For Fabric Filter Bag Rupture Detection, Third EPRI Conference on Fabric Filter Technology For Coal Fired Power Plants, Arizona, USA 1985.

B2 Dechene, R.L.; Averdieck, W.J. Triboelectricity - A New Fine Particle Measurement Parameter, Seventeenth Annual Meeting of the Fine Particles Society, California, USA 1986.

B3 Dechene, R.L.; Averdieck, W.J. Particulate Velocity Measurement by the Triboelectric Effect, Proceedings of the Powder and Bulk Solids Handling and Processing Conference, Chicago, USA 1986.

B4 Dechene, R.L.; Averdieck, W.J. Triboelectricity: A Parameter For Solids Flow Measurement, Powder and Bulk Engineering, June 1987.

B5 Dechene, R.L. Triboelectric Technology For Mass Flow Rate Measurement, Proceedings of the Powder and Bulk Solids Handling and Processing Conference, Chicago, USA 1988.

B6 Gajewski, J.B.; Szaynok, A. Charge Measurement of Dust Particles in Motion, Journal of Electrostatics, Volume 10, pp229-234, 1981.

B7 Gajewski, J.B. Charge Measurement of Dust Particles in Motion - Part II, Journal of Electrostatics, Volume 15, pp67-79, 1984.

B8 Singh, S. A Study of Electrostatic Activity in a Full Scale Pneumatic Conveying System, Proceedings of the International Conference on Pneumatic Conveying Technology, Stratford-Upon-Avon, England 1982.

B9 Shackleton, M.E. Electrodynamic Transducer For Gas/Solids Flow Measurement, Master of Philosophy Thesis, University of Bradford, England 1982.

B10 Masuda, H.; Komatsu, T.; Mitsui, N.; Iinoya, K. Electrification of Gas-Solid Suspensions Flowing in Steel and Insulating Coating Pipes, Journal of Electrostatics, Volume 2, pp341-350, 1976-77.

B11 King, P.W. Mass Flow Measurement of Conveyed Solids, By Monitoring of Intrinsic Electrostatic Noise Levels, Proceedings of the Second International Conference on the Pneumatic Transport of Solids in Pipes, Surrey, England 1973.

B12 Kittaka, S.; Masui, N.; Murata, Y. A Method For Measuring the Charge Tendency of Powder in Pneumatic Conveyance Through Metal Pipes, Journal of Electrostatics, Volume 6, pp181-190, 1979.

B13 Smeltzer, E.E.; Weaver, M.L.; Klinzing, G.E.; Individual Electrostatic Particle Interaction in Pneumatic Transport, Powder Technology, Volume 33, pp31-42, 1982.

B14 Smith, R.A.; Klinzing, G.E. Investigation of Particle Velocities in Gas-Solid Systems, Journal of the American Institute of Chemical Engineers, Volume 32, pp313-316, 1986.

B15 Klinzing, G.E.; Zaltash, A.; Myler, C.A. Particle Velocity Measurements Through Electrostatic Field Fluctuations Using External Probes, Particulate Science and Technology, Volume 5. pp95-104, 1987.

B16 Woodhead, S.R.; Coulthard, J.; Byrne, B; Barnes, R.N.; Reed, A.R. On Line Mass Flow Measurement in Low Suspension Density Pneumatic Conveying Systems Using an Electrostatic Technique, Proceedings of the Fourth International Conference on Pneumatic Conveying Technology, Glasgow, Scotland, 1990.

C1 Tsuji, Y.; Morikawa, Y. LDV Measurements of an Air-Solid Two-Phase Flow in a Horizontal Pipe, Journal of Fluid Mechanics, Volume 120, pp385-409, 1982.

C2 Riethmuller, M.L.; Ginoux, J.J. The Application of a Laser Velocimeter to the Velocity Measurement of Solid Particles Pneumatically Transported, Proceedings of the Second International Conference on the Pneumatic Transport of Solids in Pipes, Surrey, England 1973.

C3 Birchenough, A.; Mason, J.S. The Application of a Laser Anemometer in Measuring Parameters Required in the Design of a Pneumatic Conveying System. Proceedings of the Powtech'75 Conference, Harrogate U.K. 1975.

C4 Birchenough, A.; Mason, J.S. Particle Wall Velocity Measurements in a Densely Flowing Gas-Solid Suspension, Proceedings of the Third International Conference on the Pneumatic Transport of Solids in Pipes, Bath, England, April 1976.

D1 Coulthard, J.; Keech, R.P. Multichannel Correlation Applied to the Measurement of Fluid Flow, Proceedings of the International Conference on Advances in Flow Measurement Techniques, Warwick, England 1981.

D2 Beck, M.S.; Gough, J.R.; Hobson, J.H.; Jordan, J.; Menzies, P. Solid/Fluid Two Phase Flow Measurement Using Cross Correlation Techniques, Proceedings of Chemeca Conference, 1970.

D3 Beck, M.S.; Calvert, G.; Hobson, J.H.; Lee, K.T.; Mendies, P.J. Total Volume and Component Flow Measurement in Industrial Slurries and Suspensions Using Correlation Techniques, Transactions of the Institute of Measurement and Control, Volume 4, ppT133-139, 1971.

D4 Green, R.G.; Foo, S.H.; Mitchell, L.I.M. Application of a Low Cost Microcomputer to Measurement and Control of Pneumatic Conveying Systems, Proceedings of the Fifth International Conference on the Pneumatic Transport of Solids in Pipes, London, England 1980.

D5 Green, R.G.; Foo, S.H.; Philips, J.G. Flow Measurement for Optimising the Feed Rate of Pulverised Fuel to Coal Firing Systems, Proceedings of the Symposium on Fossil Energy Processes, San Francisco, USA 1981.

D6 Beck, M.S. Recent Developments and the Future of Cross Correlation Flow Meters, Proceedings of the International Conference on Advances in Flow Measurement Techniques, Warwick, England 1981.

D7 Beck, C.M.; Henry, R.M.; Lowe, B.T.; Plaskowski, A. Instrument For Velocity Measurement and Control of Solids in a Pneumatic Conveyor, Proceedings of the International Conference on Pneumatic Conveying Technology, Stratford-Upon-Avon, England 1982.

D8 Mesch, H.; Kipphan, H. Solids Flow Measurement By Correlation Methods, Optoelectronics, Volume 4, pp451-462, 1972.

D9 Boeck, T. Granucor - Mass Flow Measurement System For Pneumatically Conveyed Solids, Proceedings of the Third International Conference on Pneumatic Conveying Technology, Jersey, Channel Islands 1987.

D10 Boeck, T. Measurement of Velocity and Mass Flow Rate of Pneumatically Conveyed Solids By the Use of a Correlation Measurement Technique, Proceedings of the International Conference on the Flow of Particulate Solids, Bergen, Norway 1989.

D11 Midttveit, O; de Silva, S.R. Slip Velocity in Pneumatic Conveying, Proceedings of the Fourth International Conference on Pneumatic Conveying Technology, Glasgow, Scotland 1990.

E1 Howard, A.V. Development of Techniques for the Measurement of Concentration and Mass Flow Rate of Pneumatically Conveyed Coal Dust. Internal Report, C.E.G.B North East Region, 1980.

E2 Parkinson, M.J.; Hiorns, F.J. Mass Flowmeter for Gasborne Powders, Instrument Practice, pp197-200, March 1969.

E3 Hours, R.M.; Chen, C.P. Application of Radioactive Tracers and β-Rays Absorption Techniques to the Measurement of Solid Particles Velocity and Space Concentration in a Two Phase Air-Solid Flow at High Mass Rate, Proceedings of the Third International Conference on the Pneumatic Transport of Solids in Pipes, Bath, England, 1976.

F1 Soo, S.L. Fluid Dynamics of Multiphase Systems, Blaisdell Publishing Company, 1967.

F2 Kolansky, M.S.; Weinbaum, S.; Pfeffer, R. Drag Reduction in Dilute Gas-Solid Suspension Flow: Gas and Particle Velocity Profiles, Proceedings of the Third International Conference on the Pneumatic Transport of Solids in Pipes, Bath, England 1976.

G1 Bradley, M.S.A. Doctor of Philosophy Thesis, Thames Polytechnic, 1990.

G2 Pneumatic Conveying Technology, Short Course Notes, The Wolfson Centre for Bulk Solids Handling Technology, Thames Polytechnic, London 1989.

G3 Reed, A.R. Private Communication, Thames Polytechnic, 1988.

G4 Weber, E. Electromagnetic Fields, Theory and Applications, Volume 1 - Mapping of Fields, John Wiley and Sons Inc, New York, USA 1950.

G5 Beck, M.S.; Plaskowski, A. Cross Correlation Flowmeters - Their Design and Application, Adam Hilger, 1987.

G6 Prandtl, L. Essentials of Fluid Dynamics, With Applications to Hydraulics, Aeronautics, Meteorology and Other Subjects, Blackie and Son Limited, London 1952.

G7 Byrne, B. Private Communication, Teesside Polytechnic, May 1988.

G8 Nelkon, M.; Parker,P. Advanced Level Physics, Heinemann, London, 1977.

G9 Stroud, K.A. Engineering Mathematics 2Ed., Macmillan, U.K. 1985.

G10 Stroud, K.A. Further Engineering Mathematics, Macmillan, U.K. 1988.

G11 British Standards Institution, BS1042, Measurement of Fluid Flow in Closed Conduits, 1981.

G12 Byrne, B; Coulthard, J; Hampton, R. Private Communication, Teesside Polytechnic, May 1988.

G13 Barnes, R.N. Private Communication, Thames Polytechnic, April 1991.

Appendix 2 Particle Size Distributions

This appendix contains details of the particle size distributions of the four materials used during the various test trials of the sensors. The first is fine grade pulverised coal used for the majority of the test work. The second and third are medium and course grade pulverised coal respectively, which were used in the trials to evaluate the effect of particle size distribution on the performance of the electrostatic sensing system as detailed in Chapter 6. The fourth set of data is for the wheat flour which was used for some of the laser doppler velocimetry test work, as detailed in Chapter 4.

Particle Size Distribution of Fine Grade Pulverised Coal

System number 2349 Diode M00033

Malvern Instruments MASTER Particle Sizer M6.02 Date 01-01-84 Time 00-41

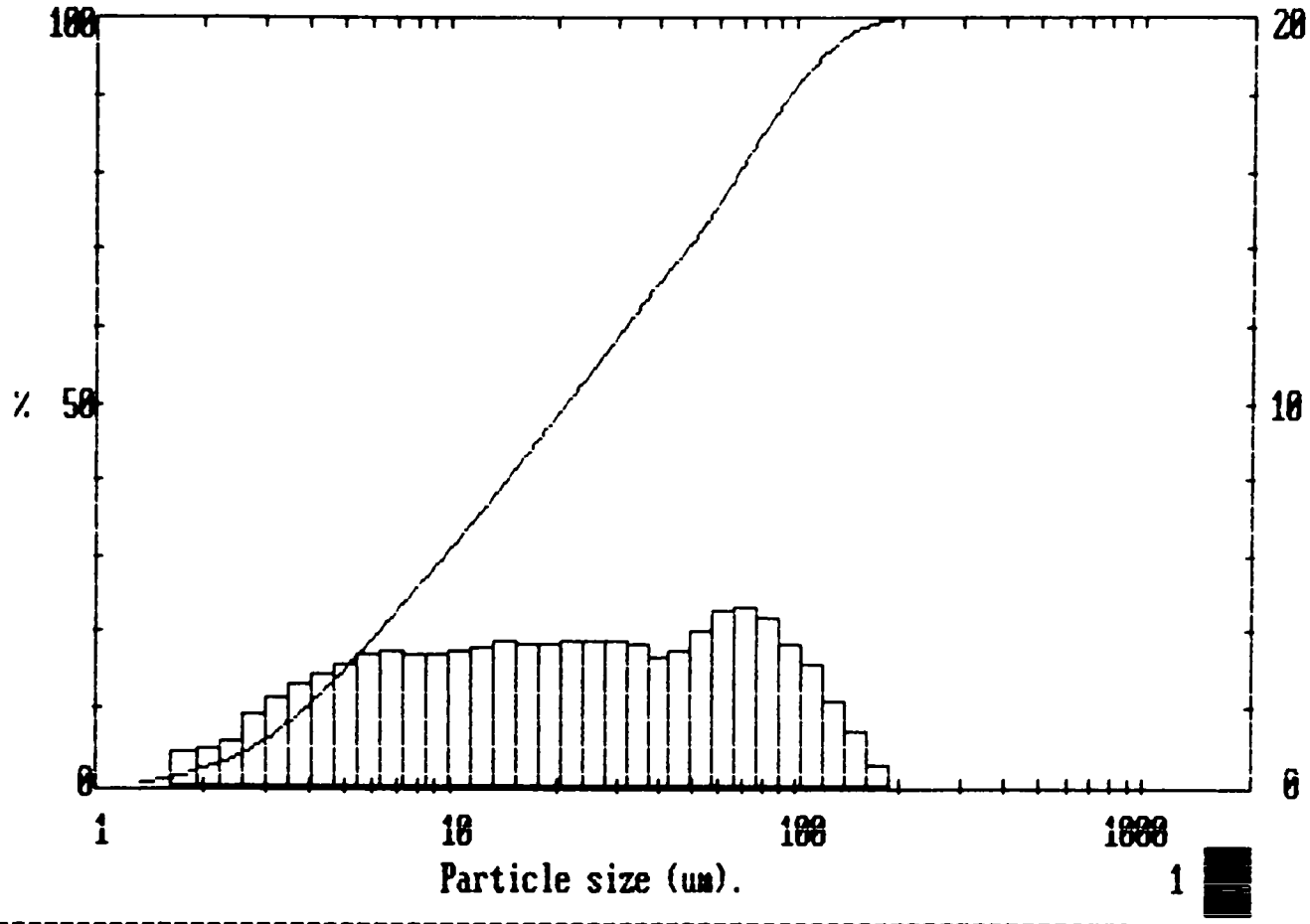

Size microns	under	% in band	Size microns	under	% in band
188.0	100.0	0.5	17.7	45.4	3.7
162.0	99.5	1.4	15.3	41.7	3.8
140.0	98.1	2.2	13.2	37.9	3.6
121.0	95.8	3.2	11.4	34.3	3.5
104.0	92.7	3.8	9.8	30.7	3.4
89.9	88.9	4.5	8.5	27.3	3.5
77.5	84.5	4.7	7.3	23.9	3.5
66.9	79.8	4.6	6.3	20.3	3.5
57.7	75.2	4.0	5.4	16.9	3.2
49.8	71.1	3.5	4.7	13.7	2.9
42.9	67.6	3.4	4.1	10.8	2.6
37.1	64.2	3.7	3.5	8.2	2.3
32.0	60.5	3.8	3.0	5.9	1.8
27.6	56.7	3.8	2.6	4.0	1.2
23.8	52.9	3.8	2.2	2.9	1.0
20.5	49.1	3.7	1.9	1.9	

Result source= Sample
Record No. = 2
Focal length = 100 mm.
Experiment type pia
Volume distribution
Beam length = 30.0 mm.
Obscuration =0.2193
Volume Conc. = 0.0027 %
Log. Diff. =1.88
Model indp

D(v,0.5) = 21.2 um
D(v,0.9) = 93.5 um
D(v,0.1) = 3.9 um
D(4,3) = 35.0 um
D(3,2) = 11.2 um
Span = 4.2
Spec. surf. area
0.6341 sq.m./cc.

Particle Size Distribution of Medium Grade Pulverided Coal

System number 2349 Diode M00033

Malvern Instruments MASTER Particle Sizer M6.02 Date 01-01-84 Time 01-02

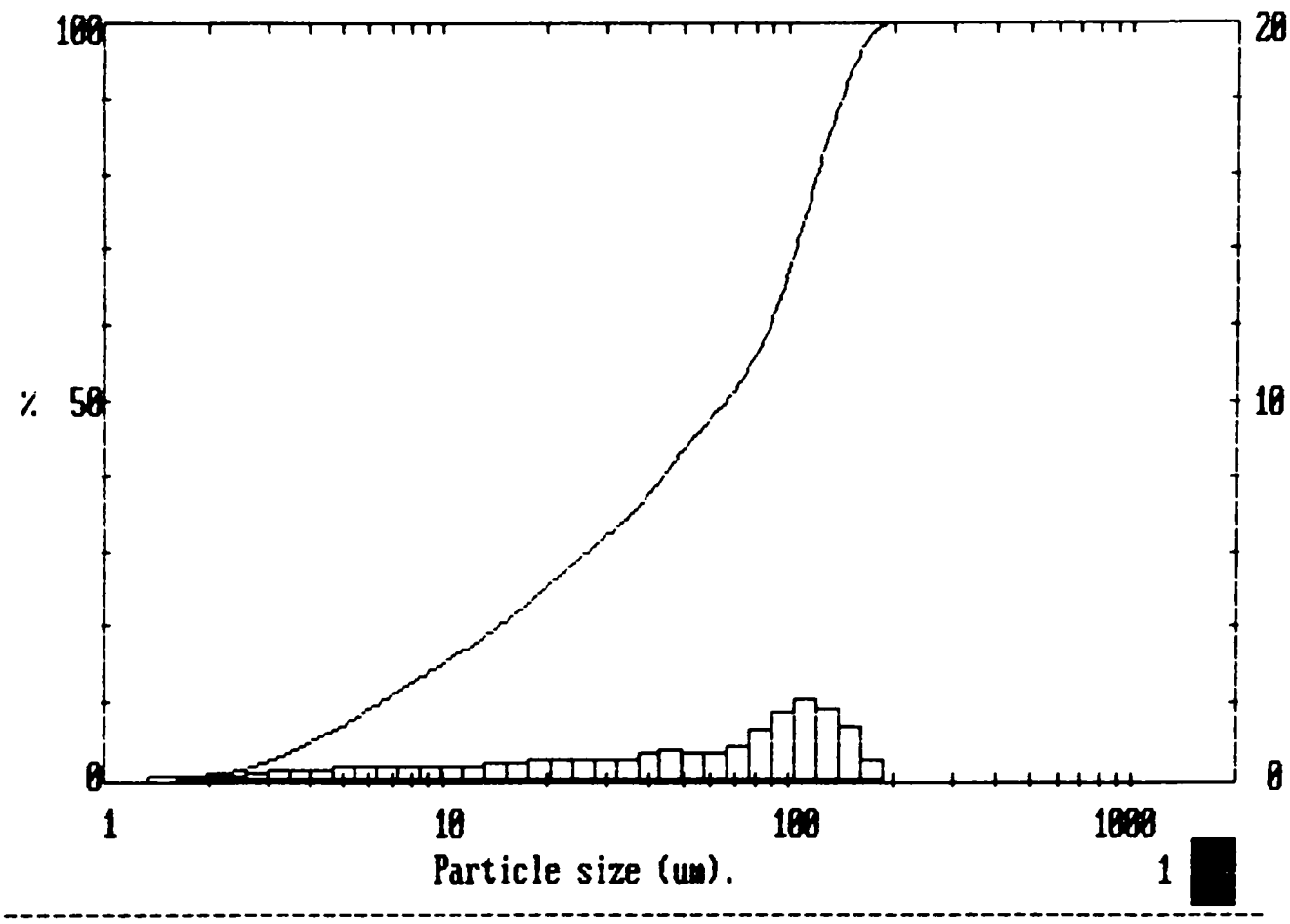

Size microns	under	% in band	Size microns	under	% in band
188.0	100.0	2.8	17.7	23.3	2.3
162.0	97.2	6.9	15.3	21.0	2.1
140.0	90.3	9.4	13.2	18.9	1.9
121.0	81.0	10.5	11.4	17.0	1.8
104.0	70.5	9.1	9.8	15.2	1.8
89.9	61.4	6.7	8.5	13.4	1.8
77.5	54.8	4.4	7.3	11.6	1.8
66.9	50.4	3.4	6.3	9.8	1.7
57.7	47.0	3.5	5.4	8.1	1.6
49.8	43.5	3.9	4.7	6.5	1.5
42.9	39.7	3.5	4.1	5.0	1.5
37.1	36.2	2.8	3.5	3.5	1.2
32.0	33.4	2.4	3.0	2.4	0.8
27.6	30.9	2.5	2.6	1.6	0.6
23.8	28.5	2.6	2.2	0.9	0.3
20.5	25.9	2.6	1.9	0.6	

Result source= Sample
Record No. = 4
Focal length = 100 mm.
Experiment type pia
Volume distribution
Beam length = 30.0 mm.
Obscuration =0.1542
Volume Conc. = 0.0034 %
Log. Diff. =2.36
Model indp

D(v,0.5) = 65.9 um
D(v,0.9) = 139.2 um
D(v,0.1) = 6.4 um
D(4,3) = 68.2 um
D(3,2) = 21.9 um
Span = 2.0
Spec. surf. area
0.3350 sq.m./cc.

Particle Size Distribution of Course Grade Pulverised Coal

System number 2349 Diode M00033

Malvern Instruments MASTER Particle Sizer M6.02 Date 01-01-84 Time 01-40

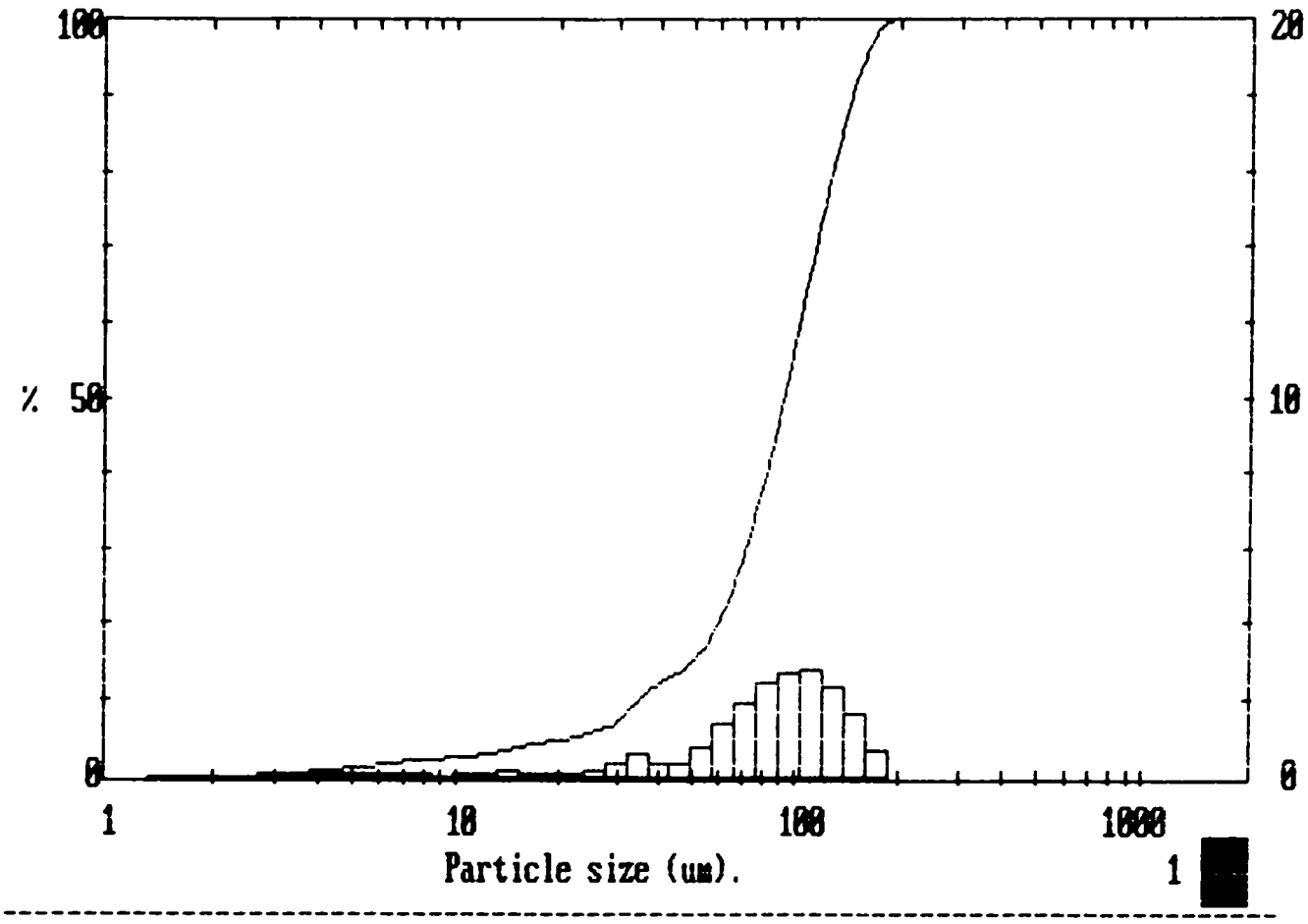

Size microns	under	% in band	Size microns	under	% in band
188.0	100.0	3.3	17.7	4.5	0.5
162.0	96.7	8.6	15.3	4.0	0.7
140.0	88.1	12.1	13.2	3.3	0.5
121.0	76.0	14.3	11.4	2.8	0.3
104.0	61.7	13.7	9.8	2.5	0.2
89.9	48.0	12.2	8.5	2.3	0.3
77.5	35.7	9.7	7.3	2.1	0.3
66.9	26.1	7.0	6.3	1.7	0.4
57.7	19.1	4.0	5.4	1.4	0.3
49.8	15.1	2.0	4.7	1.1	0.3
42.9	13.1	1.9	4.1	0.8	0.3
37.1	11.2	2.9	3.5	0.5	0.2
32.0	8.3	1.9	3.0	0.2	0.0
27.6	6.4	0.9	2.6	0.2	0.1
23.8	5.5	0.7	2.2	0.0	0.0
20.5	4.8	0.3	1.9	0.0	

Result source= Sample
Record No. = 5
Focal length = 100 mm.
Experiment type pia
Volume distribution
Beam length = 30.0 mm.
Obscuration =0.1939
Volume Conc. = 0.0130 %
Log. Diff. =4.16
Model indp

D(v,0.5) = 91.9 um
D(v,0.9) = 143.9 um
D(v,0.1) = 34.8 um
D(4,3) = 91.5 um
D(3,2) = 66.6 um
Span = 1.2
Spec. surf. area
0.1138 sq.m./cc.

Particle Size Distribution of Flour

System number 2349 Diode M00033

Malvern Instruments MASTER Particle Sizer M6.02 Date 09-01-92 Time 11-42

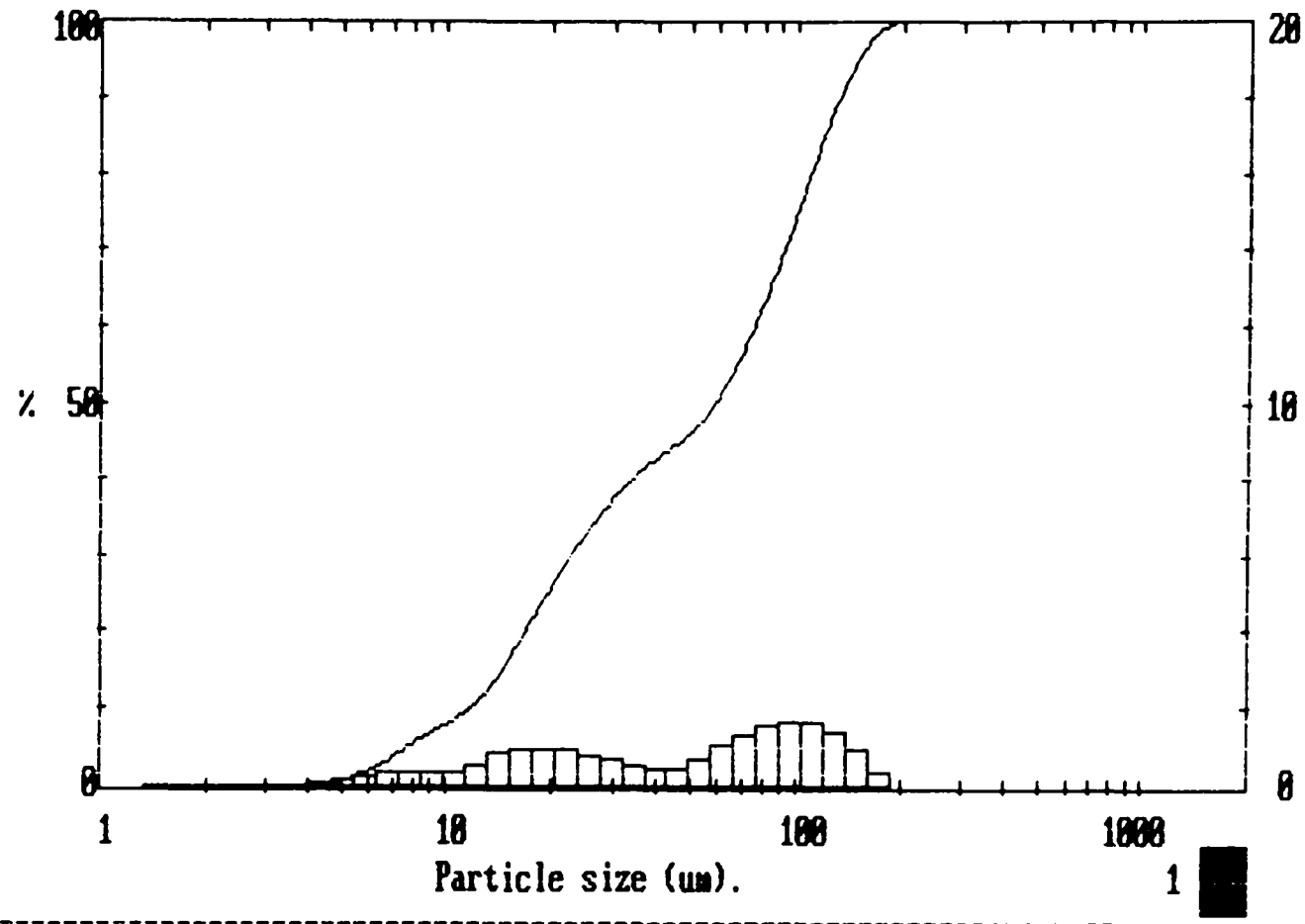

Size microns	under	% in band	Size microns	under	% in band
188.0	100.0	1.9	17.7	21.8	5.0
162.0	98.1	4.9	15.3	16.8	4.4
140.0	93.3	6.9	13.2	12.4	2.8
121.0	86.3	8.4	11.4	9.6	1.8
104.0	77.9	8.3	9.8	7.7	1.6
89.9	69.6	7.9	8.5	6.1	1.9
77.5	61.7	6.7	7.3	4.2	1.8
66.9	55.1	5.3	6.3	2.4	1.1
57.7	49.8	3.6	5.4	1.3	0.9
49.8	46.2	2.3	4.7	0.4	0.3
42.9	43.9	2.1	4.1	0.1	0.0
37.1	41.8	2.8	3.5	0.0	0.0
32.0	39.0	3.5	3.0	0.0	0.0
27.6	35.6	4.1	2.6	0.0	0.0
23.8	31.5	4.7	2.2	0.0	0.0
20.5	26.8	5.0	1.9	0.0	

Result source= Sample
Record No. = 4
Focal length = 100 mm.
Experiment type pia
Volume distribution
Beam length = 30.0 mm.
Obscuration =0.1889
Volume Conc. = 0.0064 %
Log. Diff. =4.77
Model indp

D(v,0.5) = 58.1 um
D(v,0.9) = 130.2 um
D(v,0.1) = 11.7 um
D(4,3) = 62.0 um
D(3,2) = 29.2 um
Span = 2.0
Spec. surf. area
0.2206 sq.m./cc.

Appendix 3 Laser Doppler Velocimetry Test Data

This appendix contains the tabulated test data from which the graphs associated with the laser doppler velocimetry test work were derived.

Run No.	ρ_s	V_{as}	$(V_{as}-V_{pcc})/V_{as}$ x100	$(V_{pcc}-V_{pldv})/V_{pcc}$ x100	$(V_{as}-V_{pldv})/V_{as}$ x100	n	1/n	d_{BL}	G	V_{pcc}	V_{pldv}
7	0.005	37.3	9.65	-9.04	-0.61	0.12	8.7	1.1	1.19	33.7	37.5
8	0.02	37.6	10.88	-11.14	+0.26	0.11	8.9	1.1	1.17	33.5	37.5
10	0.2	37.1	11.84	-12.02	+0.18	0.10	10.0	0.7	1.15	32.7	37.0
13	0.21	30.2	8.31	-9.72	-0.39	0.13	8.0	1.4	1.20	27.7	30.3
14	0.004	25.3	9.36	-8.14	-1.22	0.15	6.8	2.2	1.25	22.9	25.6
15	0.043	25.4	10.63	-10.78	+0.15	0.15	6.8	2.2	1.23	22.7	25.4
16	0.003	30.9	10.47	-10.68	+0.21	0.13	7.8	1.6	1.20	27.6	30.8
18	0.003	43.9	6.11	-7.70	+1.59	0.12	8.3	1.3	1.17	41.2	43.2
19	0.009	43.7	n/a	n/a	+0.71	0.12	8.1	1.4	1.19	n/a	43.4
20	0.15	43.4	10.08	-13.55	-3.47	0.11	9.4	0.9	1.12	39.1	41.9
21	0.22	25.1	11.74	-10.93	-0.81	0.13	7.9	1.5	1.21	22.2	25.3
22	0.21	30.6	11.95	-10.21	-1.74	0.10	9.6	0.8	1.18	26.9	31.1
23	0.26	37.5	10.71	-11.6	+0.89	0.10	10.1	0.7	1.14	33.5	37.2
24	0.27	30.0	8.03	-7.70	-0.33	0.10	10.1	0.7	1.16	27.6	30.1
25	0.55	30.0	8.03	-2.33	-5.70	0.07	14.3	0.2	1.17	27.6	31.7
26	0.009	37.7	10.79	-10.98	+0.19	0.13	8.0	1.4	1.19	33.7	37.6
27	0.028	25.4	13.29	-12.20	-1.09	0.14	7.2	1.9	1.23	22.0	25.7
28	0.096	37.7	12.55	-13.04	+0.49	0.12	8.6	1.2	1.18	33.0	37.5

For details of symbols used refer to Appendix 6.

Appendix 4 Electrostatic Sensor Test Data

This appendix contains the tabulated test data from which the graphs associated with the electrostatic sensor test work were derived.

Data Point Reference	V_{as}	V_{pcc}	ρ_s(actual)	ρ_s(sensor)
30(B)	21.19	19.17	0.091	1.76
30(C)	21.24	19.88	0.190	2.83
30(D)	21.14	19.91	0.237	3.39
30(E)	21.23	20.01	0.401	4.54
30(G)	21.02	19.85	1.031	6.22
30(K)	20.53	20.01	1.540	6.15
30a(B)	19.34	18.23	0.112	2.50
30a(C)	19.40	18.37	0.266	3.37
30a(E)	19.54	18.56	0.470	4.58
30a(G)	19.23	18.58	1.43	6.54
30a(J)	19.15	19.21	1.87	5.84
31(B)	20.05	18.72	0.136	2.05
31(C)	20.23	19.08	0.214	2.82
31(D)	20.13	19.06	0.250	3.51
31(E)	20.18	19.18	0.377	4.04
31(G)	20.12	19.25	0.981	6.61
32(A)	23.89	22.30	0.111	2.05
32(C)	24.02	22.80	0.130	2.79
32(D)	24.06	23.05	0.248	3.93
32(E)	23.93	22.87	0.297	4.45
32(F)	24.00	22.89	0.412	5.23
32(G)	23.80	22.50	0.817	7.62
33(A)	25.77	21.85	0.065	1.59
33(B)	25.83	23.25	0.144	2.83
33(F)	25.69	24.09	0.420	4.11
33(H)	25.64	24.09	0.662	5.14
33(K)	25.21	23.70	1.260	6.05

34(A)	28.41	24.06	0.101	2.10
34(B)	28.26	25.00	0.154	2.69
34(E)	28.49	25.61	0.203	3.32
34(G)	28.27	26.06	0.488	4.50
34(J)	27.74	25.67	0.898	5.65
35(A)	30.65	25.96	0.012	1.11
35(B)	30.58	25.84	0.087	2.14
35(C)	30.37	27.10	0.145	2.78
35(G)	30.93	27.79	0.352	4.13
35(H)	30.21	27.65	0.466	4.77
35(J)	29.96	27.49	0.845	5.93
35(K)	29.82	27.30	0.965	6.29
36(A)	31.88	27.81	0.011	1.02
36(B)	31.95	28.08	0.053	1.88
36(C)	31.80	28.98	0.112	2.83
36(F)	31.85	30.25	0.287	4.22
36(H)	31.43	30.01	0.531	5.93
37(B)	34.06	30.13	0.019	1.14
37(C)	33.93	30.01	0.049	1.90
37(D)	33.89	31.61	0.101	3.07
37(G)	33.84	32.28	0.199	3.85
37(H)	33.80	32.54	0.351	5.15
37(J)	33.56	32.29	0.532	6.67
38(C)	35.88	32.07	0.048	2.28
38(D)	35.92	32.62	0.087	2.65
38(F)	35.82	33.67	0.150	3.55
38(H1)	35.75	34.20	0.270	4.28
38(H2)	35.93	34.15	0.410	5.83

45(A)	22.22	22.07	2.73	4.63
45(B)	21.63	21.40	4.59	4.31
45(C)	21.30	21.39	5.45	4.35
46(A)	24.19	23.85	2.80	5.58
46(B)	23.61	23.40	3.70	4.95
46(C)	22.89	23.01	5.70	5.12
47(A)	26.12	25.54	2.51	6.38
47(B)	25.54	25.39	3.44	5.59
47(C)	24.72	24.72	5.13	5.27
48(A)	27.69	27.48	1.95	7.89
48(B)	28.12	27.13	2.63	7.24
48(C)	26.95	26.96	4.29	6.27
49(A)	30.07	29.24	1.77	8.13
49(B)	29.74	28.90	2.26	7.96
49(C)	28.43	28.46	3.90	7.83
50(A)	31.89	30.76	1.50	8.51
50(B)	31.58	30.36	1.91	8.27
50(C)	30.21	30.16	3.50	7.80
51(A)	34.11	32.37	1.27	8.38
51(B)	33.44	31.82	1.72	8.82
51(C)	31.93	30.94	3.02	8.73
52(A)	35.77	34.08	1.20	7.73
52(B)	35.43	-	1.41	7.84
52(C)	33.74	-	2.57	7.78
53(A)	38.26	-	0.95	7.35
53(B)	37.73	-	1.23	7.69
53(C)	35.74	-	2.20	8.22

54(A)	40.36	38.43	0.76	7.02
54(B)	39.77	37.78	1.05	7.65
54(C)	37.65	-	2.02	8.11
54(D)	36.47	-	3.16	6.93
55(A)	41.83	-	0.53	6.46
55(B)	41.27	-	0.98	7.60
55(C)	39.25	-	1.80	7.80
55(D)	38.12	-	2.44	7.65

Data Reference	ρ_s(actual)	ρ_s(sensor)
60B1	0.119	0.67
60E	0.156	1.50
60F1	0.300	2.33
60H	0.638	3.38
60K	0.775	3.74
60M	1.373	4.50
60Q	1.590	4.08
62B	0.045	1.22
62D	0.178	1.85
62F	0.372	2.55
62H	0.670	3.21
62L	0.847	3.73
63B	0.059	1.40
63D	0.164	1.75
63F	0.341	2.40
63J	0.558	2.95
63Z	0.644	3.19
63α	0.754	3.50
63β	0.969	3.73
63δ	1.665	4.30

Data Point Reference	ρ_s(actual)	ρ_s(sensor)	Relative Humidity
70G	0.52	2.67	8.6
70J	0.70	3.33	8.4
70M	1.27	4.41	8.5
70R	1.73	4.10	8.6
71C1	0.092	1.21	13.4
71C2	0.061	0.95	13.4
71E2	0.195	1.64	13.7
71G	0.570	3.0	13.3
72D	0.171	1.46	19.8

Data Reference	ρ_s(actual)	ρ_s(sensor)	C_{cc}	X
80E	0.25	2.45	0.41	∞
80H	0.61	3.10	0.42	∞
80L	0.85	3.45	0.41	∞
80P	0.94	3.64	0.38	∞
80Z	1.38	3.19	0.40	∞
81E	0.09	6.91	0.24	0.4
81H	0.48	6.00	0.21	0.4
81L	0.67	4.50	0.22	0.4
81P	0.78	4.30	0.21	0.4
81Z	0.83	4.30	0.24	0.4
82E	0.10	2.06	0.26	1.4
82H	0.46	3.29	0.26	1.4
82L	0.68	5.07	0.32	1.4
82P	0.77	5.47	0.29	1.4
82Z	0.89	4.88	0.31	1.4
83E	0.11	2.82	0.31	0.9
83H	0.36	5.04	0.32	0.9
83L	0.60	5.86	0.27	0.9
83P	0.78	6.46	0.25	0.9
83Z	0.97	6.27	0.28	0.9
84E	0.11	1.59	0.29	2.4
84H	0.37	1.84	0.34	2.4
84L	0.63	2.48	0.32	2.4
84P	0.63	2.85	0.35	2.4
84Z	1.03	3.08	0.37	2.4

85E	0.11	1.49	0.29	2.4
85H	0.35	1.85	0.32	2.4
85L	0.60	2.49	0.35	2.4
85P	0.84	2.54	0.35	2.4
86E	0.11	1.77	0.29	1.4
86H	0.37	2.54	0.29	1.4
86L	0.59	3.48	0.35	1.4
86P	0.83	4.16	0.39	1.4
86Z	1.02	4.43	0.38	1.4
87E	0.07	2.55	0.33	0.9
87H	0.39	3.69	0.35	0.9
87L	0.54	5.13	0.28	0.9
87P	0.84	5.41	0.26	0.9
87Z	1.01	5.52	0.27	0.9
88E	0.13	4.70	0.24	0.4
88H	0.37	5.61	0.21	0.4
88L	0.57	7.73	0.21	0.4
88P	0.79	7.95	0.21	0.4
88Z	0.98	7.48	0.24	0.4

90E	0.17	6.61	0.38	0.4
90H	0.35	8.52	0.25	0.4
90L	0.59	4.37	0.31	0.4
90P	0.92	3.16	0.40	0.4
90Z	1.01	3.42	0.41	0.4
91E	0.15	2.24	0.30	0.9
91H	0.37	3.50	0.26	0.9
91L	0.65	3.11	0.25	0.9
91P	0.74	3.04	0.26	0.9
91Z	1.13	2.64	0.24	0.9
92E	0.12	1.67	0.28	1.4
92H	0.35	2.43	0.29	1.4
92L	0.79	2.91	0.25	1.4
92Z	1.07	2.39	0.25	1.4
93E	0.09	1.20	0.27	2.4
93H2	0.32	1.54	0.30	2.4
93L	0.93	3.04	0.36	2.4
93Z	1.29	2.82	0.33	2.4

For details of symbols used the reader is refered to Appendix 6.

Appendix 5 Software Listings

This appendix contains listings of the software which was developed by the author during the programme of work described in this thesis.

The first section contains the listings of the real time data logging software, the purpose of which is discussed in Chapter 3. This software listing is divided into three sections. The first is the 68000 assembler code needed to allow the computer to communicate with the rig interface. The second and third sections are C code which has been split into two sections for logistic purposes. The C code was compiled into 68000 machine code modules and was then linked with the assembled assembler code to form the executable real time data logging software.

The second section of the appendix contains a listing of the software developed to calculate the mass flow rate of air through an orifice meter complying with BS1042, and was used to facilitate the calibration of the choke flow nozzles as described in Chapter 3.

The third section of the appendix contains a listing of the software developed to find the best straight line to fit a number of data points, and was used in the data processing detailed in Chapter 4.

The fourth section of the appendix contains a listing of the software developed to carry out the mathematical modelling of the electrostatic sensing head as detailed in Chapter 7.

Appendix 5 Section 1 Data Logging Software

```
            XDEF        BRDRESET
            XDEF        INDATA
            XDEF        OUTDATA
            TEXT
BRDRESET    LEA         $FA0000,A0
            TST.B       (A0)
            RTS
INDATA      MOVE.L      4(SP),D0
            LEA         $FA8000,A0
            TST.B       (A0)
            LSL.W       #01,D0
            ORI.L       #$00FB0000,D0
            MOVEA.L     D0,A0
            MOVE.W      (A0),D0
            ANDI.L      #$000000FF,D0
            RTS
OUTDATA     MOVE.L      4(SP),D0
            MOVE.L      8(SP),D1
            LSL.W       #01,D0
            LSL.W       #01,D1
            ORI.L       #$00FA8200,D0
            ORI.L       #$00FB0000,D1
            MOVEA.L     D0,A0
            MOVEA.L     D1,A1
            MOVE.W      (A0),D0
            MOVE.W      (A1),D1
            RTS
            END
```

```
#include <stdio.h>
#include <math.h>
#include <float.h>

   /* C function to initialise port chips, allocating
      chip 0 to drive one counter, and chip 1 to drive
      a second counter.
      All other chips (6) remain un initialised */

   int brdinit()

      {
      int   reg00v = 0x00; /*sets chip to mode 0 */
      int   reg02v = 0x00; /*sets port A input */
      int   reg03v = 0x00; /*sets port B input */
      int   reg04v = 0x3f; /*sets port C 6o 2i */
      int   reg06v = 0x80; /*sets port A submode 1x */
      int   reg07v = 0x80; /*sets port B submode 1x */
      int   c0r00add = 0x00; /*chip 0 reg0 address */
      int   c0r02add = 0x02; /*chip 0 reg2 address */
      int   c0r03add = 0x03; /*chip 0 reg3 address */
      int   c0r04add = 0x04; /*chip 0 reg4 address */
      int   c0r06add = 0x06; /*chip 0 reg6 address */
      int   c0r07add = 0x07; /*chip 0 reg7 address */
      int   c1r00add = 0x30; /*chip 1 reg0 address */
      int   c1r02add = 0x32; /*chip 1 reg2 address */
      int   c1r03add = 0x33; /*chip 1 reg3 address */
      int   c1r04add = 0x34; /*chip 1 reg4 address */
      int   c1r06add = 0x36; /*chip 1 reg6 address */
      int   c1r07add = 0x37; /*chip 1 reg7 address */
      int   errcount = 0;
      int   indval = 0;

      brdreset();
      outdata(reg00v,c0r00add);
      outdata(reg02v,c0r02add);
      outdata(reg03v,c0r03add);
      outdata(reg04v,c0r04add);
      outdata(reg06v,c0r06add);
      outdata(reg07v,c0r07add);
      outdata(reg00v,c1r00add);
      outdata(reg02v,c1r02add);
      outdata(reg03v,c1r03add);
      outdata(reg04v,c1r04add);
      outdata(reg06v,c1r06add);
      outdata(reg07v,c1r07add);
      indval = indata(c0r00add);
      if(indval != reg00v) ++errcount;
      indval = indata(c0r02add);
      if(indval != reg02v) ++errcount;
      indval = indata(c0r03add);
      if(indval != reg03v) ++errcount;
      indval = indata(c0r04add);
      if(indval != reg04v) ++errcount;
      indval = indata(c0r06add);
      if(indval != reg06v) ++errcount;
      indval = indata(c0r07add);
      if(indval != reg07v) ++errcount;
      indval = indata(c1r00add);
      if(indval != reg00v) ++errcount;
      indval = indata(c1r02add);
      if(indval != reg02v) ++errcount;
      indval = indata(c1r03add);
      if(indval != reg03v) ++errcount;
```

```
      indval = indata(c1r04add);
      if(indval != reg04v) ++errcount;
      indval = indata(c1r06add);
      if(indval != reg06v) ++errcount;
      indval = indata(c1r06add);
      if(indval != reg07v) ++errcount;
      return (errcount);
         }

   /* Function to input text */
void  finptext()
   {
   extern int   runnum;
   extern int   btnoz,supnoz;
   extern int   pwmfr,pwmno;
   extern char  constfname[15];
   extern char  outpfname[15];
   extern float patm;
   extern int   sudr,fudr;
   char  dumchar;

      printf("  The Wolfson Centre for Bulk Solids Handling Technology,");
      printf(" Thames Polytechnic.\n\n");
      printf("            On-Line Mass Flow Rate Measurement for Pulverised"),
      printf(" Coal in\n                                  Pneumatic Conveying");
      printf(" Systems\n\n");
      printf("                      Instrument Test and Calibration");
      printf(" Facility\n\n");
      printf("                                Please Enter the Run Number\n");
      scanf("%d %c",&runnum,&dumchar);
      printf("     Please Enter the Positions of the Blow Tank ");
      printf("Air Feed Nozzles - In Hex.\n");
      scanf("%x %c",&btnoz,&dumchar);
      printf("  Please Enter the Positions of the Supplementary ");
      printf("Air Feed Nozzles - In Hex.\n");
      scanf("%x %c",&supnoz,&dumchar);
      printf("     Please Enter the Pulse Width Modulation Fraction ");
      printf("as a Single Hex Digit\n");
      scanf("%x %c",&pwmfr,&dumchar);
      printf("     Please Enter the Pulse Width Modulation Nozzle ");
      printf("Number as a Single Intiger\n");
      scanf("%d %c",&pwmno,&dumchar);
      printf("                      Please Enter the Name of the Output File\n")
      scanf("%14s %c",outpfname,&dumchar);
      printf("                    Please Enter the Name of the Constants File\n"
      scanf("%14s %c",constfname,&dumchar);
      printf("                  Please Enter the Atmospheric Pressure in mmHg\n"
      scanf("%f %c",&patm,&dumchar);
      printf("                  Please Enter the Screen Update Rate in Seconds\n
      scanf("%d %c",&sudr,&dumchar);
      printf("                  Please Enter the File update rate in Seconds\n")
      scanf("%d %c",&fudr,&dumchar);
      }

   /* Function to initialise files */
void initfiles()
   {
   extern char  constfname[15];
   extern char  outpfname[15];
   extern FILE  *constfpoint;
   extern FILE  *outputfpoint;
   constfpoint = fopen(constfname,"r");
   outputfpoint = fopen(outpfname,"a");
   }
```

```
   /* Function to close files */
void  closefiles()
   {
   extern FILE *constfpoint;
   extern FILE *outputfpoint;
   extern int  debug;
   int   fclerror;
   if(debug == 1)
   printf("closing constants file");
   fclerror = fclose(constfpoint);
   if(debug == 1)
   printf("closing output file");
   fclerror = fclose(outputfpoint);
   if(fclerror != 0)
   printf("**** FILE CLOSE ERROR ****\n");
   }

   /* Function to input and assign constants */
void  fiaaconst()
   {
   extern FILE  *constfpoint;
   extern float uspgain,uspoffset;
   extern float btpgain,btpoffset;
   extern float sapgain,sapoffset;
   extern float lpgain,lpoffset;
   extern float ustgain,ustoffset;
   extern float ltgain,ltoffset;
   extern float escgain,escoffset;
   extern float lsgain,lsoffset;
   extern float orhgain,orhoffset;
   extern float otgain,otoffset;
   char  dumchar;

      fscanf(constfpoint,"%f %f %c",&uspgain,&uspoffset,&dumchar);
      fscanf(constfpoint,"%f %f %c",&btpgain,&btpoffset,&dumchar);
      fscanf(constfpoint,"%f %f %c",&sapgain,&sapoffset,&dumchar);
      fscanf(constfpoint,"%f %f %c",&lpgain,&lpoffset,&dumchar);
      fscanf(constfpoint,"%f %f %c",&ustgain,&ustoffset,&dumchar);
      fscanf(constfpoint,"%f %f %c",&ltgain,&ltoffset,&dumchar);
      fscanf(constfpoint,"%f %f %c",&escgain,&escoffset,&dumchar);
      fscanf(constfpoint,"%f %f %c",&lsgain,&lsoffset,&dumchar);
      fscanf(constfpoint,"%f %f %c",&orhgain,&orhoffset,&dumchar);
      fscanf(constfpoint,"%f %f %c",&otgain,&otoffset,&dumchar);
   }

   /* C functions to drive counters */
   /* Function to clear counter clock pins */
void coclrs(chipno)
   int chipno;       /* input chip no 0-7 */
   {
   int datab = 0x00;
   int addr;
   addr = (chipno << 5) | 0x0c;  /* addr = chip no shifted by 5 */
   outdata(datab,addr);          /* and ored with port C data reg addr */
   }

   /* function to initialise counter */
void coinit(chipno,countno,freqno)
   int chipno;
   int countno;
   int freqno;
   {
   int datab1;
```

```
    int datab2;
    int datab3 = 0x20;
    int addr;
    addr = (chipno << 5) | 0x0c;
    datab1 = (countno << 2) | 0x01;
    outdata(datab1,addr);
    datab2 = (freqno << 2) | 0x02;
    outdata(datab2,addr);
    outdata(datab3,addr);
    }

    /* Function to read counter */
coread(chipno,countno)
    int chipno;
    int countno;
    {
    int painput;
    int pbinput;
    int addra;
    int addrb;
    int addrc;
    int costat;
    int countval = 65537;
    addrc = (chipno << 5) | 0x0c;
    addrb = (chipno << 5) | 0x09;
    addra = (chipno << 5) | 0x08;
    costat = indata(addrc);
    costat = costat & 0x80;
    if(costat == 0)
       return(countval);
    else
       {
       painput = indata(addra);
       pbinput = indata(addrb);
       countval = (int)(pbinput << 8) | painput;
       return(countval);
       }
    }

    /* Function to input variables from counters */
void  invafrco()

    {
    extern int   c0fs[5];
    extern int   c1fs[5];
    int   lpct = 0;

    coclrs(0);
    coclrs(1);
       do
       {
       coinit(0,0,lpct);
       coinit(1,0,lpct);
          do
          c0fs[lpct] = coread(0,0);
          while(c0fs[lpct] > 65536);
          do
          c1fs[lpct] = coread(1,0);
          while(c1fs[lpct] > 65536);
          ++lpct;
       }
       while(lpct < 5);
    }
```

```
#include <stdio.h>
#include <math.h>
#include <float.h>

   /* Declaration of External or Global Variables */

   int   c0fs[5];
   int   c1fs[5];
   float uspfreq,uspgain,uspoffset,uspval;
   float btpfreq,btpgain,btpoffset,btpval;
   float sapfreq,sapgain,sapoffset,sapval;
   float lpfreq,lpgain,lpoffset,lpval;
   float ustfreq,ustgain,ustoffset,ustval;
   float ltfreq,ltgain,ltoffset,ltval;
   float escfreq,escgain,escoffset,escval,escavval;
   float lsfreq,lsgain,lsoffset,lsval,lsavval;
   float delt,mfcval,mfcavval;
   float orhfreq,orhgain,orhoffset,orhval,orhavval;
   float otfreq,otgain,otoffset,otval;
   float btmfnom,samfnom,totamfnom;
   float btamfval,samfval,totamfval;
   float slrval,patm,savval,slravval,savavval;
   float btapcval,totamfavval;

   int   runnum;
   int   btnoz;
   int   supnoz;
   int   pwmfr;
   int   pwmno;
   int   sudr;
   int   fudr;
   int   loopcount;
   int   fclerror;
   int   errorcount;
   int   debug;

   FILE  *constfpoint;
   FILE  *outputfpoint;

   char  constfname[15];
   char  outpfname[15];
   char  dumchar;
   char  rerunchar;


   /* Function to calculate nominal air flow rates */
void  fcnomamf()
   {
   extern float btmfnom;
   extern float samfnom;
   extern float totamfnom;
   extern float btapcval;
   extern int   btnoz;
   extern int   supnoz;
   extern int   pwmfr;
   extern int   pwmno;
   float noz1mod = 1.0;
   float noz2mod = 1.0;
   float noz3mod = 1.0;
   float noz4mod = 1.0;
   btmfnom = 0;
   samfnom = 0;
      switch (pwmno)
         {
```

```
    case 0: noz1mod = pwmfr/16.0;
    case 1: noz2mod = pwmfr/16.0;
    case 2: noz3mod = pwmfr/16.0;
    case 3: noz4mod = pwmfr/16.0;
    }

if((btnoz & 0x80) != 0)
   btmfnom = 0.1485;
if((btnoz & 0x40) != 0)
   btmfnom = btmfnom + 0.07999;
if((btnoz & 0x20) != 0)
   btmfnom = btmfnom + 0.04007;
if((btnoz & 0x10) != 0)
   btmfnom = btmfnom + 0.02034;
if((btnoz & 0x08) != 0)
   btmfnom = btmfnom + (noz4mod * 0.01060 );
if((btnoz & 0x04) != 0)
   btmfnom = btmfnom + (noz3mod * 0.00503  );
if((btnoz & 0x02) != 0)
   btmfnom = btmfnom + (noz2mod * 0.00260  );
if((btnoz & 0x01) != 0)
   btmfnom = btmfnom + (noz1mod * 0.00155  );

if((supnoz & 0x80) != 0)
           samfnom = 0.1482;
if((supnoz & 0x40) != 0)
   samfnom = samfnom + 0.08000;
if((supnoz & 0x20) != 0)
   samfnom = samfnom + 0.04000;
if((supnoz & 0x10) != 0)
   samfnom = samfnom + 0.02027;
if((supnoz & 0x08) != 0)
   samfnom = samfnom + 0.01010;
if((supnoz & 0x04) != 0)
   samfnom = samfnom + 0.00494;
      if((supnoz & 0x02) != 0)
         samfnom = samfnom + 0.00260;
      if((supnoz & 0x01) != 0)
         samfnom = samfnom + 0.00131;

      totamfnom = samfnom + btmfnom;
      btapcval = (btmfnom/totamfnom) * 100;
      }

   /* Function to initialise timer chip */
int   timeinit()
   {
   int   tcrdat  = 0x14;
   int   ucprdat = 0xff;
   int   mcprdat = 0xff;
   int   lcprdat = 0xff;
   int   tcraddr  = 0x50;
   int   ucpraddr = 0x53;
   int   mcpraddr = 0x54;
   int   lcpraddr = 0x55;
   int   errorcount = 0;
   int   retdata;

   outdata(tcrdat,tcraddr);
   outdata(ucprdat,ucpraddr);
   outdata(mcprdat,mcpraddr);
   outdata(lcprdat,lcpraddr);
   retdata = indata(tcraddr);
   if(retdata != tcrdat)
```

```
      ++errorcount;
   retdata = indata(ucpraddr);
   if(retdata != ucprdat)
      ++errorcount;
   retdata = indata(mcpraddr);
   if(retdata != mcprdat)
      ++errorcount;
   retdata = indata(lcpraddr);
   if(retdata != lcprdat)
      ++errorcount;
   return(errorcount);
   }


   /* Function to output to monitor */
void foptmoni()
   {
   extern float escval,escavval;
   extern float lsval,lsavval;
   extern float mfcval,mfcavval;
   extern float totamfval,totamfavval;
   extern float slrval,slravval;
   extern float savval,savavval;
   extern float orhval,orhavval;
   extern float btapcval;
   extern float btamfval;
   extern float samfval;
   extern float uspval;
   extern float btpval;
   extern float sapval;
   extern float lpval;
   extern float ustval;
   extern float otval;
   extern float ltval;
   extern float delt;
extern int   runnum;
extern int   btnoz;
extern int   supnoz;
extern int   pwmfr;
extern int   pwmno;
extern int   fudr,sudr;
extern int   loopcount;

   printf("   The Wolfson Centre For Bulk Solids Handling Technology");
   printf(", Thames Polytechnic.\n");
   printf("  On-Line Mass Flow Rate Measurement For P.F. in ");
   printf("Pneumatic Conveying Systems.\n");
   printf("                      Instrument Test And Calibration");
   printf(" Facility\n\n");
   printf("                         Test Run Number %d\n",runnum);
   printf("Nozzel Positions %2X  %2X  %2X  %2X\n",btnoz,supnoz,pwmfr,
          pwmno);
   printf("Update Rates     File = %2d     Screen = %2d\n\n",fudr,sudr);
   printf("   E.S. Conc. Value = %4.1f        Average = %4.1f\n",escval,
          escavval);
   printf("         Load Cells = %5.1f kg     Average = %5.1f kg\n"
          ,lsval,lsavval);
   printf("Coal Mass Flow Rate = %7.5f kg/s   Average = %7.5f kg/s\n",
          mfcval,mfcavval);
   printf("Air Mass Flow Rate  = %7.5f kg/s   Average = %7.5f kg/s\n",
          totamfval,totamfavval);
   printf("Solid Loading Ratio = %6.3f        Average = %6.3f \n",
          slrval,slravval);
   printf("   Superf. Air Vel. = %5.2f m/s    Average = %5.2f m/s\n",
```

```
            savval,savavval);
      printf("         Output R.H. = %5.2f         Average = %5.2f \n\n",
            orhval,orhavval);
      printf("                    Blow Tank Air Percent = %5.3f\n",btapcval);
      printf("B.T. Air M.F.R. = %5.4f kg/s   S.A. Air M.F.R. = %5.4f kg/s\n"
            ,btamfval,samfval);
      printf("N.B. U.S.Press. = %4.2f BarG   Conv. L. Press. = %4.3f BarG\n"
            ,uspval,lpval);
      printf("N.B. B.T. Press.= %4.2f BarG   N.B. Sup. Press.= %4.2f BarG\n"
            ,btpval,sapval);
      printf("      U.S. Temp. = %5.2f DegC      Output Temp. = %5.2f DegC\n"
            ,ustval,otval);
      printf("The Line Temperature is %5.2f DegC \n",ltval);
      printf("Delta = %f Seconds\n",delt);
      printf("Loopcount = %d\n\n",loopcount);
   }

   /* Function to output to file */
void foptfile()
   {
   /* output file pointer */
   extern   FILE  *outputfpoint;

   /* constants file name */
   extern   char  constfname[15];

   /* raw frequencies */
   extern   int   c0fs[5];
   extern   int   c1fs[5];

   /* variable values */
   extern   float uspval;
   extern   float btpval;
   extern   float sapval;
   extern   float lpval;
   extern   float ustval;
   extern   float ltval;
   extern   float escval;
   extern   float lsval;
   extern   float mfcval;
   extern   float orhval;
   extern   float otval;
   extern   float btamfval;
   extern   float samfval;
   extern   float totamfval;
   extern   float slrval;
   extern   float savval;
   extern   float btapcval;
   extern   float patm;

   /* averaged variable values */
   extern   float escavval;
   extern   float lsavval;
   extern   float mfcavval;
   extern   float orhavval;
   extern   float totamfavval;
   extern   float slravval;
   extern   float savavval;

   /* misc vars */
   extern   int   fudr,sudr;
   extern   int   loopcount;
   extern   float delt;
```

```
   fprintf(outputfpoint,"*\n");
   fprintf(outputfpoint,"%14s\n",constfname);
   fprintf(outputfpoint,"%5d %5d %5d %5d %5d\n",
   c0fs[0],c0fs[1],c0fs[2],c0fs[3],c0fs[4]);
   fprintf(outputfpoint,"%5d %5d %5d %5d %5d\n",
   c1fs[0],c1fs[1],c1fs[2],c1fs[3],c1fs[4]);
   fprintf(outputfpoint,"%6.3f %6.3f %6.3f\n",uspval,btpval,sapval);
   fprintf(outputfpoint,"%6.3f %6.3f %6.3f\n",lpval,ustval,ltval);
   fprintf(outputfpoint,"%7.3f %6.2f %7.4f\n",escval,lsval,mfcval);
   fprintf(outputfpoint,"%6.2f %5.2f %7.5f\n",orhval,otval,btamfval);
   fprintf(outputfpoint,"%7.5f %7.5f %6.3f\n",samfval,totamfval,slrval);
   fprintf(outputfpoint,"%6.2f %7.3f %5.1f\n",savval,btapcval,patm);
   fprintf(outputfpoint,"%7.3f %6.2f %7.4f\n",escavval,lsavval,mfcavval);
   fprintf(outputfpoint,"%6.2f \n",orhavval);
   fprintf(outputfpoint,"%7.5f %6.3f %6.2f\n",totamfavval,slravval,savavval);
   fprintf(outputfpoint,"%d %d %d %f\n",fudr,sudr,loopcount,delt);
   }

   /* Function to evaluate delta */
float delteval()
   {
   float delt;
   int   tcraddr = 0x50;
   int   stopdat = 0x14;
   int   stardat = 0x15;
   int   crdhadd = 0x57;
   int   crdmadd = 0x58;
   int   crdladd = 0x59;
   int   countread = 0;
   int   crdh;
   int   crdm;
   int   crdl;

      outdata(stopdat,tcraddr);
      crdh = indata(crdhadd);
      crdm = indata(crdmadd);
      crdl = indata(crdladd);
      outdata(stardat,tcraddr);
      countread =(((crdh << 8) | crdm) << 8) | crdl;
      delt = (16777216 - (float)countread) * 7.8125e-5;
      return(delt);
   }

void  p1calc()

   {
   extern float uspfreq;
   extern float uspgain;
   extern float uspoffset;
   extern float uspval;
      uspval = (uspfreq * uspgain) + uspoffset;
   }

void  p2calc()

   {
   extern float btpfreq;
   extern float btpgain;
   extern float btpoffset;
   extern float btpval;
      btpval = (btpfreq * btpgain) + btpoffset;
   }

void  p3calc()
```

```
    {
    extern float sapfreq;
    extern float sapgain;
    extern float sapoffset;
    extern float sapval;
       sapval = (sapfreq * sapgain) + sapoffset;
    }

void  p4calc()

    {
    extern float lpfreq;
    extern float lpgain;
    extern float lpoffset;
    extern float lpval;
       lpval = (lpfreq * lpgain) + lpoffset;
    }

void  t1calc()

    {
    extern float ustfreq;
    extern float ustgain;
    extern float ustoffset;
    extern float ustval;
       ustval = (ustfreq * ustgain) + ustoffset;

    }

void  t2calc()

    {
    extern float ltfreq;
    extern float ltgain;
    extern float ltoffset;
    extern float ltval;
       ltval = (ltfreq * ltgain) + ltoffset;

    }

void  esccalc()

    {
    extern float escfreq;
    extern float escgain;
    extern float escoffset;
    extern float escval;
       escval = (escfreq * escgain) + escoffset;

    }

void  lscalc()

    {
    extern float lsfreq;
    extern float lsgain;
    extern float lsoffset;
    extern float lsval;
       lsval = (lsfreq * lsgain) + lsoffset;

    }

void  mfccalc()
```

```
   {
   static float memlsval = 0;
   extern float lsval;
   extern float delt;
   extern float mfcval;
      mfcval = (lsval-memlsval) / delt;
      memlsval = lsval;

   }

void  rhcalc()

   {
   extern float orhfreq;
   extern float orhgain;
   extern float orhoffset;
   extern float orhval;
      orhval = (orhfreq * orhgain) + orhoffset;

   }

void  otcalc()

   {
   extern float otfreq;
   extern float otgain;
   extern float otoffset;
   extern float otval;
      otval = (otfreq * otgain) + otoffset;

   }

   /* Function to evaluate air flow rates */
int   mfacalc()

{
extern float btmfnom;
extern float samfnom;
extern float btpval;
extern float sapval;
extern float ustval;
extern float totamfnom;
extern float uspval;
extern float btamfval;
extern float samfval;
extern float totamfval;
int   errorvalue = 0;
   btamfval = btmfnom*sqrt(293.0)*(uspval+1.0)
         /(5.0*sqrt(ustval+273.15));
   samfval = samfnom*sqrt(293.0)*(uspval+1.0)
         /(5.0*sqrt(ustval+273.15));
   totamfval = totamfnom*sqrt(293.0)*(uspval+1.0)
         /(5.0*sqrt(ustval+273.15));

   if((btamfval+samfval-totamfval)>(0.001*totamfval))
   errorvalue = 1;
   if(((btpval+1.0)/(uspval+1.0))>0.68)
   errorvalue = 2;
   if(((sapval+1.0)/(uspval+1.0))>0.68)
   errorvalue = 3;

return (errorvalue);
}
```

```
   /* Function to evaluate solids loading ratio  */
void  slrcalc()

   {
   extern float totamfval;
   extern float mfcval;
   extern float slrval;
      slrval = mfcval/totamfval;

   }

   /* Function to evaluate superficial air velocity */
void  savcalc()

   {
   extern float totamfval;
   extern float lpval;
   extern float ltval;
   extern float savval;
   extern float patm;
   float pabs;
   float rho;
   float veedot;

   pabs = (lpval * 100) + (patm * 0.13332);
   rho = (3.4835 * pabs) / (ltval + 273.15);
   veedot = totamfval / rho;
   savval = veedot / 2.206e-3;
   }

      /* Averaging functions */
float avesc(escval)
   float escval;
   {
   static float escvals[10] = {0};
   float avescval;
   extern int  debug;
   extern int   loopcount;
   int   shiftcount;
   int addcount;
   if(debug == 1)
   {
   printf("escval = %f on entry to avesc\n",escval);
   printf("\nloopcount = %d at start of avesc\n",loopcount);
   }
   shiftcount = 1;
   do
      {
      if(debug == 1)
      printf("shiftcount = %d\n",shiftcount);
      escvals[10-shiftcount] = escvals[9-shiftcount];
      ++shiftcount;
      }
   while(shiftcount < 10);
   escvals[0] = escval;
      if(debug == 1)
      {
      printf("escvals0 = %f  escvals1 = %f\n",escvals[0],escvals[1]);
      printf("escvals2 = %f  escvals3 = %f\n",escvals[2],escvals[3]);
      printf("escvals4 = %f  escvals5 = %f\n",escvals[4],escvals[5]);
      printf("escvals6 = %f  escvals7 = %f\n",escvals[6],escvals[7]);
      printf("escvals8 = %f  escvals9 = %f\n",escvals[8],escvals[9]);
      }
```

```
    avescval = 0;
    if(loopcount < 10)
       {
       addcount = 0;
       do
          {
          avescval = avescval + escvals[addcount];
          ++ addcount;
          }
       while(addcount < loopcount);
       avescval = avescval/loopcount;
       }
    else
       {
       addcount = 0;
       do
          {
          avescval = avescval + escvals[addcount];
          ++ addcount;
          }
       while(addcount < 10);
       avescval = avescval/10;
       }
    if( debug == 1)
    printf("avescval equals %f\n",avescval);
    return(avescval);
    }

float avls(lsval)
    float lsval;
    {
    static float lsvals[10] = {0};
    float avlsval;
    extern int   loopcount;
    extern int   debug;
    int   shiftcount = 1;
    int   addcount;
    if( debug == 1)
    printf("loopcount = %d at start of avls\n",loopcount);
    do
       {
       lsvals[10-shiftcount] = lsvals[9 - shiftcount];
       ++ shiftcount;
       }
    while(shiftcount < 10);
    lsvals[0] = lsval;
    avlsval = 0;
    if(loopcount < 10)
       {
       addcount = 0;
       do
          {
          avlsval = avlsval + lsvals[addcount];
          ++ addcount;
          }
       while(addcount < loopcount);
       avlsval = avlsval/loopcount;
       }
    else
       {
       addcount = 0;
       do
          {
          avlsval = avlsval + lsvals[addcount];
```

```
            ++ addcount;
            }
         while(addcount < 10);
         avlsval = avlsval/10;
         }
      if(debug == 1)
      printf("avlsval equals %f\n",avlsval);
      return(avlsval);
      }

float avmfc(mfcval)
      float mfcval;
      {
      static float mfcvals[10] = {0};
      float avmfcval;
      extern int  loopcount;
      extern int  debug;
      int   shiftcount = 1;
      int   addcount;
      if(debug == 1)
      printf("loopcount = %d at the start of avmfc\n",loopcount);
      do
         {
         mfcvals[10 - shiftcount] = mfcvals[9 - shiftcount];
         ++ shiftcount;
         }
      while(shiftcount < 10);
      mfcvals[0] = mfcval;
      avmfcval = 0;
      if(loopcount < 10)
         {
         addcount = 0;
         do
            {
            avmfcval = avmfcval + mfcvals[addcount];
            ++ addcount;
            }
         while(addcount < loopcount);
         avmfcval = avmfcval/loopcount;
         }
      else
         {
         addcount = 0;
         do
            {
            avmfcval = avmfcval + mfcvals[addcount];
            ++ addcount;
            }
         while(addcount < 10);
         avmfcval = avmfcval/10;
         }
      if(debug == 1)
      printf("avmfcval equals %f\n",avmfcval);
      return(avmfcval);
      }

float avorh(orhval)
      float orhval;
      {
      static float orhvals[10] = {0};
      float avorhval;
      extern int   loopcount;
      extern int   debug;
      int   shiftcount = 1;
```

```
int   addcount;
if(debug == 1)
printf("loopcount = %d at the start of avorh\n",loopcount);
do
   {
   orhvals[10 - shiftcount] = orhvals[9 - shiftcount];
   ++ shiftcount;
   }
while(shiftcount < 10);
orhvals[0] = orhval;
avorhval = 0;
if(loopcount < 10)
   {
   addcount = 0;
   do
      {
      avorhval = avorhval + orhvals[addcount];
      ++ addcount;
      }
   while(addcount < loopcount);
   avorhval = avorhval/loopcount;
   }
else
   {
   addcount = 0;
   do
      {
      avorhval = avorhval + orhvals[addcount];
      ++addcount;
      }
   while(addcount < 10);
   avorhval = avorhval/10;
   }
   if(debug == 1)
   printf("avorhval equals %f\n",avorhval);
   return(avorhval);
   }

float avtotamf(totamfval)
   float totamfval;
   {
   static float sotamfvals[10] = {0};
   float avtotamfval;
   extern int  loopcount;
   extern int  debug;
   int   shiftcount = 1;
   int   addcount;
   if(debug == 1)
   printf("loopcount = %d at the start of avtotamf\n",loopcount);

   do
      {
      sotamfvals[10 - shiftcount] = sotamfvals[9 - shiftcount];
      ++ shiftcount;
      }
   while(shiftcount < 10);
   sotamfvals[0] = totamfval;
   avtotamfval = 0;
   if(loopcount < 10)
      {
      addcount = 0;
      do
         {
         avtotamfval = avtotamfval + sotamfvals[addcount];
```

```
            ++ addcount;
            }
         while(addcount < loopcount);
         avtotamfval = avtotamfval/loopcount;
         }
      else
         {
         addcount = 0;
         do
            {
            avtotamfval = avtotamfval + sotamfvals[addcount];
            ++addcount;
            }
         while(addcount < 10);
         avtotamfval = avtotamfval/10;
         }
         if(debug == 1)
         printf("avtotamfval equals %f\n",avtotamfval);
      return(avtotamfval);
      }

float avslr(slrval)
   float slrval;
   {
   static float slrvals[10] = {0};
   float avslrval;
   extern int  loopcount;
   extern int  debug;
   int   shiftcount = 1;
   int   addcount;
   if(debug == 1)
   printf("loopcount = %d at the start of avslr",loopcount);
   do
      {
      slrvals[10 - shiftcount] = slrvals[9 - shiftcount];
      ++ shiftcount;
      }
while(shiftcount < 10);
slrvals[0] = slrval;
avslrval = 0;
if(loopcount < 10)
   {
   addcount = 0;
   do
      {
      avslrval = avslrval + slrvals[addcount];
      ++ addcount;
      }
   while(addcount < loopcount);
   avslrval = avslrval/loopcount;
   }
else
   {
   addcount = 0;
   do
      {
      avslrval = avslrval + slrvals[addcount];
      ++ addcount;
      }
   while(addcount < 10);
   avslrval = avslrval/10;
   }
   if(debug == 1)
   printf("avslrval equals %f\n",avslrval);
```

```
    return(avslrval);
    }

float avsav(savval)
    float savval;
    {
    static float savvals[10] = {0};
    float avsavval;
    extern int  loopcount;
    extern int  debug;
    int   shiftcount = 1;
    int   addcount;
    if(debug == 1)
    printf("loopcount = %d at the start of avsav\n",loopcount);
    do
       {
       savvals[10-shiftcount] = savvals[9 - shiftcount];
       ++shiftcount;
       }
    while(shiftcount < 10);
    savvals[0] = savval;
    avsavval = 0;
    if(loopcount < 10)
       {
       addcount = 0;
       do
          {
          avsavval = avsavval + savvals[addcount];
          ++addcount;
          }
       while(addcount < loopcount);
       avsavval = avsavval/loopcount;
       }
    else
       {
       addcount = 0;
       do
          {
          avsavval = avsavval + savvals[addcount];
          ++ addcount;
          }
       while(addcount < 10);
       avsavval = avsavval/10;
       }
       if(debug == 1)
       printf("avsavval equals %f\n",avsavval);
    return(avsavval);
    }

void   fcalcs()

    {
    extern int     debug;
    extern int     errorcount;

    extern float   delt;
    extern float   escval,escavval;
    extern float   lsval,lsavval;
    extern float   mfcval,mfcavval;
    extern float   orhval,orhavval;
    extern float   totamfval,totamfavval;
    extern float   slrval,slravval;
    extern float   savval,savavval;
```

```
p1calc();
if(debug == 1)
printf("calling p2calc\n");
p2calc();
p3calc();
if(debug == 1)
printf("calling p4calc\n");
p4calc();
t1calc();
if(debug == 1)
printf("calling t2calc\n");
t2calc();
esccalc();
if(debug == 1)
printf("calling lscalc\n");
lscalc();
if(debug == 1)
printf("calling delteval\n");
delt = delteval();
if(debug == 1)
printf("calling mfccalc\n");
mfccalc();
if(debug == 1)
printf("calling rhcalc\n");
rhcalc();
if(debug == 1)
printf("calling otcalc\n");
otcalc();
if(debug == 1)
printf("calling mfacalc\n");
errorcount = mfacalc();
if(debug == 1)
printf("calling slrcalc\n");
slrcalc();
if(debug == 1)
        printf("calling savcalc\n");
        savcalc();
        if(debug == 1)
        printf("calling averaging routines\n");
        escavval = avesc(escval);
        lsavval = avls(lsval);
        mfcavval = avmfc(mfcval);
        orhavval = avorh(orhval);
        totamfavval = avtotamf(totamfval);
        slravval = avslr(slrval);
        savavval = avsav(savval);
        if(debug == 1)
        printf("exiting fcalcs\n");
        }

        /* delay routine number one */
void    delay1()
   {
   float z,theta;

   theta = 0;
   do
      {
      z = cos(theta / 1000);
      ++ theta;
      }
   while(theta < 10);
   }
```

```
      /* delay routine number two */
void delay2()
   {
   int   y =0;

   do
      {
      delay1();
      delay1();
      delay1();
      delay1();
      delay1();
      ++y;
      }
   while(y < 3);
   }
   /* MAIN PROGRAMME */
void  main()

   {
   extern int  errorcount;
   extern int  debug;
   extern int   loopcount;
   int   fileout;
   int   screenout;
   int   hit;
   int   contin;
   int   menuchoice;
   int   invscout;
   int   invfiout;

   char dumchar;
   char rerunchar;

   extern int c0fs[5];
   extern int c1fs[5];
   extern int fudr,sudr;

   extern float uspfreq,btpfreq,sapfreq;
   extern float lpfreq,ustfreq,ltfreq;
   extern float escfreq,lsfreq,orhfreq,otfreq;

   /* Start of programme - rerun starts here */
   debug = 0;
   do
   {
   contin = 1;
   hit = 0;
   errorcount = 0;
   /* call port board initialisation */
   errorcount = brdinit();

   /* call routine to input text */
   finptext();
   if(debug == 1)
   printf("calling initfiles");

   /* call routine to open constants file and output file */
   initfiles();
   if(debug == 1)
   printf("calling fiaaconst");
   /* call routine to input and assign constants */
   fiaaconst();
   if(debug == 1)
```

```
printf("calling fcnmamf");
/* call routine to evaluate nominal air mass flow rates */
fcnomamf();
if(debug == 1)
printf("calling timeinit");
/* call routine to initialise timer chip on port board */
errorcount = errorcount + timeinit();

/* initialise loopcount, fileout, screenout */
loopcount = 1;
fileout = 1;
screenout = 1;
if(debug == 1)
printf("start of programme loop");
/* start of programme loop */
do
{
do
   {
   /* call routine to input variables from counters */
   if(debug == 1)
   printf("calling invafrco");
   invafrco();

   /* programme section to assign frequency values */
   lsfreq = (float) c0fs[0];
   uspfreq = (float) c0fs[1];
   btpfreq = (float) c0fs[2];
   sapfreq = (float) c0fs[3];
   ustfreq = (float) c0fs[4];

   orhfreq = (float) c1fs[0];
   otfreq = (float) c1fs[1];
   ltfreq = (float) c1fs[2];
   lpfreq = (float) c1fs[3];
escfreq = (float) c1fs[4];

/* call function to call calcs functions */
if(debug == 1)
printf("calling fcalcs\n");
fcalcs();

/* if screenout equals 1 output to screen */
if(debug == 1)
printf("calling foptmoni if applicable\n");
if(screenout == 1)
foptmoni();

/* if fileout equals 1 output to file */
if(debug == 1)
printf("calling foptfile if applicable  fileout = %d\n",fileout);
if(fileout == 1)
foptfile();

/* incrument loopcount */
++ loopcount;

/* evaluate fileout, and screen out for new value of loopcount */
invscout = loopcount % sudr;
invfiout = loopcount % fudr;
if(invscout == 0)
   screenout = 1;
if(invscout != 0)
   screenout = 0;
```

```
    if (invfiout == 0)
       fileout = 1;
    if (invfiout != 0)
       fileout = 0;

    /* call delay routine */
    delay2();

    /* has there been a keyboard hit ? */
    if(debug == 1)
    printf("evaluating keyboard hit\n");
    hit = kbhit();
    if(debug == 1)
    printf("hit = %d\n",hit);
    }
while(hit == 0);

/* print menu for options  */

printf("\n\n\n");
printf("   The Wolfson Centre for Bulk Solids Handling Technology,");
printf("Thames Polytechnic\n\n");
printf("           On-Line Mass Flow Rate Measurement for Pulverised Coal")
printf(" in\n                              Pneumatic Conveying Systems\n\n");
printf("                      Instrument Test and Calibration");
printf(" Facility\n\n\n\n");
printf("                                  MENU\n\n\n");
printf("    1. Continue Test Run.\n\n");
printf("    2. Change Screen Update Rate.\n\n");
printf("    3. Change File Update Rate.\n\n");
printf("    4. Terminate Test Run.\n\n");
printf("    Please Enter Option Number.\n");

/* input character which caused kbhit =  1    */
scanf("%c",&dumchar);

/* input menu choice     */
scanf("%d %c",&menuchoice,&dumchar);

/* if menu choice = 1 no action needed, as continue already = 1 */
/* if menu choice = 2 input new value for sudr   */
if(menuchoice == 2)
   {
   printf("Enter New Value for Screen Update Rate");
   scanf("%d %c",&sudr,&dumchar);
   }

/* if menu choice = 3 input new value for fudr   */
if(menuchoice == 3)
   {
   printf("Enter New Value for File Update Rate");
   scanf("%d %c",&fudr,&dumchar);
   }

/* if menu choice = 4 contin = 0   */
if(menuchoice == 4)
   contin = 0;
}

while(contin == 1);

/* if menuchoice = 4 (exit), close files   */
if(debug == 1)
printf("calling closefiles");
```

```
closefiles();

/* rerun programme  */
printf("   Do you wish to carry out another run ?\n");
scanf("%c %c",&rerunchar,&dumchar);
}
while(rerunchar == 'Y');
}

                        /* END OF MAIN */
```

Appendix 5 Section 2 Orifice Meter Software

```
#include <stdio.h>
#include <math.h>

   /* C Program To Calculate The Mass Flow Rate Through

      An Orifice Plate Conforming To BS1042     */


   /* Inputs   d     Orifice Diameter in Meters
               delP  Differential Pressure in mm of Water
               P1    Upstream Gauge Pressure in BarG
               Pat   Atmospheric Pressure in mm of Mercury  */


   /* Outputs  C1    Initial Discharge Coefficient
               Q1    Initial Mass Flow Rate
               C2    Final Value of Discharge Coefficient
               Q2    Final Value of Mass Flow Rate
               n     Number of Iterations to Reach Tolerance   */

   /* Function to Print Program Title  */

   void  printtit()
         {
         printf ("  Program to Calculate the Air Mass Flow Rate\n");
         printf ("Through an Orifice Plate Conforming to BS 1042.\n\n");
         printf ("An Internal Pipe Diameter of 52.3mm is Assumed.\n\n");
         }

   /* Function to Input and Echo Orifice Diameter */

   float inputd()
         {
      float d;
      char  dumchar;

         printf ("Enter the Orifice Diameter in Meters.\n");
         scanf  ("%f %c",&d,&dumchar);
         printf ("%.5f\n",d);
         return (d);
         }

/* Function to Input and Echo Differential Pressure */

float inputdelP()
         {
      float delP;
      char  dumchar;

         printf ("Enter the Differential Pressure in mm of Water.\n");
         scanf  ("%f %c",&delP,&dumchar);
         printf ("%.2f\n",delP);
         return (delP);
         }

/* Function to Input and Echo Upstream Pressure */

float inputP1()
         {
      float P1;
      char  dumchar;

         printf ("Enter the Upstream Gauge Pressure in mmH20.\n");
         scanf  ("%f %c",&P1,&dumchar);
```

```
      printf ("%.3f\n",P1);
      return (P1);
      }

/* Function to Input and Echo Atmospheric Pressure */

float inputPat()
      {
   float Pat;
   char  dumchar;

      printf ("Enter the Atmospheric Pressure in mm Mercury.\n");
      scanf  ("%f %c",&Pat,&dumchar);
      printf ("%.2f\n",Pat);
      return (Pat);
      }

/* Function to Calculate Beta */

float calcBeta1(d,D)
   float d;
   float D;
      {
   float Beta;
      Beta = d / D;
      return (Beta);
      }

/* Functions to Calculate Beta Raised to Various Powers */

float calcBeta201(Beta)
   float Beta;
      {
   float Beta201;
      Beta201 = pow(Beta,2.1);
      return (Beta201);
      }

float calcBeta205(Beta)
   float Beta;
      {
   float Beta205;
      Beta205 = pow(Beta,2.5);
      return (Beta205);
      }

float calcBeta3(Beta)
   float Beta;
      {
   float Beta3;
      Beta3 = pow(Beta,3.0);
      return (Beta3);
      }

float calcBeta4(Beta)
   float Beta;
      {
   float Beta4;
      Beta4 = pow(Beta,4.0);
      return (Beta4);
      }

float calcBeta8(Beta)
   float Beta;
```

```
      {
   float Beta8;
      Beta8 = pow(Beta,8.0);
      return (Beta8);
      }

/* Function to calculate C05, the constant term of the expression
                              for C    */

float PrecalcC(Beta201,Beta3,Beta8)
   float Beta201;
   float Beta3;
   float Beta8;
      {
   float C05;
      C05 = 0.5994 + .0312 * Beta201 - .0337 * 0.4700 * Beta3
      - 0.1840 * Beta8;
      return (C05);
      }

/* Function to calculate C, using the above precalculation */

float calcC(C05,Beta205,Rnum)
   float C05;
   float Beta205;
   float Rnum;
      {
   float C;
      C = C05 + 0.00290 * Beta205 * pow ( 1.0e6 / Rnum, 0.75);
      return (C);
      }

/* Function to Calculate E  */

float calcE(Beta4)
   float Beta4;
      {
   float E;
      E = pow((1 - Beta4), -0.5);
      return (E);
      }

/* Function to Calculate the Differential Pressure in Pascals */

float convDelP(delP)
   float delP;
      {
   float delPPa;
      delPPa = 9.780 * delP;
      return (delPPa);
      }

/* Function to calculate the Absolute upstream pressure in Pa */

float calcPabsPa(P1,Pat)
   float P1;
   float Pat;
      {
   float PabsPa;
      PabsPa = 9.780 * P1 + 133.4 * Pat;
      return (PabsPa);
      }

/* Function to Calculate Eta */
```

```
float calcEta(Beta4,delPPa,PabsPa)
   float Beta4;
   float delPPa;
   float PabsPa;
      {
   float Eta;
      Eta = 1 - (( 0.41 + 0.35 * Beta4 ) * (delPPa/(1.390 *
            PabsPa)));
      return (Eta);
      }

/* Function to Calculate Rho */

float calcRho(PabsPa)
   float PabsPa;
      {
   float Rho;
      Rho = PabsPa * 1.166e-5;
      return (Rho);
      }

/* Function to Calculate Value for Qm05, the Constant
                  term of the  Mass Flow Rate  Equation  */

float PrecalcQm(delPPa,Rho,d,E,Eta)
   float delPPa;
   float Rho;
   float d;
   float E;
   float Eta;
      {
   float IVF1;
   float Qm05;
      IVF1 = sqrt ( 2 * delPPa * Rho );
      Qm05 = IVF1 * pow ( d,2.0 ) * E * Eta * 3.1416 / 4;
      return ( Qm05 );
      }

/* Function to Calculate the Mass Flow Rate Using
         the Above Precalculation  */

float calcQm(Qm05,C)
   float Qm05;
   float C;
      {
   float Qm;
      Qm = Qm05 * C;
      return (Qm);
      }

/* Function to Calculate Reynolds Number  */

float calcRnum(Qm,D)
   float Qm;
   float D;
      {
   float Rnum;
      Rnum = ( 4.0 * Qm ) / ( 3.1416 * D * 1.82e-5 );
      return ( Rnum );
      }
```

```
void  main ()
        {
      float D = 0.0523;
      float Rnum = 1.0e6;
      float d;
      float delP;
      float P1;
      float Pat;
      float Beta1;
      float Beta201;
      float Beta205;
      float Beta3;
      float Beta4;
      float Beta8;
      float PreC;
      float C;
      float delPPa;
      float E;
      float PabsPa;
      float Eta;
      float Rho;
      float QmA;
      float QmB;
      float PreQm;
      float delQm;
      int loopcount;
      char loopchar;
      char dumchar;

            do
            {

         printtit();
         d = inputd();
         delP = inputdelP();
         P1 = inputP1();
         Pat = inputPat();
         Beta1 = calcBeta1(d,D);
         Beta201 = calcBeta201(Beta1);
         Beta205 = calcBeta205(Beta1);
         Beta3 = calcBeta3(Beta1);
         Beta4 = calcBeta4(Beta1);
         Beta8 = calcBeta8(Beta1);
         E = calcE(Beta4);
         delPPa = convDelP(delP);
         PabsPa = calcPabsPa(P1,Pat);
         Eta = calcEta(Beta4,delPPa,PabsPa);
         Rho = calcRho(PabsPa);
         PreC = PrecalcC(Beta201,Beta3,Beta8);
         PreQm = PrecalcQm(delPPa,Rho,d,E,Eta);
         C = calcC(PreC,Beta205,Rnum);
         QmA = calcQm(PreQm,C);
         printf("The Initial Value For the Mass  Flow Rate\n");
         printf("Was %9.7f\n",QmA);
         loopcount = 0;
         do
            {
            ++loopcount;
            QmB = QmA;
            Rnum = calcRnum(QmB,D);
            C = calcC(PreC,Beta205,Rnum);
            QmA = calcQm(PreQm,C);
            delQm = abs(QmA-QmB);
```

```
    }
while(delQm>=1.0e-5);
printf("The Final Value For the Mass Flow Rate\n");
printf("is %9.7f\n",QmA);
printf("The Previous Value Was %9.7f\n",QmB);
printf("Reynolds Number is %7f\n",Rnum);

      printf("Do you wish to rum the program again?\n");
      printf("Enter Y or N \n");
      scanf ("%c %c",&loopchar,&dumchar);
}
      while( loopchar == 'Y');

}
```

Appendix 5 Section 3 Best Fit Straight Line Software

```
#include <stdio.h>

    /*  This programme will find the best straight line fit for
        a set of points using the least squares technique  */

int main(void)

{

    /*  Declaration of Variables */

    float   xvals[100];
    float   yvals[100];
    float   sumx;
    float   sumy;
    float   sumx2;
    float   sumxy;
    float   a;
    float   b;
    float   n;
    float   syon;
    float   sxyosx;
    float   sxon;
    float   sx2osx;

    int     loopc1;
    int     loopc2;
    int     loopc3;
    int     loopc4;
    int     nop;
    int     progrun;
    int     status[100];
    int     notomod;
    int     notochst;
    int     loopcon;
    char    dumchar;
    char    moption;
    char    stchfl;
    char    hit;


    /*  Print programme explanation  */

    printf("        This programme will calculate the equation for the\n");
    printf("        best fit straight line for the given set of points\n\n");

    /*  Request the number of sets of points  */

    printf("        Please enter the number of sets of points to be\n");
    printf("        processed (maximum 100)\n\n");

    /*  Input number of sets of points  */

    scanf("%d",&nop);

    /* Initialise status array elements  */

    for(loopc3 = 1; loopc3 <= nop; loopc3++)
        status[loopc3] = 1;

    /*  Output general message to ask for data points  */
    /*  Giving required format  */
```

```
printf("        Please input each of the data points giving first\n");
printf("        the X value and then the Y, separated by a space \n");

/*  Loop to input data points  */

loopc1 = 1;
for ( loopc1 = 1; loopc1 <= nop; loopc1++ )
    {
    printf("        Point No. %d ?\n",loopc1 );
    scanf("%f %f",&xvals[loopc1],&yvals[loopc1]);
    }
/* Initialise programme continuation variable  */

progrun = 1;

/* Start of do loop for main part of programme  */

do
    {

    /*  Loop to Echo Point Set  */

    printf("   Point No.\tX\t\tY\t    Status\n\n");

    for ( loopc2 = 1; loopc2 <= nop; loopc2++ )
        {
    printf("\t%d\t%f\t%f\t%d\n",\
        loopc2,xvals[loopc2],yvals[loopc2],status[loopc2]);
        }

    /*  wait for keyboard Hit  */

    hit = 0;
    do
        {
        hit = kbhit();
        }
while(hit == 0);
scanf("%c",&dumchar);

/*  Print Menu  */

printf("\n                MENU\n\n");
printf("    Press  M to Modify point value\n\n");
printf("    Press  S to Change Status of a point\n\n");
printf("    Press  C to Calculate best fit\n\n");
printf("    Press  E to Exit Programme\n\n");

/*  Input reply  */

scanf("%c %c",&dumchar,&moption);

/*  switch statement to select option  */

switch(moption)

    {

/*  section to modify point value  */

    case 'm':
        {
/*  input number of point to be modified  */
```

```
        printf("    Enter the number of the point to be modified\n");
        scanf("%d",&notomod);

/*  input new values for point  */

        printf("    Enter the new X value followed by the new Y\
        value,seperated by a space\n");
        scanf("%f %f",&xvals[notomod],&yvals[notomod]);

        }
        break;

/*  section to change point status  */

    case 's':
        {
/*  input number of point for status change  */

        printf("\tEnter number of the point requiring status change\n"
        scanf("%d",&notochst);

/*  Print current status of point  */

        printf("\tThe current status of this point is %d\n\n",\
        status[notochst]);

/*  Start of do loop  */
        do
        {
    loopcon = 0;
/*  Request status change  */

        printf("\tDo you wish to change the status ? (type y or n)\n")
        scanf("%c %c",&dumchar,&stchfl);

/*  Switch for stchfl value  */

        switch(stchfl)
        {

/*  If stchfl = y, toggle status array element  */

        case 'y':
        {
        if(status[notochst] == 1)
            status[notochst] = 0;
        else
            status[notochst] = 1;
        break;
        }

/*  If stchfl = n, break and continue rest of programme   */

        case 'n':
        break;

/*  If stchfl |= y or n display error message and loop back */

        default:
        {
        printf("Input Character not valid - Try again\n");
        loopcon = 1;
        }
        break;
```

```
        }
        }
        while(loopcon ==1);
        }
        break;

/*  Section to calculate best fit straight line  */

    case 'c':
        {

/*  calculate the sum of the x,y,xy and x2 values  */
/*  also calculate n  */

    sumx = 0;
    sumy = 0;
    sumxy = 0;
    sumx2 = 0;
    n = 0;
    for(loopc4 = 1; loopc4 <= nop; loopc4++)
    {
    if(status[loopc4] == 1)
    {
    sumx = sumx + xvals[loopc4];
    sumy = sumy + yvals[loopc4];
    sumxy = sumxy + (xvals[loopc4]*yvals[loopc4]);
    sumx2 = sumx2 + (xvals[loopc4]*xvals[loopc4]);
    n++;
    }
    else if(status[loopc4] |= 0)
    printf("\tIncorrect character in status array at \
    loopcount 4 = %d\n",loopc4);
    }

/*  calculate intermediate variables  */

            syon = sumy/n;
            sxyosx = sumxy/sumx;
            sxon = sumx/n;
            sx2osx = sumx2/sumx;

        /*  calculate a and b  */

            b = (syon - sxyosx)/(sxon - sx2osx);
            a = syon - (b * sxon);

        /*  print equation  */

            printf("\t The equation of the best fit straight line is :-\n\n");
            printf("\t\t\tY = %fX + %f\n",b,a);
                }
            break;

            case 'e':
            progrun = 0;
            break;

            default:
            printf("\tInvalid input character - Try again\n");
            break;
            }
}
while(progrun == 1);
```

Appendix 5 Section 4 Sensor Modelling Software

```
#include <stdio.h>
#include <math.h>

        /*  This programme will calculate the charge on an equipotential plane
            with a point charge above it */

float   qcalc(X1,X2,Y1,Y2,H,DELTAX)

float   X1,X2,Y1,Y2;
float   H;
float   DELTAX;

{
/* Declaration of variables   */

float   XA,XB;
float   QSA,QSB;
float   QACC,QW,QSS;
float   MDELTQS;
float   HO2PI;
float   DEN1,DEN2,RDEN3;
float   HSQ,Y1SQ,Y2SQ;

int     LOOPC;

        /*  initiate variables for loop  */

 QACC = 0.0;
 XA = X1;
 LOOPC = 0;
 HO2PI = H/(2*3.14159);
 HSQ = H*H;
 Y1SQ = Y1*Y1;
 Y2SQ = Y2*Y2;
 DEN1 = sqrt(Y1SQ+(XA*XA)+HSQ);
 DEN2 = sqrt(Y2SQ+(XA*XA)+HSQ);
 RDEN3 = 1/(HSQ+(XA*XA));
 QSB = RDEN3*(Y1/DEN1-Y2/DEN2);

        /*  start of integration loop  */

do
        {
        QSA = QSB;
        XB = X1 + (LOOPC+1)*DELTAX;

        /*  calc value for new QSB  */

        DEN1 = sqrt(Y1SQ+(XB*XB)+HSQ);
        DEN2 = sqrt(Y2SQ+(XB*XB)+HSQ);
        RDEN3 = 1/(HSQ+(XB*XB));
        QSB = RDEN3*(Y1/DEN1-Y2/DEN2);

        /*  find modulus of difference  */

        MDELTQS = fabs(QSA-QSB);

        /*  find smallest  */

        if(QSA > QSB)
        QSS = QSB;
        else
        QSS = QSA;
```

```
        /*  calculate volume of slice  */

        QW = (QSS+MDELTQS/2)*DELTAX;


        /*  add to QACC  */

        QACC = QACC+QW;

        /*  incrument loopc  */

        ++LOOPC;
        }
        while((XB+DELTAX/10) < X2);

        QACC = QACC*HO2PI;


return(QACC);
}

int main(void)

{
        /*  declare main variables  */

float   xbegin,xend,xstart,xstop;
float   el,ew;
float   h;
float   xcent,xstep;
float   ctot;
float   intres;
float   xbegef,xendef;
float   qnew;
float   xsams,xsoms,xsapl,xsopl;
float   qminus,qplus;
float   y1,y2;

int     nosteps,notraps;
int     loopc1;
int     debug = 0;

char    rerun;
char    dumchar1;
char    dumchar2;
char    outfname[25];

FILE    *outfpoint;

rerun = 'n';

do
{
        /*  print programme explanation  */

printf("\tThis programme will model the charge induced on an \n\
        \telectrode as a charged particle moves over it\n");

        /*  input variables  */

printf("\t\tplease input the start and stop x cordinates\n");
scanf("%f %f",&xbegin,&xend);
printf("\t\tplease input the length and width of the electrode\n");
scanf("%f %f",&el,&ew);
```

```
printf("\t\tplease input the number of steps required\n");
scanf("%d",&nosteps);
printf("\t\tplease input the number of trapeziums to be used over e.l.\n");
scanf("%d",&notraps);
printf("\t\tplease input the height of the point charge\n");
scanf("%f",&h);
printf("\t\tplease input the output filename\n");
scanf("%24s",outfname);

xstep = (xend-xbegin)/nosteps;

intres = el/notraps;

outfpoint = fopen(outfname,"a");

xbegef = xbegin - el/2;
xendef = xend + el/2;

xstart = xbegef;
xstop = xbegef + el;

y1 = 0.0 - ew/2;
y2 = 0.0 + ew/2;

if(debug == 1)
{
printf("xstart = %f xstop = %f\n",xstart,xstop);
printf("y1 = %f y2 = %f intres = %f\n",y1,y2,intres);
}
qnew = qcalc(xstart,xstop,y1,y2,h,intres);

xcent =xstart + (xstop - xstart)/2.0;

fprintf(outfpoint,"%f %f\n",xcent,qnew);

loopc1 = 0;

do
{       xsams = xstart + (loopc1*xstep);
        xsoms = xstart + ((loopc1+1)*xstep);

        xsapl = xstop + (loopc1*xstep);
        xsopl = xstop + ((loopc1+1)*xstep);

if(debug == 1)
{
printf("xsams=%f xsoms=%f y1=%f y2=%f intres=%f\n",xsams,xsoms,y1,y2,intres);
printf("xsapl=%f xsopl=%f\n",xsapl,xsopl);
}

        qminus = qcalc(xsams,xsoms,y1,y2,h,intres);
        qplus  = qcalc(xsapl,xsopl,y1,y2,h,intres);

        qnew = qnew - qminus + qplus;

        xcent =xsoms + (xsopl - xsoms)/2;

        fprintf(outfpoint,"%f %f\n",xcent,qnew);

        ++loopc1;

}
while(xsopl+(intres/10) < xendef);
```

```
fclose(outfpoint);

        /*  rerun request  */

printf("\t\t\tRun complete\n\t\tDo you wish to run again (y or n)\n");

if(debug == 1)
printf("rerun = %c\n",rerun);

scanf("%c %c %c",&dumchar1,&dumchar2,&rerun);

if(debug == 1)
printf("rerun = %c\n",rerun);
}
while(rerun == 'Y');

return(1);
}
```

Appendix 6 Nomenclature

This appendix contains a listing of definitions of the symbols used in this thesis which the author did not consider to be self evident. It also contains a listing of some of the more specialised terms used in the thesis, along with the authors interpretation of their meaning.

Nomenclature

b	Radius of laser beam at laser window.
b_0	Radius of laser beam at cross over point.
d_{BL}	Boundry Layer Width
d_{ia}	Diameter of interrogated area.
d_{ph}	Diameter of pin hole.
f_d	Doppler frequency.
f_L	Focal length of lens.
G	Ratio of peak particle velocity to average particle velocity.
n	The power of the power law model used to model the particle velocity distributions determined by the laser doppler velocimetry instrumentation.
Q	Electrostatic charge.
Q_{total}	Total electrostatic charge.
Re.	Reynolds number.
RH	Relative humidity.
$R_{xy}(\tau)$	Cross Correlation Function
t	Time
V	Volume of revolution.
V_{as}	Superficial air velocity. That is the average air velocity of the air in the pipeline were no solids present.
V_p	Discrete particle velocity.
V_{pa}	The actual average particle velocity.

V_{pcc}	Average particle velocity as evaluated by the cross correlator.
V_{pldv}	Average particle velocity as evaluated by the laser doppler velocimetry instrumentation. That is the average particle velocity calculated from the the velocity profile.
x,y,z	Distances in a mutually perpendicular coordinate geometry system.
ρ_s	Suspension density. That is the mass of solids divided by the volume of air throughout which the solids are distributed.
ρ_s(sensor)	Reading of the electrostatic suspension density sensor.
$\Delta X, \Delta Y, \Delta Z$	Perpendicular dimentions of sample illuminated volume.
δ	Laser doppler velocimetry fringe spacing
θ	Value of an angle in degrees
λ	Wavelength of laser light
σ	Electrostatic charge density.
τ	Time delay

Appendix 7 Publications

This appendix contains copies of two publications written and published by the author during the tenure of the programme of work detailed in this thesis.

1. Presented at the Fourth International Conference on Pneumatic Conveying Technology, Glasgow, Scotland, 1990.

2. Published in Powder Handling and Processing, Volume 2, Number 2, June 1990.

ON LINE MASS FLOW MEASUREMENT IN LOW SUSPENSION DENSITY PNEUMATIC CONVEYING SYSTEMS USING AN ELECTROSTATIC TECHNIQUE

S R Woodhead*#, J Coulthard$, B Byrne$, R N Barnes#, A R Reed#

#The Wolfson Centre For Bulk Solids Handling Technology
The School of Engineering
Thames Polytechnic
London
U K

$The School of Information Engineering
Teesside Polytechnic
Middlesborough
Cleveland
U K

Abstract

As a direct result of increased energy costs - both financial, and environmental, the instrumentation and control processes in coal fired boiler and kiln plant have come under close scrutiny in an attempt to improve overall efficiency.

One technique which has been identified which will improve overall efficiency, is that of monitoring the flow rates of pulverised and granular coal as they are conveyed through the pneumatic injection system. This information can then be fed to the plant control system to permit the plant to operate with all the burners in a balanced condition, and thereby more efficiently.

Unfortunately, a system to measure the mass flow rate of fuel reliably under the conditions encountered in most pulverised coal injection systems is not widely available. Several experimental systems have been developed in various parts of the world, but none have found widespread acceptance, due either to technical problems or excessive cost.

1.0 Principle of the Measurement System

It has been widely recognised for some years now that in order to carry out an on line measurement of mass flow rate in a pneumatic conveying pipeline, two independent measurements must be made. One is that of the average particle velocity, and the other is that of the suspension density, which is defined as the mass of fuel per unit volume of conveying air.

The major obstacle to the development of a widely applicable technique has been the inability to evaluate these two variables accurately using non-intrusive sensors. It is imperative that the sensors are of a non-intrusive design since any intrusion would be subject to high levels of erosive wear.

Accordingly, several non-intrusive techniques have undergone development and on line trials on various scales. The widely documented capacitive technique (Ref. 1-4) has proved to be moderately successful, particularly when the flowing suspension is of a relatively high density. A number of other techniques have been documented (Ref. 5) including attenuation of ionising radiation and

electrostatic techniques.

The sensors used in the tests reported in this paper were of the electrostatic ring type, manufactured at Teesside Polytechnic. Two sensors were used spaced axially along the pipeline. The general configuration of a single sensor is shown in Figure 1. Each sensing ring is connected to the input of a charge amplifier and then to some signal processing electronics.

The average particle velocity is obtained by cross correlation of the signals from the two axially spaced sensors. The cross correlator used was of a type specially developed for velocity measurement at the School of Information Engineering, Teesside Polytechnic, in collaboration with an industrial organisation. The density of the suspension was obtained from the average value of the signal originating from a single ring sensor.

2.0 Outline of the Test Plant

In order to test such a measurement system, it is necessary to install the sensors in the pneumatic conveying pipeline of a suitably instrumented test plant. A specially commissioned test plant has been constructed at The Wolfson Centre for Bulk Solids Handling Technology, Thames Polytechnic for this purpose. The position of the sensors within the plant is illustrated in Figure 2.

The superficial air velocity within the test section was evaluated in the following manner. The air flow into the system was controlled by a bank of calibrated choke flow nozzles under computer control, thus allowing the mass flow rate of air into the system to be evaluated. Pressure and temperature sensors were installed in the test section, thus allowing the volumetric flow rate of air to be evaluated using the ideal gas equation. The cross sectional area of the test section was determined from the known test section pipeline bore of 53 mm, thereby permitting the superficial air velocity to be calculated. (The superficial air velocity is defined as the average velocity of the air if there were no fuel present)

The suspension density was determined in the following manner. The pulverised coal is conveyed into a receiving hopper, where the fuel is disengaged from the carrying air by a fabric filter. The receiving hopper is mounted on load cells, the readings from which were recorded by a computerised data logging system, along with the readings from the other sensors. From the logged load cell readings, the mass flow rate of coal was determined by a numerical differentiation and averaging algorithum. The suspension density was then determined by dividing the mass flow rate of fuel by the volumetric flow rate of air.

3.0 Test Work and Results

Two sets of tests were conducted to evaluate the measurement system. The superficial air velocity was compared with the average particle velocity as determined by the cross correlator. This resulted in the graph shown in Figure 3. The suspension density as determined from the load cell and other sensor readings was compared with the suspension density output signal from the electrostatic sensing system. This resulted in the graph shown in Figure 4.

3.1 Velocity Tests

With reference to Figure 3 it may be seen that the average particle velocity as determined by the cross correlator bears good relation to the superficial air velocity. The relationship is not perfect, and this maybe due to a number of factors. It is widely accepted (Ref. 6&7) that the particles in a pneumatic conveying system 'slip' within the air stream with the value of this 'slip' thought to be dependent upon a number of factors such as particle size and superficial air velocity. With this in mind, it may be noted from Figure 3 that the average particle velocity is consistently lower than the superficial air velocity. There is notable scatter of the points on the graph, which is clearly undesirable for such a measurement system. This may be partially accounted for by the fact that the combined error of the sensors used to evaluate the superficial air velocity was approximately 3%, and is therefore significant.

3.2 Suspension Density Tests

Suspension density tests were carried out at two nominal flow velocities. This was in order to evaluate the sensitivity of the density sensor to the flow velocity as well as the suspension density, since it was suspected that the density sensor also had some sensitivity to the former. It may be seen from Figure 4 that the sensor output voltage is well correlated with the suspension density. It may also be seen that the sensor output voltage is in fact sensitive to the flow velocity.

4.0 Conclusions

It is considered that the measurement system tested forms the basis of a workable technique in the area of low suspension density pneumatic conveying systems. One potential problem area is that of the sensitivity of the suspension density sensor to the flow velocity. However, the two values for velocity and suspension density must be combined to provide a value for mass flow rate, and provided that the velocity is known, and its effect is known on the suspension density sensor, this effect may be compensated for in the combination of the two values.

The results quoted cover the range of suspension densities from 1.7 upwards, which corresponds to a solids to air ratio of 1.3 : 1 by mass. It is expected that the authors will be undertaking tests in the range below this value in the near future, the results of which will be equally applicable in the field of pneumatic feeds to combustion processes.

It is however anticipated that the suspension density sensing arrangement may not be fully applicable at very low suspension densities in the region of 0.1 kg/m^3, and that a new type of sensor will be required to operate under these conditions. Such a system is already under development jointly at Teesside and Thames Polytechnics.

Acknowledgements

The authors would like to thank the following organisations for supporting the work presented in this paper :

Babcock Energy
Blue Circle Cement
The Department of Energy
Kent Industrial Measurements
Kevex Corperation (U.K.)
The Science and Engineering Research Council
Tealgate
The Wolfson Foundation

References

1. Green, R G ; Cunliffe, J M. "On line measurement of two phase fluid flow with an F.M. capacitance transducer", Proc. of the International Conference on Advances in Flow Measurement Techniques", Warwick, U.K., September 1981.

2. Hammer, E A ; Green, R G. "The spatial filtering effect of capacitance transducer electrodes", J. Physics E, Volume 16, 1983.

3. Boeck, T. "Measurement of Velocity and mass flow rate of pneumatically conveyed solids by the use of the correlation measurement technique", Proc. of the Conference on the Flow of Particulate Solids, Bergen, Norway, August 1986.

4. Boeck, T. "Granucor - Mass flow measuring system for pneumatically conveyed solids", Proc. of the Third International Conference on Pneumatic Conveying Technology, Jersey, C.I., March 1987.

5. Woodhead, S R ; Barnes, R N ; Reed, A R. "On line mass flow measurement in pulverised coal injection systems", Interbulk Seminar, Pneumatic Conveying : Potentials and Capabilities, Birmingham, Sept. 1989.

6. Lech, M. "Some aspects of radioisotropic measurement of concentration and mass flow rate of powder", Proc. of the Fifth International Conference on the Pneumatic Transport of Solids in Pipes, April 1980.

7. Birchenough, A. "The application of laser measurement techniques to the pneumatic transport of fine particles", PhD Thesis, Thames Polytechnic, London, September 1975.

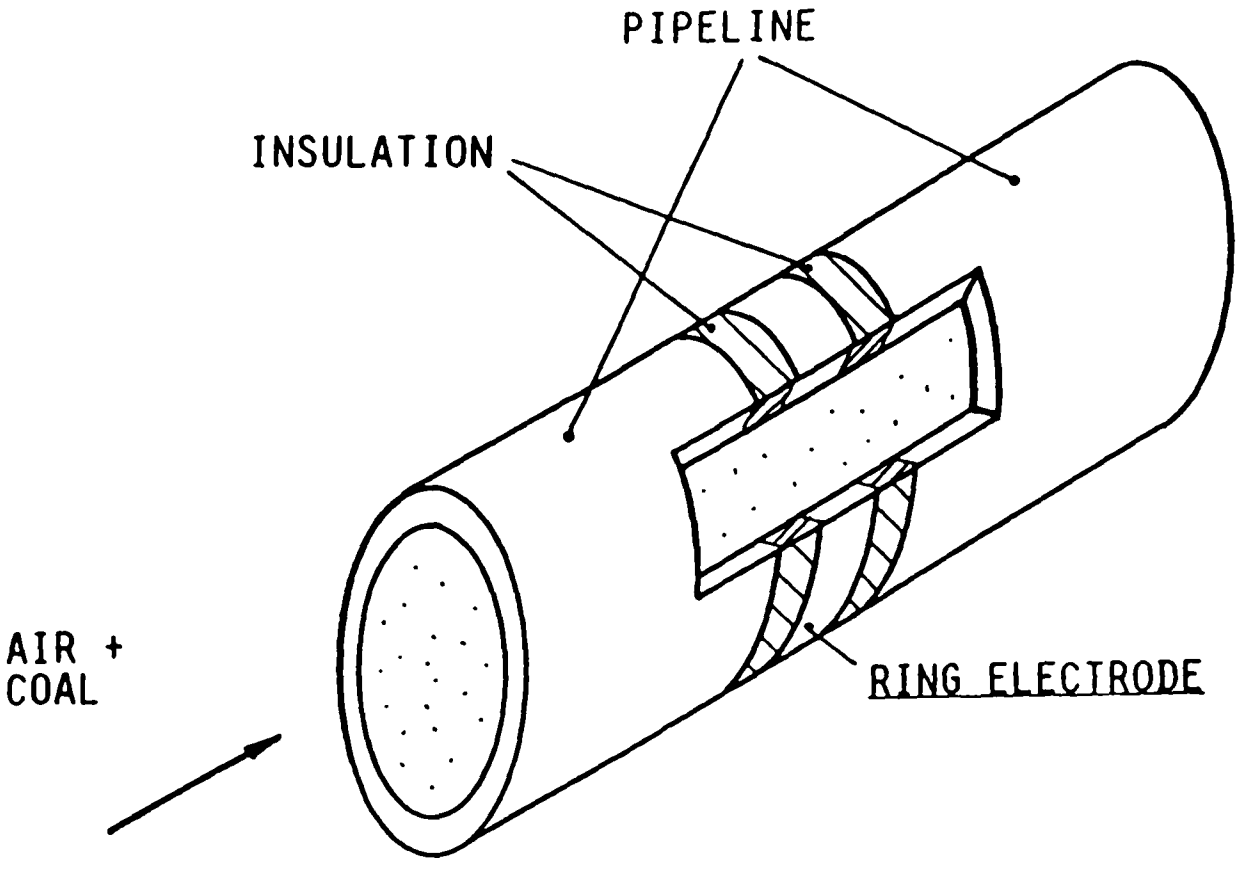

FIGURE 1 GENERAL CONFIGURATION OF A SINGLE PIPELINE SENSOR

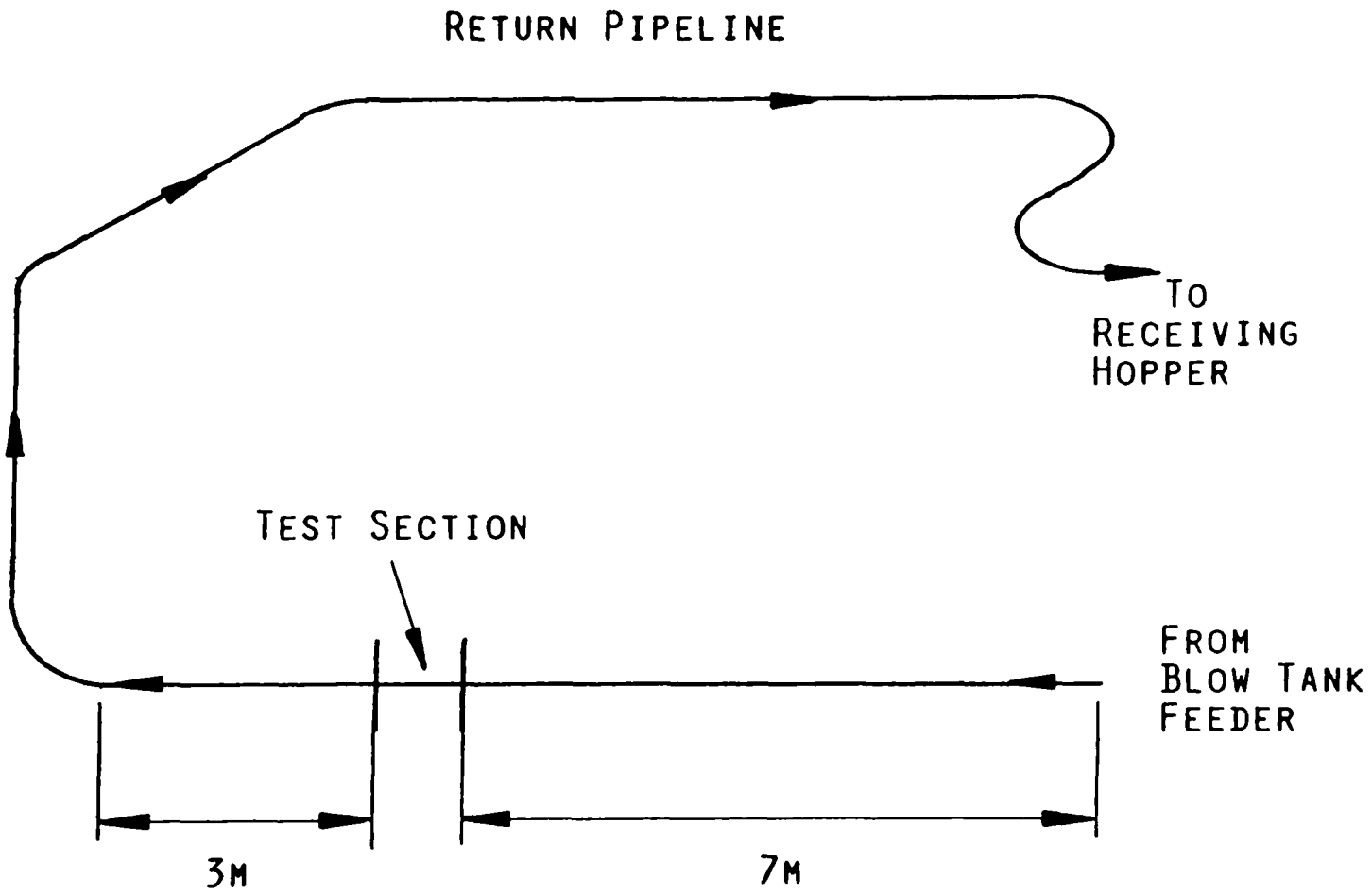

FIGURE 2 POSITION OF THE TEST SECTION WITHIN THE TEST PLANT

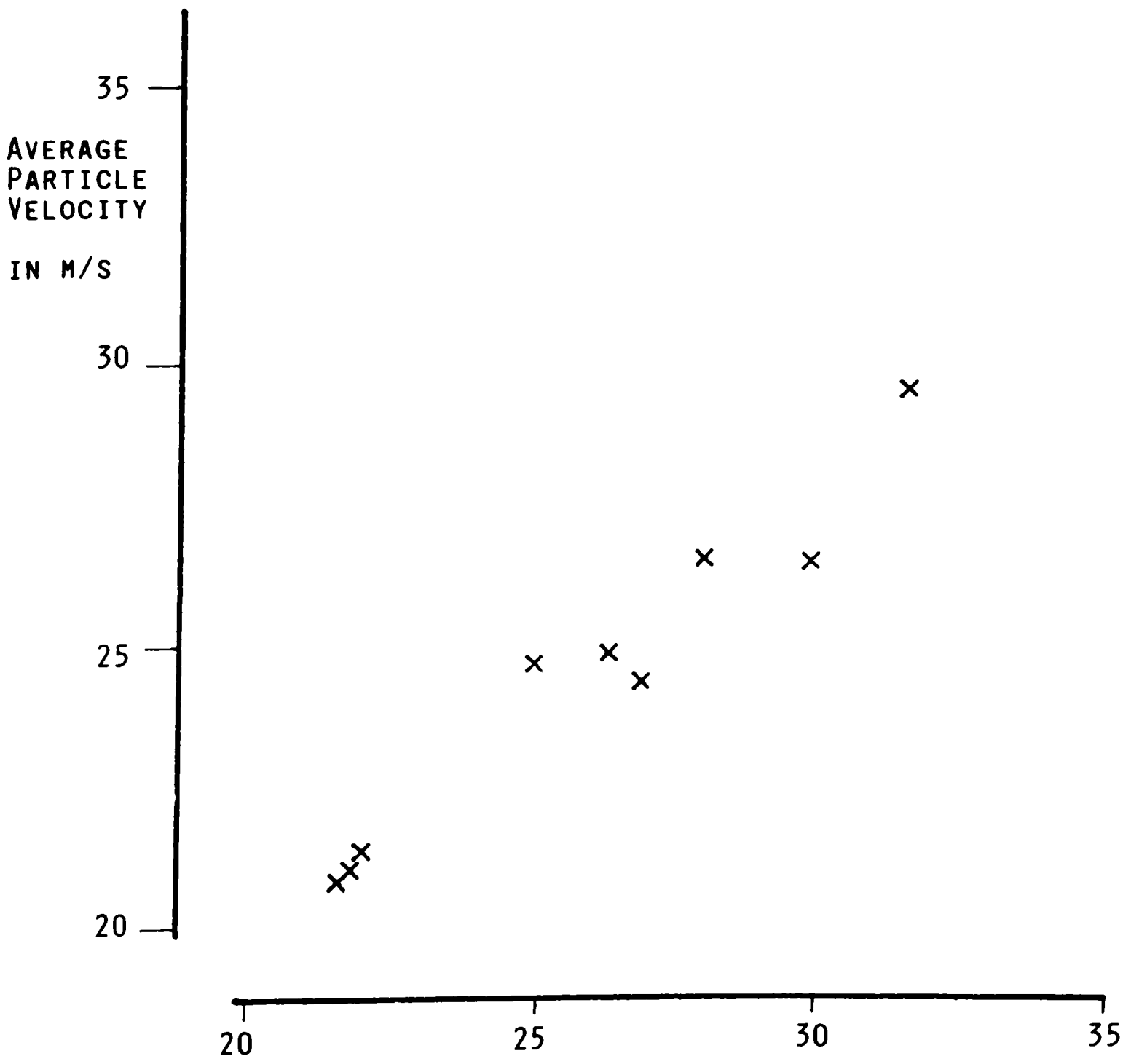

FIGURE 3 GRAPH OF AVERAGE PARTICLE VELOCITY AGAINST SUPERFICIAL AIR VELOCITY

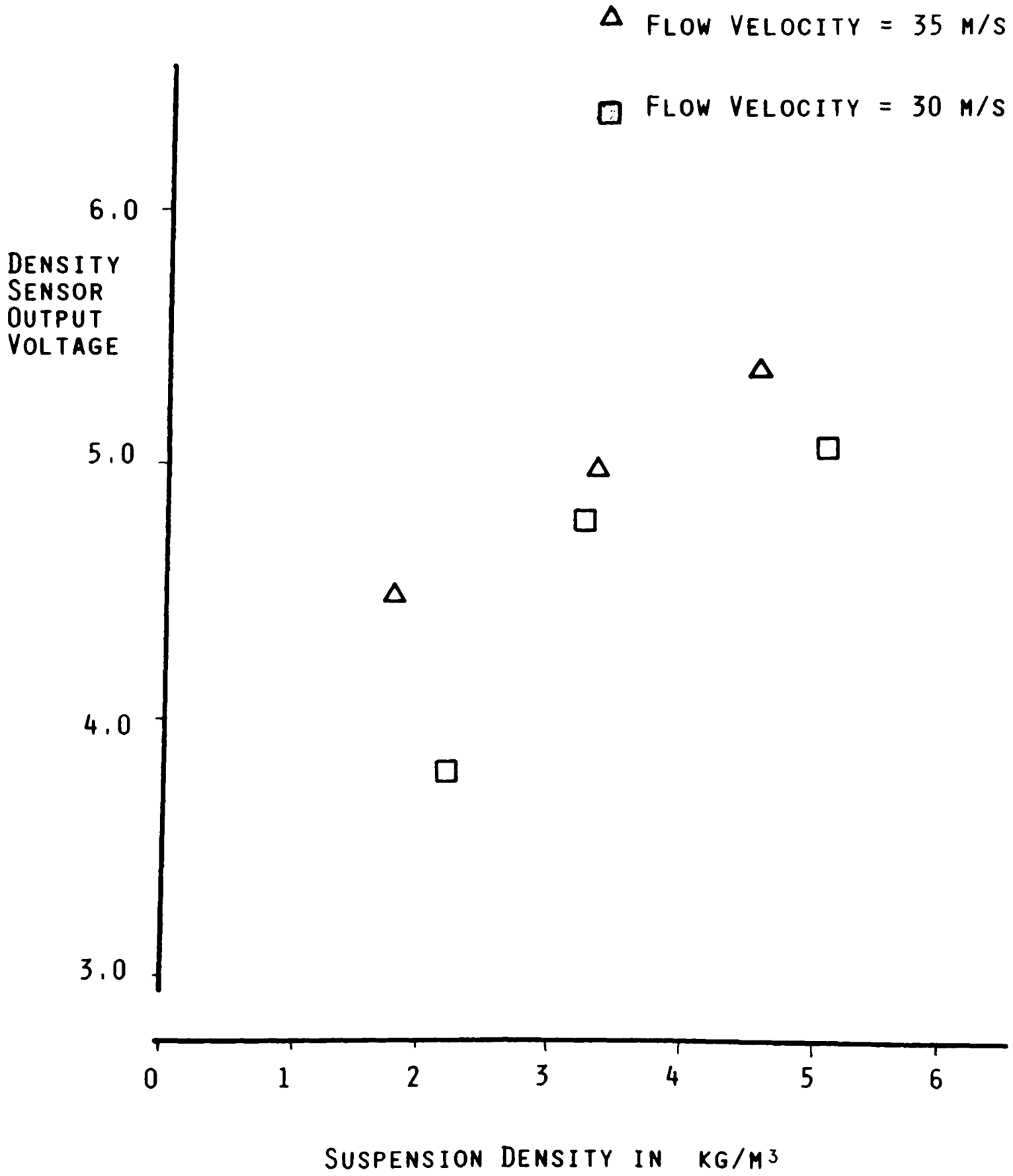

FIGURE 4 GRAPH OF DENSITY SENSOR OUTPUT VOLTAGE AGAINST SUSPENSION DENSITY

powder handling & processing Volume 2, Number 2, June 1990

On-Line Mass Flow Measurement in Pulverised Coal Injection Systems

S.R. Woodhead, R.N. Barnes and A.R. Reed, U.K.

Summary

This paper reviews the principles of a number of techniques applicable to on-line mass flow rate measurement in pulverised fuel injection systems, and indeed pneumatic conveying systems in general.

It has been established for some years now, that two independent measurements are required in order to obtain the coal mass flow rate in pneumatic conveying pipelines. The first measurement is that of the average velocity of the particles being conveyed through the pipeline. The second is that of the concentration of coal in the pipeline. These two values can then be combined to obtain the required coal mass flow rate.

The techniques reviewed in this paper are:

for concentration measurement:

i) capacitive sensors
ii) electrostatic sensors
iii) flow modulated ionizing radiation;

for velocity measurement:

i) cross correlation of axially spaced sensors.
ii) an estimated particle slip technique.

1. Introduction

In recent years there has been an increased demand in the electrical power, cement and steel industries for greater energy efficiency. At the same time there has been an increased dependency on plant automation in these and other industries. Throughout all of these types of plant, the pneumatic transport of powdered and granular materials through pipelines is commonplace. For example, in power generation pulverised coal is fed to the boilers by pneumatic means. In the steel and cement industries, pulverised or granular coal is also injected into the blast furnaces and kilns pneumatically. Pneumatic conveying of powdered and granular materials is also used extensively in other industries.

Accordingly, some years ago a need was identified for an on-line mass flow rate measurement technique, which could provide a reliable real time value for the amount of product being transported through a pipeline at any given time. Such a technique would enable much more efficient direct automatic control of boilers, kilns and blast furnaces which are recognised as being major problem areas in terms of such control. The technique would also be invaluable to operators of process plant, such as with batch mixing systems, where the masses of each constituent ingredient could be evaluated as the process proceeds. Provided the mass flow rate measurement technique is sufficiently accurate, this would then eliminate the need to install costly, and sometimes less than accurate load cell and belt weighing systems.

Initial efforts to provide such a technique were focused on adaptations of techniques originally devised for measuring the flow rate of single phase flows - for example, orifice plates and venturi meters [1]. However, for various reasons, these proved to be less than satisfactory. Realising that this approach was fundamentally flawed, movement was made towards the development of techniques specifically for two phase, gas-solids flow applications. Almost all of these new techniques rely upon the independent evaluation of the average particle velocity and the concentration of product in the pipeline. The two values, together with a calibration factor, are then multiplied to obtain the product mass flow rate. Many of these specialised systems are still the subject of research or on-going development. Indeed, there is, to the authors' knowledge, only one system of this type in use in industry, and it is known that the conditions under which this will operate satisfactorily are somewhat limited.

In this paper the authors will initially examine the possible techniques for the measurement of concentration. The principles of the velocity measurement techniques will then be outlined. Most of this material is taken from work, which is either on-going, or is scheduled for investigation in the very near future at The Wolfson Centre for Bulk Solids Handling Technology, Thames Polytechnic, London, UK, utilising the purpose built test rig shown in Fig. 1.

2. Concentration Measurement Techniques

There are currently three possible techniques applicable to concentration measurement, under investigation. The most established technique will be dealt with first and then attention will focus on those approaches which are less well established.

2.1 Capacitive Techniques [2-12]

This approach involves the use of insulated sections of pipeline. The capacitance between the insulated section and the rest of the pipeline is then measured by incorporating the capacitor in an oscillator circuit. As particulate product is introduced into the pipeline the dielectric of the capacitor will change, thus causing the capacitor value, and hence the oscillator frequency to change. Depending on the flow conditions, two different configurations of transducers are in use, Fig. 2.

The transducer electronics are arranged as shown in Fig. 3. The oscillator output is fed to an FM demodulator, which provides a voltage output as a function of capacitance. In order to keep the FM. demodulator within the linear region, feedback is applied by using a low pass filtered version of the output to feed a varicap diode in the oscillator circuit. An

For information on authors - see pages 196/197

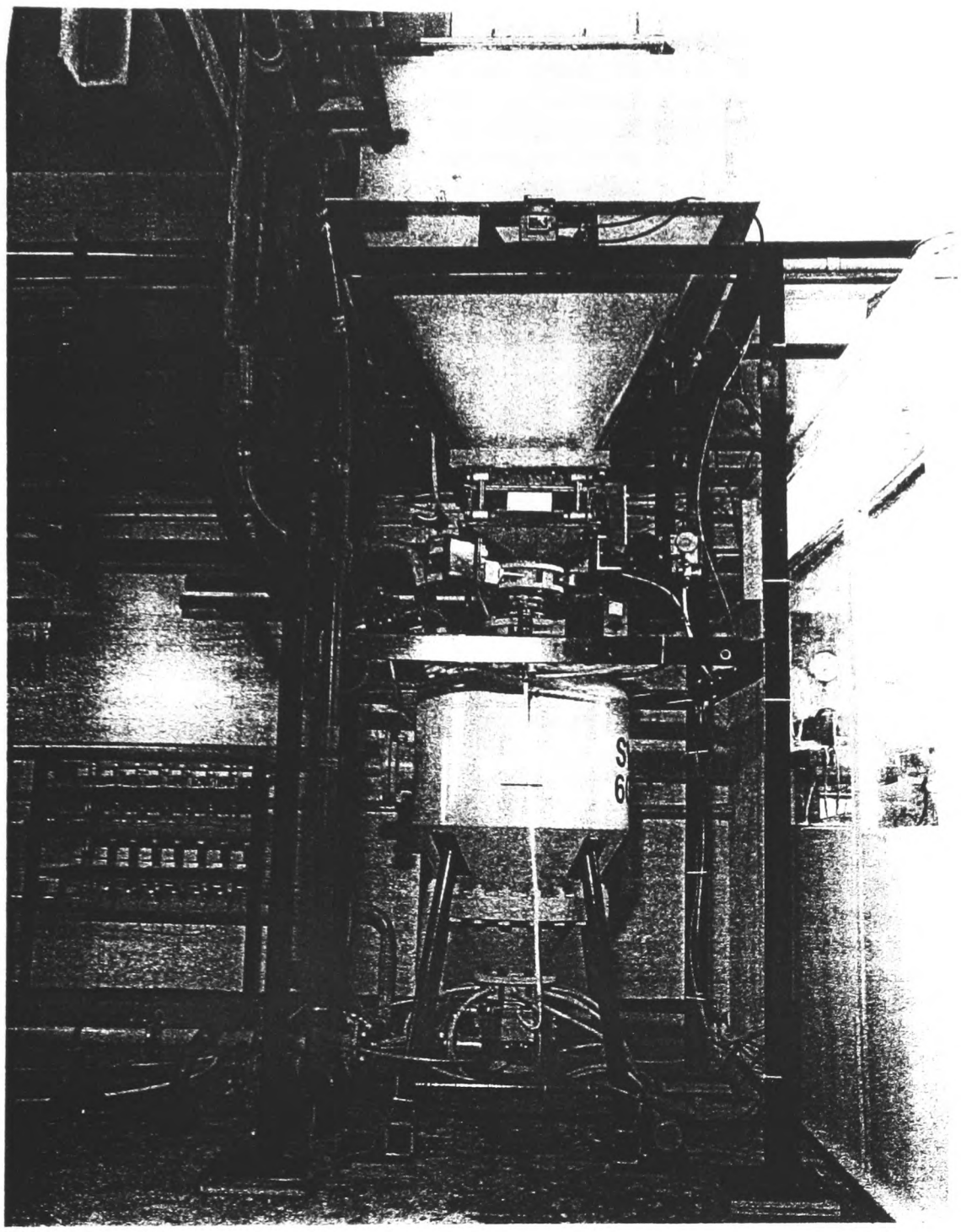

Fig. 1: Flow measurement test rig at the Wolfson Centre, Thames Polytechnic

A.C. amplifier is then added to the F.M. demodulator output to provide the transducer output. The output from the transducer will then constitute an A.C. signal. It has been found that the amplitude of the A.C. signal is a function of the product concentration in the pipeline.

The range of product to air mass flow ratios over which these systems will operate is somewhat limited and one manufacturer [2] does not recommend their use in systems operating at product to air mass flow ratios below the values of 2 to 7 – depending upon the particular product under consideration. This is due to the fact that the change in the dielectric becomes very small at the low solids loadings. Unfortunately, many pneumatic conveying systems operate below these values – particularly in the power, cement and steel industries, where there is a considerable need for such a system. Thus, to date, applications have been somewhat limited. It is expected that in the near future such a system will undergo extensive trials at The Wolfson Centre in the specially commissioned test plant. It is the object of this work to determine the exact limits of applicability of this technique for coal and other materials.

2.2 Electrostatic Techniques [13-19]

This technique involves the use of pipeline sections similar to those already shown in Fig. 2b. However, rather than incorporating the sensor in an oscillator circuit, as in the capacitive transducer, the insulated ring section is connected to the input of a charge amplifier. As the particles pass along the pipeline they will

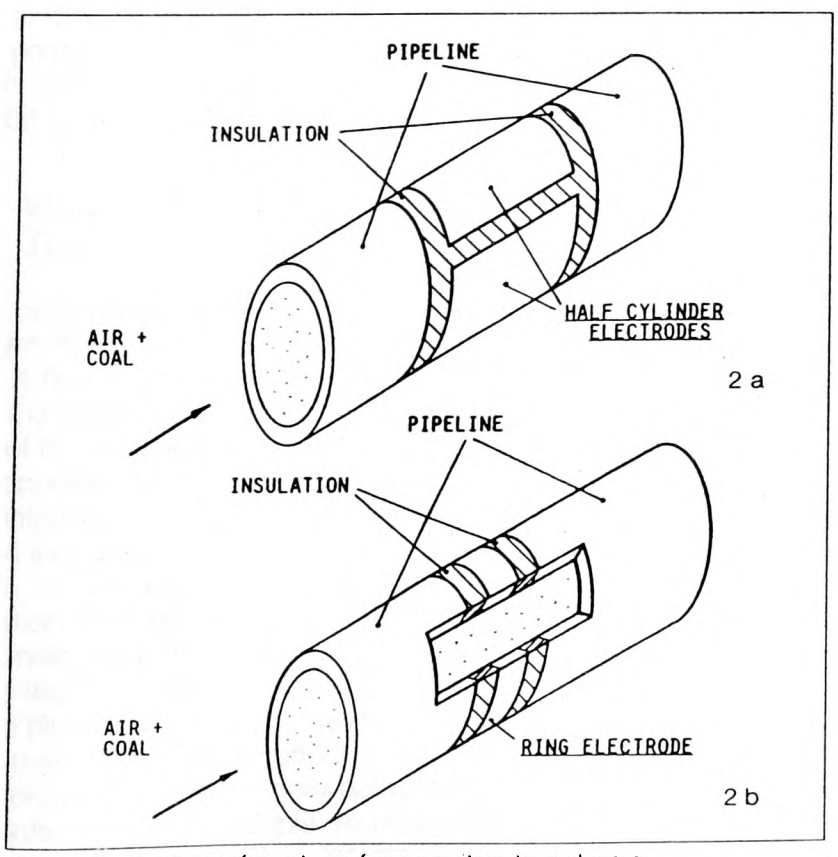

Fig. 2. Electrode configurations for capacitive transducers

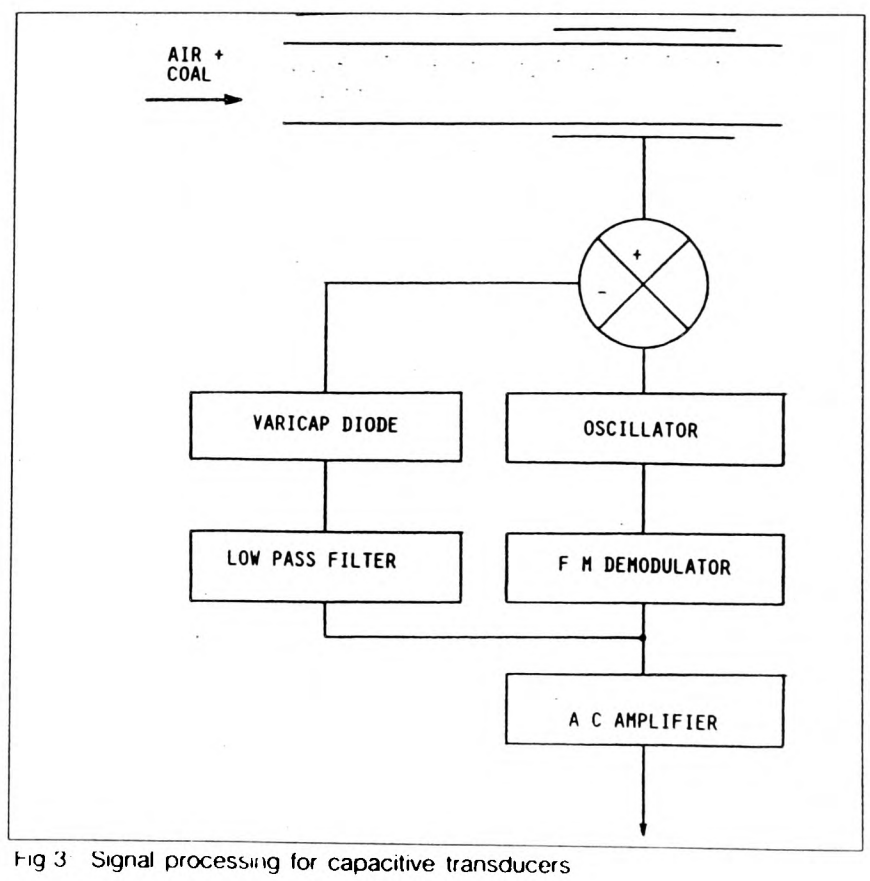

Fig 3 Signal processing for capacitive transducers

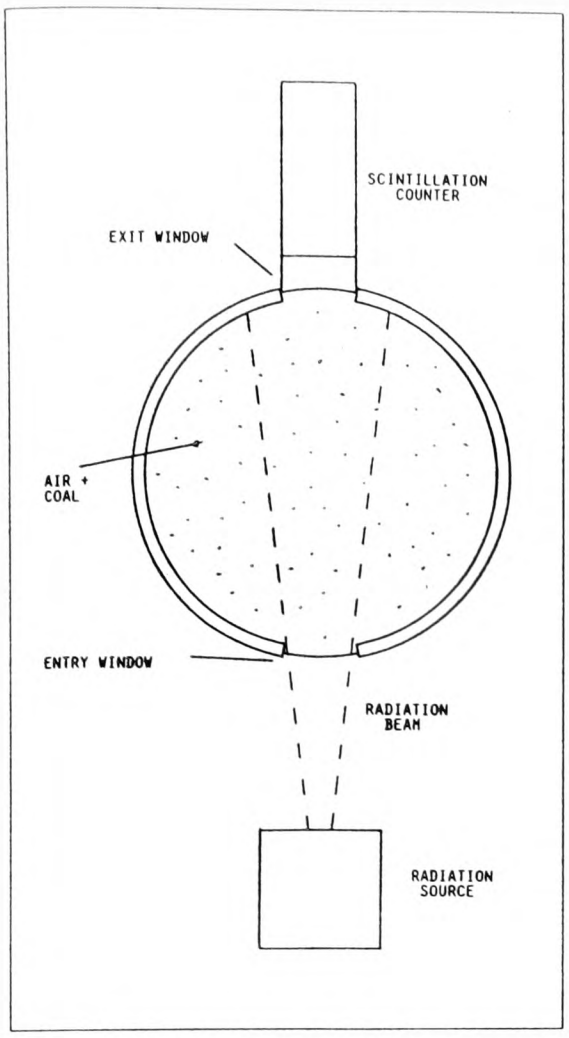

Fig 4: Principle of the flow modulated radiation technique

cause the value of the electrostatic charge on the ring sensor to vary. Once again a noise signal is obtained and the RMS value of this noise is a function of the concentration of product in the pipeline.

Initial tests indicate that this type of transducer may operate more effectively at the low product to air mass flow rate ratios encountered in the power generation and other industries. However, a full test program is not yet complete and it is expected that more reliable information will be available in the near future.

2.3 Flow Modulated Radiation Techniques [20]

The basic principle of this technique is shown in Fig. 4. Radiation, either Gamma, X-Ray or Beta particle is introduced into the pipeline via a window. The intensity of the radiation is then measured on the opposite side of pipeline, usually with a scintillation counter. It can be seen from Fig. 4 that only a small part of the pipeline cross section will be interrogated by the radiation from the single source. This is the main weakness of this technique, since the distribution of the product within the pipe cross section is rarely uniform, because of the 'roping' effect [21]. Consequently, movement is now being made towards the use of multiple sources and counters in an attempt to interrogate a larger proportion of the pipeline cross section. The basic principle of operation is very simple. As product is introduced into the pipeline, the radiation will undergo attenuation across the pipeline. The attenuation will be a function of the product concentration.

The research and development being carried out into this technique is based in a number of areas:

i) The 'window' material – in order to minimise the attenuation caused by the window itself.

ii) The types and the configuration of the sources and counters in order to minimise both cost and radiation hazards, and maximise the proportion of the cross section being interrogated.

iii) The processing of the signal produced by the counter(s) – the laws governing the attenuation of ionizing radiation suggest that the process is not linear and some signal processing is needed. This problem becomes particularly acute with multiple sources and counters.

Although a small amount of work has already been undertaken to explore the possibilities of this technique, clearly, there is much still to be done. This technique is therefore one which the authors shall be continuing to examine in some detail.

3. Velocity Measurement Techniques

As previously mentioned, evaluation of both the coal concentration and the average particle velocity is necessary in order to obtain the mass flow rate of coal in the conveying pipeline. Two techniques applicable to the measurement of the average particle velocity will now be discussed. Again, the most established technique first, which will be followed with a newer, lesser known method.

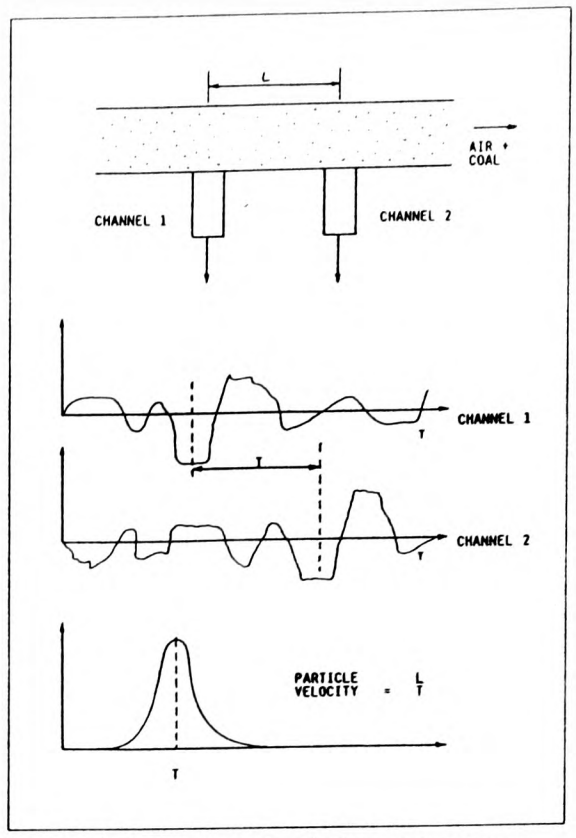

Fig. 5: Average particle velocity measurement using the cross correlation technique

3.1 Cross Correlation of Axially Spaced Concentration Sensors

The principle of this technique is shown diagramatically in Fig. 5. Two concentration sensors are spaced axially along the pipeline, and assuming that the flow pattern remains constant along the short length between the sensors, two signals will be obtained as shown. It should be noted that, as we would expect the signals are similar, and time delayed by period T. By obtaining the cross correlation function of the two signals, in real time, it is possible to evaluate the delay period and hence (assuming that the sensor separation is known) the average particle velocity. In principle, it should be possible to employ any of the concentration measurement techniques for the axially spaced sensors. Both the capacitive and electrostatic techniques have been used

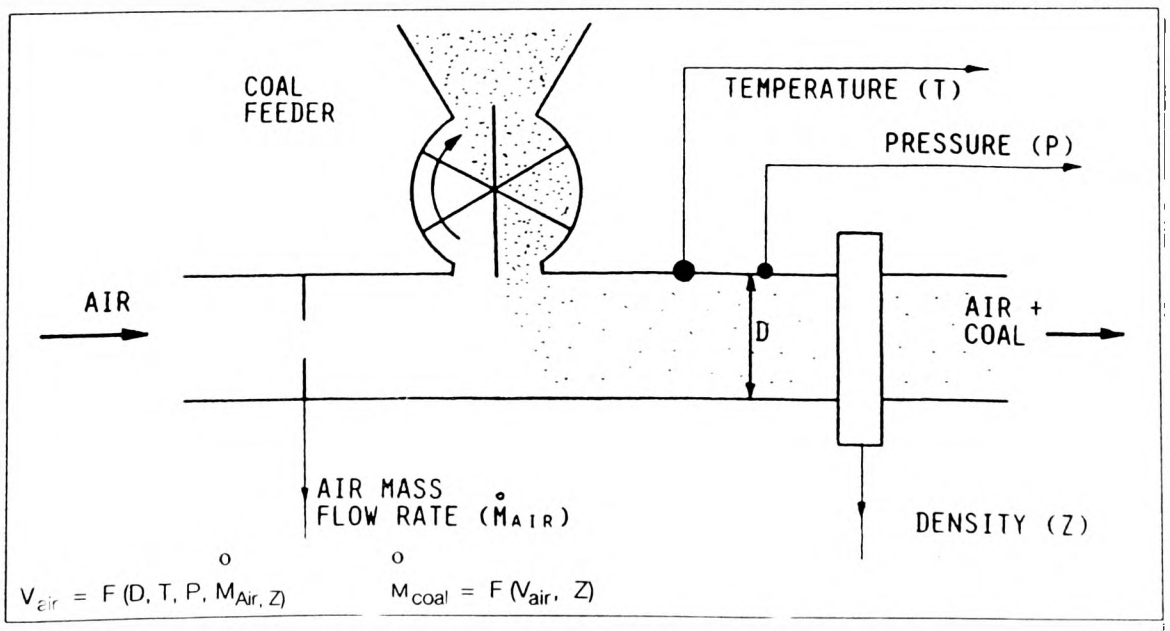

Fig 6 Principle of the estimated slip technique

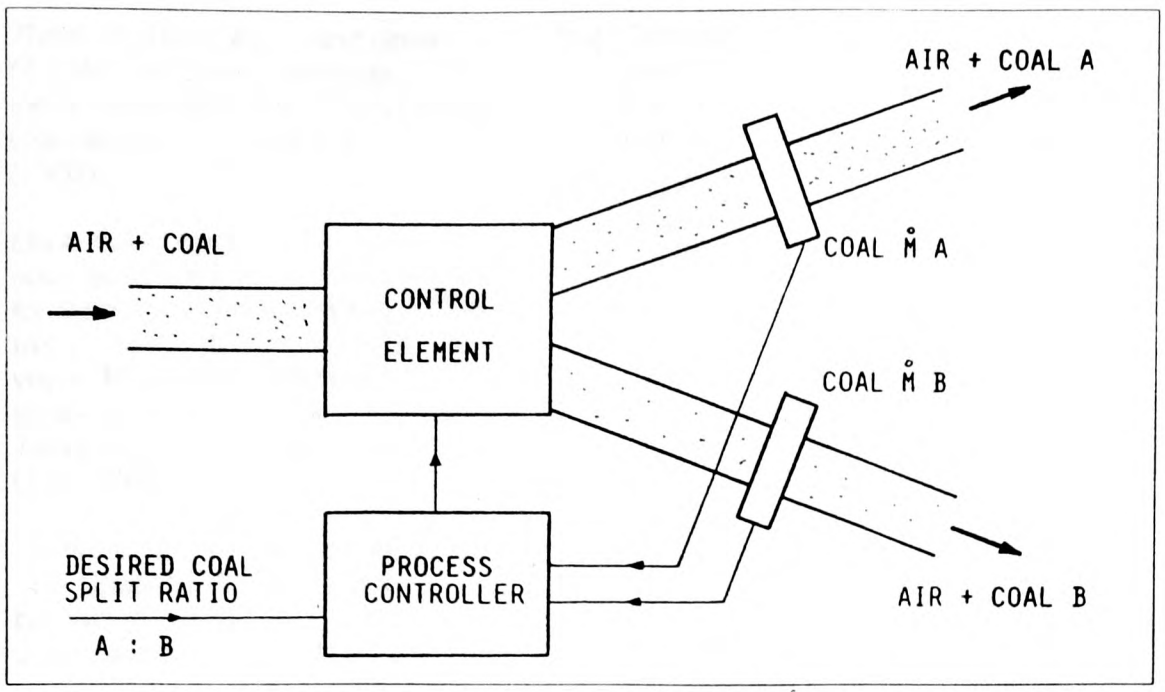

Fig. 7. Principle of the flow splitting control system

with some degree of success. However, once again the results of exhaustive tests are not yet available. To the authors' knowledge, none of the radiation techniques have been combined with the cross correlation technique, for use in pneumatic conveying applications. However they have been utilised in other two-phase flow applications [26].

3.2 The Estimated Particle Slip Technique

This technique is based upon the assumption that the mass flow rate of the air entering the system can be measured. The principle of the technique is shown in Fig. 6. If the mass flow rate of the incoming air can be determined by some conventional technique, such as an orifice plate or a critical flow nozzle, and the temperature, pressure and pipeline bore are known at a given point in the pipeline, it is possible to calculate the superficial air velocity (the air velocity with no product present).

It is known that under most conditions experienced in pneumatic conveying systems, the average particle velocity and the superficial air velocity are not the same. The average particle velocity is always less than the superficial air velocity and the particles are therefore said to 'slip'. Unfortunately, the slip ratio (ratio of particle to superficial air velocity) is not constant. The value changes according to a number of factors, such as product density, particle size, conveying velocity, whether the pipeline is horizontal or vertical and the distance from the last bend or other obstruction to flow.

However, it is possible to measure the slip ratio using a specialised facility incorporating Laser Doppler Velocimetry Instrumentation [23-25]. Such a facility already exists at the Wolfson Centre and if slip ratios for various products under various conveying conditions can be evaluated, this technique could then form the basis of a particle velocity measurement system.

If the particle velocity could be predicted with sufficient accuracy this approach could be particularly cost effective, since much existing process plant is already instrumented to give the mass flow rate of the air intake. All that would then be needed would be a low cost microprocessor based signal processing system, and some means of measuring the product concentration. This technique also forms part of an on going research project at The Wolfson Centre.

4. Concluding Remarks

This paper has reviewed a number of techniques which it is hoped will form the basis for a reliable instrument. One particularly important application of such an instrument would be to provide a feedback signal for flow splitting control systems.

Flow splitting of pneumatic conveying pipelines is used extensively in the power generation industry, and controlling the splitting process is notoriously difficult. The principle of such a technique is shown in Fig. 7.

However, it can be seen that in order to split the flow, a control element is also needed. The development of control elements for flow splitting is the subject of another current research project at The Wolfson Centre, and the development of a complete control system is a matter which the authors shall be investigating in the near future.

Acknowledgements

The authors thank the following organisations for supporting the research programmes outlined in this paper:

Babcock Energy
Blue Circle Cement
The Department of Energy
Kevex Corporation (U.K.)
The School of Information Engineering, Teeside Polytechnic
The Science and Engineering Research Council
Tealgate Limited
The Wolfson Foundation.

This paper is based on a presentation made at the Interbulk Seminar in Pneumatic Conveying: Potentials and Capabilities, Birmingham, U.K., Sept. 1989.

References

[1] *McVeigh, J.C.* and *Craig, R.W.*: Metering of Solid Gas Mixtures Using an Annular Venturi Meter; Proc. Pneumotransport 1 Conference, Cambridge, 1972.

[2] *Beck, M.S.* and *Wainwright, N.*: Flow Failure Detector for Powdered and Granular Materials; Control, pp. 52-56, January, 1969.

[3] *Green, R.G., Foo, S.H.* and *Mitchell, S.*: Application of Low Cost Microcomputer to Measurement and Control of Pneumatic Conveying Systems; Proc. Fifth International Conference on the Pneumatic Transport of Solids in Pipes, London, 1980.

[4] *Beck, M.S.*: Recent Developments and the Future of Cross Correlation Flow Meters; Proc. International Conference on Advances in Flow Measurement Techniques, Warwick, U.K., 1981.

[5] *Cardon, M., Green, R.G.* and *John R.*: Applications in Monitoring Particulate Mass Flow Rates of Abrasive Materials; Proc. International Conference on Advances in Flow Measurement Techniques, Warwick, U.K., 1981.

[6] *Green, R.G.* and *Cunliffe, J.M.*: On line measurement of two phase fluid flow with an F.M. Capacitance Transducer; Proc. International Conference on Advances in Flow Measurement Techniques, Warwick, U.K., 1981.

[7] *Green, R.G., Foo, S.H.* and *Philips J.G.*: Flow Measurement for Optimising the Feed Rate of Pulverised Fuel to Coal Fired Boilers; Symposium on Fossil Energy Processes, San Francisco, 1981.

[8] *Thom, R., Beck, M. S.* and *Green, R. G.*: Non-Intrusive Methods of Velocity Measurement in Pneumatic Conveying; J. Physics E., Vol. 15 (1982).

[9] *Beck, C.M., Henry, R.M., Lowe, B.T.* and *Plaskowski, A.*: Instrumentation for Velocity Measurement and Control of Solids in a Pneumatic Conveyor; Proc. First International Conference on Pneumatic Conveying Technology, Stratford-upon-Avon, U.K., 1983.

[10] *Hammer, E. A.* and *Green, R. G.*: The Spatial Filtering Effect of Capacitance Transducer Electrodes; J. Physics E., Vol. 16 (1983).

[11] *Boeck, T.*: Measurement of Velocity and Mass Flow Rate of Pneumatically Conveyed Solids by the Use of the Correlation Measurement Technique; Proc. Conference on the Flow of Particulate Solids, Bergen, 1986.

[12] *Boeck, T.*: Granucor – Mass Flow Measuring System for Pneumatically Conveyed Solids; Proc. Third International Conference on Pneumatic Conveying Technology, Jersey, 1987.

[13] *Shackleton, M.E.*: Electrodynamic Transducer for Gas Solids Flow Measurement; MPhil Thesis, University of Bradford, 1983.

[14] *Gajewski, J. B.*: Charge Measurement of Dust Particles in Motion, Part II; J. Electrostatics, Vol. 15 (1984), p. 67.

[15] *Coulthard, J.* and *Corbett, M.J.*: Metering of Pulverised and Granular Coal; Energy Transport in Pipelines, Institute of Measurement and Control, London, 1987.

[16] *Dechene, R.L.* and *Averdieck, W.J.*: Triboelectricity – A New Fine Particle Measurement Parameter; 17th Annual Meeting of the Fine Particle Society, San Francisco, 1986.

[17] *Dechene, R.L.* and *Averdieck, W.J.*: Particulate Velocity Measurement by the Triboelectric Effect; Proc. Powder and Bulk Solids Handling and Processing Conference, Chicago, 1987.

[18] *Dechene, R.L.* and *Averdieck, W.J.*: Triboelectricity: A Parameter for Solids Flow Measurement; Powder & Bulk Engineering, 1987.

[19] *Dechene, R.L.*: Triboelectric Technology for Mass Flow Measurement; Proc. Powder and Bulk Solids Handling and Processing Conference, Chicago, 1988.

[20] Howard, *A.V.*: Development of Techniques for the Measurement of Concentration & Mass Flow Rate of Pneumatically Conveyed Coal Dust; Internal Report, CEGB NE Region.

[21] *Cook, D.* and *Hurworth, N.R.*: Recent Research on Pulverised Fuel Settlement in Power Station Pipelines, and the Significance of 'Roping'; Proc. Pneumotransport 5 Conference, London 1980.

[22] *Lech, M.*: Some Aspects of Radioisotropic Measurement of Concentration and Mass Flow Rate of Powder; Proc. Fifth International Conference on the Pneumatic Transport of Solids in Pipes, 1980.

[23] *Birchenough, A.*: The Application of Laser Measurement Techniques to the Pneumatic Transport of Fine Particles; Doctor of Philosophy Thesis, Thames Polytechnic London, 1975.

[24] *Riethmuller, M.L.* and *Ginoux, J.J.*: The Application of a Laser Doppler Velocimeter to the Velocity Measurement of Solid Particles Pneumatically Transported; Proc. of Pneumotransport 2 Conference, Guilford, 1973.

[25] *Birchenough, A.* and *Mason, J.S.*: An Industrial Application of the Laser Velocimeter in Gas-Solid Flows; Proc. Pneumotransport 5 Conference, London, 1980.

[26] *Byrne, B., Coulthard, J.* and *Hampton, R.*: Comparison of Ultrasonic and Radiological Cross Correlation Measurements in Air Water Mixtures; Proc. Intl. Conference on Mass Flow Rate Measurement - Direct and Indirect; London, 1989.